Dissertation

submitted to the
Combined Faculties of the Natural Sciences and Mathematics
of the Ruperto Carola University of Heidelberg, Germany,
for the degree of
Doctor of Natural Sciences

Put forward by
Julian Heeck

Born in Telgte, Germany
Oral examination: May 14th, 2014

Neutrinos and Abelian Gauge Symmetries

Referees:
Dr. Werner Rodejohann
Prof. Dr. Joerg Jaeckel

Abstract

We study the intimate connection between neutrinos and simple abelian gauge symmetries $U(1)'$, starting from the observation that the full global symmetry group of the Standard Model, $\mathcal{G} = U(1)_{B-L} \times U(1)_{L_e-L_\mu} \times U(1)_{L_\mu-L_\tau}$, can be promoted to a local symmetry group by introducing three right-handed neutrinos—automatically making neutrinos massive. The unflavored part $U(1)_{B-L}$ is linked to the Dirac vs. Majorana nature of neutrinos; we discuss the $B-L$ landscape—including lepton-number-violating Dirac neutrinos—and implications for neutrinos, the baryon asymmetry, and experiments. Flavored subgroups $U(1)' \subset \mathcal{G}$ can shed light on the peculiar leptonic mixing pattern and mass ordering; we show how normal, inverted, and quasi-degenerate mass hierarchy can arise from a $U(1)'$ in a simple and testable manner. We furthermore present all $U(1)' \subset \mathcal{G}$ that can enforce viable texture zeros in the neutrino mass matrices. Beyond $\mathcal{G}$, symmetries $U(1)_{\rm DM}$ in the dark matter sector can give rise to naturally light sterile neutrinos, which provide a new portal between visible and dark sector, and also resolve some longstanding anomalies in neutrino experiments. Further topics under consideration are the mixing of vector bosons with the Z boson, as well as the Stückelberg mechanism. The latter raises the question why the photon should be massless—or stable for that matter!

Zusammenfassung

Wir befassen uns mit der innigen Verbindung zwischen Neutrinos und einfachen abelschen Eichsymmetrien $U(1)'$, der Feststellung folgend, dass die volle globale Symmetriegruppe des Standardmodells, $\mathcal{G} = U(1)_{B-L} \times U(1)_{L_e-L_\mu} \times U(1)_{L_\mu-L_\tau}$, nach Einführung dreier rechtshändiger Neutrinos geeicht werden kann – was Neutrinos automatisch massiv macht. Der generationsunabhängige Teil $U(1)_{B-L}$ hängt dabei mit der Dirac- oder Majorana-Natur der Neutrinos zusammen; wir untersuchen die $B-L$ Landschaft – Leptonenzahl-verletzende Dirac-Neutrinos eingeschlossen – und Implikationen für Neutrinos, die Baryonasymmetrie und Experimente. Generationsabhängige $U(1)' \subset \mathcal{G}$ können die eigentümlichen leptonischen Mischungs- und Massenparameter erklären; wir zeigen wie normale, invertierte und quasi-entartete Massenhierarchien in einfacher und testbarer Weise durch solche $U(1)'$ erzeugt werden können. Des Weiteren bestimmen wir alle Untergruppen $U(1)' \subset \mathcal{G}$ die zu erlaubten Textur-Nullen in Neutrino-Massenmatrizen führen. Jenseits von $\mathcal{G}$ können abelsche Eichsymmetrien $U(1)_{\rm DM}$ im Sektor der dunklen Materie auf natürliche Weise zu leichten sterilen Neutrinos führen, welche nicht nur ein neues Portal zwischen dem sichtbaren und dem dunklen Sektor öffnen, sondern auch seit langem bestehende Anomalien in einigen Neutrinoexperimenten auflösen. Als weitere Themen behandeln wir die Mischung von Vektorbosonen mit dem Z, sowie den Stückelberg-Mechanismus, welcher die Frage aufwirft, warum das Photon masselos sein sollte – oder stabil!

Contents

Disclaimer

The research presented in this thesis contains original results already published in peer-reviewed journals. This is indicated at the appropriate places—typically at the beginning of the chapters—but in essence it comes down to this:

- Chapter 2 contains work published in "Neutrinoless quadruple beta decay" [1] (in collaboration with W. Rodejohann) (Sec. 2.3.3) and "Leptogenesis with lepton-number-violating Dirac neutrinos" [2] (Sec. 2.3.4).
- Chapter 3 contains work published in "Neutrino hierarchies from a gauge symmetry" [3] (in collaboration with W. Rodejohann) (Secs. 3.1 and 3.2), "Gauged $L_\mu - L_\tau$ symmetry at the electroweak scale" [4] (in collaboration with W. Rodejohann) (Sec. 3.3), and "Vanishing minors in the neutrino mass matrix from abelian gauge symmetries" [5] (in collaboration with T. Araki and J. Kubo (Sec. 3.4), as well as the proceedings found in Refs. [6, 7].
- Chapter 4 is a slightly rewritten version of "Exotic charges, multicomponent dark matter and light sterile neutrinos" [8] (in collaboration with H. Zhang).
- Appendix A.2 contains almost verbatim the paper "How stable is the photon?" [9].
- In appendix B.2 we present the results from "Kinetic and mass mixing with three abelian groups" [10] (in collaboration with W. Rodejohann).

In order to keep the thesis pithy and topically coherent, we will not cover all work that has been published during the course of this Ph.D. (having already displaced potentially distracting topics adjacent to the main part to the appendices). In particular, we omit a discussion of the papers

- "Hidden $O(2)$ and $SO(2)$ symmetry in lepton mixing" [11] (in collaboration with W. Rodejohann)—connecting the small neutrino-mixing parameters Δm^2_{12} and θ_{13} with an approximate global symmetry.
- "Seesaw parametrization for n right-handed neutrinos" [12]—studying the effects of a varying number $n \neq 3$ of right-handed neutrinos in the seesaw mechanism, especially on neutrino mass anarchy.
- "Sterile neutrino anarchy" [13] (in collaboration with W. Rodejohann)—extending the neutrino mass anarchy framework to the $3 + 2$ scenario of light sterile neutrinos.

Acknowledgments

Many people deserve my gratitude for their help and support during my studies and the writing of this thesis. First and foremost I thank Werner Rodejohann, not only for scientific discussions and sound advice, but also for providing a stimulating and open work environment, allowing and encouraging me to participate in numerous international conferences, and supporting me in the pursuit of my own projects.

I thank Manfred Lindner and all members of the Max Planck Institute for Nuclear Physics, past and present, for many interesting discussions and seminars, and an overall inspiring atmosphere to work in. For enduring my various idiosyncrasies, I give thanks to my office mates over the years, James Barry, Tibor Frossard, and Stefan Brünner.

Jisuke Kubo, Morimitsu Tanimoto, Werner, and Manfred made possible a two-month research stay and follow-up symposium in Kanazawa, Japan; this was a fascinating experience not only concerning my scientific training, and I wholeheartedly thank the theory group of Kanazawa University for their kind hospitality.

Further thanks goes to my collaborators of the various papers presented in this thesis, He Zhang, Takeshi Araki, and the aforementioned Werner and Kubo, for fruitful joined efforts. I also want to thank Joerg Jaeckel for kindly accepting the duty of second referee, and Klaus Blaum and Klaus Pfeilsticker for their quick agreement to partake in my examination. For the time-consuming task of proofreading parts of this thesis, I am indebted to Michael Dürr, Martin Holthausen, and Kher Sham Lim.

Chapter 1

Introduction

The Standard Model (SM) is the pinnacle of about a century's worth of particle physics. Its framework unifies the description of the strong force, responsible for the inner structure of protons and neutrons, and the electroweak force, which governs radioactive decays and electromagnetism. It successfully describes physics down to length scales of 10^{-18} m, corresponding to energy scales up to TeV. With the discovery of a Higgs-like particle at the LHC in 2012 [14, 15], the entire SM particle content seems to be accounted for. Nevertheless, the SM cannot be the final theory, as a number of observations lie beyond its realm. Some of them, for example neutrino oscillations, can be relatively easy accommodated by extensions of the SM; others, such as gravity, have proven to be an almost insurmountable obstacle. In all cases no *unique* solution to any of the problems exists, spawning a plethora of competing models which await scrutiny by future experiments. In the mean time we have only Ockham's razor—simplicity and minimality—and personal preference to select a solution to work on. Since the truly minimal explanations offer only limited potential for a whole new thesis, we will discuss slightly non-minimal scenarios, to be motivated below. We still keep an eye on simplicity and testability of our models, hoping for either veri- or falsification by experiments. This thesis is not meant to provide a review of the SM, nor of its shortcomings and solutions thereof. We will rather introduce only topics and concepts that are of relevance to the original work presented in the later chapters, sacrificing generality to conciseness. Reviews can be readily found, should an interested reader stumble upon this thesis ill-prepared.

The SM is a quantum field theory with gauge group $G_{\rm SM} \equiv SU(3)_C \times SU(2)_L \times U(1)_Y$ and particle content listed in Tab. 1.1. A brief inspection shows that it does not allow for any gauge-invariant fermion or gauge boson masses;[1] masses are rather generated by spontaneous symmetry breaking of $SU(2)_L \times U(1)_Y$ to the electromagnetic gauge group $U(1)_{\rm EM}$ by the vacuum expectation value (VEV) of the Higgs doublet:

$$H = \begin{pmatrix} G^0 \\ G^- \end{pmatrix} \to \begin{pmatrix} v/\sqrt{2} \\ 0 \end{pmatrix}, \quad \text{with} \;\; v/\sqrt{2} \simeq 174\,\text{GeV}\,. \tag{1.1}$$

This electroweak symmetry breaking (EWSB) generates the masses for the W^-_μ and Z_μ vector bosons, but leaves the photon A_μ massless. Gauge invariance renders some of the scalars unphysical, and one colloquially says that G^- and $\mathrm{Im}\, G^0$ are "eaten" by the massive gauge bosons, which however just corresponds to a particular choice of gauge fixing. In this unitary gauge, only the real scalar $h \equiv \sqrt{2}\mathrm{Re}\, G^0$ survives—the famous Higgs particle. Fermion masses

[1] An arguable exception being an allowed Stückelberg mass for the hypercharge gauge boson; see App. A for details of the mechanism and A.2 for a discussion of the induced photon mass.

gauge group	$Q_{L,j}$	$u^c_{R,j}$	$d^c_{R,j}$	L_j	$e^c_{R,j}$	H
$SU(3)_C$	$\mathbf{3}$	$\overline{\mathbf{3}}$	$\overline{\mathbf{3}}$	$\mathbf{1}$	$\mathbf{1}$	$\mathbf{1}$
$SU(2)_L$	$\mathbf{2}$	$\mathbf{1}$	$\mathbf{1}$	$\mathbf{2}$	$\mathbf{1}$	$\mathbf{2}$
$U(1)_Y$	$+\frac{1}{6}$	$-\frac{2}{3}$	$+\frac{1}{3}$	$-\frac{1}{2}$	$+1$	$-\frac{1}{2}$

Table 1.1: $G_{\rm SM} = SU(3)_C \times SU(2)_L \times U(1)_Y$ representations of left-handed fermions and the SM Higgs H. The generation index j runs from 1 to 3, electric charge after symmetry breaking is $Q = T_3 + Y$, and the components of the fermion doublets are denoted as $Q_{L,j} = (u_{L,j},\, d_{L,j})^T$ and $L_j = (\nu_j,\, e_{L,j})^T$.

arise from the Yukawa couplings

$$-\mathcal{L}_{\rm Yuk} = \overline{e}_{R,j}\,(y_e)_{jk}\,\tilde{H}^\dagger L_k + \overline{u}_{R,j}\,(y_u)_{jk}\,H^\dagger Q_{L,k} + \overline{d}_{R,j}\,(y_d)_{jk}\,\tilde{H}^\dagger Q_{L,k} + \text{h.c.}, \tag{1.2}$$

where we also defined the conjugate doublet $\tilde{H} \equiv -i\sigma_2 H^* = (-G^+, G_0^*)^T$ for convenience, which transforms as $(\mathbf{1}, \mathbf{2}, +1/2)$. Inserting the VEV $\langle G_0 \rangle = v/\sqrt{2}$ generates the 3×3 mass matrix $M_e = v y_e/\sqrt{2}$ for the charged leptons, and

$$\begin{aligned} M_u &= v y_u/\sqrt{2} = (U^{u_R})^\dagger\, \text{diag}(m_u, m_c, m_t)\, U^{u_L}\,, \\ M_d &= v y_d/\sqrt{2} = (U^{d_R})^\dagger\, \text{diag}(m_d, m_s, m_b)\, U^{d_L}\,, \end{aligned} \tag{1.3}$$

for the up- and down-type quarks, respectively.

Let us focus on the quark fields first; as already indicated by the bi-unitary transformation in the above equation, the mass matrices $M_{u,d}$ can be diagonalized by rotating the fields to the mass basis, denoted with primes:

$$d'_{R,j} \equiv U^{d_R}_{jk} d_{R,k}\,, \quad d'_{L,j} \equiv U^{d_L}_{jk} d_{L,k}\,, \quad u'_{R,j} \equiv U^{u_R}_{jk} u_{R,k}\,, \quad u'_{L,j} \equiv U^{u_L}_{jk} u_{L,k}\,, \tag{1.4}$$

U^A being unitary 3×3 matrices. This automatically diagonalizes the interactions with the physical Higgs field h in unitary gauge

$$-\mathcal{L}_{\rm Yuk} \;\supset\; \sum_{q=u,d,c,s,t,b} m_q\, \overline{q}'_R\, q'_L\, (1 + h/v) + \text{h.c.}, \tag{1.5}$$

so there are no flavor-changing Higgs interactions. The remaining quark interactions come from the gauge sector via the coupling to the covariant derivative D_μ:

$$\mathcal{L} \;\supset\; \overline{Q}_{L,j}(i\not{D})Q_{L,j} + \overline{u}_{R,j}(i\not{D})u_{R,j} + \overline{d}_{R,j}(i\not{D})d_{R,j}\,. \tag{1.6}$$

The rotations (1.4) of the right-handed quark fields do not change these kinetic terms; however, if $U^{u_L} \neq U^{d_L}$, and hence $V_{\rm CKM} \equiv U^{u_L}(U^{d_L})^\dagger \neq \mathbb{1}$, the doublet structure of $Q_L = (u_L, d_L)^T$ is destroyed and charged-current interactions can jump across families:

$$\mathcal{L} \;\supset\; \frac{g}{\sqrt{2}} \overline{u}'_{L,j} \gamma^\mu (V_{\rm CKM})_{jk} d'_{L,k} W^+_\mu + \text{h.c.} \tag{1.7}$$

These are the only flavor-violating interactions of the SM, induced by the unitary Cabibbo–Kobayashi–Maskawa (CKM) matrix $V_{\rm CKM}$. Having rewritten all quark interactions in terms of the physical mass eigenstates, we can drop the primes on the spinors for convenience. Note that a unitary 3×3 matrix has in general 9 parameters—3 mixing angles and 6 phases. All but one of the phases can however be redefined into the right-handed quark fields, rendering them unphysical.

Decades' worth of experiments have provided plenty of information about the CKM matrix, checking its unitarity, measuring the magnitude of its entries, as well as its CP-violating phase. Of relevance for us are only the magnitudes [16]

$$|(V_{\rm CKM})_{jk}| \simeq \begin{pmatrix} 0.974 & 0.225 & 0.004 \\ 0.225 & 0.973 & 0.041 \\ 0.009 & 0.040 & 0.999 \end{pmatrix}, \tag{1.8}$$

from which we learn that the off-diagonal entries are small, so the mixing matrix of the quark sector is close to the identity matrix $\mathbb{1}$. This is to be compared to the leptonic mixing matrix in the next section, which looks quite different.

Performing analogous rotations in the lepton sector shows that the lack of right-handed neutrinos ν_R—or, more generally, the absence of *any* neutrino mass terms—allows us to rotate the ν_L arbitrarily; in particular, we can rotate them in the same way as e_L, keeping the doublet structure of $L = (\nu_L, e_L)^T$ intact. As a result, there are no flavor-changing charged-current interactions in the lepton sector of the SM. We will see in the next section how this changes once neutrinos are made massive.

1.1 Neutrinos Oscillate and Have Mass

The observation of neutrino oscillations has provided conclusive proof of non-vanishing neutrino masses, and hence physics beyond the SM. Our introduction will be the other way around, showing first how neutrino masses lead to oscillations. At the end of the section we will also comment on neutrino properties which are unobservable in oscillation experiments.

The addition of any neutrino mass term to Eq. (1.2)—to be defined below—forbids us to freely perform rotations among the three neutrino families, because it introduces a preferred basis. Now we need to diagonalize both the charged-lepton mass matrix

$$M_e = v y_e/\sqrt{2} = (U^{e_R})^\dagger \,\mathrm{diag}(m_e, m_\mu, m_\tau)\, U^{e_L}\,, \tag{1.9}$$

by rotating to the charged-lepton mass eigenstates

$$e'_{L,j} \equiv U^{e_L}_{jk} e_{L,k}\,, \quad e'_{R,j} \equiv U^{e_R}_{jk} e_{R,k}\,, \tag{1.10}$$

and the neutrino mass matrix, defining the mass eigenstates $\nu'_{L,j} \equiv U^{\nu_L}_{jk}\nu_{L,k}$. In complete analogy to the quark sector in the previous section, a mismatch in U^{e_L} and U^{ν_L} breaks the doublet structure and leads to flavor-changing charged-current interactions:

$$\mathcal{L}_{cc} = \frac{g}{\sqrt{2}} \overline{e}'_{L,j} \gamma^\mu (U_{\rm PMNS})_{jk} \nu'_{L,k} W^-_\mu + \frac{g}{\sqrt{2}} \overline{\nu}'_{L,j} \gamma^\mu (U_{\rm PMNS})^\dagger_{jk} e'_{L,k} W^+_\mu\,. \tag{1.11}$$

The 3×3 unitary Pontecorvo–Maki–Nakagawa–Sakata (PMNS) matrix $U_{\text{PMNS}} \equiv U^{e_L}(U^{\nu_L})^\dagger$ is conventionally parametrized using three mixing angles and three phases, absorbing three unphysical phases into the right-handed charged leptons:

$$\begin{aligned} U_{\text{PMNS}} &= \begin{pmatrix} 1 & 0 & 0 \\ 0 & c_{23} & s_{23} \\ 0 & -s_{23} & c_{23} \end{pmatrix} \begin{pmatrix} c_{13} & 0 & e^{-i\delta}s_{13} \\ 0 & 1 & 0 \\ -e^{i\delta}s_{13} & 0 & c_{13} \end{pmatrix} \begin{pmatrix} c_{12} & s_{12} & 0 \\ -s_{12} & c_{12} & 0 \\ 0 & 0 & 1 \end{pmatrix} P \\ &= \begin{pmatrix} c_{12}c_{13} & s_{12}c_{13} & s_{13}e^{-i\delta} \\ -c_{23}s_{12} - s_{23}s_{13}c_{12}e^{i\delta} & c_{23}c_{12} - s_{23}s_{13}s_{12}e^{i\delta} & s_{23}c_{13} \\ s_{23}s_{12} - c_{23}s_{13}c_{12}e^{i\delta} & -s_{23}c_{12} - c_{23}s_{13}s_{12}e^{i\delta} & c_{23}c_{13} \end{pmatrix} P\,, \end{aligned} \tag{1.12}$$

with the Majorana-phase matrix $P = \text{diag}(1, e^{i\varphi_1/2}, e^{i\varphi_2/2})$. Here we used the abbreviations $s_{ij} \equiv \sin\theta_{ij}$ and $c_{ij} \equiv \cos\theta_{ij}$ for the three mixing angles. We will often discard the subscript PMNS on the mixing matrix U in the following when no confusion is possible.

We can again omit the primes on the fermion fields, having rewritten all interactions in terms of the physical mass eigenstates. In comparison to the quark sector, it proves convenient to keep the notion of neutrino flavor, because the neutrino masses are observed to be tiny. When *one* of the neutrino mass eigenstates is created via a charged-current interaction (1.11), it is typically kinematically possible to create *all three*.[2] Since the mass differences of the neutrinos are extremely small, the three coherent neutrino wave packets only slowly run apart, behaving for a while like *one* neutrino with a certain flavor. Beta decay will, for example, create an electron-neutrino ν_e, which is a linear combination $\sum_j U_{ej}\nu_j$ of mass eigenstates ν_j. We will denote flavor eigenstates with Greek indices, ν_α, $\alpha = e, \mu, \tau$, and mass eigenstates with Latin indices, ν_i, $i = 1, 2, 3$. The conversion between these two sets is just the PMNS matrix: $\nu_\alpha = U_{\alpha i}\nu_i$, using the Einstein summation convention.

1.1.1 Oscillations

The previous paragraph already provided the crucial ingredients for neutrino oscillations, to which we turn now. We follow the standard derivation below, which has the minor drawback of being wrong; since it nevertheless leads to the correct result and is quite intuitive, we only refer to Ref. [18] for a proper treatment involving either wave packets or full quantum field theory. Our discussion starts with the observation that neutrinos barely interact with the other particles, and hence with matter. They have couplings to the Z and W^- bosons, and maybe to the Higgs or some other scalar, depending on how neutrino masses are introduced, but these scalar couplings are typically highly suppressed. The neutral-current coupling to the Z has been used to "count" the number of light neutrinos ($N_\nu = 2.984 \pm 0.008$ [16]) via the invisible Z width at LEP—comprising only of $Z \to \overline{\nu}\nu$ in the SM—and is also crucial to understand elastic scattering of neutrinos in matter. These interactions are however flavor-diagonal and can therefore not be used to measure leptonic mixing. For neutrino oscillation experiments, the charged-current interactions from Eq. (1.11) are the relevant ones, as they allow an incoming neutrino ν_i to scatter inelastically in matter, producing a charged lepton ℓ

[2] Atomic decays of a metastable state $|e\rangle \to |g\rangle + \gamma + \nu_i + \nu_j$ can in principle provide energies sensitive to the neutrino-mass thresholds, visible in the photon spectrum [17]; tiny rates render this approach experimentally challenging.

that can be readily detected using standard methods like Čerenkov radiation; the amplitude for this process would be proportional to $U_{\ell i}$ and allow us to probe leptonic mixing. However, as already discussed above, it is very difficult to actually create just a single neutrino mass eigenstate ν_i; typically, all three of them will be created coherently, which means we should take the creation process of the neutrino into account as well.

Starting with the charged-current creation of a neutrino in flavor state $\nu_\alpha(t_0) = U_{\alpha j}\nu_j(t_0)$ at time $t_0 = 0$, the propagation is given by the time evolution of the mass eigenstates

$$\nu_j(t) = e^{-iE_j t}\nu_j(0)\,, \tag{1.13}$$

assuming plane waves instead of more appropriate wave packets. Due to the smallness of the neutrino masses m_j compared to typical creation energies E, we can use the ultra-relativistic limit for the individual energies $E_j = \sqrt{|\boldsymbol{p}_j|^2 + m_j^2} \simeq E + m_j^2/2E$. In this limit, we can also replace the propagation time t by the distance traveled $L \simeq t$. The probability for detecting the flavor state ν_β at distance L from the creation is then simply

$$P(\nu_\alpha \to \nu_\beta) = |\,\langle \nu_\beta | \nu_\alpha(t)\rangle\,|^2 = \Big|\sum_j U_{\beta j} e^{-i\Delta m^2_{j1} L/2E} (U^\dagger)_{j\alpha}\Big|^2 . \tag{1.14}$$

Writing out these expressions is bothersome, but let us make note of the most important properties. First, one of the time-propagation phase factors can be eliminated in this absolute square, making only mass-squared *differences* $\Delta m^2_{ij} \equiv m_i^2 - m_j^2$ physically relevant. Inserting the parametrization from Eq. (1.12) shows that the Majorana phases φ_1 and φ_2 drop out of the oscillation formula; we will comment later on their possible physical effects. Another useful form of the oscillation probability (1.14) can be obtained by multiplying-out the absolute square:

$$\begin{aligned} P(\nu_\alpha \to \nu_\beta) = \delta_{\alpha\beta} &- 4\sum_{i>j} \mathrm{Re}\left(U^*_{\alpha i} U_{\beta i} U_{\alpha j} U^*_{\beta j}\right) \sin^2\left(\frac{\Delta m^2_{ij} L}{4E}\right) \\ &+ 2\sum_{i>j} \mathrm{Im}\left(U^*_{\alpha i} U_{\beta i} U_{\alpha j} U^*_{\beta j}\right) \sin\left(\frac{\Delta m^2_{ij} L}{2E}\right). \end{aligned} \tag{1.15}$$

The last sum only contributes if the CP phase δ is not zero, because otherwise all matrix elements $U_{\ell j}$ are real. The name-giving oscillatory behavior in L is apparent from the phase factors in Eq. (1.14) and the sines in Eq. (1.15). Typical values are $\Delta m^2 \simeq 10^{-3}\,\mathrm{eV}^2$ and $E \simeq 1\,\mathrm{GeV}$, leading to an oscillation length of about a thousand kilometers—an utterly impressive length for a quantum effect!

With the theoretical description from above in our hands, it seems like all but a minor experimental issue to actually measure all of the neutrino parameters in Eq. (1.12). The long time span of about forty years from the discovery of neutrinos to an observation of their oscillations is however already a testament to the difficulties of this endeavor. The small cross sections of the charged-current interactions (1.11), e.g. $\sigma_{cc} \simeq 10^{-2}\,\mathrm{pb}\,(E_\nu/\mathrm{GeV})$ for neutrino–nucleon scattering [16], make necessary huge detector targets in order to achieve appreciable rates. The Super-Kamiokande detector, for example, consists of 50.000 tons of ultra-pure water with ten thousand photomultipliers at the edge to detect Čerenkov light, and is situated

parameter	best fit $\pm 1\sigma$	3σ range
$\sin^2\theta_{12}$	0.306 ± 0.012	0.271–0.346
$\sin^2\theta_{23}$	$(0.446 \pm 0.007) \oplus \left(0.587^{+0.032}_{-0.037}\right)$	0.366–0.663
$\sin^2\theta_{13}$	$0.0229^{+0.0020}_{-0.0019}$	0.0170–0.0288
Δm^2_{21} $[10^{-5}\text{eV}^2]$	$7.45^{+0.19}_{-0.16}$	6.98–8.05
Δm^2_{31} $[10^{-3}\text{eV}^2]$ (NH)	$+2.417 \pm 0.013$	2.247–2.623
Δm^2_{32} $[10^{-3}\text{eV}^2]$ (IH)	-2.410 ± 0.062	(-2.602)–(-2.226)

Table 1.2: Neutrino oscillation parameters from a global data fit, taken from Ref. [19].

a thousand meters underground to minimize unwanted cosmic-ray backgrounds. Obviously we cannot do justice to all the impressive experimental efforts to pin down the neutrino mixing parameters; numerous experiments have probed these oscillation probabilities for various flavors, distances, and energies, culminating in a consistent set of parameters given in Tab. 1.2.[3]

While the mixing angles θ_{ij} and the absolute values of the mass-squared differences $|\Delta m^2_{ij}|$ are by now well known, there are only statistically insignificant hints for the CP-violating phase δ, which can still take any value from 0 to 2π at 3σ level. Also unresolved is the octant of θ_{23} ($s^2_{23} \lessgtr 1/2$), should data continue to hint at a non-maximal angle ($s^2_{23} \neq 1/2$). Furthermore, experiments are not yet able to distinguish the two different possible mass orderings: normal hierarchy (NH), with $\Delta m^2_{31} \simeq \Delta m^2_{32} > 0$, or inverted hierarchy (IH), with $\Delta m^2_{31} < 0$. The question of the neutrino mass hierarchy is, of course, more than a mere labeling issue and might be phrased more physically as: Is the mass eigenstate with the largest electron component (defined as ν_1) the lightest or the second-to-lightest eigenstate? Solar neutrino oscillations have already shown that $m_2 > m_1$, but the ordering relative to ν_3 is still undetermined. Fig. 1.1 illustrate the two hierarchies, which will become important in Sec. 3.1, where we connect them to abelian gauge symmetries. With only mass-squared differences accessible in neutrino-oscillation experiments, the actual mass scale, e.g. the mass of the lightest neutrino, remains unknown. In this regard, one further defines the quasi-degenerate (QD) neutrino mass regime $m_j \gg \sqrt{|\Delta m^2_{31,32}|} \simeq 0.05\,\text{eV}$. While not yet as precisely measured as the CKM matrix of the quark sector (Eq. (1.8)), we can nevertheless already conclude that leptonic mixing looks drastically different, with much larger off-diagonal entries [19]:

$$|(U_{\text{PMNS}})_{\alpha j}|_{3\sigma} \simeq \begin{pmatrix} 0.799\text{–}0.844 & 0.515\text{–}0.581 & 0.130\text{–}0.170 \\ 0.214\text{–}0.525 & 0.427\text{–}0.706 & 0.598\text{–}0.805 \\ 0.234\text{–}0.536 & 0.452\text{–}0.721 & 0.573\text{–}0.787 \end{pmatrix}. \tag{1.16}$$

[3] Note that the 1 and 3σ ranges in Tab. 1.2 correspond to $\Delta\chi^2$ deviations from the *global* minimum (at IH). This leads to reduced intervals around the second (local) minimum (at NH), as can be seen in e.g. Δm^2_{31} (NH). Confidence intervals under the prior assumption of a hierarchy can be obtained from the plots in Ref. [19].

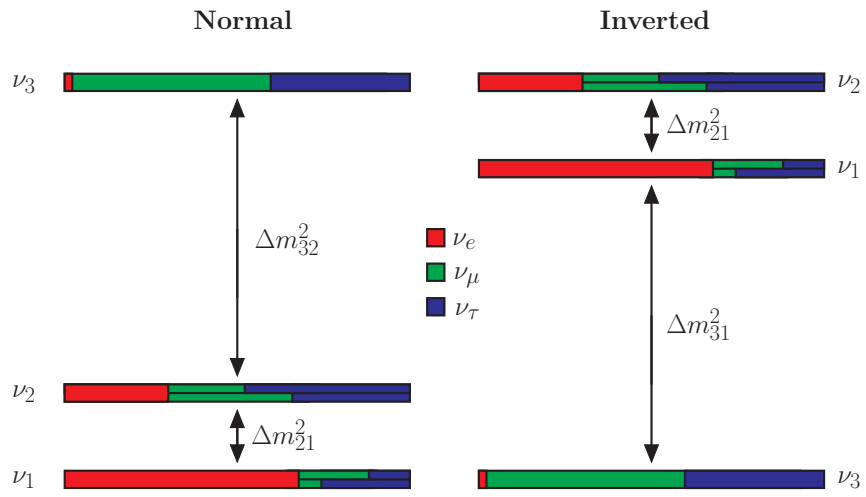

Figure 1.1: Illustration of normal and inverted mass ordering of neutrinos, left and right, respectively. The colors illustrate the flavor content $|U_{\ell j}|^2$ of the mass eigenstates ν_j using the best-fit values from Tab. 1.2. The μ/τ content of $\nu_{1,2}$ depends on the CP angle δ and lies between the extremal values $\delta = 0$ (upper rows) and $\delta = \pi$ (lower rows).

The two large mixing angles—and in particular the former compatibility with the values $s^2_{23} = 1/2$, $s^2_{12} = 1/3$, and $s^2_{13} = 0$—have spawned a plethora of theoretical ideas regarding their origin. For the most part these make use of *discrete global* symmetries in order to explain the mixing angles geometrically. For this, the leptons and neutrinos are put into representations of a non-abelian discrete symmetry such as S_4, A_4, or $\Delta(96)$, while the quarks and the Higgs transform trivially. The goal is then to break the new symmetry into two different remnant subgroups, one for charged leptons, one for neutrinos, in order to explain the mismatch encoded in the PMNS matrix. This symmetry breaking is achieved with a couple of so-called flavon fields ϕ_j, which have to obtain VEVs in specific directions of flavor space; typically, even more fields and symmetries are necessary to achieve the desired vacuum alignment, i.e. the "angles" between the VEVs $\langle\phi_j\rangle$, without fine-tuning. After this, we are still faced with the problem of connecting the flavon VEVs to the actual lepton mass matrices. The usual Yukawa couplings employed so far, e.g. $\overline{e}_R \tilde{H}^\dagger L$, are *forbidden* by the new symmetry, so we are forced to consider non-renormalizable effective operators of the form $\phi_j \overline{e}_R \tilde{H}^\dagger L/\Lambda$ in order to actually generate lepton masses (using the seesaw mechanism (Sec. 2.2.1) for the neutrinos). Inserting the flavon VEVs, one can then achieve a lepton–neutrino mismatch of geometrical origin, for example tri-bimaximal mixing: $s^2_{23} = 1/2$, $s^2_{12} = 1/3$, and $s^2_{13} = 0$. With the recent observation of $\theta_{13} \neq 0$, the discrete-group ansatz to the lepton flavor problem has become yet more involved, with a widespread hope to generate a valid θ_{13} by higher-order corrections. Note that the higher-dimensional operators necessary for this framework might be obtained from a renormalizable model, at the prize of introducing even more particles and parameters. Predictivity of the discrete-group ansatz is limited to the neutrino parameters, as all the newly introduced particles are assumed to be extremely heavy. After this heavily biased and incomplete diatribe, it should be clear that we will not follow the approach of *discrete*

non-abelian global symmetries in this thesis. Instead, we present an alternative based on *continuous abelian local* symmetries in chapter 3, which requires just one symmetry-breaking scalar and a handful of parameters, and is furthermore renormalizable and testable outside of the neutrino sector. For an equally biased—but in the opposite direction—pedagogical review of the discrete-group ansatz, we refer to Ref. [20].

Let us also note that some observations hint at deviations from the above three-neutrino oscillation picture—typically interpreted and explained in a framework with even *more* neutrinos. The PMNS matrix is then promoted to a $(3+n)\times(3+n)$ matrix, and the n new states are assumed to be light, typically eV. Consequently, they would contribute to the invisible width of the Z boson, which is however strongly consistent with $n = 0$. The n new light states of these so-called $3 + n$ models are hence not allowed to carry any G_{SM} quantum numbers, and are therefore referred to as *sterile* neutrinos [21]. Such light sterile neutrinos will be the topic of Ch. 4, where a longer introduction can be found.

1.1.2 Mass

Having discussed mixing angles, we turn to masses. Oscillation experiments aside, there are, of course, other ways determine neutrino properties. One comes from cosmology, where the nonzero neutrino masses contribute to the energy density of the Universe, leaving imprints in the cosmic microwave background (CMB) [22]. The relevant quantity here is the sum of neutrino masses, and recent Planck data, including data from WMAP and baryon acoustic oscillations, give an upper bound of $\sum_j m_j < 0.23\,\text{eV}$ at 95% C.L. [23]. This limit strongly depends on the combined data sets and model assumptions, but is still of utmost importance for the quasi-degenerate neutrino mass regime.

A different upper bound on neutrino masses can be obtained by measuring the end-point energy of the electron spectrum in beta decays. For massive neutrinos, not all the available energy in a beta decay $(A, Z) \to (A, Z+1)+e^-+\overline{\nu}_e$ can be transferred to the electron, because at least the amount $\Delta E = m_{\nu_e}$ is needed to create the electron anti-neutrino. Measuring the highest possible electron energy very precisely can therefore give information about m_{ν_e}. From the discussion in this section, it is clear that m_{ν_e} is not the mass of just one mass eigenstate, but rather a parameter describing the incoherent emission of all three neutrinos. In terms of our notation from above, this parameter takes the form $m_{\nu_e} = \sqrt{\sum_j |U_{ej}|^2 m_j^2}$. The current limit is $m_{\nu_e} < 2.3\,\text{eV}$ at 95% C.L. [24], but is expected to be improved in the near future by an order of magnitude by the KATRIN experiment [25].

1.1.3 Neutrinoless Double Beta Decay

In order to introduce the last type of neutrino-mass experiment, we have to take a step back. Our discussion so far did not require any knowledge about the *type* of neutrino mass—a question only relevant for neutral fermions like the neutrino. The conceptually simplest is a Dirac mass: In direct analogy to the quark sector, we can introduce right-handed neutrino (RHN) partners ν_R to the SM in order to write down Yukawa couplings

$$\Delta\mathcal{L}_{\text{Yuk}} = -\overline{\nu}_{R,j}\,(y_\nu)_{j\,\alpha}\,H^\dagger L_\alpha + \text{h.c.}, \tag{1.17}$$

leading to an up-type Dirac mass matrix $m_D = y_\nu v/\sqrt{2}$, and the neutrino mass eigenstates are Dirac particles of the form $\nu = \nu_L + \nu_R$. In this case, the Majorana phases φ_1 and φ_2 in Eq. (1.12) can be absorbed into the ν_R fields and are rendered unphysical. In order to write down the above Yukawa couplings, the ν_R have to be complete gauge singlets, i.e. $\nu_R \sim (\mathbf{1},\mathbf{1},0)$, and will therefore not lead to new effects beyond neutrino mass.[4] Such Dirac neutrinos will be discussed more thoroughly in the sections 2.1, 2.3.3, and 2.3.4.

A different type of mass term arises because the neutrinos are total singlets under the unbroken SM group $SU(3)_C \times U(1)_{\rm EM}$, allowing for mass terms like $m\,\overline{\nu}_L^c \nu_L$. Basically, the neutrinos can form *their own* right-handed neutrino partners Ψ_R by use of parity-changing charge conjugation $\Psi_R = (\nu_L)^c \equiv \nu_L^c \equiv \mathcal{C}\overline{\nu}_L^T$. The neutrinos are then self-conjugate Majorana fields of the form $\nu = \nu_L + \nu_L^c = \nu^c$. Even though we apparently did not introduce new fields to the SM, new physics is still required to generate this Majorana mass, because the term $m\,\overline{\nu}_L^c \nu_L$ is not invariant under $SU(2)_L \times U(1)_Y$, but only under the unbroken subgroup $U(1)_{\rm EM}$. If the new physics behind the Majorana mass is heavy and can be integrated out, it will effectively give rise to the *fully* gauge-invariant higher-dimensional Weinberg operator [27]

$$\mathcal{L}_{\rm eff} = -\frac{g_{\alpha\beta}}{\Lambda}(\overline{L}_\alpha^c \tilde{H})(H^\dagger L_\beta) + \text{h.c.}, \tag{1.18}$$

leading to a Majorana neutrino mass matrix $\mathcal{M}_{\alpha\beta} = g_{\alpha\beta} v^2/\Lambda$ after EWSB, suppressed by the new-physics scale Λ at which this operator is induced. Small neutrino masses $m_j \lesssim 1\,\text{eV}$ can then be understood as the result of a large scale $\Lambda \gtrsim 10^{14}\,\text{GeV}$ instead of small Yukawa couplings $y_\nu \simeq 10^{-11}(m_\nu/1\,\text{eV})$.

Seeing as this Weinberg operator is of mass dimension five—and actually the only $d = 5$ operator of the SM—it would give the dominant next-order term in an expansion of the SM as an effective field theory below Λ:

$$\mathcal{L}_{\rm full} = \mathcal{L}_{\rm SM} + \mathcal{O}_{d=5}/\Lambda + \mathcal{O}_{d=6}/\Lambda^2 + \ldots \tag{1.19}$$

Neutrino masses of *Majorana* type can hence be interpreted as the natural first sign of physics beyond the SM. No sign of the $\mathcal{O}_{d=6}$ operators has emerged yet, which could give rise to proton decay, an electric dipole moment for the neutron, or lepton-flavor-violating processes such as $\mu \to e\gamma$ [28], all under thorough experimental scrutiny. We stress that this argument should not be misunderstood in the way that physics beyond the SM *necessarily* gives rise to Majorana neutrinos, as the operator $\mathcal{O}_{d=5}$ could easily be forbidden by symmetries (see Ch. 2), allowing only for Dirac masses.

The most famous renormalizable realization of the Weinberg operator (1.18), the seesaw mechanism, will be discussed in Sec. 2.2.1 but is of no importance right now. Let us rather discuss the physical impact of the Majorana nature and possible differences to the Dirac case. First off, the Majorana neutrino mass matrix of whatever origin—written in the basis where the charged-lepton mass matrix is diagonal—takes the form

$$\mathcal{L} \;\supset\; -\frac{1}{2}\,\overline{\nu}_{L,\alpha}^c \mathcal{M}_{\alpha\beta} \nu_{L,\beta} + \text{h.c.} \tag{1.20}$$

[4] The Yukawa coupling $\overline{\nu}_R H^\dagger L$ can also be written down for an $SU(2)_L$ triplet $\nu_R \sim (\mathbf{1},\mathbf{3},0)$, which would bring with it two additional charged particles per generation and hence a more complicated phenomenology [26].

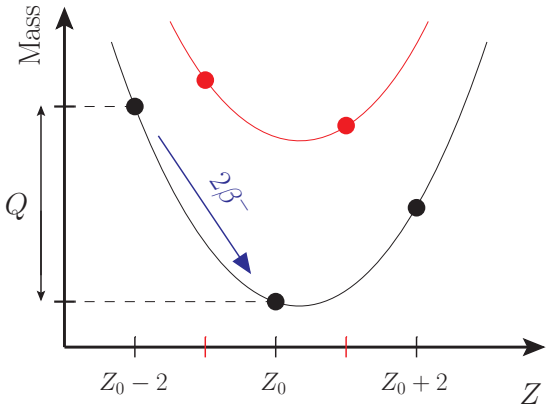

Figure 1.2: Mass parabolas for isobars (A, Z), following the Bethe–Weizsäcker formula. Masses of even–even (odd–odd) nuclei lie on the black (red) parabola. The state $(A, Z_0 - 2)$ cannot undergo beta decay into $(A, Z_0 - 1)$, but *can* decay via $2\nu2\beta$ or $0\nu2\beta$ into the energetically favorable (A, Z_0). The two electrons (in $2\nu2\beta$ also the neutrinos) carry away the energy difference Q.

The object $\overline{\nu}^c_{L,\alpha}\nu_{L,\beta}$ can be shown to be symmetric under the exchange $\alpha \leftrightarrow \beta$, so $\mathcal{M}$ is some complex *symmetric* matrix. Similar to the Dirac case discussed at the beginning of this section, a unitary rotation of the neutrino fields $\nu_{L,\alpha} = U_{\alpha j}\nu'_{L,j}$ can be used to diagonalize the mass matrix $\mathcal{M} = U^* \mathrm{diag}(m_1, m_2, m_3) U^\dagger$. m_j is then the mass of the Majorana field $\nu'_j = (\nu'_j)^c$, and we again drop the primes for convenience. The rotation matrix U is again the PMNS matrix from Eq. (1.12), but with one crucial difference to the Dirac case: The Majorana phases φ_1 and φ_2 are now physical, because they cannot be absorbed by the "right-handed fields" $\Psi_R = (\nu_L)^c$. They are, of course, still unobservable in neutrino oscillation experiments, as discussed above, and cosmology as well as measurements of the electron spectrum in beta decays are similarly insensitive to the Majorana nature of neutrinos.

How does one then distinguish Majorana and Dirac neutrinos? The most promising way to determine the neutrino nature are *neutrinoless double beta decays*. Some nuclei with an even number of protons and neutrons (even–even) are stable against single beta decay $(A, Z) \to (A, Z + 1) + e^- + \overline{\nu}_e$, because the odd–odd daughter nucleus has a lower binding energy and hence higher mass (see Fig. 1.2 for an illustration), caused by the pairing term in the semi-empirical Bethe–Weizsäcker formula. The stability is however only guaranteed in the first order of perturbation series, double beta decay

$$(A, Z) \to (A, Z + 2) + 2\,e^- + 2\,\overline{\nu}_e \qquad (2\nu2\beta) \tag{1.21}$$

allows the nucleus to skip the forbidden odd–odd state and go straight to the energetically allowed even–even nucleus at the bottom of the mass-parabola. At quark level, $2\nu2\beta$ describes the process $2\,d \to 2\,u + 2\,e^- + 2\,\overline{\nu}_e$. Double beta decay, being second order in the weak coupling strength $G_F = 1/\sqrt{2}v^2$, is a highly suppressed process with measured lifetimes exceeding 10^{19} yr. Now, if neutrinos are Majorana particles, a competing decay channel opens up, *neutrinoless* double beta decay

$$(A, Z) \to (A, Z + 2) + 2\,e^- \qquad (0\nu2\beta)\,, \tag{1.22}$$

corresponding to $2\,n \to 2\,p + 2\,e^-$ at hadron level or $2\,d \to 2\,u + 2\,e^-$ at quark level. Basically, the Majorana mass term $m_{ee}\overline{\nu}^c_e\nu_e$ can be interpreted as a vertex at which the electron neutrino changes into an anti-neutrino. This allows the neutrino in normal double beta decay to remain virtual, as can be seen pictorially in Fig. 1.3. In this simple form, the amplitude

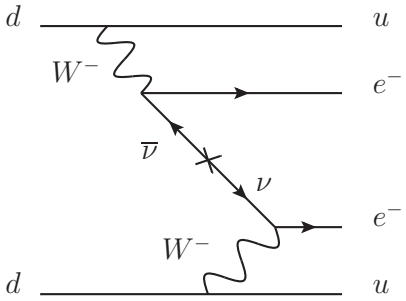

Figure 1.3: Neutrinoless double beta decay $0\nu2\beta$ at quark level. Only a self-conjugate *Majorana* neutrino $\nu = \overline{\nu}$ can remain virtual; the cross denotes the Majorana neutrino mass m_{ee}, interpreted as an interaction vertex.

for $0\nu2\beta$ is still second order in G_F, and furthermore suppressed by the "interaction vertex" $m_{ee}/q \lesssim \text{eV}/100\,\text{MeV}$—$q$ being a typical nuclear energy scale—so it seems hopelessly suppressed compared to the already small $2\nu2\beta$. However, the phase space for $0\nu2\beta$ is much larger because fewer particles are emitted, enough to make $0\nu2\beta$ feasible. Better yet, with at most some MeV of released energy (the Q value), the recoil of the daughter nucleus is irrelevant for the kinematics, resulting in two back-to-back electrons with sharp energy of $Q/2$. This is to be compared to the continuous energy spectrum for the $2\nu2\beta$ electrons, shown in Fig. 1.4. The strategy for $0\nu2\beta$ observation is then to take a large amount of promising nuclei (i.e. stable against beta decay, large Q value to reduce unwanted radioactive background) and measure the deposited energy of emitted electrons. A small sharp peak at $Q/2$ (or Q if the summed electron energy is taken) is then a sign for the existence of neutrinoless double beta decay, and ultimately the Majorana nature of neutrinos—a statement that remains valid independent of the underlying mechanism behind $0\nu2\beta$, be it mediation of light Majorana neutrinos as in Fig. 1.3 or other new physics [29].

Experiments have so far only put lower limits on the $0\nu2\beta$ lifetime of various nuclei, which can be converted into upper limits on the Majorana mass $m_{ee}\overline{\nu}_e^c\nu_e$ with the knowledge of the relevant nuclear matrix elements. The recent 90% C.L. limit of $\tau_{1/2}^{0\nu2\beta} > 2.1 \times 10^{25}\,\text{yr}$ for the germanium isotope ${}^{76}_{32}\text{Ge}$ (with Q value $\simeq 2\,\text{MeV}$) by GERDA [30] can for example be translated into the bound $m_{ee} < (0.2\text{–}0.4)\,\text{eV}$, subject to nuclear-physics uncertainties. In order to connect this limit to the standard neutrino oscillation parameters, we write out the ee entry of the Majorana mass matrix $\mathcal{M}_\nu = U^*\text{diag}(m_1, m_2, m_3)U^\dagger$ using the PMNS matrix from Eq. (1.12):

$$m_{ee} \equiv |(\mathcal{M}_\nu)_{ee}| = |\sum_j U_{ej}^2 m_j| = |m_1 c_{13}^2 c_{12}^2 + m_2 c_{13}^2 s_{12}^2 e^{i\varphi_1} + m_3 s_{13}^2 e^{i(\varphi_2 - 2\delta)}|\,. \tag{1.23}$$

The last expression clearly shows the dependence of this parameter of the Majorana phases φ_1 and φ_2, which finally have a measurable effect. Using the global-fit values for the mixing angles from Tab. 1.2, one can show that m_{ee} could actually vanish for specific values of the lightest neutrino mass ($m_{\text{lightest}} \sim 4\,\text{meV}$) and phases, although only for NH. Correspondingly, even Majorana neutrinos do not *necessarily* lead to (measurable) $0\nu2\beta$ rates. IH on the other hand predicts $m_{ee} \gtrsim 10^{-2}\,\text{eV}$, potentially testable at future experiments. In the QD mass regime one finds roughly $m_{ee} > 4 \times 10^{-2}\,\text{eV}$ and cannot distinguish NH and IH with just m_{ee} alone. There is, of course, more to be said about $0\nu2\beta$, be it experimental (status of current experiments, prospects for the future, nuclear uncertainties) or theoretical (non-

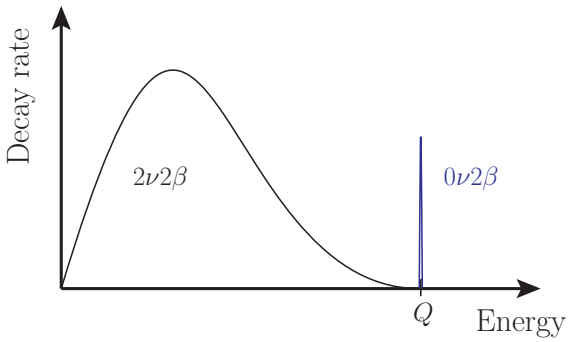

Figure 1.4: Summed energy spectrum of the emitted electrons in (neutrinoless) double beta decay ($0\nu2\beta$) $2\nu2\beta$. The $0\nu2\beta$ spectral line (blue) sits at the Q value of the decay, at most some MeV. The two decay rates are *not* to scale.

standard mechanisms behind $0\nu2\beta$, well-motivated predictions); we refer to Ref. [31] as one of a number of recent reviews on the subject.

1.1.4 Summary of Open Questions in Neutrino Physics

Neutrino oscillations succeeded in measuring the leptonic mixing angles and neutrino mass-squared differences (Tab. 1.2), while upper limits on neutrino-mass parameters come from cosmology, beta-decay, and neutrinoless double beta decay experiments. The unanswered questions in the neutrino sector are hence:

- What is the absolute neutrino mass scale, e.g. the mass of the lightest neutrino?
- What is the nature of this mass, are neutrinos Majorana or Dirac particles?
- What is the mass ordering, do neutrinos have a normal or inverted hierarchy?
- Is there CP violation in the lepton sector, what are the values of δ, φ_1, and φ_2?
- In which octant lies θ_{23}, or can it even be maximal?

The answer to all these questions can, of course, only come from experiment, and at least some will most likely be answered in the next decade. From the theoretical point of view it is nonetheless intriguing to speculate about deeper reasons behind these issues, ultimately trying to motivate or predict an answer and provide connections to other observables or areas of physics [32]. This is the path taken in this thesis, and the above questions should be kept in mind while reading the later chapters.

1.2 Baryon Asymmetry of the Universe

Neutrinos are the main focus of this thesis, but along the way we will also come across other areas in need of physics beyond the SM. Two relevant subjects here are the baryon asymmetry of the Universe (BAU) and dark matter, which both turn out to be linked to neutrinos and abelian gauge symmetries in the later chapters of this thesis. We start with an introduction of the former.

Antiparticles are a general requirement for a consistent quantum field theory like the SM, and have been produced and detected in a multitude of ways. Since particles and antiparticles can per definition annihilate, e.g. into photons, our very existence proves that Earth is composed only of matter, not antimatter. The moon landing has long since confirmed that the Moon, too, is made of matter instead of antimatter or cheese, and unmanned probes extend this observation to other planets. The non-annihilation of solar-wind particles with planets shows that the Sun is really not an anti-Sun. For stars outside our solar system, the arguments are not as clear; stars and anti-stars look the same, as the spectra of elements and anti-elements are identical and consist of the same photons. If other regions of the Universe—be it solar systems, galaxies, or clusters—would indeed consist of antimatter, we would however expect strong annihilations at the boundary region to the matter part we know. Non-observations of the signature gamma lines, e.g. 511 keV photons from $e^+e^- \to \gamma\gamma$, lead us to believe that the whole observable Universe consists of matter. We will work under this paradigm and refer to Ref. [33] for an overview of antimatter regions in the Universe.

In standard Big Bang cosmology our Universe cooled down to its current state by expansion, essentially diluting its contents. The Universe thus used to be a hot plasma of particles and antiparticles in high densities, which have left imprints in certain observables—allowing us to quantify the matter–antimatter asymmetry at different stages of cosmological evolution. Note that we define matter today to consist of protons, neutrons, and electrons; seeing as electric charge is conserved to an incredible degree [16] and the Universe carries very little, if any, net charge [34], the number of electrons is fixed to the number of protons, allowing us to talk about a *baryon* asymmetry rather than a matter asymmetry.

The observed value for the BAU is typically expressed in terms of number densities of baryons n_B and antibaryons $n_{\overline{B}}$ relative to the photon density n_γ

$$\left.\frac{n_B - n_{\overline{B}}}{n_\gamma}\right|_{\text{today}} \simeq 6 \times 10^{-10}\,, \tag{1.24}$$

or relative to the entropy density $s = 2\pi^2 g_* T^3/45$:

$$Y_{\Delta B} \equiv \left.\frac{n_B - n_{\overline{B}}}{s}\right|_{\text{today}} \simeq 8 \times 10^{-11}\,, \tag{1.25}$$

g_* being the effective number of degrees of freedom in the Universe at temperature T. These asymmetries can be inferred either from Big Bang nucleosynthesis (BBN) [35] or the power spectrum of temperature fluctuations in the CMB [23,36]. The CMB consists of the photons left over from recombination at temperature $T \simeq 0.3\,\text{eV}$, when electrons and protons first formed neutral hydrogen and the opaque Universe became clear, while BBN probes the Universe at a temperature $T \simeq 2\,\text{MeV}$. The consistently determined $Y_{\Delta B}$ at these two different scales is a marvelous confirmation of our nuclear physics and cosmology models.

The dominance of matter over antimatter in our Universe raises the obvious question about the *why*, but also about the *how*: The BAU cannot simply be imposed as an initial condition for inflationary Big Bang cosmology,[5] because the energy density of conserved

[5] Cosmic inflation describes the enormously rapid expansion of our Universe shortly after the Big Bang, blowing its volume up by a factor $(e^{60})^3 \simeq 10^{78}$ [37]. Inflation of the small causally connected region gives rise to the *flat*, *homogeneous*, and *isotropic* Universe we observe (using CMB data), naively without the need for unnatural fine-tuning (see however Ref. [38] for a critical view).

baryons would not allow for sufficient inflation [39]. In order to nevertheless obtain matter dominance, a *dynamical* generation of the BAU is required. In the standard framework of CPT-conserving quantum field theories, the conditions for such a dynamical *baryogenesis* have been determined by Sakharov [40] to be

- baryon number violation,
- violation of both charge conjugation (C) and charge parity (CP), and
- out-of-equilibrium interactions.

The SM fulfills these conditions qualitatively: Baryon number B is violated by nonperturbative processes in the early Universe (to be explained in Sec. 1.4), C and CP are violated by the weak interactions and the complex phase in the CKM matrix (1.8), and the expansion of the Universe provides out-of-equilibrium interactions. The resulting baryon asymmetry is however orders of magnitude smaller than the observed one [33].

Since the BAU cannot be explained within the SM, this either hints at new particle physics, or a problem with the assumed underlying inflationary Big Bang cosmology. Since the latter seems to be in very good agreement with complementary observations of the CMB [23], we will study some new-physics explanations of the BAU in this thesis (mainly in Ch. 2). As we will review in Sec. 2.2.2, baryogenesis via leptogenesis can give a simple explanation of the BAU and at the same time shed light on the small neutrino masses.

1.3 Dark Matter

We come to the third problem unaddressed by the SM relevant for this thesis: dark matter (DM). Velocity dispersion of galaxies in clusters, unexplainable just with luminous matter, served as the original hint for non-luminous, i.e. dark, matter. By now, several other observations apparently confirm this hypothesis, among them gravitational lensing, the Bullet Cluster, large scale structure, and distant supernovae. Of great importance are further DM imprints in the CMB, which can be used to accurately measure the density Ω_{DM} of DM today [23]

$$\Omega_{\mathrm{DM}} h^2 = 0.1199 \pm 0.0027\,, \tag{1.26}$$

given in units of the critical density $\rho_c \simeq 10^{-26}\,\mathrm{kg/m^3}$ that renders our Universe flat (as observed), and conventionally multiplied by h^2, $h \simeq 0.67 \pm 0.01$ being the Hubble constant in units of $100\,\mathrm{km\,s^{-1}\,Mpc^{-1}}$. The DM density $\Omega_{\mathrm{DM}} h^2$ is about five times larger than the density of baryons, $\Omega_B h^2 = 0.02205 \pm 0.00028$, which make up all the stars and galaxies we observe. The remaining, and by far dominant, part of the energy density today ($\Omega_\Lambda \simeq 1 - \Omega_{\mathrm{DM}} - \Omega_B \simeq 0.7$) takes the form of dark energy, and seems to be well-described by Einstein's cosmological constant Λ.

Being particle physicists, we will only be concerned with *particle dark matter* in this thesis, more specifically WIMP-like DM [41]. The idea behind this type of weakly interacting massive particles (WIMPs) is based on the freeze-out mechanism: Let us consider a new stable particle Ψ with mass $m_\Psi \simeq 10\,\mathrm{GeV}$–TeV and some weak interactions with SM particles,

which are, however, strong enough to keep Ψ in thermal equilibrium with the SM in the early Universe. As the temperature drops below $T \sim m_\Psi$, Ψ production stops and the number density n_Ψ decreases with an exponential Boltzmann factor $e^{-m_\Psi/T}$ because of Ψ annihilations into the SM. The expansion of the Universe can however effectively stop this annihilation by diluting the Ψ gas, which happens when the annihilation rate $\Gamma \sim n_\Psi \sigma$ drops below the Hubble expansion rate $H(T) \simeq \sqrt{g_*} T^2/M_{\rm Pl}$. At this time, typically at temperature $T_f \simeq m_\Psi/20$, the DM number density is frozen out, allowing us to calculate the resulting thermal relic density [42]

$$\Omega_\Psi h^2 \simeq \frac{0.1\,\text{pb}}{\sigma}\,. \tag{1.27}$$

In the above we defined the *thermally averaged* annihilation cross section $\sigma \equiv \langle \sigma(\Psi\Psi \to \text{SM})\, v \rangle$, v being the DM velocity. The fact that the observed relic density (1.26) seemingly requires typical weak (in the $SU(2)_L \times U(1)_Y$ sense) cross sections $\sigma \sim 1\,\text{pb}$ is known as the WIMP miracle and strongly motivates DM searches around the electroweak scale.

The necessary interactions of the WIMP with the SM can be probed at colliders (looking for $\text{SM}\,\text{SM} \to \Psi\Psi$), indirect astrophysical signals (annihilations $\Psi\Psi \to \text{SM}$ from e.g. galaxies), or in direct detection experiments (scattering of Ψ off recoiling nuclei). The latter are particularly effective in the WIMP mass region $m_\Psi \simeq 10\,\text{GeV–TeV}$, providing strong DM–nucleon cross-section limits of $\sigma_{\text{DM}\text{–}N} \lesssim 10^{-7}\text{–}10^{-9}\,\text{pb}$ [43]. This puts some pressure on the WIMP miracle, as the cross sections required for the relic density are orders of magnitude above these limits. One typical solution of this paradox is a resonantly enhanced s-channel annihilation cross section, e.g. via an intermediate boson X, that does not show up in t-channel direct detection scattering—at the prize of fine-tuning $m_\Psi \simeq m_X/2$.

In this thesis we do not actually set out to solve the DM issue; it just so happens that several models in chapters 3 and 4—motivated by the neutrino sector—give rise to additional stable particles, enforced by consistency requirements. The unavoidable occurrence of DM in these models is particularly intriguing as it points to a deeper connection between the neutrino and DM sectors.

1.4 Baryon and Lepton Numbers

After the introduction of the three areas of beyond-the-SM physics relevant for this thesis, we slowly move towards the motivational part. Before turning to the title-giving abelian *gauge* symmetries, we will take a look at the abelian *global* symmetries of the SM.

As already stated above, the Standard Model is a quantum field theory with gauge group $G_{\text{SM}} = SU(3)_C \times SU(2)_L \times U(1)_Y$ and particle content from Tab. 1.1. The requirement of gauge and Lorentz invariance severely restricts the allowed terms in the Lagrangian, and renormalizability of the theory finally cuts down the—still infinite—amount of conceivable operators to those with mass dimension $d \leq 4$. As a result of these theoretical demands, the SM Lagrangian features a couple of accidental global symmetries. The phases of all quark fields Q_j, d_j, and u_j, can be shifted by a common amount without changing the Lagrangian; the conserved quantity connected to this global $U(1)_B$ symmetry by Noether's theorem is called baryon number B, and is normalized by assigning $B = 1/3$ to all quarks—resulting in

$B = 1$ for the name-giving baryons proton and neutron. The conserved baryon current can be written in terms of the quark fields as

$$j_B^\mu = \sum_{\text{fermions } f} B(\Psi_f)\,\overline{\Psi}_f \gamma^\mu \Psi_f = \frac{1}{3} \sum_{\text{families}} \left(\overline{Q}_L \gamma^\mu Q_L + \overline{u}_R \gamma^\mu u_R + \overline{d}_R \gamma^\mu d_R \right) , \tag{1.28}$$

with implicit isospin and color contractions.

The SM with massless neutrinos further allows to shift the phases of the lepton fields L_j and $e_{R,j}$ of each generation, leading to the global symmetry group $U(1)_{L_e} \times U(1)_{L_\mu} \times U(1)_{L_\tau}$ and the conservation of electron, muon, and tauon numbers L_e, L_μ, and L_τ, respectively. The conserved currents take the form

$$j_{L_\alpha}^\mu = \overline{L}_\alpha \gamma^\mu L_\alpha + \overline{e}_{R,\alpha} \gamma^\mu e_{R,\alpha} \,. \tag{1.29}$$

The *classical* global symmetry group of the SM is hence abelian and given by

$$U(1)_B \times U(1)_{L_e} \times U(1)_{L_\mu} \times U(1)_{L_\tau} \,. \tag{1.30}$$

As discussed in Sec. 1.1, neutrino oscillation measurements have by now conclusively proven that the individual lepton numbers are, in fact, not conserved, and that it is necessary to extend the SM to account for neutrino masses, but we will postpone a discussion of this for later and continue on with the SM.

The quantities B, L_e, L_μ, and L_τ are actually not even exactly conserved in the SM with massless neutrinos, because they are violated by quantum anomalies. Specifically, Adler–Bell–Jackiw-anomalies [44, 45] arise at one-loop level and lead to a non-vanishing divergence of the classically conserved currents:

$$\partial_\mu j_B^\mu = \partial_\mu j_L^\mu = 3\,\partial_\mu j_{L_\alpha}^\mu = \frac{3}{32\pi^2} \left(\frac{e^2}{\cos^2\theta_W} B_{\mu\nu} \tilde{B}^{\mu\nu} - \frac{e^2}{\sin^2\theta_W} W_{\mu\nu}^A \tilde{W}^{\mu\nu A} \right) , \tag{1.31}$$

$W_{\mu\nu}^A$ and $B_{\mu\nu}$ being field strength tensors of $SU(2)_L$ and $U(1)_Y$, respectively, and $\tilde{W}_{\mu\nu}^A \equiv \frac{1}{2}\varepsilon_{\mu\nu\alpha\beta} W^{\alpha\beta A}$ and $\tilde{B}_{\mu\nu} \equiv \frac{1}{2}\varepsilon_{\mu\nu\alpha\beta} B^{\alpha\beta}$ their duals. Here we have also defined the total lepton number $L \equiv L_e + L_\mu + L_\tau$. While B and the L_α are no longer conserved, one can easily identify conserved linear combinations from Eq. (1.31), e.g. $B - L$ and the lepton-number differences $L_\alpha - L_\beta$. It is therefore more useful to go to a different basis for the generators of the classically conserved global SM symmetries (1.30):

$$U(1)_B \times U(1)_{L_e} \times U(1)_{L_\mu} \times U(1)_{L_\tau} \to U(1)_{B+L} \times U(1)_{B-L} \times U(1)_{L_e - L_\mu} \times U(1)_{L_\mu - L_\tau} \,. \tag{1.32}$$

This rewriting is somewhat trivial, as we are still describing the same abelian symmetry group $U(1)^4$, but in this basis all currents except for the $B + L$ current $j_{B+L}^\mu \equiv j_B^\mu + j_L^\mu$ in Eq. (1.31) are conserved. What are then the phenomenological implications of $\partial_\mu j_{B+L}^\mu \neq 0$? Even though the right-hand side of Eq. (1.31) can be written as a total divergence, the nontrivial topological group structure of $SU(2)_L$ can give rise to a non-vanishing integral $\int \mathrm{d}^4x\, W_{\mu\nu}^A \tilde{W}^{\mu\nu A}$ in the action. This integral takes on discrete values for different field configurations and divides the vacuum into an infinite number of topologically inequivalent states.

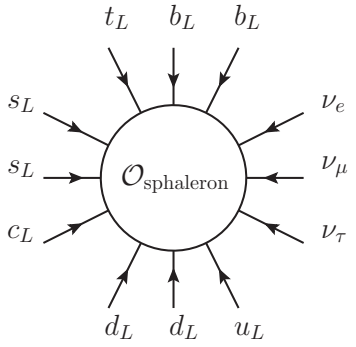

Figure 1.5: One possible effective twelve-fermion interaction mediated by sphalerons [48], induced by the effective operator in Eq. (1.33).

There exist nonperturbative effects, so-called instantons, which correspond to quantum tunneling between the different vacua, and in effect break baryon number by three units and the individual lepton numbers by one unit: $\Delta B = 3$, $\Delta L_\alpha = 1$. Consequently, $\Delta(B+L) = 6$, while $B - L$ and $L_\alpha - L_\beta$ are conserved in these transitions. At zero temperature, these instanton solutions are suppressed by an exponential factor $e^{-(4\pi)^2 \sin^2\theta_W/e^2} \simeq 10^{-173}$ [46], rendering any baryon or lepton number violation in the SM unobservably small.

At nonzero temperature $T \neq 0$ however, small tunneling rates can be replaced by thermal fluctuations over the potential barrier between the vacua, and these so-called sphaleron solutions are of utmost relevance in the early Universe to understand the dominance of matter over antimatter (see Sec. 1.2). Since the nonperturbative instanton or sphaleron solutions are quite abstract, it is useful to illustrate their effects with an effective operator. Seeing as the sphalerons are inherently connected to the $SU(2)_L$ anomalies of j_B and j_L (1.31), this effective operator should involve only (and all of) the chiral doublets Q_L^j and L_j, leading us to

$$\mathcal{O}_{\text{sphaleron}} = \prod_{\text{families } j} Q_L^j Q_L^j Q_L^j L_j \,, \tag{1.33}$$

with implicit $SU(3)_C$ and $SU(2)_L$ contractions. A diagrammatic example of a possible process is shown in Fig. 1.5. This twelve-fermion operator indeed violates $B + L$ by six units, but conserves $B - L$ and $L_\alpha - L_\beta$, in accordance to our discussion above. A proper analysis shows that the $(B+L)$-violating rates are rapid for $T \gg m_W \simeq 80\,\text{GeV}$, and that sphalerons are in equilibrium with the rest of the SM fields for temperatures between the electroweak phase transition (EWPT) and $T \simeq 10^{12}\,\text{GeV}$ [47].

To summarize, the classical SM Lagrangian has the global symmetry group $U(1)_B \times U(1)_{L_e} \times U(1)_{L_\mu} \times U(1)_{L_\tau}$. $B + L$ turns out to be not a symmetry at all, since it is violated at quantum level, leaving us with the actual *global symmetry group of the SM*

$$\mathcal{G} \equiv U(1)_{B-L} \times U(1)_{L_e - L_\mu} \times U(1)_{L_\mu - L_\tau} \,, \tag{1.34}$$

where we have chosen a specific basis in flavor space. $\mathcal{G}$ is more commonly written in terms of the three non-anomalous quantities $B/3 - L_\alpha$ as $\prod_\alpha U(1)_{B/3-L_\alpha}$ (see for example Ref. [47]), but we will stick to the above decomposition in this thesis, which just corresponds to different linear combinations of generators.

1.5 Motivation of Symmetries

As the last part of this introductory chapter, we finally come to the motivation behind this thesis. Following some technical arguments we will point out the title-giving connection between neutrinos and abelian gauge symmetries that will guide us through subsequent chapters. Though part of the introduction, this section should not be skipped, as it contains results originally published in the papers "Kinetic and mass mixing with three abelian groups" [10] (in collaboration with W. Rodejohann) and "Vanishing minors in the neutrino mass matrix from abelian gauge symmetries" [5] (in collaboration with T. Araki and J. Kubo).

In the last section we have rederived the well-known result that the SM has the global abelian symmetry group $\mathcal{G} = U(1)_{B-L} \times U(1)_{L_e-L_\mu} \times U(1)_{L_\mu-L_\tau}$. Now, seeing as $\mathcal{G}$ is already an anomaly-free *global* symmetry of the SM Lagrangian, it is tempting to try to promote it to a *local* symmetry, following the enormous success of the gauge principle in the SM. As a local symmetry, $\mathcal{G}$ gives rise to additional triangle anomalies (to be discussed below), which necessitate the introduction of new anomaly-canceling chiral fields. As we will show below (and pointed out in our paper [5]), it suffices to introduce just three right-handed SM-singlet neutrinos ν_R to cancel *all* arising anomalies and gauge $\mathcal{G}$. This *automatically* results in massive neutrinos, alleviating one of the major shortcomings of the Standard Model. We can take this as an *a posteriori* motivation that our promotion of the non-anomalous global symmetries to local symmetries is worthwhile and goes in the right direction; however, the connection between these symmetries and neutrinos goes actually beyond the mere introduction of RHNs, as we will show in this thesis.

Anomalies in *global* symmetries like B are not problematic and simply show that the symmetry is broken, but anomalies in *local* symmetries would destroy gauge invariance and the renormalizability of the theory. It is therefore important to ensure a cancellation of the chiral-fermion contributions to one-loop triangle diagrams like Fig. 1.6.[6] Attaching gauge bosons with group indices a, b, and c to the triangle diagrams, one can show that the amplitudes are proportional to an anomaly coefficient

$$\operatorname{tr}\left[\left(T^a_{\mathcal{R}} T^b_{\mathcal{R}} + T^b_{\mathcal{R}} T^a_{\mathcal{R}}\right) T^c_{\mathcal{R}}\right], \tag{1.35}$$

where $T^a_{\mathcal{R}}$ denotes the generating group matrix for the left-handed fermions in the (reducible) representation $\mathcal{R}$.[7] For an anomaly-free $U(1)$ gauge group, this simply means that the cubes of all charges have to sum to zero ($\sum Q^3 = 0$), which unfortunately looks a little more complicated for non-abelian gauge groups (1.35). A different potential anomaly arises from the coupling to gravity [50], proportional to $\operatorname{tr}[T^a_{\mathcal{R}}]$. Since only the matrix generators of abelian groups have non-vanishing traces, the absences of gravitational anomalies simply requires the charges of all $U(1)$ gauge group factors to sum to zero ($\sum Q = 0$). The SM gauge group G_{SM} with field content from Tab. 1.1 is, of course, non-anomalous, albeit not obviously so [51]; the seemingly miraculous anomaly cancellation per fermion generation can be attributed

[6] An alternative would be the implementation of the Green–Schwarz mechanism [49] to cancel anomalies. Since anomaly-canceling fermions turn out to have far more interesting/testable effects, we will not discuss this here.

[7] Here we take all fermions to be left-handed, which can be trivially realized by rewriting any right-handed Ψ_R as a left-handed charge conjugate $\phi_L \equiv (\Psi_R)^c \equiv \Psi^c_R = \mathcal{C}\overline{\Psi_R}^T$.

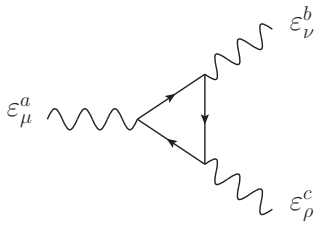

Figure 1.6: Triangle diagram relevant for gauge anomalies. The polarization vectors ε^a_μ belong to gauge bosons X^a_μ with group index a.

to an embedding of the SM gauge group G_{SM} into a non-abelian group such as $SO(10)$, each family forming an irreducible representation, e.g. $\mathbf{16}_{SO(10)}$. While such Grand Unified Theories (GUTs) also often lead to additional abelian factors $G_{\text{SM}} \times U(1)'$ at intermediate stages of symmetry breaking, the phenomenology and underlying motivation is quite different from the abelian gauge symmetries discussed in this thesis, and will not be discussed further.

Let us rather go back to our well-motivated group $\mathcal{G}$ from Eq. (1.34) and discuss the arising anomalies in an SM extension by *one* of the $U(1) \subset \mathcal{G}$ factors, starting with $U(1)_{B-L}$. We are required to introduce particles beyond the SM to gauge $B-L$, as can be seen already by the non-vanishing anomaly involving only $B-L$ gauge bosons

$$\begin{aligned}\mathcal{A}\left[U(1)^3_{B-L}\right] &= \sum (B-L)^3 = \sum B^3 - \sum L^3 \\ &= N_g N_C \left[2 \times \left(\frac{1}{3}\right)^3 + \left(-\frac{1}{3}\right)^3 + \left(-\frac{1}{3}\right)^3\right] + N_g \left[2 \times (-1)^3 + (+1)^3\right] \\ &= -N_g \,,\end{aligned} \tag{1.36}$$

with the number of generations $N_g = 3$ and number of colors $N_C = 3$. Extending the SM particle content of Tab. 1.1 by three RHNs $\nu_R \sim (\mathbf{1}, \mathbf{1}, 0)$—carrying lepton numbers $L_e = 1$, $L_\mu = 1$, and $L_\tau = 1$, respectively—contributes $\Delta\mathcal{A}\left[U(1)^3_{B-L}\right] = 3 \times (+1)^3$ and successfully cancels the anomaly. The gravitational anomaly is similarly canceled by the RHNs ν_R:

$$\begin{aligned}\mathcal{A}\left[U(1)_{B-L}\right] &= \sum (B-L) = \sum B - \sum L \\ &= N_g N_C \left[2 \times \left(\frac{1}{3}\right) + \left(-\frac{1}{3}\right) + \left(-\frac{1}{3}\right)\right] + N_g \left[2 \times (-1) + (+1)\right] + 3 \times (+1) \\ &= 0 \,.\end{aligned} \tag{1.37}$$

This leaves us with the anomalies involving SM gauge bosons, which do not couple to the SM-singlets ν_R. It is already clear from Eq. (1.31) that there cannot be any cross-anomalies of $B-L$ with the SM, because the current j_{B-L} is exactly conserved even at quantum level. Still, we will calculate some anomaly-coefficients explicitly, if only for illustration purposes. We start with the triangle anomaly with two $SU(3)_C$ gauge bosons

$$\begin{aligned}\mathcal{A}\left[SU(3)^2_C U(1)_{B-L}\right] &= \sum_{\text{quarks}} (B-L) \\ &= N_g N_C \left[2 \times \left(\frac{1}{3}\right) + \left(-\frac{1}{3}\right) + \left(-\frac{1}{3}\right)\right] \\ &= 0 \,,\end{aligned} \tag{1.38}$$

two $SU(2)_L$ gauge bosons

$$\mathcal{A}\left[SU(2)_L^2 U(1)_{B-L}\right] = \sum_{\text{doublets}} (B-L) = N_g N_C \left(\frac{1}{3}\right) + N_g(-1) = 0\,, \tag{1.39}$$

two hypercharge gauge bosons

$$\mathcal{A}\left[U(1)_Y^2 U(1)_{B-L}\right] = \sum Y^2 (B-L) = 0\,, \tag{1.40}$$

and, finally, one hypercharge gauge boson

$$\mathcal{A}\left[U(1)_Y U(1)_{B-L}^2\right] = \sum Y (B-L)^2 = 0\,. \tag{1.41}$$

With the above equations, we have proven the well-known fact that $G_{\text{SM}} \times U(1)_{B-L}$ is a consistent anomaly-free theory once three RHNs are introduced. Let us move on to the other $U(1)$ factors in $\mathcal{G}$, which couple to lepton-number differences $L_\alpha - L_\beta$ (1.34). This time we omit the calculation of the cross-anomalies with the SM, which cancel due to Eq. (1.31). This leaves

$$\mathcal{A}\left[U(1)_{L_\alpha - L_\beta}^3\right] = \sum (L_\alpha - L_\beta)^3 = \sum_{\alpha \text{ leptons}} L_\alpha^3 - \sum_{\beta \text{ leptons}} L_\beta^3 = 0\,, \tag{1.42}$$

and

$$\mathcal{A}\left[U(1)_{L_\alpha - L_\beta}\right] = \sum (L_\alpha - L_\beta) = \sum_{\alpha \text{ leptons}} L_\alpha - \sum_{\beta \text{ leptons}} L_\beta = 0\,. \tag{1.43}$$

One of the lepton number differences $L_\alpha - L_\beta$ can therefore be consistently gauged in addition to the SM. This actually works even without the RHNs, as shown long ago [52–54], making $U(1)_{L_\alpha - L_\beta}$ the only new symmetry that can be gauged with the SM particle content.

So far, we have shown that every *factor* of the non-anomalous global symmetry

$$\mathcal{G} = U(1)_{B-L} \times U(1)_{L_e - L_\mu} \times U(1)_{L_\mu - L_\tau}\,, \tag{1.44}$$

and by extension *every* $U(1)$ subgroup of $\mathcal{G}$, can be promoted to a local symmetry once right-handed neutrinos are introduced. It has to our knowledge never been emphasized, though, that the ν_R are already enough to make the entire group $G_{\text{SM}} \times \mathcal{G}$ anomaly free. Having already shown that all the cross-anomalies of $\mathcal{G}$ with the SM cancel, we only have to consider cross-anomalies within $\mathcal{G}$, following our papers [5, 10]. We show the purely leptonic part

$$\sum (L_\alpha - L_\beta)^2 (L_\beta - L_\gamma) = \sum_{\beta \text{ leptons}} L_\beta^3 = 2 \times (+1)^3 + (-1)^3 + (-1)^3 = 0\,, \tag{1.45}$$

$$\sum (L_\alpha - L_\beta)(L_\beta - L_\gamma)^2 = -\sum_{\beta \text{ leptons}} L_\beta^3 = 0\,, \tag{1.46}$$

$$\sum (L_\alpha - L_\beta)(L_\beta - L_\gamma) Y = -\sum_{\beta \text{ leptons}} L_\beta^2 Y = 0\,, \tag{1.47}$$

and the anomalies involving $B - L$:

$$\sum (B-L)(L_\alpha - L_\beta)^2 \propto \sum_{\beta \text{ leptons}} L_\beta = 2 \times (+1) + (-1) + (-1) = 0\,, \tag{1.48}$$

$$\sum (B-L)(L_\alpha - L_\beta)(L_\beta - L_\gamma) = \sum_{\beta \text{ leptons}} L_\beta^3 = 0\,, \tag{1.49}$$

$$\sum (B-L)(L_\alpha - L_\beta)Y = \sum_{\alpha \text{ leptons}} (B-L)Y - \sum_{\beta \text{ leptons}} (B-L)Y = 0\,, \tag{1.50}$$

$$\sum (B-L)^2(L_\alpha - L_\beta) = \sum_{\alpha \text{ leptons}} (B-L)^2 - \sum_{\beta \text{ leptons}} (B-L)^2 = 0\,, \tag{1.51}$$

where the last two relations follow from the universality of Y and $B-L$ [10]. This means that the full *global* symmetry group of the SM

$$\mathcal{G} = U(1)_{B-L} \times U(1)_{L_e - L_\mu} \times U(1)_{L_\mu - L_\tau}\,, \tag{1.52}$$

can be promoted to a *local* symmetry group just with the introduction of three right-handed neutrinos. Before diving into the physical implications of this result, let us make two technical comments about the obtained result:

- First, note that even though we can formally consider the much larger group

$$\begin{aligned} &G_{\text{SM}} \times U(1)_{B - x_e L_e - x_\mu L_\mu - x_\tau L_\tau} \times U(1)_{y_e L_e + y_\mu L_\mu + y_\tau L_\tau} \\ &\quad \times U(1)_{L_e - L_\mu} \times U(1)_{L_\mu - L_\tau} \times U(1)_{L_\tau - L_e} \end{aligned} \tag{1.53}$$

  and show that it is anomaly-free for $\sum x_\alpha = 3$ and $\sum y_\alpha = 0$, the decompositions

$$L_e - L_\tau = (L_e - L_\mu) + (L_\mu - L_\tau)\,, \tag{1.54}$$

$$y_e L_e + y_\mu L_\mu - (y_e + y_\mu) L_\tau = y_e (L_e - L_\mu) + (y_e + y_\mu)(L_\mu - L_\tau)\,, \tag{1.55}$$

  and

$$\begin{aligned} &B - x_e L_e - x_\mu L_\mu - (3 - x_e - x_\mu) L_\tau \\ &\quad = (B-L) + (1-x_e)(L_e - L_\mu) + (2 - x_e - x_\mu)(L_\mu - L_\tau)\,, \end{aligned} \tag{1.56}$$

  show that the generators of the five new abelian groups are not independent, and only two of the lepton-number differences can be gauged. Stated in another way: One of the gauge bosons of $U(1)_{L_e - L_\mu} \times U(1)_{L_\mu - L_\tau} \times U(1)_{L_\tau - L_e}$ can be rotated away, i.e. made non-interacting, so it suffices to consider $U(1)_{L_e - L_\mu} \times U(1)_{L_\mu - L_\tau}$ (with kinetic mixing). The same argument holds for the other linear combinations.

- Second, there is a more elegant way to derive all the vanishing anomalies. By taking another basis for the flavor-dependent part of $\mathcal{G}$ (acting on three-dimensional flavor space), namely

$$L_e - L_\mu = \text{diag}(1, -1, 0)\,, \quad (L_e - L_\mu) + 2\,(L_\mu - L_\tau) = \text{diag}(1, 1, -2)\,, \tag{1.57}$$

  we see that these two generators form the Cartan sub-algebra of a rank-2 $SU(3)_\ell$. In fact, putting the leptons in the representations

$$(L_e, L_\mu, L_\tau)^T \sim \mathbf{3}_\ell\,, \quad (e_R, \mu_R, \tau_R)^T \sim \mathbf{3}_\ell\,, \quad (\nu_{R,e}, \nu_{R,\mu}, \nu_{R,\tau})^T \sim \mathbf{3}_\ell\,, \tag{1.58}$$

immediately shows that they form a vector-like representation of $SU(3)_\ell$, so the anomaly $\mathcal{A}[SU(3)_\ell^3]$ vanishes in direct analogy to the quarks in $SU(3)_C$. Anomalies with other nonabelian group factors vanish trivially, so the only possible anomalies are

$$\begin{aligned}\mathcal{A}[SU(3)_\ell^2 U(1)_Y] &= \sum_{\mathbf{3}_\ell} Y = 3 \times [2\,Y(L_e) + Y(e_R^c)] = 0\,,\\ \mathcal{A}[SU(3)_\ell^2 U(1)_{B-L}] &= \sum_{\mathbf{3}_\ell} (B-L) = 3 \times [2\,(-1) + (+1) + (+1)] = 0\,,\end{aligned} \tag{1.59}$$

which means that $G_{\text{SM}} \times U(1)_{B-L} \times SU(3)_\ell$ is anomaly-free. Since the $SU(3)_\ell$ is badly broken by the Yukawa couplings in the charged lepton sector—seeing as electron, muon, and tauon have vastly different masses—we will not use it in the following. This is not to say that a discussion of $SU(3)_\ell$ might not be worthwhile, but is beyond the scope of this thesis.

After many technical arguments, we can finally summarize our motivation for this thesis: We have shown that with the introduction of just three right-handed neutrinos ν_R, the full *global* symmetry group $U(1)^3$ of the SM can be promoted to a *local* symmetry group, i.e. that

$$\underbrace{SU(3)_C \times SU(2)_L \times U(1)_Y}_{G_{\text{SM}}} \times \underbrace{U(1)_{B-L} \times U(1)_{L_e - L_\mu} \times U(1)_{L_\mu - L_\tau}}_{\mathcal{G}}\,, \tag{1.60}$$

is free of anomalies. The remainder of this thesis is devoted to a discussion of this abelian gauge group or subgroups of $\mathcal{G}$, but let us make a couple more comments:

- The three ν_R will couple to the left-handed lepton doublet L via typical Yukawa couplings $\overline{\nu}_{R,j}\,(y_\nu)_{j\,\alpha}\,H^\dagger L_\alpha$, giving rise to a Dirac mass matrix for the neutrinos $m_D = y_\nu \langle H \rangle$ (see Secs. 1 and 1.1). Gauge invariance under $\mathcal{G}$ only allows for a diagonal m_D, and the charged-lepton mass matrix M_e is automatically diagonal as well. Neutrinos are hence *massive*, but do not *mix*, which shows that at least the flavored gauge group factor $U(1)_{L_e - L_\mu} \times U(1)_{L_\mu - L_\tau}$ has to be broken. The specifics of this breakdown can however shed light on various neutrino properties, as we will show in chapter 3.

- Every $U(1)'$ subgroup of $\mathcal{G}$, generated by a linear combination $Y' = \alpha(B-L) + \beta(L_e - L_\mu) + \gamma(L_\mu - L_\tau)$, is in itself a well-motivated anomaly-free gauge-group extension of the SM, which can be envisioned as the last step of a full breakdown $\mathcal{G} \to$ nothing. We will only work with such $U(1)'$ subgroups, as they are simpler to handle and already give rise to fascinating phenomenology.

- Our derivation of $\mathcal{G}$ involved symmetries that act on SM fields. It is, of course, trivial to extend G_{SM} by a gauge group G_{DM} under which the SM particles are uncharged, G_{DM} typically being connected to dark matter. Even though the SM fields are uncharged under G_{DM}, this can still lead to interesting phenomenology, and we will show in chapter 4 that an intimate connection to neutrinos can arise even in this case. Neutrinos are good mediators to the G_{DM} sector because they are gauge singlets of the unbroken SM group $SU(3)_C \times U(1)_{\text{EM}}$, and can therefore mix with gauge-singlet fermions of the (broken) group G_{DM}.

All of this should suffice as an introduction and motivation for this thesis. In the next chapter, we will discuss the unflavored $\mathcal{G}$ subgroup $U(1)_{B-L}$ in its various phases: unbroken exact $B-L$ in Sec. 2.1, the more commonly discussed case of Majorana $B-L$ ($B-L$ spontaneously broken by two units) in Secs. 2.2.1 and 2.2.2, and finally our very own Dirac $B-L$ in Secs. 2.3.3 and 2.3.4, where $B-L$ is broken spontaneously by *four* units, giving rise to Dirac neutrinos with lepton-number-violating interactions. This chapter connects the very nature of neutrinos, i.e. whether they are Dirac or Majorana fermions, to an abelian gauge symmetry.

Chapter 3 is devoted to a discussion of flavor-dependent $U(1)'$ subgroups of $U(1)_{B-L} \times U(1)_{L_e-L_\mu} \times U(1)_{L_\mu-L_\tau}$, which can help us to understand the peculiar leptonic mixing pattern and neutrino mass hierarchy in a very simple manner. In its most extreme case, such an abelian gauge symmetry can even enforce texture zeros in the neutrino mass matrix, leading to testable relations in the mixing parameters (Sec. 3.4). In all cases, the abelian gauge symmetries are connected to neutrino properties and the employed models are particularly simple and testable.

The above-mentioned possibility of gauge groups G_{DM} not acting on SM fermions will be discussed in chapter 4. Following the title of this thesis, we are only concerned with abelian gauge groups $G_{\text{DM}} = U(1)_{\text{DM}}$. Despite the fact that the SM fermions do not couple to G_{DM}, the new force can have very interesting consequences for neutrino physics, and can in particular provide a natural explanation for new *light sterile neutrinos* at the eV scale.

We will briefly summarize our findings in Ch. 5, together with an outlook. Longer conclusions can be found at the end of each individual chapter, or even section. Some topics (and associated original work) that are not *directly* related to the topic of this thesis, but not far off either, have been put in the appendix in an effort to improve readability. App. A introduces the Stückelberg mechanism for abelian gauge boson masses. While we will use this mechanism in the main text in our discussion of unbroken $B-L$ (Sec. 2.1), it primarily serves as a motivation for the paper "How stable is the photon?" [9] in App. A.2, where we employ it to motivate a finite photon mass (and lifetime). App. B on the other hand deals with kinetic mixing, and Z–Z' mixing in general. Based on the paper "Kinetic and mass mixing with three abelian groups" [10] (in collaboration with W. Rodejohann), it is actually very relevant to the topic of (multiple) abelian gauge symmetries discussed in this thesis, but has by itself little to do with neutrinos. As such, it might be too distracting if included in the main text. We urge the reader to peruse these appendices with the same commitment as the main text.

Chapter 2

Unflavored Symmetries

Having motivated an abelian gauge group extension

$$G_{\text{SM}} \to G_{\text{SM}} \times U(1)_{B-L} \times U(1)_{L_e-L_\mu} \times U(1)_{L_\mu-L_\tau} \equiv G_{\text{SM}} \times \mathcal{G} \tag{2.1}$$

in Sec. 1.5, we devote this chapter to an overview of $U(1)_{B-L}$, the unique *unflavored* subgroup of $\mathcal{G}$. Because of its generation-independent couplings, $B-L$ is incapable to shed light on the peculiar leptonic mixing pattern (Sec. 1.1); $B-L$ *is*, however, connected to the very nature of neutrinos. We identify three distinct possibilities for the gauge group $U(1)_{B-L}$, each with fascinating implications, especially for neutrino physics. Although rarely presented in this manner, the discussions of unbroken $B-L$ in Sec. 2.1 and "Majorana $B-L$" in Secs. 2.2.1 and 2.2.2, contain no new results and serve as a topical overview and introduction to relevant concepts like the seesaw and various leptogenesis mechanisms. Secs. 2.3.3 and 2.3.4 then extend the known framework and introduce the idea of lepton-number-violating Dirac neutrinos, following very closely the papers "Neutrinoless quadruple beta decay" [1] (in collaboration with W. Rodejohann) and "Leptogenesis with lepton-number-violating Dirac neutrinos" [2].

2.1 Unbroken $B-L$

We start our discussion of $G_{\text{SM}} \times U(1)_{B-L}$ with a particularly interesting, and not often discussed, possibility: exact and unbroken $B-L$ [55]. The active neutrinos then form Dirac fermions together with the anomaly-canceling RHNs ν_R. To be more precise, the Yukawa couplings $\overline{\nu}_{R,j}\,(y_\nu)_{j\,\alpha}\,H^\dagger L_\alpha$ in a basis where the charged-lepton mass matrix is diagonal lead to the Dirac-neutrino mass matrix

$$m_D = y_\nu \langle H \rangle = V_R^\dagger \,\text{diag}(m_1^\nu, m_2^\nu, m_3^\nu)\, U_{\text{PMNS}}^\dagger\,, \tag{2.2}$$

the unitary matrix V_R being unphysical (see Ch. 1). The smallness of neutrino masses m^ν compared to the other fermions can either be attributed to small Yukawa couplings $y_\nu \simeq 10^{-11}(m^\nu/1\,\text{eV})$—which can be explained in a more natural way by extended dynamics [56–58]—or via the small VEV of a second Higgs doublet $y_\nu \simeq \mathcal{O}(1)(1\,\text{eV}/\langle H_2 \rangle)$ [59–61]. The latter will be discussed in Sec. 2.3.4, we will stick to small Yukawas in this section, their origin being irrelevant for the most part. Neutrinoless double beta decays are, of course, absent in this framework, because neutrinos are Dirac and $B-L$ is conserved (see Sec. 1.1).

2.1.1 $B - L$ Gauge Boson

Dirac neutrinos aside, an unbroken $U(1)_{B-L}$ brings with it only one more particle, the gauge boson Z', coupled to the $B - L$ current j^μ_{B-L} via

$$\begin{aligned}\mathcal{L} \supset\ & g' Z'_\mu j^\mu_{B-L} \\ =\ & g' Z'_\mu \sum_{\text{families}} \left[\frac{1}{3}\left(\overline{Q}_L \gamma^\mu Q_L + \overline{u}_R \gamma^\mu u_R + \overline{d}_R \gamma^\mu d_R\right) - \overline{L}\gamma^\mu L - \overline{e}_R \gamma^\mu e_R - \overline{\nu}_R \gamma^\mu \nu_R\right], \end{aligned} \tag{2.3}$$

with suppressed color, isospin, and family indices. All fermions—including neutrinos—are described by Dirac fermions after EWSB, leading to *vector-like* Z' couplings to these mass eigenstates

$$g' Z'_\mu j^\mu_{B-L} \to g' Z'_\mu \sum_{\text{families}} \left[\frac{1}{3}\left(\overline{u}\gamma^\mu u + \overline{d}\gamma^\mu d\right) - \overline{e}\gamma^\mu e - \overline{\nu}\gamma^\mu \nu\right]. \tag{2.4}$$

Most importantly, the rotation to the fermion mass basis (see Ch. 1) does not lead to any flavor-changing neutral currents mediated by the Z'. The above interactions—in particular the coupling to electrons, and the quark-induced coupling to baryons—can now be used to search for this new $U(1)_{B-L}$ force, i.e. the Z'. If massless, this photon-like gauge boson would couple to the huge number of *neutrons* in astrophysical objects, such as stars and planets, because the contributions of protons and electrons would exactly cancel in electrically neutral bodies. Tests of the weak equivalence principle then put strong bounds on the fine-structure constant of this new force [62]:

$$\alpha_{B-L} \equiv g'^2/4\pi < 10^{-49} \text{ at } 95\% \text{ C.L.}, \tag{2.5}$$

as already recognized in early papers concerned with long-range forces acting on baryons [63] and leptons [64]. A tiny gauge coupling is, of course, no argument *against* an unbroken $B - L$ symmetry, unnatural as it might seem. Furthermore, we can actually evade the above constraint by using the Stückelberg mechanism to generate a mass for Z' without breaking $B - L$. We postpone a detailed discussion of this mechanism to App. A and merely summarize the result: Gauge bosons of abelian symmetries are permitted a mass by means of the Stückelberg mechanism—retaining gauge invariance, unitarity, and renormalizability. With this in mind, one can start to probe the two-dimensional parameter space $(\alpha_{B-L}, M_{Z'})$ in a general way.[1] The above limit (2.5) holds for long-range forces, i.e. for gauge boson masses $M_{Z'} \ll 10^{-13}\,\text{eV} \simeq 1/10^7\,\text{m}$, while a short-range limit

$$M_{Z'}/g' > 6\,\text{TeV} \text{ at } 95\% \text{ C.L.} \tag{2.6}$$

is valid for $M_{Z'} \gg \sqrt{s}_{\text{LEP}} \simeq 200\,\text{GeV}$ [66,67], obtained from a study of effective four-fermion operators at LEP. An even more stringent limit can be obtained from global fits to electroweak precision data [68]:

$$M_{Z'}/g' > 7\,\text{TeV} \text{ at } 99\% \text{ C.L.}, \tag{2.7}$$

[1] Let us note that small values for both g' and $M_{Z'}$ are technically natural in the sense of 't Hooft [65], in that all radiative corrections are again proportional to g' and $M_{Z'}$, respectively.

which can be translated into a 95% C.L. bound of about 9 TeV. Limits for the vast mass region in between ($10^{-13}\,\mathrm{eV} < M_{Z'} < 200\,\mathrm{GeV}$) arise from various data sources such as neutrino–nucleon scattering, beam-dump experiments, and successful BBN, but cannot be cast in such simple forms as the above limiting cases (2.5) and (2.7), and have to our knowledge not been completely explored. At least for $M_{Z'} \lesssim 10^{-5}\,\mathrm{eV} \simeq 1/0.1\,\mathrm{m}$ and $M_{Z'} \gtrsim 1\,\mathrm{keV}$ limits can be found in Refs. [62] and [69], respectively. The remaining region $10^{-5}\,\mathrm{eV} < M_{Z'} < 1\,\mathrm{keV}$ can be constrained, for example, with tests of Coulomb's law and stellar evolution, similar to hidden photons (cf. Ref. [70]).

The LHC phenomenology of a Z' with $M_{Z'} \sim$ TeV is well covered in the literature, e.g. Ref. [71], and is not the focus of this thesis. Let us make but a couple of remarks: The decay width into fermions is given by

$$\Gamma(Z' \to \overline{f} f) = \tfrac{1}{3}\alpha_{B-L} M_{Z'} \left(1 + 2\frac{m_f^2}{M_{Z'}^2}\right) \sqrt{1 - 4\frac{m_f^2}{M_{Z'}^2}} \times \begin{cases} 1, & f = \text{lepton}, \\ 1/3, & f = \text{quark}. \end{cases} \tag{2.8}$$

The branching ratios into leptons and quarks are then fixed for a specified mass $M_{Z'}$, and can be used to distinguish this Z' from other vector bosons (see for example Ref. [72]). Most importantly, the rates are *flavor-universal*, at least for large $M_{Z'}$, so one expects the same decay rates into e.g. electron and muon. This will no longer be the case for the flavored $U(1)'$ symmetries employed in Ch. 3, and serve as an important discrimination tool. Let us further note that the invisible width of Z' is governed by the decay into the light Dirac neutrinos $\nu = \nu_L + \nu_R$:

$$\Gamma_{\text{inv}}(Z') = 3 \times \Gamma(Z' \to \overline{\nu}\nu) = \alpha_{B-L} M_{Z'}\,, \tag{2.9}$$

which effectively counts the number of light neutrinos, in complete analogy to the invisible width of the Z, which however only counts the number of light *left-handed* neutrinos.

Even though an unbroken $U(1)_{B-L}$ symmetry has naively only one parameter, the coupling strength g', we have remarked above (and shown in App. A) that a mass term $M_{Z'}$ for the gauge boson is also allowed. This mass term does *not* introduce yet more parameters or particles—as a Higgs mechanism unavoidably would—so unbroken $U(1)_{B-L}$ seems to introduce only two parameters (plus neutrino masses and mixing). There is however a third parameter associated with the Z' boson of any abelian gauge group extension of the SM: *kinetic mixing* [73]. This type of mixing arises in any gauge theory with two abelian factors $U(1)_1 \times U(1)_2$, because the associated field-strength tensors $F_{1,2}^{\mu\nu}$ are gauge invariant objects by themselves—compared to non-abelian ones, which transform covariantly but non-trivial—allowing us to write down the kinetic terms

$$\mathcal{L} \supset -\frac{1}{4} F_1^{\mu\nu} F_{1,\mu\nu} - \frac{1}{4} F_2^{\mu\nu} F_{2,\mu\nu} - \frac{\sin\chi}{2} F_1^{\mu\nu} F_{2,\mu\nu}\,, \tag{2.10}$$

where we introduced the kinetic-mixing angle χ. The vector fields need to be re-defined using non-unitary transformations in order to arrive at conventionally-normalized physical mass eigenstates—which then couple to *both* currents j_1^μ and j_2^μ. Effectively, kinetic mixing introduces a coupling of j_1^μ to A_μ^2. In the case of interest, this means that the Z' boson of our new $U(1)_{B-L}$ will also couple to the hypercharge current j_Y^μ, with strength $\frac{e}{\cos\theta_W}\sin\chi$.

Note that a small but nonzero χ will typically be generated radiatively even if $\chi = 0$ at some scale. Unbroken $B-L$ is hence a three-parameter—plus neutrino masses and mixing—extension of the SM. For a Z' above MeV, constraints on g', $M_{Z'}$ and χ have been derived in Ref. [69]. In this chapter and the next, we will ignore the effects of kinetic mixing for simplicity, but come back to it briefly in Ch. 4. Instead, App. B is devoted to a proper study of kinetic mixing, also extending the framework to gauge groups with three abelian factors $U(1)_a \times U(1)_b \times U(1)_c$ (following the paper "Kinetic and mass mixing with three abelian groups" [10] (in collaboration with W. Rodejohann)). This is of obvious interest following our motivation for the gauge group $U(1)_{B-L} \times U(1)_{L_e-L_\mu} \times U(1)_{L_\mu-L_\tau}$ in Sec. 1.5.

It should be mentioned that unbroken $B-L$ is not compatible with GUT scenarios where $G_{\rm SM} \times U(1)_{B-L}$ is embedded into a simple non-abelian group such as $SO(10)$. While the fermion content of SM+ν_R nicely fits into an irreducible representation $\mathbf{16}_{SO(10)}$ per family—strongly motivating RHNs and $U(1)_{B-L}$ extensions—the overlying non-abelian structure does not allow for any Stückelberg mass terms. Additionally, all four gauge couplings of $G_{\rm SM} \times U(1)_{B-L}$ are generated by renormalization-group running of a single $SO(10)$ gauge coupling from the breaking scale $\Lambda \sim 10^{16}$ GeV to electroweak energies, making it impossible to end up with a $B-L$ coupling small enough to satisfy Eq. (2.5). So, while $U(1)_{B-L}$ can be easily considered part of a GUT, it has to be *broken*. The Majorana $B-L$ case of Sec. 2.2 can for example be envisioned as part of a larger GUT framework, in which the high $SO(10)$ breaking scale naturally suppresses neutrino masses via the seesaw mechanism. Since GUTs require increasingly complex scalar sectors to evade constraints, we will not discuss them any further and continue on with our much simpler *abelian* gauge symmetries.

2.1.2 Dirac Leptogenesis

We will now turn our attention to the biggest challenge of our unbroken $B-L$ scenario: the dynamical generation of the matter–antimatter asymmetry of our Universe (see Sec. 1.2). It is well known that the $(B+L)$-violating sphalerons in the SM (introduced in Sec. 1.4) would wash out any baryon asymmetry in the early Universe if we start with $B-L=0$. Since fine-tuned initial conditions are not compatible with inflationary cosmology and we *never break* $B-L$, it seems impossible to explain or even accommodate the BAU in our unbroken $B-L$ framework. However, the minor addition of RHNs to the SM makes possible baryogenesis even for initial values $B=L=0$ and without breaking $B-L$. This mechanism is called Dirac leptogenesis or *neutrinogenesis* [74], and we will give a brief qualitative overview in this section.

Processes and particles are in equilibrium in the early Universe at temperature T if the equilibrating rates Γ are fast compared to the Hubble expansion rate $H(T)$

$$\Gamma \gg H(T) \simeq 1.66\sqrt{g_*}\,T^2/M_{\rm Pl}\,, \tag{2.11}$$

with the Planck mass $M_{\rm Pl} \simeq 10^{19}$ GeV and the effective number of degrees of freedom g_*. In our case the SM degrees of freedom give $g_* = \mathcal{O}(100)$ above $T \gtrsim 1$ TeV. All SM particles are in equilibrium above the EWPT, due to the rather strong gauge couplings. Also in equilibrium at these temperatures are the aforementioned sphalerons, which violate $B+L$ by six units but conserve $B-L$ [46,75]. These sphalerons will (partially) transfer any lepton asymmetry to the baryon sector, which makes possible *baryo*genesis via *lepto*genesis. The question remains how

we can generate any asymmetry if $B-L$ is unbroken, and here the tiny Yukawa couplings of our Dirac neutrinos turn out to be crucial. Ignoring the $B-L$ gauge interactions for a moment, our RHNs only couple to the SM via the Yukawa couplings $\overline{\nu}_R y_\nu H^\dagger L$. Typical rates to produce ν_R above the EWPT will then take the form $\Gamma \sim y_\nu^2 g^2 T$, g being a gauge coupling or the Yukawa coupling of the top quark [74]. With Eq. (2.11) we see that the ν_R are *not* in thermal equilibrium above the EWPT, because the Yukawas $y_\nu \sim m_\nu/100\,\text{GeV}$ are simply too small. Only at much lower temperatures will the ν_R be connected to the SM again, but by that time the sphalerons will have gone out of equilibrium and the BAU has been fixed.

On to the actual neutrinogenesis mechanism: The key idea is to generate an asymmetry Δ_L in the left-handed neutrinos that is exactly canceled by an asymmetry $\Delta_R = -\Delta_L$ in the RHNs, so neither lepton number L nor $B-L$ are violated. According to the above discussion, Δ_R will be hidden from the rest of the plasma, so the sphalerons will effectively only see a nonzero Δ_L and transfer that to a baryon asymmetry. A simple way to generate the needed $\Delta_L = -\Delta_R \neq 0$ structure is to introduce two new heavy Higgs doublets $\Psi_{1,2} \sim (\mathbf{1}, \mathbf{2}, -1/2)$, which do not acquire VEVs:

$$\mathcal{L} \supset \sum_{j=1,2} F_j^{\alpha\beta} \overline{L}_\alpha \Psi_j \nu_{R,\beta} + G_j^{\alpha\beta} \overline{L}_\alpha \tilde{\Psi}_j e_{R,\beta} + \text{h.c.} \tag{2.12}$$

The out-of-equilibrium decay of the lightest Ψ_j into $\overline{L}\,\nu_R$ and $L\,\overline{\nu}_R$ will in general violate CP at one-loop level, due to the complex nature of the Yukawa matrices F_j and G_j. Consequently, the asymmetry $\Delta_L = -\Delta_R \neq 0$ can indeed be generated, and it has been shown in Refs. [56, 74] that the BAU (1.24) can be quantitatively explained in this way. We stress once again that $B-L$ is exactly conserved during this entire process; we ignored the effect of the Z' boson in the above discussion by assuming a tiny gauge coupling (2.5) or a very large Stückelberg mass $M_{Z'}$. Choosing parameters $(g', M_{Z'})$ that make the Z' relevant for neutrinogenesis goes unfortunately beyond the scope of this thesis.

A word about relativistic degrees of freedom: Light Dirac neutrinos would effectively double the number of neutrino species in cosmological considerations compared to the SM; in turn, more relativistic particles would increase the expansion rate of the Universe, seeing as the Hubble rate $H(T)$ is proportional to $\sqrt{g_*}$. BBN is a crucial testing ground here, because a change of $H(T_\text{BBN} \sim 1\,\text{MeV})$ directly affects the proton-to-neutron ratio, and hence the helium abundance of the Universe. Resulting limits on g_* at T_BBN are usually given in terms of the effective number of neutrino species N_eff—with $g_* = 5.5 + \frac{7}{4} N_\text{eff}$—but can, of course, stem from various sources other than neutrinos. Neutrino heating increases the naive SM estimate from 3 to $N_\text{eff}^\text{SM} \simeq 3.046$ [16], and recent Planck data constrains $N_\text{eff} = 3.30 \pm 0.27$ at 68% C.L. [23] (strongly dependent on the combination of data sets). While past results hinted at far larger values for N_eff, it now seems that additional light states are disfavored by Planck. In particular, three RHN partners for our SM neutrinos seem to be vastly excluded, as they would yield $N_\text{eff} \simeq 6$. However, in the neutrinogenesis mechanism discussed above, the RHNs are necessarily *not* thermalized in order to be hidden from the sphalerons at temperatures above EWSB. For the small neutrino masses allowed by experiments (Sec. 1.1.2), the RHNs remain out of equilibrium during BBN, and subsequently *do not* contribute to N_eff. In Sec. 2.3.4 we will present a different Dirac leptogenesis mechanism that works the other way around: It requires *thermalized* RHNs and yields $N_\text{eff} > 3$, so future data might distinguish these two scenarios.

The neutrinogenesis mechanism presented here is interesting not only for the usage of *Dirac* neutrinos, but that it takes crucial advantage of their small masses—heavier neutrinos simply would make neutrinogenesis impossible! While this connection between small neutrino masses and leptogenesis is not as direct as in the Majorana $B-L$ scenario of the next section, it does hint at a link between these two subjects.

This already concludes our brief overview of the unbroken realization of a local $U(1)_{B-L}$. In absence of any observed B or L violating interactions, unbroken $B-L$ remains an interesting and simple possibility. It automatically gives rise to neutrino masses—solving the biggest shortcoming of the SM—and can, with some additional scalars, give rise to a leptogenesis mechanism. The main prediction is, of course, the Dirac nature of neutrinos and consequent absence of neutrinoless double beta decay. The gauge boson Z' properties g', $M_{Z'}$, and χ can in principle take on any value, so further searches for it can only be encouraged; we stress in particular that $M_{Z'}$ is not in any way connected to other scales—unlike the Z' of the next section—so it can be searched for in various experiments, not only at the energy frontier. That being said, it remains a lamppost search, as there is also no reason why g', $M_{Z'}$, and χ should take on values detectable by us.

2.2 Majorana $B - L$

We will now move on to the more popular scenario of spontaneously broken $B - L$ [76, 77], starting with the part of parameter space that gives rise to Majorana neutrinos, the seesaw mechanism, and standard thermal leptogenesis. In Sec. 2.2.3 we will discuss the simple scalar potential of our model—Higgs doublet H plus SM-singlet scalar S—that is used many times throughout this thesis.

2.2.1 Seesaw Mechanism

In this section we will discuss the framework of Majorana $B - L$, i.e. a local $U(1)_{B-L}$ spontaneously broken by the VEV of an SM-singlet scalar S with $B - L$ charge 2. The relevant part of the Lagrangian takes the form

$$-\mathcal{L} \supset V(H,S) + \overline{\nu}_{R,j}\,(y_\nu)_{j\,\alpha}\,H^\dagger L_\alpha + \frac{1}{2}\overline{\nu}_{R,j}K_{jk}\nu^c_{R,k}\,S^* + \text{h.c.}, \tag{2.13}$$

$K_{jk} = K_{kj}$ being a complex symmetric Yukawa-coupling matrix. Assuming the scalar potential $V(H,S)$ to have a minimum at $\langle H\rangle| \equiv v/\sqrt{2} \neq 0$ and $|\langle S\rangle| \equiv v_S/\sqrt{2} \neq 0$—to be discussed in Sec. 2.2.3—the following mass terms for the neutral fermions are generated:

$$\begin{aligned} -\mathcal{L} &\supset (m_D)_{j\alpha}\,\overline{\nu}_{R,j}\nu_{L,\alpha} + \frac{1}{2}(\mathcal{M}_R)_{jk}\,\overline{\nu}_{R,j}\nu^c_{R,k} + \text{h.c.} \\ &= \frac{1}{2}\begin{pmatrix}\overline{\nu}^c_L & \overline{\nu}_R\end{pmatrix}\begin{pmatrix}0 & m_D^T \\ m_D & \mathcal{M}_R\end{pmatrix}\begin{pmatrix}\nu_L \\ \nu^c_R\end{pmatrix} + \text{h.c.}, \end{aligned} \tag{2.14}$$

with the Dirac mass matrix $m_D \equiv vy_\nu/\sqrt{2}$, the right-handed Majorana mass matrix $\mathcal{M}_R \equiv v_S K/\sqrt{2}$, and an implicit matrix/vector notation in the last line. Without loss of generality we can work in a basis where $\mathcal{M}_R$ is diagonal, $\mathcal{M}_R = \text{diag}(M_1, M_2, M_3)$, because the diagonalization merely redefines m_D.

The mass matrix in Eq. (2.14) gives rise to six massive Majorana fermions when diagonalized by a unitary 6×6 matrix W:

$$\begin{pmatrix} 0 & m_D^T \\ m_D & \mathcal{M}_R \end{pmatrix} = W^* \,\mathrm{diag}(m_1,\ldots,m_6)\, W^\dagger\,, \tag{2.15}$$

the mass eigenstates being admixtures of ν_L and ν_R. However, the successful three-neutrino oscillation picture presented in Sec. 1.1 strongly hints at a separation of scales, with three light and three unobserved heavy (mostly sterile) neutrinos. This limiting case occurs naturally for $\mathcal{M}_R \gg m_D$, the famous seesaw limit [78–81]. The three heavy mass eigenstates (with masses $\simeq M_j$) then consist mostly of ν_R and can be effectively integrated out of the Lagrangian, generating the low-energy Majorana neutrino mass

$$\mathcal{M}_\nu \simeq -m_D^T \mathcal{M}_R^{-1} m_D = -\frac{1}{\sqrt{2}}\frac{v^2}{v_S}\, y_\nu^T K^{-1} y_\nu\,. \tag{2.16}$$

The three light neutrino masses are naturally suppressed by the ratio $m_D/\mathcal{M}_R \ll 1$, or $v/v_S \ll 1$ in our $U(1)_{B-L}$ framework, without the need of choosing tiny Yukawa couplings. Indeed, with Yukawa couplings of order one, the $B-L$ breaking scale suggested by the seesaw mechanism would be $\mathcal{M}_R \sim v_S \sim 10^{15}\,\mathrm{GeV}$. The heavy RHNs with mass matrix $\mathcal{M}_R$ can furthermore naturally lead to leptogenesis, as we will see in Sec. 2.2.2. Diagonalization of $\mathcal{M}_\nu$ can be performed in the following way

$$\mathcal{M}_\nu = U_{\mathrm{PMNS}}^* \,\mathrm{diag}(m_1,m_2,m_3)\, U_{\mathrm{PMNS}}^\dagger\,, \tag{2.17}$$

with the PMNS matrix from Eq. (1.12). The neutrino mass eigenstates $\nu_j = (U_{\mathrm{PMNS}}^\dagger)_{j\alpha}\nu_\alpha$ consist mostly of the active left-handed neutrinos ν_L, but have a small admixture of the sterile ν_R, suppressed by $m_D/\mathcal{M}_R$. Furthermore, U_{PMNS} is actually *not unitary*, as it is just the upper-left 3×3 submatrix of the proper diagonalization matrix W from Eq. (2.15). This can be ignored in the strong seesaw limit, as the non-unitary corrections to U_{PMNS} are suppressed by $m_D/\mathcal{M}_R$, but can lead to observable effects in low-scale seesaw scenarios, strongly constrained by data [82]. With natural seesaw scales $\mathcal{M}_R \sim 10^{15}\,\mathrm{GeV}$ far beyond experimental reach, considerable effort has been put into the construction and discussion of such low-scale seesaws, with detection possibilities at colliders or via induced lepton flavor violation. Being sterile and typically heavy, the search for the seesaw partners is certainly not easy [83]. In our gauged $B-L$ context however, all neutrinos are coupled to the Z', which leads to new signatures and could simplify the search, as discussed e.g. in Ref. [71].

In the limit $\mathcal{M}_R \sim v_S \gg 100\,\mathrm{GeV}$, the only testable prediction of the seesaw mechanism—and more or less of Majorana $B-L$—is the Majorana nature of neutrinos. As already discussed in Sec. 1.1.3, this can facilitate neutrinoless double beta decay, i.e. the $\Delta(B-L)=2$ process $2\,n \to 2\,p + 2\,e^-$. Unobserved as of yet, the detection depends only on the entry $(\mathcal{M}_\nu)_{ee}$ of the neutrino mass matrix; using the decomposition $\mathcal{M}_\nu = U^*\mathrm{diag}(m_1,m_2,m_3)U^\dagger$ with the values from Tab. 1.2 shows that $(\mathcal{M}_\nu)_{ee}$ *could* vanish (or be unobservably small), even though neutrinos *are* Majorana particles. Neutrinoless double beta decay is therefore not a hard prediction of Majorana $B-L$—reasonable as it might be—and care has to be taken in the interpretation of continuing non-observation. The combination of $0\nu2\beta$ with

other neutrino-mass experiments (see Sec. 1.1.2) can in principle lay the question to rest, but only under the assumption that no *additional* new physics interferes with the results. At least the vanilla Majorana $B-L$ model presented here, i.e. just three light Majorana neutrinos, is falsifiable.

We note that the seesaw mechanism (Eqs. (2.14) and (2.16)) is obviously of interest far beyond our local $B-L$ model, and usually discussed independently. Simply introducing n RHNs to the SM leads to the same mass terms—$\mathcal{M}_R$ (m_D) now being an $n \times n$ ($n \times 3$) matrix—because $\overline{\nu}_{R,j}\nu^c_{R,k}$ is then automatically gauge invariant. Without a gauged $U(1)_{B-L}$, the number n of RHNs is not restricted to $n = 3$ on theoretical grounds; to account for the two measured $\Delta m^2_{31,21}$, at least *two* ν_R are required in absence of other physics beyond the SM, and the same holds for successful leptogenesis [84]. Models with $n \gg 2$ can give rise to interesting effects—see our paper [12]—but typically $n = 3$ is chosen for aesthetic reasons.

More could be said about the seesaw mechanism, but the above suffices for the purposes of the later chapters. Let us rather turn to the leptogenesis mechanism accompanying seesaw, before we discuss the scalar potential of our $U(1)_{B-L}$ model in Sec. 2.2.3.

2.2.2 Thermal Leptogenesis

Having discussed the famous seesaw mechanism as an explanation for the lightness of neutrinos, we turn to the equally famous accompanying leptogenesis mechanism [85]. We assume a very high $B-L$ breaking scale $v_S \gg 10^9\,\text{GeV}$ in the following, and also assume the Z' and s bosons to be sufficiently heavy or weakly coupled to be irrelevant at temperatures below the mass of the lightest RHN ($\nu_{R,1}$) at $T \sim M_1 > 10^9\,\text{GeV}$. This simply ensures that we can work within the standard thermal leptogenesis scenario, without the additional bothersome interactions mediated by Z' and s. A discussion of the parameter space where the new bosons are important goes unfortunately beyond the scope of this thesis. Our discussion of this leptogenesis mechanism will once again be more qualitative, details can be found, for example, in Ref. [84].

Below the $B-L$ breaking scale, but above the EWPT, the right-handed neutrinos ν_R interact only via their Yukawa couplings

$$-\mathcal{L} \supset \overline{\nu}_{R,j}\,(y_\nu)_{j\,\alpha}\,H^\dagger L_\alpha + \frac{1}{2}(\mathcal{M}_R)_{jk}\,\overline{\nu}_{R,j}\nu^c_{R,k} + \text{h.c.} \tag{2.18}$$

We can again choose $\mathcal{M}_R$ to be diagonal, with entries M_i; the chiral right-handed fermions $\nu_{R,i}$ can then be written in terms of Majorana fermions $N_i = \nu_{R,i} + \nu^c_{R,i} = N^c_i$. Due to their self-conjugate nature, these heavy neutrinos can decay either into LH^* or L^cH via the Yukawa couplings in Eq. (2.18), providing the necessary lepton number violation (LNV) for a lepton asymmetry. Since the Yukawas are complex in general, CP-violating loop corrections to these decays (depicted in Fig. 2.1) can yield different rates for $\Gamma(N \to LH^*)$ and $\Gamma(N \to L^cH)$. The decay of these heavy N in the early Universe would then result in a lepton asymmetry, provided the decay takes place out of equilibrium. This lepton asymmetry will then be converted to a baryon asymmetry by the sphalerons, as discussed already in Sec. 1.4 and Sec. 2.1.

Let us make the above discussion more quantitative: At tree level, the total decay rate of

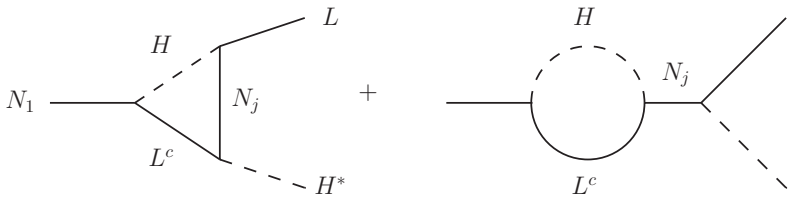

Figure 2.1: CP-violating vertex and self-energy loop corrections to the LNV decay of the lightest Majorana neutrino $N_1 \to LH^*$ relevant for leptogenesis.

N_i is given by

$$\Gamma_{N_i} \equiv \Gamma(N_i \to LH^*) + \Gamma(N_i \to L^c H) = (y_\nu^\dagger y_\nu)_{ii} M_i / 8\pi \,, \tag{2.19}$$

where no summation over the indices is assumed, but implicit matrix multiplication of $y_\nu^\dagger y_\nu$. We will assume a hierarchy $M_1 \ll M_{2,3}$ for simplicity, so we are only concerned with the decay of the lightest RHN N_1. According to the famous Sakharov conditions [40], a dynamical asymmetry generation requires departure from thermal equilibrium. Since the Universe expands with a Hubble rate $H(T) \simeq 1.66\sqrt{g_*}T^2/M_{\rm Pl}$ (2.11), departure from equilibrium can be achieved if the interaction rate Γ_{N_1} is much smaller than $H(T)$ when the temperature drops below M_1:[2]

$$\Gamma_{N_1} \ll H(M_1) \simeq 1.66\sqrt{g_*} M_1^2 / M_{\rm Pl} \,. \tag{2.20}$$

We define the CP asymmetry of the decay as

$$\varepsilon \equiv \frac{\Gamma(N_1 \to LH^*) - \Gamma(N_1 \to L^c H)}{\Gamma(N_1 \to LH^*) + \Gamma(N_1 \to L^c H)} \simeq -\frac{3}{16\pi} \sum_{j=2,3} \frac{\mathrm{Im}[(y_\nu^\dagger y_\nu)_{1j}^2]}{(y_\nu^\dagger y_\nu)_{11}} \frac{M_1}{M_j} g\left(\frac{M_1^2}{M_j^2}\right), \tag{2.21}$$

where we already evaluated the one-loop contributions from Fig. 2.1, introducing the loop function

$$g(x) = \left(-\frac{2}{3}\right) \frac{x - 2x^2 + (x^2-1)\log(1+x)}{(1-x)x^2} = 1 + \frac{5}{9}x + \mathcal{O}(x^2) \,. \tag{2.22}$$

The asymmetry ε obviously vanishes in case of real Yukawas, but also in the absence of $N_{2,3}$—or, equivalently, in the limit $M_{2,3} \to \infty$. This can be understood by noticing that a generic 1×3 matrix y_ν in Eq. (2.18) can be transformed into $(z, 0, 0)$ with real z simply by means of a flavor rotation in L_α, rendering the Yukawas real again. Effectively we move the CP violation to a sector of the Lagrangian irrelevant to the N_1 decay, a feat that proves impossible in the presence of more than one RHN.

To calculate the final $B - L$ asymmetry, one needs to solve the Boltzmann equations that describe the decay and inverse decay of N_1, leading to $Y_{\Delta(B-L)} \simeq 10^{-3}\eta\varepsilon$ [47]. The efficiency factor $\eta \leq 1$ depends on the validity of Eq. (2.20) and the initial abundance of N_1. With

[2] We assume a sufficiently high reheating temperature after inflation so that the RHNs have been in thermal equilibrium with the SM, be it via Yukawa couplings or $B - L$ gauge interactions.

this $B-L$ asymmetry, one can then calculate the final baryon asymmetry by considering the chemical potentials of the SM at temperatures far below M_1; it turns out that the sphaleron conversion rate leads to $Y_{\Delta B} = \frac{28}{79} Y_{\Delta(B-L)}$ [86], which can then be matched to the observed value from Eq. (1.25). A typical value for the CP asymmetry would be $\varepsilon \sim 10^{-6}$, but it depends on the details of production and washout processes [84]. Let this suffice as an introduction to thermal leptogenesis, as we have introduced all that we need later on.

2.2.3 Scalar Sector

After seesaw and leptogenesis, we turn to the other implications of this "Majorana $B-L$" scenario, namely the scalar sector and differences in the Z' phenomenology compared to the discussion in Sec. 2.1. The following discussion will prove useful throughout the different chapters of this thesis, as it can be readily adapted to the different models. Let us first discuss the scalar potential $V(H,S)$, following our paper [3]. Since this is arguably the simplest scalar-potential extension of the SM, it is well covered in the literature; let us single out Ref. [87] specifically, as it pertains our $U(1)_{B-L}$ scenario. With just the usual Higgs doublet H and one additional SM-singlet scalar S, the potential has the simple form

$$V(H,S) = -\mu_1^2|H|^2 + \lambda_1|H|^4 - \mu_2^2|S|^2 + \lambda_2|S|^4 + \delta|S|^2|H|^2\,, \tag{2.23}$$

where we assume $\mu_i^2 > 0$ to generate nonzero VEVs $v \equiv \sqrt{2}|\langle H\rangle| \simeq 246\,\text{GeV}$ and $v_S \equiv \sqrt{2}|\langle S\rangle|$. The positivity of the potential gives the constraints $\lambda_i > 0$ and $\lambda_1\lambda_2 > \delta^2/4$. In unitary gauge the charged component G^- of $H = (G^0, G^-)^T$ is absorbed by W^-, the pseudoscalar neutral component $\text{Im}\,G^0$ by Z, and the pseudoscalar component $\text{Im}\,S$ of S by the $B-L$ vector boson Z', hence we may go to the physical basis $H \to ((h+v)/\sqrt{2}, 0)^T$, $S \to (s+v_S)/\sqrt{2}$, which after the replacement of μ_i^2 by the VEVs gives the potential:

$$\begin{aligned} V(h,s) = {} & \lambda_1 v^2 h^2 + \lambda_2 v_S^2 s^2 + \delta v v_S hs \\ & + \lambda_1 v h^3 + \frac{\lambda_1}{4}h^4 + \lambda_2 v_S s^3 + \frac{\lambda_2}{4}s^4 + \frac{\delta}{4}h^2 s^2 + \frac{\delta}{2}vhs^2 + \frac{\delta}{2}v_S h^2 s\,. \end{aligned} \tag{2.24}$$

The resulting mass matrix for the physical neutral scalars h and s can be read off the first line to be

$$\mathcal{M}^2_{\text{scalar}} = \begin{pmatrix} 2\lambda_1 v^2 & \delta v v_S \\ \delta v v_S & 2\lambda_2 v_S^2 \end{pmatrix}, \tag{2.25}$$

leading to the mass eigenstates ϕ_1 and ϕ_2

$$\begin{pmatrix}\phi_1\\ \phi_2\end{pmatrix} = \begin{pmatrix}\cos\alpha & -\sin\alpha\\ \sin\alpha & \cos\alpha\end{pmatrix}\begin{pmatrix}h\\ s\end{pmatrix}, \quad \text{with} \quad \tan 2\alpha = \frac{\delta v v_S}{\lambda_2 v_S^2 - \lambda_1 v^2}\,, \tag{2.26}$$

and masses $m^2_{1,2} = \lambda_1 v^2 + \lambda_2 v_S^2 \mp \sqrt{(\lambda_2 v_S^2 - \lambda_1 v^2)^2 + \delta^2 v_S^2 v^2}$. In the seesaw limit $v_S \gg v$ we are mostly concerned with, the mixing angle is naturally suppressed, $\alpha \simeq \delta v / 2\lambda_2 v_S$, and the lighter mass eigenstate ϕ_1 corresponds to the Higgs-like particle recently found at the LHC [14, 15], with $m_1^2 \simeq 2(\lambda_1 - \delta^2/4\lambda_2)v^2 \simeq (125\,\text{GeV})^2$.

The mass for our new vector boson Z' generated after spontaneous symmetry breaking by the VEV $\langle S\rangle = v_S/\sqrt{2}$ takes the form

$$M_{Z'} = |(B-L)(S)g'v_S| = 2|g'v_S|\,, \tag{2.27}$$

so we can translate the LEP bound on $M_{Z'}/g'$ from Eq. (2.7) into the constraint $v_S > 3.5\,\text{TeV}$. The couplings of the Higgs ϕ_1 to fermions and gauge bosons are then modified by $\cos\alpha$ with respect to the SM, while the new scalar boson inherits all SM-Higgs couplings, multiplied by $\sin\alpha$. This, of course, also works the other way around, generating a coupling of the 125 GeV Higgs particle ϕ_1 to the right-handed neutrinos proportional to $\sin\alpha$. Assuming all RHNs and also ϕ_2 to be heavier than $m_1/2 \simeq 62\,\text{GeV}$, the branching ratios of ϕ_1 are SM-like, and only the production cross sections are suppressed, yielding the bound $\cos^2\alpha > 0.66$ at 95% C.L. [88]. There are, of course, also bounds on ϕ_2 from direct searches, but we will skip a discussion and simply work in the limits $\alpha \ll 1$ and $m_2 \simeq m_s \simeq \sqrt{2\lambda_2}v_S \gg m_1$ implied by seesaw.

Other than the new scalar $\phi_2 \simeq s$, the collider phenomenology of the gauge boson Z' is similar to the unbroken $B-L$ case of Sec. 2.1.1. An interesting difference arises however in the invisible Z' width, still dominated by $Z' \to \nu\nu$. If all Majorana neutrinos, including the "heavy" ν_R, are much lighter than the Z', the width coincides with the Dirac case (Eq. (2.9)), because all six neutrinos are kinematically accessible. In Majorana $B-L$, there is however no reason why $\mathcal{M}_R \ll M_{Z'}$ should hold, seeing as both are generated by the VEV v_S. Some of the RHNs might hence be heavier than $M_{Z'}/2$ and not contribute to $\Gamma_{\text{inv}}(Z')$. The invisible Z' width can therefore tell us something about the neutrino nature: Dirac neutrinos give $\Gamma_{\text{inv}}(Z') = \alpha_{B-L}M_{Z'}$, while Majorana neutrinos lead to $y\,\alpha_{B-L}M_{Z'}$, with $\frac{1}{2} \le y \le 1$ depending on the actual mass spectrum.

This ends our section on Majorana $B-L$. A large VEV $\langle S\rangle \sim 10^{15}\,\text{GeV}$ generates large masses for the right-handed neutrinos, making possible thermal leptogenesis to explain the BAU and naturally small Majorana masses for the active neutrinos via seesaw; the new bosons Z' and s are also naturally heavy. In this high-scale limit, we only expect neutrinoless double beta decay as a signature of $B-L$ breaking and the Majorana nature of the neutrinos (see Sec. 1.1.3). Lowering the $(B-L)$-breaking VEV to TeV values makes the model testable at colliders, and the seesaw mechanism is still effective. However, leptogenesis is harder to achieve in this case and requires modifications to the mechanism presented above; specifically, a *resonant* leptogenesis is necessary, which has been discussed for the Majorana $B-L$ case in Ref. [89].

2.3 Dirac $B-L$

In the previous sections of this chapter we have given an overview over the two cases of unbroken $B-L$ (Sec. 2.1), and $B-L$ spontaneously broken by two units—Majorana $B-L$—leading to the seesaw mechanism (Sec. 2.2.1) and thermal leptogenesis (Sec. 2.2.2). The next two sections are motivated by the following observation: Other than interesting phenomenology, there is no compelling reason why $B-L$ has to be broken by *two* units. We will show that a spontaneous breaking by *four* units can lead to the interesting framework of lepton-number-violating Dirac neutrinos, with previously undiscussed experimental signatures. We

present effective $\Delta(B-L)=4$ operators in Sec. 2.3.1 that aid us in the search for worthwhile processes to study in detail; an economic renormalizable model to generate these operators is then introduced in Sec. 2.3.2. Having laid the groundwork for LNV Dirac neutrinos, we then identify candidates for their signature nuclear decay in Sec. 2.3.3: neutrinoless *quadruple* beta decay. Here we follow closely our paper "Neutrinoless quadruple beta decay" [1] (in collaboration with W. Rodejohann). In Sec. 2.3.4 we will finally present a leptogenesis mechanism for this framework, based on our paper "Leptogenesis with lepton-number-violating Dirac neutrinos" [2].

2.3.1 Effective $\Delta(B-L)=4$ Operators

Before delving into model-specific calculations, let us make some model-independent considerations. If $B-L$ is broken by $n\neq 2$ units, neutrinos are Dirac particles, and processes violating $B-L$ by n, $2n$, $3n$, ... units are still allowed. We are interested in possible effects of such LNV Dirac neutrinos, assuming that $B-L$ is broken by n units at a high scale Λ. This allows us to integrate out the heavy new physics, generating higher-dimensional operators of the SM fields from Tab. 1.1 plus the RHNs required for gauged $B-L$ (and, of course, to form Dirac neutrinos $\nu=\nu_L+\nu_R$). These operators can then be studied without knowing the details of the high-energy completion.[3] What value of $n=\Delta(B-L)$ should be studied in our quest for testable effects? $\Delta(B-L)=2$ operators are necessarily forbidden if neutrinos are of Dirac type; seeing as all SM+ν_R fermions carry an *odd* $B-L$ charge and we need an *even* number of fermions in order to construct Lorentz invariant operators, there will be no operators with odd $B-L$, making $n=4=\Delta(B-L)$ the dominant possible source of LNV. As such, we will focus on these operators in the following.

Using $\gamma_5\nu_R=\nu_R$ and $\overline{\nu}_R^c\gamma^\mu\nu_R=0$, we obtain the unique $\Delta(B-L)=4$ operator at mass dimension $d=6$:

$$\mathcal{O}^{d=6}=\overline{\nu}_R^c\nu_R\;\overline{\nu}_R^c\nu_R\,, \tag{2.28}$$

suppressing flavor indices. This simplest $\Delta(B-L)=4$ operator describes for example the Dirac-neutrino scattering $\nu\nu\to\overline{\nu}\overline{\nu}$, which violates lepton number by four units and lends our framework its name. The tensor $(\sigma^{\mu\nu}\equiv\frac{i}{2}[\gamma^\mu,\gamma^\nu])$ coupling $(\overline{\nu}_R^c\sigma^{\mu\nu}\nu_R)(\overline{\nu}_R^c\sigma_{\mu\nu}\nu_R)$ can be decomposed into operators of the form $\mathcal{O}^{d=6}$ using Fierz identities. Gauge invariant $d=8$ operators can be constructed with the Weinberg operator $(\overline{L}^c\tilde{H})(H^\dagger L)$ from Eq. (1.18):

$$\mathcal{O}_1^{d=8}=|H|^2\;\overline{\nu}_R^c\nu_R\;\overline{\nu}_R^c\nu_R\,, \tag{2.29}$$

$$\mathcal{O}_2^{d=8}=(\overline{L}^c\tilde{H})(H^\dagger L)\;\overline{\nu}_R^c\nu_R\,, \tag{2.30}$$

A possible vector coupling is equivalent to $\mathcal{O}_2^{d=8}$ after a Fierz transformation, while a possible tensor contraction in $\mathcal{O}_2^{d=8}$ simply vanishes. There is also a coupling to the hypercharge field strength tensor:

$$\mathcal{O}_3^{d=8}=F_Y^{\mu\nu}\overline{\nu}_R^c\sigma_{\mu\nu}\nu_R\;\overline{\nu}_R^c\nu_R\,, \tag{2.31}$$

[3] $\Delta L=2$ operators up to and including mass dimension $d=11$ have been derived and discussed in the literature [90], the motivation being contributions to $0\nu2\beta$ and Majorana neutrino masses. We refer the reader to these papers for a concise introduction to the underlying effective-field-theory framework of such higher-dimensional operators.

which is reminiscent of a magnetic-moment operator, were it not for the second fermion bilinear. We ignore operators involving derivatives, e.g. $\overline{\nu}_R^c \partial^2 \nu_R \; \overline{\nu}_R^c \nu_R$, which do not lead to qualitatively new interactions.

As for $\Delta(B-L)=4$ operators with mass dimension $d=9$, the only possibility $u_R^c d_R^c d_R^c \nu_R^3$ contains three left- and three right-handed fermions, which cannot be coupled to a Lorentz scalar. The obvious $d=10$ operators are the square of the Weinberg operator

$$\mathcal{O}_1^{d=10} = (\overline{L}^c \tilde{H})(H^\dagger L) \; (\overline{L}^c \tilde{H})(H^\dagger L)\,, \tag{2.32}$$

the replacement of two ν_R by two $(H^\dagger L)^c$ in $\mathcal{O}_j^{d=8}$, making also possible a coupling to the $SU(2)_L$ field strength tensors $W_a^{\mu\nu}$ (τ^a, $a=1,2,3$, denote the $SU(2)_L$ Pauli matrices)

$$\mathcal{O}_2^{d=10} = |H|^2 (\overline{L}^c \tilde{H})(H^\dagger L) \; \overline{\nu}_R^c \nu_R\,, \tag{2.33}$$

$$\mathcal{O}_3^{d=10} = F_Y^{\mu\nu} (\overline{L}^c \tilde{H}) \sigma_{\mu\nu} (H^\dagger L) \; \overline{\nu}_R^c \nu_R\,, \tag{2.34}$$

$$\mathcal{O}_4^{d=10} = F_Y^{\mu\nu} (\overline{L}^c \tilde{H})(H^\dagger L) \; \overline{\nu}_R^c \sigma_{\mu\nu} \nu_R\,, \tag{2.35}$$

$$\mathcal{O}_5^{d=10} = W_a^{\mu\nu} (\overline{L}^c \tilde{H}) \sigma_{\mu\nu} (H^\dagger \tau^a L) \; \overline{\nu}_R^c \nu_R\,, \tag{2.36}$$

$$\mathcal{O}_6^{d=10} = W_a^{\mu\nu} (\overline{L}^c \tilde{H})(H^\dagger \tau^a L) \; \overline{\nu}_R^c \sigma_{\mu\nu} \nu_R\,, \tag{2.37}$$

and finally those that arise by multiplying $\mathcal{O}^{d=6}$ with any term in the SM Lagrangian $\mathcal{L}_{\rm SM}$, as those all have mass dimension $d=4$. There are even more though, as gauge and Lorentz contractions can be more intricate. At this mass dimension, quarks also come into play, allowing for baryon-number-violating $\Delta(B-L)=4$ operators, for example

$$\mathcal{O}_7^{d=10} = (\overline{u}_R d_R^c)(\overline{d}_R H^\dagger L)(\overline{\nu}_R^c \nu_R)\,, \tag{2.38}$$

which describes the neutron coupling $(\overline{n}\nu_L)(\overline{\nu}_R^c \nu_R)$ at low energies and could lead to the $\Delta(B-L)=4$ decay $n \to 3\nu$, strongly constrained by experiment: $\tau(n \to \text{inv}) > 6\times 10^{29}$ yr [91]. For obvious reasons we omit an exhaustive list of $d \geq 10$ operators. Note that $\Delta L = 4$ operators with charged leptons and gauge bosons can be obtained using covariant derivatives:

$$\mathcal{O}^{d=18} = \left[(\overline{L}^c \tilde{H})(H^\dagger D_\mu L)\right]^2 \supset (\overline{\nu}_L^c W_\mu^+ e_L)(\overline{\nu}_L^c W^{+\mu} e_L)\,, \tag{2.39}$$

$$\mathcal{O}^{d=20} = \left[(\overline{(D_\mu L)}^c \tilde{H})(H^\dagger D_\nu L)\right]^2 \supset (\overline{e}_L^c W_\mu^+ W_\nu^+ e_L)(\overline{e}_L^c W^{+\mu} W^{+\nu} e_L)\,. \tag{2.40}$$

The square includes the appropriate contraction of Lorentz indices, as should be obvious. Here we also gave the most interesting induced operator upon EWSB, in order to illustrate the effect.

Most operators from above can be constrained using existing experimental data, but do not offer a good *detection* channel for $\Delta(B-L)=4$. This is because the distinction between neutrino and anti-neutrino is a difficult experimental endeavor, making it impossible to distinguish e.g. the $\Delta(B-L)=4$ decay $n \to 3\nu$ from the $\Delta(B-L)=0$ decay $n \to \nu\overline{\nu\nu}$. *Charged* leptons are required to actually observe $\Delta(B-L)=4$, so operators like $\mathcal{O}^{d=20}$ are of particular interest. Since it is difficult to collide W bosons to test $\mathcal{O}^{d=20}$, let us write down a $\Delta(B-L)=4$ operator involving only charged first-generation particles, which can be easily produced and detected. At lowest mass dimension we find the $\Delta L = 4$ operator

$$\mathcal{O}^{d=18} = (\overline{d}_R d_R^c \; \overline{u}_R^c u_R \; \overline{e}_R^c e_R)(\overline{d}_R d_R^c \; \overline{u}_R^c u_R \; \overline{e}_R^c e_R)\,. \tag{2.41}$$

This operator should encode the prime detection process for $\Delta(B-L)=4$, and hence our LNV Dirac neutrinos—it describes $4\,d \to 4\,u + 4\,e^-$, or $4\,n \to 4\,p + 4\,e^-$ at baryon level. We will show in Sec. 2.3.3 that certain nuclei could indeed be sensitive to this *neutrinoless quadruple beta decay*. First off, however, we will turn away from the effective operators of this section and present a simple renormalizable realization of LNV Dirac neutrinos.

2.3.2 Lepton-Number-Violating Dirac Neutrinos

Following our introduction, we briefly present the simplest model for lepton-number-violating Dirac neutrinos, first brought forward in our paper [1]. We work again with a gauged $B-L$ symmetry, three RHNs $\nu_R \sim -1$ to cancel anomalies, one scalar $\phi \sim 4$ to break $B-L$, and one additional scalar $\chi \sim -2$ as a mediator, all of which are singlets under the SM gauge group. (Note that χ^* has exactly the same quantum numbers as S from Sec. 2.2.1; we denote it differently here as it serves another purpose and has a distinct phenomenology.) The Lagrangian takes a form very similar to Eq. (2.13), except for the scalar potential

$$\mathcal{L} = \mathcal{L}_{\rm SM} + \mathcal{L}_{\rm kinetic} + \mathcal{L}_{Z'} - V(H,\phi,\chi) - \left(\overline{\nu}_{R,j}\,(y_\nu)_{j\alpha}\,H^\dagger L_\alpha + \frac{1}{2}\overline{\nu}_{R,j}K_{jk}\nu^c_{R,k}\,\chi + \text{h.c.}\right). \tag{2.42}$$

If χ does not acquire a VEV, the neutrinos will be Dirac particles $\nu = \nu_L + \nu_R$ with mass matrix $m_D = y_\nu v/\sqrt{2}$, just like in the unbroken $B-L$ case of Sec. 2.1. The smallness of neutrino masses is in this simple model a result of very small couplings, $y_\nu \lesssim 10^{-11}$. The symmetric Yukawa-coupling matrix $K_{ij} = K_{ji}$ is nondiagonal and complex in general, which is important for our leptogenesis application in Sec. 2.3.4. The scalar potential takes the form

$$V(H,\phi,\chi) \equiv \sum_{X=H,\phi,\chi}\left(\mu_X^2|X|^2 + \lambda_X|X|^4\right) + \sum_{\substack{X,Y=H,\phi,\chi\\ X\neq Y}}\frac{\lambda_{XY}}{2}|X|^2|Y|^2 - \mu\left(\phi\chi^2 + \text{h.c.}\right), \tag{2.43}$$

with symmetric couplings $\lambda_{XY} = \lambda_{YX}$. Choosing the structure $\mu_H^2, \mu_\phi^2 < 0 < \mu_\chi^2$, one can easily realize a potential with minimum at $\langle\chi\rangle = 0$, $\langle H\rangle \neq 0 \neq \langle\phi\rangle$, which breaks $SU(2)_L \times U(1)_Y \times U(1)_{B-L}$ to $U(1)_{\rm EM} \times \mathbb{Z}_4^L$. An exact $\mathbb{Z}_4^L$ symmetry remains, under which leptons transform as $\ell \to -i\,\ell$ and $\chi \to -\chi$, making the neutrinos Dirac particles but still allowing for $\Delta L = 4$ LNV processes.[4] The crucial μ term in the potential induces a mass splitting between the two real scalars Ξ_j contained in $\chi = (\Xi_1 + i\,\Xi_2)/\sqrt{2}$:

$$m_1^2 = m_c^2 - 2\mu\langle\phi\rangle\,, \quad m_2^2 = m_c^2 + 2\mu\langle\phi\rangle\,, \tag{2.44}$$

where m_c is a mass term common to both

$$m_c^2 \equiv \mu_\chi^2 + \lambda_{H\chi}\langle H\rangle^2 + \lambda_{\chi\phi}\langle\phi\rangle^2\,. \tag{2.45}$$

Note that we can choose μ and $\langle\phi\rangle$ real and positive w.l.o.g. using phase and $B-L$ gauge transformations.

[4] Conservation of lepton number modulo $n > 2$ as a means to forbid Majorana neutrino masses was also mentioned in Ref. [92].

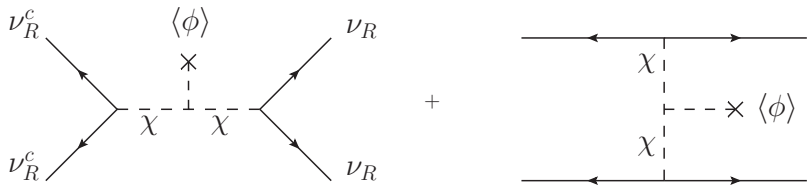

Figure 2.2: Tree-level realization of the $\Delta L = 4$ operator $(\overline{\nu}_R^c \nu_R)^2$ describing for example the neutrino–neutrino scattering $\nu_R^c \nu_R^c \to \nu_R \nu_R$.

We stress again that the neutrinos in our model are Dirac particles, but we also obtain effective $\Delta L = 4$ four-neutrino operators by integrating out χ—or more appropriately the mass eigenstates Ξ_j—at energies $E \ll m_{1,2}$:

$$\mathcal{L}_{\text{eff}}^{\Delta L=4} \supset \frac{1}{8}\left(m_2^{-2} - m_1^{-2}\right)\left(K_{ij}\overline{\nu}_{R,i}\nu_{R,j}^c\right)^2 + \text{h.c.}, \tag{2.46}$$

see Fig. 2.2 for the relevant Feynman diagrams. This is precisely the $d = 6$ operator from Eq. (2.28), but now with a renormalizable completion on top. We emphasize that this operator was not difficult to construct, all we needed was one more complex scalar than in Sec. 2.2. For simplicity, we will assume physics at the TeV scale as the source of our four-neutrino operators throughout this thesis, i.e. only discuss the effects of effective operators like the above (2.46); a discussion of more constrained *light* mediators, as well as of other and more complicated models that generate effective four-neutrino operators with left-handed neutrinos, will be presented elsewhere. We note that our particular example uses a gauged $B - L$ framework; in general however, the observation and the model building possibilities that might lead to LNV Dirac neutrinos are, of course, much broader.

2.3.3 Neutrinoless Quadruple Beta Decay

Our model from the last section gave us the effective dimension-six $\Delta L = 4$ operator $(\overline{\nu}_R \nu_R^c)^2$, which can lead to an interesting signature in beta decay measurements: Four nucleons undergo beta decay, emitting four neutrinos which meet at the effective $\Delta L = 4$ vertex and remain virtual. We only see four electrons going out, so at parton level we have $4\,d \to 4\,u + 4\,e^-$, and on hadron level $4\,n \to 4\,p + 4\,e^-$ (Fig. 2.3). This is precisely the signature we identified in Sec. 2.3.1 with the help of effective operators as the prime observation channel for $\Delta(B - L) = 4$. Obviously this neutrinoless quadruple beta decay ($0\nu4\beta$) is highly unlikely—more so than $0\nu2\beta$, as it is of fourth order—but one can still perform the exercise of identifying candidate isotopes for the decay and estimating the lifetime; constraining the lifetime experimentally is, of course, also possible. Besides $0\nu4\beta$, one can imagine analogous processes such as neutrinoless quadruple electron capture ($0\nu4\text{EC}$), neutrinoless quadruple positron decay ($0\nu4\beta^+$), neutrinoless double electron capture double positron decay ($0\nu2\text{EC}2\beta^+$), etc. We will find potential candidates for $0\nu4\beta$, $0\nu2\text{EC}2\beta^+$, $0\nu3\text{EC}\beta^+$, and $0\nu4\text{EC}$.

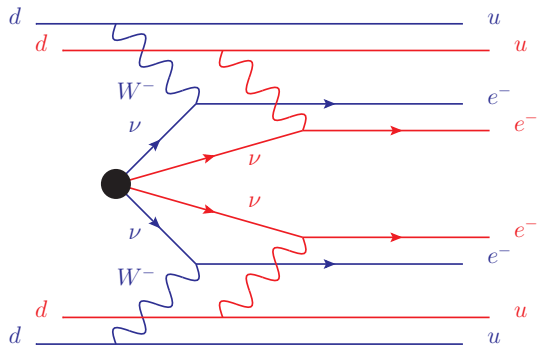

Figure 2.3: Neutrinoless quadruple beta decay via a $\Delta L = 4$ operator $(\overline{\nu}^c \nu)^2$ (filled circle). Arrows denote flow of lepton number, colors are for illustration purposes.

Candidates for $0\nu4\beta$

We will now identify candidate isotopes for $\Delta L = 4$ processes. We need to find isotopes which are more stable after the flip $(A, Z) \to (A, Z \pm 4)$. Normal beta decay has to be forbidden in order to handle backgrounds and make the mother nucleus sufficiently stable. Using nuclear data charts [93], we found seven possible candidates: three for $0\nu4\beta$, four for neutrinoless quadruple electron capture and related decays. They are listed in Tab. 2.1, together with their Q values, competing decay channels, and natural abundance. It should be obvious that not all $0\nu2\beta$ candidates (A, Z) make good $0\nu4\beta$ candidates, as $(A, Z + 4)$ can have a larger mass than (A, Z); it is *less* obvious that there exist no $0\nu4\beta$ candidates with beta-unstable daughter nuclei. Using the semi-empirical Bethe–Weizsäcker mass formula, one can however show that

$$\frac{M[{}^A(Z-2)] - M[{}^A(Z+2)]}{M[{}^A(Z-1)] - M[{}^A(Z+1)]} = 2\,, \tag{2.47}$$

where $M[{}^AZ]$ denotes the mass of the neutral atom ${}^AZ$ in its ground state. Applied to our problem, this means that the mass splitting of the odd–odd states in Fig. 2.4 (colored in red) is expected to be smaller than the mass splitting of the two $\Delta Z = 4$ nuclei (which is just the Q value, see below), which implies that beta-stable $0\nu4\beta$ candidates will decay into *beta-stable* nuclei (this simple argument is confirmed with data charts [93]).

The Q values in Tab. 2.1 can be readily calculated in analogy to $0\nu2\beta$. In general, the total kinetic energy of the emitted electrons/positrons in a $0\nu n\beta^\mp$ decay,

$${}^AZ \to {}^A(Z \pm n) + n\, e^\mp\,, \tag{2.48}$$

is given by the Q value, and can be calculated via

$$Q_{0\nu n\beta^-} = M[{}^AZ] - M[{}^A(Z+n)]\,, \tag{2.49}$$

$$Q_{0\nu n\beta^+} = M[{}^AZ] - M[{}^A(Z-n)] - 2n\, m_e\,. \tag{2.50}$$

The term $-2n\, m_e$ in $Q_{0\nu n\beta^+}$ already makes $0\nu2\beta^+$ very rare, but neutrinoless quadruple positron decay $0\nu4\beta^+$ *impossible*. Electron capture with the emission of up to two positrons is however permitted, as the Q value for the EC-process

$${}^AZ + k\, e^- \to {}^A(Z-n) + (n-k)\, e^+ \tag{2.51}$$

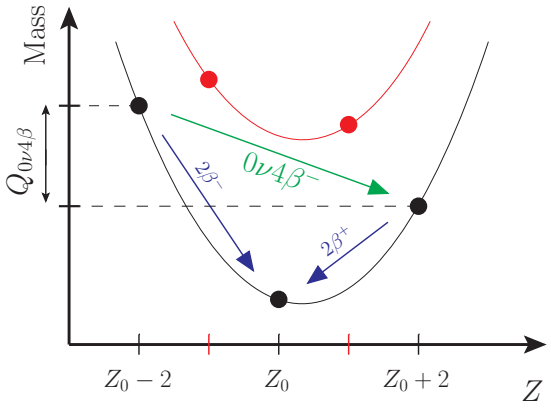

Figure 2.4: Three beta-stable even–even nuclei on their mass parabola (black). The heaviest isobar $(A, Z_0 - 2)$ can decay either via double beta decay into the lowest state (A, Z_0), or via $0\nu4\beta$ (green arrow) into the medium state $(A, Z_0 + 2)$. Also shown are the "forbidden" odd–odd states in between (red).

is given by $Q_{0\nu k\mathrm{EC}(n-k)\beta^+} = Q_{0\nu n\beta^+} + 2k\, m_e$, allowing above all for neutrinoless quadruple electron capture $0\nu4\mathrm{EC}$ in four isotopes (Tab. 2.1).

Having identified all $\Delta L = 4$ candidates, we discuss their experimental prospects and challenges in more detail. Let us first take a look at the most promising isotope for $0\nu4\beta$: neodymium ^{150}Nd. The following decay channels are possible (see also Fig. 2.4):

- $^{150}_{60}\mathrm{Nd} \to {}^{150}_{62}\mathrm{Sm}$ via $2\nu2\beta$, i.e. via the forbidden intermediate odd–odd state $^{150}_{61}\mathrm{Pm}$. Two neutrinos and two electrons are emitted; the electrons hence have a continuous energy spectrum and total energy $E_{e,1} + E_{e,2} < 3.371\,\mathrm{MeV}$. This decay has already been observed with a half-life of $7 \times 10^{18}\,\mathrm{yr}$.

- $^{150}_{60}\mathrm{Nd} \to {}^{150}_{64}\mathrm{Gd}$ via $0\nu4\beta$. Four electrons with continuous energy spectrum and summed energy $Q_{0\nu4\beta} = 2.079\,\mathrm{MeV}$ are emitted. In this special case, the daughter nucleus is α-unstable with half-life $\tau^{\alpha}_{1/2}({}^{150}_{64}\mathrm{Gd} \to {}^{146}_{62}\mathrm{Sm}) \simeq 2 \times 10^6\,\mathrm{yr}$.

- There is also the possibility of a decay into an excited state, $^{150}_{60}\mathrm{Nd} \to {}^{150}_{64}\mathrm{Gd}^*$ via $0\nu4\beta$. The excited final state will reduce the effective Q value—by $0.638\,\mathrm{MeV}$ $(1.207\,\mathrm{MeV})$ for the lowest 2^+ (0^+) state—and produce additional detectable photons.

- We note that if neutrinos were Majorana particles, the decay $^{150}_{60}\mathrm{Nd} \to {}^{150}_{62}\mathrm{Sm}$ via $0\nu2\beta$ would possible. Two mono-energetic electrons would be emitted with total energy $Q_{0\nu2\beta} = 3.371\,\mathrm{MeV}$. This decay is, of course, forbidden in our model of LNV Dirac neutrinos.

A sketch of the summed electron energy spectrum is shown in Fig. 2.5. The $Q_{0\nu4\beta}$ peak will always sit somewhere in the middle of the continuous spectrum, so one would have to identify the four electrons in order to remove the $2\nu2\beta$ background. This still leaves other backgrounds to be considered, e.g. the scattering of the two $2\nu2\beta$ electrons off of atomic electrons, which can effectively lead to four emitted electrons (and two neutrinos). Since $Q_{0\nu4\beta} < Q_{2\nu2\beta}$, the sum of the electron energies will be continuously distributed and can overlap the discrete $Q_{0\nu4\beta}$ peak. A dedicated discussion of this and other possible backgrounds goes far beyond the scope of this thesis.

As an alternative to direct searches, one could even omit an energy measurement and just look at the transmutation $^{150}\mathrm{Nd} \to {}^{150}\mathrm{Gd}$, using, for example, chemical methods. The

element	$Q_{0\nu4\beta}$	other decays	NA in %
$^{96}_{40}\mathrm{Zr} \to {}^{96}_{44}\mathrm{Ru}$	0.629 MeV	$\tau^{2\nu2\beta}_{1/2} \simeq 2 \times 10^{19}\,\mathrm{yr}$	2.8
$^{136}_{54}\mathrm{Xe} \to {}^{136}_{58}\mathrm{Ce}$	0.044 MeV	$\tau^{2\nu2\beta}_{1/2} \simeq 2 \times 10^{21}\,\mathrm{yr}$	8.9
$^{150}_{60}\mathrm{Nd} \to {}^{150}_{64}\mathrm{Gd}$	2.079 MeV	$\tau^{2\nu2\beta}_{1/2} \simeq 7 \times 10^{18}\,\mathrm{yr}$	5.6
	$Q_{0\nu4\mathrm{EC}}$		
$^{124}_{54}\mathrm{Xe} \to {}^{124}_{50}\mathrm{Sn}$	0.577 MeV	–	0.095
$^{130}_{56}\mathrm{Ba} \to {}^{130}_{52}\mathrm{Te}$	0.090 MeV	$\tau^{2\nu2\mathrm{EC}}_{1/2} \sim 10^{21}\,\mathrm{yr}$	0.106
$^{148}_{64}\mathrm{Gd} \to {}^{148}_{60}\mathrm{Nd}$	1.138 MeV	$\tau^{\alpha}_{1/2} \simeq 75\,\mathrm{yr}$	–
$^{154}_{66}\mathrm{Dy} \to {}^{154}_{62}\mathrm{Sm}$	2.063 MeV	$\tau^{\alpha}_{1/2} \simeq 3 \times 10^{6}\,\mathrm{yr}$	–
	$Q_{0\nu3\mathrm{EC}\beta^+}$		
$^{148}_{64}\mathrm{Gd} \to {}^{148}_{60}\mathrm{Nd}$	0.116 MeV	$\tau^{\alpha}_{1/2} \simeq 75\,\mathrm{yr}$	–
$^{154}_{66}\mathrm{Dy} \to {}^{154}_{62}\mathrm{Sm}$	1.041 MeV	$\tau^{\alpha}_{1/2} \simeq 3 \times 10^{6}\,\mathrm{yr}$	–
	$Q_{0\nu2\mathrm{EC}2\beta^+}$		
$^{154}_{66}\mathrm{Dy} \to {}^{154}_{62}\mathrm{Sm}$	0.019 MeV	$\tau^{\alpha}_{1/2} \simeq 3 \times 10^{6}\,\mathrm{yr}$	–

Table 2.1: Candidates for the nuclear $\Delta L = 4$ processes neutrinoless quadruple beta decay and electron capture, the corresponding Q values, competing (observed) decay channels with half-life $\tau^{j}_{1/2}$, and natural abundance (NA) of the candidate isotopes.

background for $^{150}\mathrm{Nd} \to {}^{150}\mathrm{Gd}$ is basically nonexistent, as the SM-allowed $4\nu4\beta$ is killed by the Q-dependence of the eight-particle phase space $G_{4\nu4\beta} \sim Q^{23}$ (compared to the four-particle phase space $G_{0\nu4\beta} \sim Q^{11}$), and $0\nu2\beta$ would most likely be seen long before we ever see the double $0\nu2\beta$ that mimics $0\nu4\beta$. Hence, this transmutation suffices to test $0\nu4\beta$. In case of $^{150}\mathrm{Nd}$, the instability of the daughter nucleus $^{150}\mathrm{Gd}$ can even be advantageous, as the resulting alpha particle provides an additional handle to look for the decay.[5] The necessary macroscopic number of daughter elements will, of course, result in weak limits compared to dedicated $0\nu4\beta$ searches in $0\nu2\beta$ experiments. However, for elements not under consideration in $0\nu2\beta$ experiments, this could be a viable and inexpensive way to test $0\nu4\beta$.

All the above holds similarly for $^{96}\mathrm{Zr}$ and $^{136}\mathrm{Xe}$ as well. Both have much smaller Q values—which theoretically reduces the rate—but α-stable daughter nuclei. The non-solid structure of xenon makes it, in principle, easier to check for the transmutation into cerium; furthermore, the EXO [94] $0\nu2\beta$ experiment is currently running and could check for $0\nu4\beta$, should their detector be sensitive at these energies and not flooded by backgrounds. $^{96}\mathrm{Zr}$ is a better candidate due to a higher Q value, but there are no dedicated $^{96}\mathrm{Zr}$ experiments planned. Still, the NEMO collaboration could set limits on $^{96}\mathrm{Zr} \xrightarrow{0.629} {}^{96}\mathrm{Ru}$ by reanalyzing their data from Ref. [95]. Overall, $^{150}\mathrm{Nd}$ is by far the best candidate, due to the high $Q_{0\nu4\beta}$ value and availability. Coincidentally, it also has a high $Q_{0\nu2\beta}$ value, which makes it a popular isotope to test for $0\nu2\beta$, with some existing and planned experiments [31]. Once again, NEMO might

[5] The alpha decay is however too slow to be used in coincidence with $0\nu4\beta$.

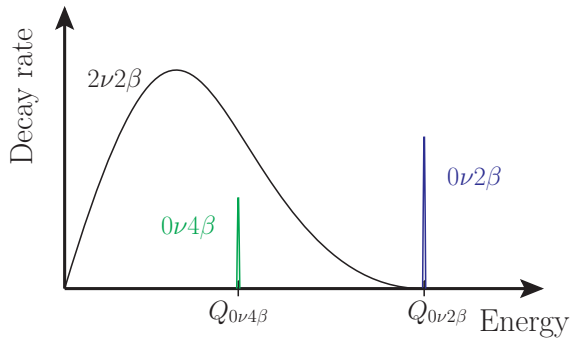

Figure 2.5: Sum of kinetic electron energies in the beta decays $0\nu2\beta$ (blue), $2\nu2\beta$ (black), and $0\nu4\beta$ (green). Relative contributions not to scale.

already be able to constrain ^{150}Nd $\xrightarrow{2.079}$ ^{150}Gd with their data from Ref. [96].

The $0\nu4$EC channels in Tab. 2.1 lead to a similar transmutation behavior as discussed above for $0\nu4\beta^-$, and can be checked in the same way. Note that the energy gain $Q_{0\nu4\text{EC}}$ will here be carried away by *photons* instead of electrons; the captured electrons will be taken out of the K and L shells, resulting in a subsequent cascade of X-ray photons. The Q values of ^{148}Gd and ^{154}Dy are high enough to also undergo $0\nu3\text{EC}\beta^+$; ^{154}Dy is the only isotope capable of $0\nu2\text{EC}2\beta^+$. This can give rise to distinguishable signatures due to the additional 511 keV photons from electron–positron annihilation. The comparatively fast α decay of ^{148}Gd and ^{154}Dy—and the fact that they have to be synthesized from scratch—make them however very challenging probes for $\Delta L = 4$, despite their large Q values. ^{124}Xe might then be the best element to test for $0\nu4$EC—unfortunately, the enriched xenon used by EXO contains almost no ^{124}Xe, so $0\nu4$EC is currently hard to test (dark matter experiments using xenon can in principle be used, as they contain ^{124}Xe). Resonant enhancement of the $0\nu4$EC rates, as discussed for the $0\nu2$EC mode (for an overview, see Ref. [97]), might boost the signal.

Following the above discussion, $\Delta L = 4$ signals are apparently easier to test via the $0\nu4\beta$ channels, with both ^{96}Zr and ^{150}Nd as more favorable isotopes when it comes to Q values and natural abundance.

Rates for $0\nu4\beta$

Having identified the candidates and signatures to test $0\nu4\beta$ experimentally, let us estimate some rates. Similar to $0\nu2\beta$, the half-life of $0\nu4\beta$ can approximately be factorized as

$$\left[\tau_{1/2}^{0\nu4\beta}\right]^{-1} = G_{0\nu4\beta}|\mathcal{M}_{0\nu4\beta}|^2\,, \tag{2.52}$$

where $G_{0\nu4\beta}$ denotes the phase space and $\mathcal{M}_{0\nu4\beta}$ the nuclear transition matrix element (including the particle physics parameters) facilitating the process. Using an effective $\Delta L = 4$ vertex $(\overline{\nu}_L \nu_L^c)^2/\Lambda^2$ gives $\mathcal{M}_{0\nu4\beta} \propto G_F^4/p_\nu^4\Lambda^2$, simply by counting propagators. For the virtual neutrino momentum p_ν we will use the inverse distance between the decaying nucleons, $p_\nu \sim |q| \sim 1\,\text{fm}^{-1} \simeq 100\,\text{MeV}$. The phase-space factor for the four final particles is the same as the one in $2\nu2\beta$ (proportional to Q^{11} for $Q \gg m_e$ [98]), which also tells us that each of the four electrons will be distributed just like the electrons in $2\nu2\beta$, with a different Q value, of course. Purely on dimensional grounds we can then estimate the dependence of the half-life

on our parameters as

$$\left[\tau_{1/2}^{0\nu4\beta}\right]^{-1} \propto Q^{11} \left(\frac{G_F^4}{q^4\Lambda^2}\right)^2 q^{18}\,, \tag{2.53}$$

where the last factor is included to obtain the correct overall mass dimension. The above estimate is only valid for large Q values, as it assumes massless electrons; the low $Q_{0\nu4\beta}$ of most elements in Tab. 2.1 render (some of) the four electrons non-relativistic and require a more accurate calculation of the phase space. To partially cancel the uncertainties, we can approximate that the phase space for $0\nu4\beta$ and $2\nu2\beta$ is overall similar and consider the ratio (for ^{150}Nd and $|q| \simeq 100\,\text{MeV}$)

$$\frac{\tau_{1/2}^{0\nu4\beta}}{\tau_{1/2}^{2\nu2\beta}} \simeq \left(\frac{Q_{0\nu2\beta}}{Q_{0\nu4\beta}}\right)^{11} \left(\frac{\Lambda^4}{q^{12}G_F^4}\right) \simeq 10^{46} \left(\frac{\Lambda}{\text{TeV}}\right)^4. \tag{2.54}$$

This is, of course, only a rough estimate, and a better calculation (dropping the implicitly used closure approximation, including effects of the nuclear Coulomb field etc.) will certainly change this rate. To this effect we point out a difference between $0\nu2\beta$ and $0\nu4\beta$: While the former decay proceeds via a kinematically forbidden intermediate state, the latter also features an energetically preferred intermediate state X, only to rush past it on the mass parabola (see Fig. 2.4). Since excited states of X can still have a lower mass than our initial nucleus, the summation over all these states is important and cannot be approximated away as easily as the excited states of an already forbidden intermediate state.

Finally, in our simple model from above, we generate the $\Delta L = 4$ operator with RHNs, $(\overline{\nu}_R \nu_R^c)^2$, so each of the neutrinos in Fig. 2.3 requires a mass-flip in order to couple to the W bosons. The particle-physics amplitude is therefore further suppressed by a factor $(m_\nu/q)^4 \simeq 10^{-37}$, making this process all the more unlikely. These mass-flips can be avoided in left–right-symmetric extensions of our model [99–101], at the price of replacing the four W bosons in Fig. 2.3 with their heavier W_R counterparts.

Even with all our approximations leading to the above estimates, one can safely conclude that the half-life for neutrinoless quadruple beta decay is very large, at least if physics at the TeV scale is behind it in any way. This may be a too conservative approach, because four-neutrino interactions do not suffer from such stringent constraints as other four-fermion interactions [102]. The effective LNV operator $(\overline{\nu}_L \nu_L^c)^2/\Lambda^2$ discussed here has not been constrained so far, and the contribution to the well-measured invisible Z width via $Z \to 4\nu$ only gives $\Lambda > 1/(\mathcal{O}(10)\sqrt{G_F}) \sim 20\,\text{GeV}$. This, of course, only holds if the mediator is heavy enough to be integrated out in the first place. Light mediators can significantly increase the rate, and the life-time will be minimal if the exchanged particles have masses of the order of $|q| \simeq 100\,\text{MeV}$. For neutrinoless double beta decay the gain factor for the half-life is about 10^{16} [103, 104], and we can expect something similar here. Given that we have four neutrino propagators, the rate might be enhanced by a sizable factor, and therefore experimental searches for $0\nu4\beta$ should be pursued.

While the expected rates for $0\nu4\beta$ in our proof-of-principle model are unobservably small, more elaborate models—invoking resonances—might overcome this obstacle. Most importantly, the experimental and nuclear-physics aspects of $0\nu4\beta$ are completely independent of the underlying mechanism, and can therefore be readily investigated.

2.3.4 New Dirac Leptogenesis

Having introduced the concept of LNV Dirac neutrinos and identified possible experimental signatures, we will show in this subsection how the associated $\Delta L = 4$ interactions can give rise to a novel Dirac leptogenesis mechanism. We have already presented a Dirac leptogenesis mechanism in Sec. 2.1, dubbed neutrinogenesis [74], that made use of the tiny Yukawa couplings $y_\nu \sim m_\nu/\langle H\rangle \lesssim 10^{-11}$ connecting the RHNs ν_R to the SM. The non-thermalization of the ν_R then made it possible to hide a lepton asymmetry in the ν_R sector, invisible to the sphalerons. Neutrinogenesis can therefore provide an explanation of the observed BAU for every model in which Dirac neutrinos are light because of a small Yukawa coupling, be it put in by hand or generated effectively.

An interesting and very different route to motivate light Dirac neutrinos has been discussed in Refs. [59–61], where a second Higgs doublet H_2 is introduced, which couples exclusively to neutrinos [105]. A small VEV, say $\langle H_2\rangle \sim 1\,\text{eV}$, is then the reason for small neutrino masses, while the Yukawa couplings can be large. This leads to distinctive collider signatures [106], but also makes standard neutrinogenesis impossible. In this section we will provide a new kind of Dirac leptogenesis, which *relies* on thermalized RHNs and therefore works for the neutrinophilic two-Higgs-doublet solution of small Dirac masses. Our mechanism uses the framework of LNV Dirac neutrinos to create a lepton asymmetry from the CP-violating decay of a heavy particle.[6] As such, the mechanism is actually more reminiscent of standard leptogenesis than neutrinogenesis, even though it contains Dirac neutrinos.

Asymmetries

As seen above, neutrinos are Dirac particles in our model, yet $B - L$ is broken, which makes possible a real Dirac lepto*genesis*, where a lepton asymmetry is created by the CP-violating $\Delta L = 4$ decay of some heavy particle. In order for this to work, the decay has to take place after $B - L$ breaking and before the EWPT, so that sphalerons can convert the lepton asymmetry to the baryons (assuming $\Delta B = 0$ as induced in our model).

For a simple realization, we use the framework Sec. 2.3.2 and add second copies of both the mediator scalar $\chi = (\Xi_1 + i\Xi_2)/\sqrt{2}$ and the Higgs doublet H. In order to break $B - L$ by only four units, both χ_j are required to stay VEV-less, which can be easily realized in the scalar potential. Below the $B - L$ breaking scale, χ_1 and χ_2 now split into *four* real scalars Ξ_j, with decay channels $\nu_{R,\alpha}\nu_{R,\beta}$ and $\nu^c_{R,\alpha}\nu^c_{R,\beta}$. The second copy χ_2 is necessary to obtain CP violation in these decays (depicted in Fig. 2.6), as we will see below. The out-of-equilibrium decay of the lightest Ξ_j has then all the necessary qualitative features to create an asymmetry Δ_{ν_R} in the RHNs (i.e. fulfills Sakharov-like conditions). This in itself would not suffice for baryogenesis, as the sphalerons do not see the right-handed Δ_{ν_R}, and the Higgs Yukawa couplings $y \sim m_\nu/\langle H_1\rangle$ from Eq. (2.42) are too small to efficiently convert Δ_{ν_R} to the left-handed lepton doublets. This is where the second Higgs doublet H_2 comes in, as it can have large enough Yukawa couplings $w_{\alpha\beta}\overline{L}_\alpha H_2 \nu_{R,\beta}$ to thermalize ν_R and transfer $\Delta_{\nu_R} \to \Delta_L$. From there, sphalerons take over to convert Δ_L to the baryons Δ_B in the usual leptogenesis fashion (see Sec. 2.2.2).

[6] Prior to Ref. [1], it was already mentioned in Ref. [107] that LNV Dirac neutrinos could lead to interesting effects in the early Universe.

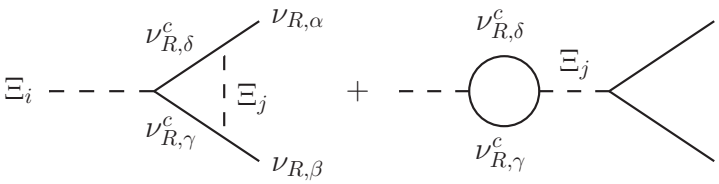

Figure 2.6: CP-violating vertex and self-energy loop corrections to the LNV decay $\Xi_i \to \nu_{R,\alpha}\nu_{R,\beta}$ relevant for leptogenesis.

The second Higgs doublet H_2 will be chosen neutrinophilic, i.e. with a small VEV [61]. While this is not strictly necessary for our version of Dirac leptogenesis—for example, a VEV-less H_2 with large Yukawas would work as well, the neutrinos gaining mass via H_1—it is the most interesting two-Higgs-doublet model for our purposes, as it additionally sheds light on the small neutrino masses. To this effect, let us mention briefly how the neutrinophilic nature of H_2 can be realized in our context. Following Ref. [60], we impose an additional global $\mathbb{Z}_2$ symmetry (or a $U(1)$ as in Ref. [61]) under which only H_2 and ν_R are charged, forbidding all H_2 Yukawa couplings except for $w_{\alpha\beta}\overline{L}_\alpha H_2 \nu_{R,\beta}$. The new global symmetry is broken softly by a term $\mu_{12}^2 H_1^\dagger H_2$ in the scalar potential; a small μ_{12}^2 is technically natural and will induce a small VEV for H_2, $\langle H_2\rangle/\langle H_1\rangle = \mu_{12}^2/M_{H_2}^2$, which gives naturally small Dirac neutrino masses $m_D = w|\langle H_2\rangle|$. We stress that our additional $B-L$ symmetry and scalars, compared to Refs. [60, 61], do in no way complicate or interfere with this realization of a neutrinophilic H_2, so we will not go into any more details.

After these qualitative statements, let us delve into a more quantitative analysis of our leptogenesis mechanism. The scalar potential for ϕ, $H_{1,2}$ and $\chi_{1,2}$ is more involved than before (Eq. (2.43)), but the only qualitatively new terms are

$$V(\phi, H_{1,2}, \chi_{1,2}) \;\supset\; m_{12}^2\, \overline{\chi}_1\chi_2 + \mu_{12}\,\phi\,\chi_1\chi_2 + \text{h.c.}, \tag{2.55}$$

as they lead to a mixing of the four real fields Ξ_j contained in $\chi_{1,2}$ after breaking $B-L$. The 4×4 mass matrix for the Ξ_j is not particularly illuminating, and a diagonalization merely redefines the couplings $\kappa^j_{\alpha\beta}$ to the RHNs (see Eq. (2.42)). Since the resulting couplings are the only relevant ones for leptogenesis, we can skip all these steps and just work with four real scalar fields Ξ_j with masses m_j and complex symmetric Yukawa couplings $V^j_{\alpha\beta} = V^j_{\beta\alpha}$

$$\mathcal{L} \;\supset\; \frac{1}{2}V^j_{\alpha\beta}\,\Xi_j \overline{\nu}_{R,\alpha}\nu^c_{R,\beta} + \frac{1}{2}\overline{V}^j_{\alpha\beta}\,\Xi_j\overline{\nu}^c_{R,\alpha}\nu_{R,\beta}\,, \tag{2.56}$$

where implicit sums are understood and $\overline{V}^j_{\alpha\beta} \equiv (V^j_{\alpha\beta})^*$.

The Z' interactions will keep the SM particles and the new scalars and RHNs in equilibrium above $T_{Z'} \simeq (\sqrt{g_*}\langle\phi\rangle^4/M_{\rm Pl})^{1/3}$, $g_* \simeq 100$ being the effective number of degrees of freedom at temperature T and $M_{\rm Pl} \simeq 10^{19}$ GeV the Planck mass. Below $T_{Z'}$, the real scalars Ξ_j will only be coupled to the SM via Higgs portal (assumed to be small for simplicity) and the RHN interactions from Eq. (2.56). The out-of-equilibrium condition for the decay of the lightest Ξ_i then reads

$$\Gamma(\Xi_i \to \nu_R\nu_R, \nu^c_R\nu^c_R) \ll H(T\sim m_i) \simeq 1.66\,\sqrt{g_*}\,\frac{m_i^2}{M_{\rm Pl}}\,, \tag{2.57}$$

$H(T)$ being the Hubble expansion rate of the Universe at temperature T (not to be confused with the Higgs fields H_j). As with the bulk of leptogenesis models, this condition is most naturally fulfilled for very heavy decaying particles, as can be seen by inserting the total decay rate $\Gamma(\Xi_i) = \mathrm{tr}(\overline{V}^i V^i)\, m_i/4\pi$, leading to

$$\mathrm{tr}(\overline{V}^i V^i)/10^{-6} \ll m_i/10^{11}\,\mathrm{GeV}\,, \tag{2.58}$$

which can be satisfied with either small Yukawa couplings or large masses, in complete analogy to the standard leptogenesis with heavy right-handed Majorana neutrinos (Sec. 2.2.2).

Assuming the out-of-equilibrium condition (2.58) to be satisfied, the decay of the lightest Ξ_i then leads to a CP asymmetry due to interference of tree-level and one-loop diagrams (Fig. 2.6):

$$\varepsilon_i \equiv 2\,\frac{\Gamma\left(\Xi_i \to \nu_R\nu_R\right) - \Gamma\left(\Xi_i \to \nu_R^c\nu_R^c\right)}{\Gamma\left(\Xi_i \to \nu_R\nu_R\right) + \Gamma\left(\Xi_i \to \nu_R^c\nu_R^c\right)}\,, \tag{2.59}$$

where we already summed over flavor indices and included a factor of two because two RHNs are created per decay. A straightforward calculation yields the asymmetries from the vertex (ε^{v}) and self-energy correction (ε^{s}):

$$\begin{aligned}
\varepsilon_i^{\mathrm{v}} &= \frac{1}{4\pi}\frac{1}{\mathrm{tr}(\overline{V}^i V^i)}\sum_{k\neq i} F(\eta_k)\,\mathrm{Im}\left[\mathrm{tr}\left(\overline{V}^i V^k \overline{V}^i V^k\right)\right],\\
\varepsilon_i^{\mathrm{s}} &= -\frac{1}{24\pi}\frac{1}{\mathrm{tr}(\overline{V}^i V^i)}\sum_{k\neq i} G(\eta_k)\,\mathrm{Im}\left[\left\{\mathrm{tr}\left(\overline{V}^i V^k\right)\right\}^2\right],
\end{aligned} \tag{2.60}$$

with $\eta_k \equiv m_i^2/m_k^2 < 1$ and the loop functions

$$\begin{aligned}
F(x) &\equiv \frac{x - \log(1+x)}{x} = \frac{x}{2} - \frac{x^2}{3} + \mathcal{O}(x^3),\\
G(x) &\equiv \frac{x}{1-x} = x + x^2 + \mathcal{O}(x^3).
\end{aligned} \tag{2.61}$$

As quick crosschecks, one can easily verify that the $k = i$ contribution to the sums in Eq. (2.60) vanishes, because the trace of an hermitian matrix is real. One can also convince oneself that the second χ_2 is indeed necessary for the CP asymmetry, as the couplings of just one field $\chi = (\Xi_1 + i\Xi_2)/\sqrt{2}$ would lead to the Yukawa-coupling relation $V^2 = iV^1$ and ultimately $\varepsilon^{\mathrm{s}} = 0 = \varepsilon^{\mathrm{v}}$. Let us consider one last limiting case before we move on: Neglecting the χ_1–χ_2 mixing terms in the scalar potential (2.55) gives $\chi_1 = (\Xi_1 + i\Xi_2)/\sqrt{2}$, $\chi_2 = (\Xi_3 + i\Xi_4)/\sqrt{2}$ and the relations $V^2 = iV^1$ and $V^4 = iV^3$. Assuming Ξ_1 to be the lightest of the four scalars, Ξ_2 does not contribute to ε by the argument given above. The contributions of Ξ_3 and Ξ_4 are opposite in sign, so that $\varepsilon^{\mathrm{v}} \propto F(\eta_3) - F(\eta_4)$ and $\varepsilon^{\mathrm{s}} \propto G(\eta_3) - G(\eta_4)$. The asymmetry therefore vanishes for $m_3 = m_4$, as it should, because this would imply $B - L$ conservation.

Compared to other leptogenesis scenarios, the asymmetries from vertex and self-energy corrections in our model depend on different flavor parameters—even in the unflavored case—because $\mathrm{tr}(A^2) \neq (\mathrm{tr}A)^2$ for a general matrix A. The asymmetries are nevertheless qualitatively reminiscent of standard leptogenesis, with the same rough behavior

$$\varepsilon \sim 10^{-7}\left(\eta/10^{-2}\right)\left(V/10^{-2}\right)^2, \tag{2.62}$$

ignoring the complex matrix structure of V and assuming a hierarchy $\eta_k \ll 1$. A low-scale resonant leptogenesis is, of course, also possible in our framework, but goes beyond the scope of this thesis.

The total lepton asymmetry, i.e. the RHN number density n_{ν_R} relative to the entropy density $s = (2\pi^2/45) g_* T^3$ is then given by

$$Y_{\nu_R} \equiv \frac{n_{\nu_R}}{s} \sim \frac{\varepsilon_i^{\mathrm{v}} + \varepsilon_i^{\mathrm{s}}}{g_*} \,. \tag{2.63}$$

Since we assume equilibrium of the SM particles with the RHNs as well as the sphalerons, we can use chemical potentials to describe the plasma. (Note that $B - L$ is effectively conserved once the Ξ_j have dropped out.) Consequently, the chemical potential for the RHNs has to be added to the usual set of equations [86], resulting in the equilibrium condition $3B + L = 0$, or

$$Y_B = \frac{1}{4} Y_{B-L} \,, \qquad\qquad Y_L = -\frac{3}{4} Y_{B-L} \,, \tag{2.64}$$

for three generations (and an arbitrary number of Higgs doublets), compared to $Y_B = \frac{28}{79} Y_{B-L}$ for standard leptogenesis with one Higgs doublet (Sec. 2.2.2). The condition $3B + L = 0$ can also be understood with the help of Ref. [108], where it was pointed out that $3B + L$ vanishes if only left-handed fermions and the sphalerons are in equilibrium. Since we introduce fully thermalized right-handed partners to all left-handed fermions, it is no surprise that $3B+L = 0$ remains valid.

With all of the above, it should be clear that our LNV Dirac neutrinos can accommodate the observed baryon asymmetry $Y_B \sim 10^{-10}$ (Eq. (1.25)) in this novel leptogenesis scenario. We refrain from a parameter scan, as the Yukawa couplings V^j and masses m_j are in any way hardly constrained by other processes or related to other observables, at least for the very heavy Ξ_j considered here. This leptogenesis mechanism is testable nonetheless, because it requires additional interactions for the RHNs. Let us therefore discuss the last crucial piece of the puzzle: the thermalization of the RHNs.

Asymmetry Transfer

The ν_R asymmetry needs to be transferred to the left-handed sector before the EWPT in order to generate the baryon asymmetry of the Universe. Correspondingly, we need stronger-than-usual interactions for the RHNs, in our case by means of the second Higgs doublet H_2 in $w_{\alpha\beta} \overline{L}_\alpha H_2 \nu_{R,\beta}$. At temperatures above the electroweak scale, the interaction rates go with $w^2 T$, which equilibrates the RHNs if $w \gtrsim 10^{-8}$ [74]. This does not lead to problems, because below the EWPT, the interaction rate drastically changes its form; the charged Higgs H_2^+ for example mediates an $\ell^+ \ell^- \leftrightarrow \overline{\nu}_R \nu_R$ scattering with rate $w^4 T^5 / m_{H_2^+}^4$, i.e. suppressed by the mass. The RHN decoupling temperature $T_{\nu_R}^{\mathrm{dec}}$ is then given by the condition

$$w^4 \left(T_{\nu_R}^{\mathrm{dec}}\right)^5 / m_{H_2^+}^4 \sim H\left(T_{\nu_R}^{\mathrm{dec}}\right) , \tag{2.65}$$

at least for large w. If the RHNs decouple before the left-handed neutrinos, i.e. $T_{\nu_R}^{\mathrm{dec}} > T_{\nu_L}^{\mathrm{dec}} \sim 1\,\mathrm{MeV}$, the RHN contribution to the effective number of relativistic degrees of freedom N_{eff}

will be diluted [61]:

$$N_{\text{eff}} \simeq 3 + 3\left[g_*(T_{\nu_L}^{\text{dec}})/g_*(T_{\nu_R}^{\text{dec}})\right]^{4/3}. \tag{2.66}$$

We have $g_*\left(T_{\nu_L}^{\text{dec}}\right) = 43/4$, and recent Planck data constrains $N_{\text{eff}} = 3.30 \pm 0.27$ at 68% C.L. [23] (dependent on the combination of data sets). The RHNs therefore have to decouple before the QCD phase transition, $T_{\nu_R}^{\text{dec}} > 150$–$300\,\text{MeV}$, which yields with Eq. (2.65) a bound on the Yukawa couplings [61]:

$$|w| \lesssim \frac{1}{30}\left(\frac{m_{H_2^+}}{100\,\text{GeV}}\right)\left(\frac{1/\sqrt{2}}{|U_{\ell i}|}\right). \tag{2.67}$$

Earlier decoupling is, of course, possible, but we always expect *some* contribution of the RHNs to N_{eff}, namely $3.14 \lesssim N_{\text{eff}} \lesssim 3.29$ for $150\,\text{MeV} \lesssim T_{\nu_R}^{\text{dec}} \lesssim 200\,\text{GeV}$, assuming only SM degrees of freedom. These values can even explain the long-standing deviation of the best-fit value of N_{eff} from the SM value 3.046, as recently emphasized in Ref. [109]. Consequently, the second Higgs doublet H_2 puts the RHNs in equilibrium above the EWPT to generate the baryon asymmetry, then naturally decouples them to satisfy and ameliorate cosmological constraints. Taking the flavor structure of the Yukawa couplings $w_{\alpha\beta}$ into account will modify the discussion a bit, but goes beyond the scope of this thesis. We refer to Refs. [61, 106] for a detailed discussion of the phenomenology of the neutrinophilic H_2, which is still valid for our extension with lepton-number-violating Dirac neutrinos.

In summary, Dirac neutrinos with lepton-number-violating interactions make possible a new way to create a lepton asymmetry in the early Universe. In the simplest model presented here, this asymmetry resides in the RHN sector and requires a second Higgs doublet to transfer it to the left-handed leptons and ultimately baryons. If the second doublet couples exclusively to neutrinos, its small vacuum expectation value can in addition provide a natural explanation for the smallness of the neutrino masses without invoking small Yukawa couplings. The unavoidable partial thermalization of the RHNs distinguishes this mechanism from neutrinogenesis (Sec. 2.1.2), as it contributes to the relativistic degrees of freedom in perfect agreement with the persisting observational hints. Together with the ensuing collider phenomenology of the second Higgs doublet and, of course, the predicted absence of neutrinoless double beta decay, this model can be falsified in current and upcoming experiments.

2.4 Conclusion

In this chapter we have studied various realizations of an abelian $B-L$ gauge symmetry. Seeing as this corresponds to the only *unflavored* subgroup of the greater symmetry $\mathcal{G}$ motivated in Sec. 1.5, it is, of course, incapable to shed any light on the peculiar mixing pattern displayed by neutrinos; $B-L$ *is*, however, directly connected to the question whether neutrinos are Majorana or Dirac particles, and of crucial importance for understanding the matter–antimatter asymmetry of our Universe. If the gauged $U(1)_{B-L}$ is broken spontaneously by a scalar carrying *two* units of $B-L$, Majorana masses for the right-handed neutrinos ν_R are generated, which trickle down to naturally small Majorana masses for the active neutrinos via the seesaw mechanism—most likely inducing the signature process of this framework:

neutrinoless double beta decay ($0\nu2\beta$). In addition, the decay of the heavy ν_R can give rise to a lepton asymmetry in the early Universe, transferred to a baryon asymmetry by sphalerons. This well-known scenario is however not the only possible fate of the $U(1)_{B-L}$. As we have pointed out, current data is completely compatible with an *unbroken* $B-L$ gauge symmetry, the gauge boson acquiring a gauge-invariant mass by means of the Stückelberg mechanism. Neutrinos are then necessarily Dirac particles and there even exists a leptogenesis mechanism to explain our matter–antimatter asymmetry. This *neutrinogenesis* relies crucially on the non-thermalization of the right-handed neutrino partners, effectively hiding them from the sphalerons. Unbroken $B-L$ predicts Dirac neutrinos, the absence of $0\nu2\beta$, and, like all models in this chapter, a new vector boson Z'. For unbroken $B-L$, however, the Z' mass is a completely independent parameter, and can therefore be probed not only at colliders, but also in low-energy experiments.

Besides unbroken $B-L$ and Majorana $B-L$, we also proposed here a third phenomenologically interesting realization of $U(1)_{B-L}$, spontaneously broken by *four* units. Neutrinos are then Dirac particles (like in unbroken $B-L$) but lepton number *is* violated (similar to Majorana $B-L$). These appropriately named lepton-number-violating Dirac neutrinos arise in simple models and can mediate $\Delta L=4$ interactions (more generally $\Delta(B-L)=4$). Such interactions unavoidably involve many particles and are even more challenging to explore than the already difficult $\Delta(B-L)=2$ processes associated with Majorana $B-L$. Still, following the same arguments that lead to neutrinoless *double* beta decay $0\nu2\beta$ as the prime option to probe $\Delta(B-L)=2$, we consider neutrinoless *quadruple* beta decay ($0\nu4\beta$) as a probe for $\Delta(B-L)=4$. Surprisingly, there actually are some beta-stable nuclei that could, in principle, undergo $0\nu4\beta$ (see Tab. 2.1)—always competing with the SM-allowed double beta decay $2\nu2\beta$—with appreciable energy release, e.g. $Q_{0\nu4\beta}\simeq 2\,\text{MeV}$ in ^{150}Nd. If the experimental challenges for the detection of such a process can be overcome, it should be possible to use $0\nu4\beta$ to set interesting bounds on $\Delta(B-L)=4$ interactions. Alas, theoretical estimates for the lifetime of $0\nu4\beta$ in our toy model are beyond discouraging, and it is conceivable that even more elaborate model-building extensions cannot lead to observable rates.

Besides $0\nu4\beta$, lepton-number-violating Dirac neutrinos can in any case play an important role in the early Universe. In the hot dense plasma, the $\Delta(B-L)=4$ interactions can easily be relevant and generate a lepton asymmetry. As a simple realization, we considered the $\Delta(B-L)=4$ decay of newly introduced scalars into two right-handed neutrinos ν_R, generating an asymmetry Δ_{ν_R}. Since the Dirac-neutrino masses are too small to transfer this asymmetry to the left-handed fermions, a second Higgs doublet has been introduced to thermalize the ν_R and ultimately generate a baryon asymmetry out of Δ_{ν_R}. Not only is this a novel leptogenesis mechanism for Dirac neutrinos, the necessary thermalization of the ν_R makes it testable, as they will contribute $\Delta N_{\text{eff}}\simeq 0.14$–$0.29$ to the relativistic degrees of freedom in the early Universe $N_{\text{eff}}^{\text{SM}}\simeq 3.05$, in perfect agreement with recent measurements.

Should the Dirac nature of neutrinos be experimentally confirmed by a combination of neutrino-mass results, we can not conclude that lepton number is a conserved quantity, as often stated. Lepton number, or more appropriately $B-L$, *can* be exactly conserved, but it can also be broken by higher units than two, motivating experimental efforts to explore these new signatures and theoretical studies to provide more testable models.

Chapter 3

Flavored Symmetries

In Sec. 1.5 we have shown that with three right-handed neutrinos in addition to the SM particle content, the much larger group

$$G_{\text{SM}} \times \mathcal{G} = SU(3)_C \times SU(2)_L \times U(1)_Y \times U(1)_{B-L} \times U(1)_{L_e-L_\mu} \times U(1)_{L_\mu-L_\tau}\,, \tag{3.1}$$

is free of anomalies, motivating a study of $\mathcal{G}$. Every $U(1)'$ subgroup of $\mathcal{G}$ is, of course, automatically anomaly-free and many of them have already been discussed in the literature (for an incomplete list see Refs. [110–118]). A discussion of the full breakdown $\mathcal{G} \to$ nothing—and its connection to neutrino mass and mixing—lies outside the realm of this thesis, as it involves many parameters and new scalars. Instead, we focus on an effective model of a possible last step of the breakdown $\mathcal{G} \to U(1)'$, i.e. we consider only $U(1)'$ subgroups of $\mathcal{G}$, generated by Y', a linear combination of the generators:

$$Y' = \alpha(B-L) + \beta(L_e - L_\mu) + \gamma(L_\mu - L_\tau)\,. \tag{3.2}$$

$U(1)'$ models have the advantage of a simple scalar sector with tree-level couplings to the RHNs, almost identical to the case discussed in Sec. 2.2.3. A more elaborate embedding of our $U(1)'$ models into the larger group $G_{\text{SM}} \times \mathcal{G}$ is, of course, desirable, should any of the approaches presented in this chapter be experimentally verified. In the following, we will only consider *Majorana* neutrinos and make use of the seesaw mechanism introduced in Sec. 2.2.1. The $U(1)'$ groups considered here will then typically only allow for some select Majorana mass terms $(\mathcal{M}_R)_{ij}$, all others being induced by spontaneously breaking the $U(1)'$ with an SM-singlet scalar.

The question thus arises which subgroup of $\mathcal{G}$ should be chosen, i.e. what values α, β, and γ in Eq. (3.2) are most interesting. We have already discussed the *unflavored* part (with $\beta = \gamma = 0$) in Ch. 2, so we will turn on the flavor in this chapter. With non-vanishing β or γ, the *flavored* abelian gauge symmetry $U(1)'$ will have significant influence on leptonic mixing, which might help us to understand the peculiar mixing pattern observed in neutrinos (see Sec. 1.1). (Note that all $U(1)' \subset \mathcal{G}$ are unflavored when it comes to quarks, and can thus not explain the pattern of the CKM matrix (1.8).) Symmetry origins of neutrino mixing are a popular topic of research, typically using *discrete non-abelian global* symmetries to generate precisely the observed mixing angles from Tab. 1.2 (see Ref. [20] for a review). Efforts in this direction have reached an uncomfortably baroque complexity in order to remain valid, with dozens of unobservably heavy particles and parameters, not to mention typical problems such as vacuum alignment and domain walls. In this chapter we instead motivate the use of *continuous abelian local* symmetries to learn something about lepton mixing, which are very economic—few additional parameters and particles—and renormalizable.

As far as *approximate flavor symmetries* in the Majorana neutrino mass matrix $\mathcal{M}_\nu$ go, three interesting cases for abelian symmetries have been identified already in Ref. [119] (see also Ref. [120]):

- L_e symmetry for normal hierarchy (NH),
- $\overline{L} \equiv L_e - L_\mu - L_\tau$ for inverted hierarchy (IH), and
- $L_\mu - L_\tau$ for quasi-degenerate neutrinos (QD),

with corresponding neutrino mass matrices of the form

$$\mathcal{M}_\nu^{L_e} \sim \begin{pmatrix} 0 & 0 & 0 \\ 0 & \times & \times \\ 0 & \times & \times \end{pmatrix}, \qquad \mathcal{M}_\nu^{\overline{L}} \sim \begin{pmatrix} 0 & \times & \times \\ \times & 0 & 0 \\ \times & 0 & 0 \end{pmatrix}, \qquad \mathcal{M}_\nu^{L_\mu - L_\tau} \sim \begin{pmatrix} \times & 0 & 0 \\ 0 & 0 & \times \\ 0 & \times & 0 \end{pmatrix}, \tag{3.3}$$

where $\times$ denotes a nonzero entry. Small corrections to one of these matrices can then lead to valid neutrino mass and mixing parameters. This already hints at a deep connection between abelian symmetries and neutrino properties, to be exploited in Secs. 3.1 (NH), 3.2 (IH), and 3.3 (QD), where we promote the corresponding approximate global symmetries to *gauge* symmetries.[1] Besides motivating neutrino hierarchies and the structure of mixing angles, such *local* flavor symmetries bring with them a new vector boson Z' to test the symmetry in complementary ways outside of the neutrino sector, making them not only simple, but also testable.

In Sec. 3.4 we will take a different approach and discuss flavor symmetries $U(1)' \subset \mathcal{G}$ that generate texture zeros or vanishing minors in the neutrino mass matrix $\mathcal{M}_\nu$. Two independent zeros (or vanishing minors) in the active neutrino mass matrix $\mathcal{M}_\nu$ then imply four constraints on the nine low-energy parameters (m_1, m_2, m_3), $(\theta_{23}, \theta_{12}, \theta_{13})$ and $(\delta, \varphi_1, \varphi_2)$ (CP violating phases), making them in principle distinguishable with future data. Our approach not only provides new testing ground for flavor symmetries, but also allows to check for the flavor symmetry behind the texture zeros at the LHC.

This chapter is based on the publications "Neutrino hierarchies from a gauge symmetry" [3], "Gauged $L_\mu - L_\tau$ symmetry at the electroweak scale" [4] (both in collaboration with W. Rodejohann), and "Vanishing minors in the neutrino mass matrix from abelian gauge symmetries" [5] (in collaboration with T. Araki and J. Kubo), as well as the proceedings in Refs. [6, 7].

3.1 Neutrino Hierarchies: Normal Spectrum

As already mentioned in the introduction to this chapter, the mixing parameters from Tab. 1.2 for NH hint at an approximate L_e symmetry in the Majorana-neutrino mass matrix $\mathcal{M}_\nu = U_{\text{PMNS}}^* \text{diag}(m_1, m_2, m_3) U_{\text{PMNS}}^\dagger$, i.e. the pattern

$$\mathcal{M}_\nu^{L_e} \sim \begin{pmatrix} 0 & 0 & 0 \\ 0 & \times & \times \\ 0 & \times & \times \end{pmatrix}. \tag{3.4}$$

[1] Except for $L_\mu - L_\tau$, these symmetries have so far only been considered as global [120–129] or anomalous [130] symmetries.

This structure arises simply by imposing a $U(1)_{L_e}$ symmetry, i.e. invariance under $\nu_e \to e^{i\theta}\nu_e$, on $\overline{\nu}^c_{L,\alpha}\mathcal{M}_{\alpha\beta}\nu_{L,\beta}$, and leads to a massless $\nu_1 = \nu_e$ and two massive neutrinos $\nu_{2,3}$ (mixtures of ν_μ and ν_τ). This is a good approximation to the NH case, as can be seen already from Fig. 1.1; corrections $\Delta\mathcal{M}_\nu$ to $\mathcal{M}_\nu^{L_e}$ are, of course, necessary to mix some of ν_e into the mass eigenstates $\nu_{2,3}$, i.e. generate a nonzero θ_{12} and θ_{13}. For a *global* $U(1)_{L_e}$, these symmetry-breaking corrections $\Delta\mathcal{M}_\nu$ need to be put in by hand, because spontaneous breaking would result in a potentially problematic Goldstone boson. Not much can be learned this way, so we will try to impose the structure $\mathcal{M}_\nu^{L_e}$ by a *gauge* symmetry, $\Delta\mathcal{M}_\nu$ being generated by spontaneous symmetry breaking, necessary anyways to generate the Z' mass $M_{Z'}/g' \gtrsim \mathcal{O}(\text{TeV})$ (similar to the bounds of Sec. 2.1.1).

3.1.1 The Right Symmetry

$U(1)_{L_e}$ is not easily promoted to a gauge symmetry, due to the anomalies mentioned in Sec. 1.5. We can, however, simply take the $\mathcal{G}$ subgroup $B - 3L_e$, which is anomaly-free with three RHNs and has the same effect as $U(1)_{L_e}$ in the lepton sector. Surprisingly, this approach still fails, at least when a seesaw mechanism similar to Sec. 2.2.1 is used: The $U(1)_{B-3L_e}$ symmetry imposes the structure (3.4) on the *right-handed* mass matrix $\mathcal{M}_R^{L_e}$, while the Dirac mass matrix m_D can be taken to be diagonal. The naive seesaw formula $\mathcal{M}_\nu \simeq -m_D^T(\mathcal{M}_R^{L_e})^{-1}m_D$ is not applicable, because $\mathcal{M}_R^{L_e}$ is *not invertible*. Even if we introduce small corrections $\Delta\mathcal{M}_R$ that make $\mathcal{M}_R \equiv \mathcal{M}_R^{L_e} + \Delta\mathcal{M}_R$ invertible, we will *not* end up with a matrix $\mathcal{M}_\nu$ that has an approximate L_e symmetry. Roughly said, two matrices $\mathcal{M}$ and $\mathcal{M}^{-1}$ can only have the same approximate symmetry if $\mathcal{M}$ is *invertible* in the exact-symmetry limit. This is not the case for the L_e symmetry in Eq. (3.4).

Counterintuitively, the appropriate gauge symmetry for NH via seesaw—yielding an approximate $\mathcal{M}_\nu^{L_e}$—is the anomaly-free $\mathcal{G}$ subgroup $U(1)_{B+3\overline{L}}$. To see this, we show the Dirac and Majorana mass matrices in the case of unbroken $B + 3\overline{L}$:

$$m_D = \begin{pmatrix} a & 0 & 0 \\ 0 & b & c \\ 0 & d & e \end{pmatrix}, \qquad \mathcal{M}_R^{\overline{L}} = \begin{pmatrix} 0 & X & Y \\ X & 0 & 0 \\ Y & 0 & 0 \end{pmatrix}. \tag{3.5}$$

The matrix $\mathcal{M}_R^{\overline{L}}$ is again singular, so the usual seesaw formula $\mathcal{M}_\nu \simeq -m_D^T(\mathcal{M}_R^{\overline{L}})^{-1}m_D$ for the light neutrinos in the limit $X, Y \gg (m_D)_{ij}$ is not applicable. Instead of the $3\,\nu_{\text{light}} + 3\,\nu_{\text{heavy}}$ scheme known from seesaw, the diagonalization of the full 6×6 matrix leads to the hierarchy $2\,\nu_{\text{heavy}} + 2\,\nu_{\text{electroweak}} + 2\,\nu_{\text{light}}$, not in agreement with experiments.

Since the model looks quite different after $U(1)'$ breaking, let us introduce an SM-singlet complex scalar field $S \sim (\mathbf{1},\mathbf{1},0)(+6)$ which acquires a VEV $\langle S\rangle \gtrsim \mathcal{O}(\text{TeV})$ in complete analogy to the Majorana $B - L$ scenario of Sec. 2.2. S couples to the RHNs via $\overline{S}\,\overline{\nu}^c_{R,e}\nu_{R,e}$ etc. in such a way that all the zeros in $\mathcal{M}_R^{\overline{L}}$ are filled by entries A, B, C, D, all proportional to $\langle S\rangle$. As a result, $\mathcal{M}_R = \mathcal{M}_R^{\overline{L}} + \Delta\mathcal{M}_R$ is in general an invertible matrix after $B + 3\overline{L}$ breaking:

$$\mathcal{M}_R = \begin{pmatrix} A & X & Y \\ \cdot & B & C \\ \cdot & \cdot & D \end{pmatrix}, \quad \mathcal{M}_R^{-1} = -\frac{1}{\det\mathcal{M}_R}\begin{pmatrix} C^2 - BD & DX - CY & BY - CX \\ \cdot & Y^2 - AD & AC - XY \\ \cdot & \cdot & X^2 - AB \end{pmatrix}. \tag{3.6}$$

The scaling $X, Y \gg \langle S\rangle \gg (m_D)_{ij}$ leads to the order-of-magnitude structure of the low-energy neutrino mass matrix

$$\mathcal{M}_\nu \simeq -m_D^T \mathcal{M}_R^{-1} m_D \sim \begin{pmatrix} 0 & 0 & 0 \\ \cdot & 1 & 1 \\ \cdot & \cdot & 1 \end{pmatrix} + \begin{pmatrix} \varepsilon^2 & \varepsilon & \varepsilon \\ \cdot & 0 & 0 \\ \cdot & \cdot & 0 \end{pmatrix}, \tag{3.7}$$

with $\varepsilon \equiv \langle S\rangle / X$. Consequently, a low $B + 3\overline{L}$ breaking scale $\varepsilon \sim 0.1$ actually leads to a mass matrix that approximately conserves L_e (3.4), as we have claimed above (and was already noted in Refs. [123, 129]).

Our spontaneously broken $U(1)_{B+3\overline{L}}$ symmetry does however not generate the most *general* L_e symmetric matrix, because the zeroth-order mass matrix has the structure

$$\mathcal{M}_\nu \sim \begin{pmatrix} 0 & 0 & 0 \\ \cdot & (dX - bY)^2 & (dX - bY)(eX - cY) \\ \cdot & \cdot & (eX - cY)^2 \end{pmatrix} + \mathcal{O}(\varepsilon)\,, \tag{3.8}$$

which gives only *one* massive neutrino $\nu_3 \sim (dX - bY)\,\nu_\mu + (eX - cY)\,\nu_\tau$ at leading order. This is easily understood by noting that $\mathcal{M}_R$ has rank 2 in the symmetry limit, i.e. only two massive ν_R. The third ν_R gains a much smaller mass from $\langle S\rangle \sim \Delta\mathcal{M}_R \ll \mathcal{M}_R^{\overline{L}}$, that is however the *dominant* effect in $\mathcal{M}_\nu \sim \mathcal{M}_R^{-1}$, making *one* of the active neutrinos way heavier than the other two. At leading order, the $U(1)_{B+3\overline{L}}$ symmetry thus generates one massive neutrino $\nu_3 = s_{23}\nu_\mu + c_{23}\nu_\tau$, which is a good approximation for the normal neutrino hierarchy spectrum (cf. Fig. 1.1). The solar mixing angle is still undefined at this order, due to an accidental $O(2)$ symmetry of the matrix—the two approximately massless neutrinos can still be rotated into each other (see Ref. [11]). Since the symmetry allows for mixing of μ and τ, the charged lepton mass matrix is not diagonal in general and contributes to θ_{23}. The atmospheric mixing angle will therefore receive a contribution from the charged-lepton mixing *and* from the neutrino diagonalization

$$\tan\theta_{23}^\nu \simeq \frac{dX - bY}{eX - cY}\,, \tag{3.9}$$

so we expect large but non-maximal mixing for θ_{23}.

Analytical expressions for the $\mathcal{O}(\varepsilon)$ corrections to the above picture can be obtained in a straightforward but bothersome manner. For a qualitative overview, we rather show the distribution of the mixing angles θ_{12} and θ_{13} in Fig. 3.1. For these we generated random Yukawa couplings $|(m_D)_{ij}| \leq 1$, symmetry-breaking parameters $|A|, |B|, \cdots < \varepsilon$, and $\overline{L}$ symmetric $\mathcal{M}_R$ entries $|X|, |Y| > 1$ that lead to neutrino mixing parameters in their 3σ range [131].[2] Here we restrict the parameters to real values for simplicity, resulting in vanishing CP-violating phases in the mixing matrix. In any case, since the Yukawa couplings can have arbitrary phases, we do not expect our model to be able to predict the CP-violating phases. The solar angle tends to be large, while the reactor angle θ_{13} is generally small, but in good agreement with the recent results of $\sin^2\theta_{13} \simeq 0.025$–$0.03$. The units of m_D and $\mathcal{M}_R$ have not been specified yet, because they only fix the overall neutrino mass scale—and

[2] Not much would change using the newer data from Tab. 1.2.

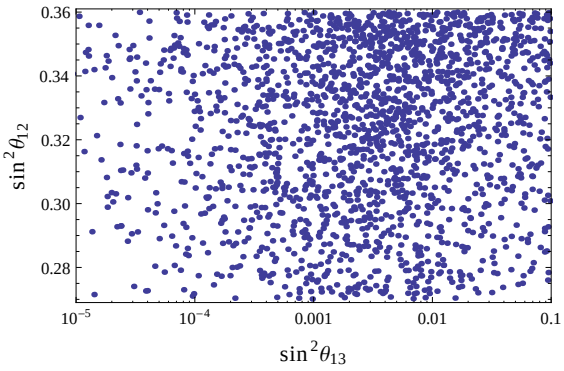

Figure 3.1: Scatter plots using the broken $B + 3\overline{L}$ low-energy neutrino mass matrix (3.7) ($\varepsilon = 0.05$) that leads to NH. The accepted values of the mixing parameters satisfy the 3σ bounds from Ref. [131], except for θ_{23}, because it can be arbitrarily adjusted by the charged-lepton contribution.

hence the Δm^2_{ij}—but not the mixing angles. In the usual seesaw manner, the magnitude $m_D^2/\mathcal{M}_R \simeq 0.1\,\text{eV}$ does not fix the seesaw scale, but naturalness hints at a high scale.

We have thus succeeded in connecting the normal hierarchy of neutrinos to an abelian gauge symmetry $U(1)_{B+3\overline{L}}$. While this approach can not predict *precise* values for the neutrino parameters, it does motivate their qualitative structure—large θ_{23} and θ_{12}, small θ_{13}—already impressive considering the simplicity of the model. The size of the corrections ε necessary for viable neutrino mixing then fixes the ratio of $U(1)$ symmetry-breaking VEV $\langle S\rangle$ to the seesaw scale $X \sim \langle S\rangle/\varepsilon$. Note that $0\nu2\beta$ rates are expected to be small, seeing as $m_{ee} \sim \varepsilon^2$ in this model.

A word about previous work: The gauge symmetry $U(1)_{B+3\overline{L}}$ was proposed in Ref. [117] as an origin for R-parity, noting that $B+3\overline{L}$ successfully forbids dangerous proton decay via higher-dimensional operators such as $QQQL$. This operator conserves $B-L$, the most popular R-parity extension, but violates $B-\sum_\ell x_\ell L_\ell$ if $x_\ell \neq 1$; spontaneous symmetry breaking of $B+3\overline{L}$ via $S \sim 6$, as necessary for viable neutrino phenomenology, then results in a remnant $\mathbb{Z}_6$ symmetry that renders the proton completely stable—a welcome additional feature of $U(1)_{B+3\overline{L}}$. It should be stressed that even though we are taking a non-supersymmetric model for simplicity, a similar discussion holds for the supersymmetric case of Ref. [117]. Supersymmetric particles aside, the main difference is the need for a second complex scalar (super-)field to fill the vanishing entries in the neutrino mass matrix. The model (superpotential, mass spectrum etc.) is then similar to supersymmetric $B-L$ models, which are intensively discussed in e.g. Refs. [132–134]. Assuming similar vacuum expectation values for both scalars makes the discussion of neutrino masses identical to our discussion here.

3.1.2 Gauge Boson

Before we move on to gauge-symmetry realizations of an inverted neutrino spectrum in the next section, let us comment on the boson sector of our flavored $U(1)'$ symmetries. The scalar potential of our $U(1)_{B+3\overline{L}}$ model is the same as for $U(1)_{B-L}$ in Sec. 2.2.3, because we just introduced an SM-singlet complex scalar $S \sim (\mathbf{1},\mathbf{1},0)(+6)$ with a VEV $\langle S\rangle = v_S/\sqrt{2}$—generating a Z' mass $M_{Z'} = 6|g'v_S|$. The mixing of $\text{Re}\,S$ and the Higgs h is therefore not particularly helpful to distinguish the various $U(1)'$ symmetries discussed in this thesis.

The Z' phenomenology of $U(1)_{B+3\overline{L}}$ is, however, different enough from $U(1)_{B-L}$ to distinguish the cases: The coupling to quarks/baryons is identical, but the Z' branching ratios into

leptons will differ significantly, for example

$$\frac{\mathrm{BR}\left(Z'_{B+3\overline{L}} \to \overline{e}e\right)}{\mathrm{BR}\left(Z'_{B+3\overline{L}} \to \overline{b}b\right)} = 9 \times \frac{\mathrm{BR}\left(Z'_{B-L} \to \overline{e}e\right)}{\mathrm{BR}\left(Z'_{B-L} \to \overline{b}b\right)} \,. \tag{3.10}$$

The gauge boson of $U(1)_{B+3\overline{L}}$ can even lead to effects at energies $E \ll M_{Z'}$, for example loop-induced deviations from lepton universality. More specifically, we expect slightly different cross sections for electrons than for muons and tauons (which are universal under $U(1)_{B+3\overline{L}}$). No such deviation has been observed so far, but might arise in the future. The prospects of detecting the heavy Z' at the LHC were discussed in Ref. [117]; for $g' = 0.1$ the final stage of the LHC ($\sqrt{s} = 14\,\mathrm{TeV}$, integrated luminosity $L \simeq 100\,\mathrm{fb}^{-1}$) can probe the model up to $M_{Z'} \simeq 3.6\,\mathrm{TeV}$ via the dilepton Z' resonance.

Let us present some actual bounds on the gauge boson of our $U(1)_{B+3\overline{L}}$ scenario after all these qualitative considerations. Extending the SM gauge group $G_{\mathrm{SM}} \equiv SU(3)_C \times SU(2)_L \times U(1)_Y$ by $U(1)'$ leads to possible Z–Z' mixing, either from the VEV of a scalar in a non-trivial representation of $SU(2)_L \times U(1)_Y$ *and* $U(1)'$, or via the kinetic mixing angle χ that connects the $U(1)$ field strength tensors (see App. B for details). The relevant Lagrange density $\mathcal{L} = \mathcal{L}_{\mathrm{SM}} + \mathcal{L}_{Z'} + \mathcal{L}_{\mathrm{mix}}$ after breaking $SU(2)_L \times U(1)_Y \times U(1)'$ to $U(1)_{\mathrm{EM}}$ then consists of

$$\begin{aligned}
\mathcal{L}_{\mathrm{SM}} &= -\frac{1}{4}\hat{B}_{\mu\nu}\hat{B}^{\mu\nu} - \frac{1}{4}\hat{W}^a_{\mu\nu}\hat{W}^{a\mu\nu} + \frac{1}{2}\hat{M}_Z^2\hat{Z}_\mu\hat{Z}^\mu - \frac{\hat{e}}{\hat{c}_W}j_Y^\mu\hat{B}_\mu - \frac{\hat{e}}{\hat{s}_W}j^{a\mu}_{SU(2)}\hat{W}^a_\mu \,, \\
\mathcal{L}_{Z'} &= -\frac{1}{4}\hat{Z}'_{\mu\nu}\hat{Z}'^{\mu\nu} + \frac{1}{2}\hat{M}^2_{Z'}\hat{Z}'_\mu\hat{Z}'^{\mu} - \hat{g}'j'^{\mu}\hat{Z}'_\mu \,, \\
\mathcal{L}_{\mathrm{mix}} &= -\frac{\sin\chi}{2}\hat{Z}'^{\mu\nu}\hat{B}_{\mu\nu} + \delta\hat{M}^2\hat{Z}'_\mu\hat{Z}^\mu \,.
\end{aligned} \tag{3.11}$$

Since the above gauge eigenstates have a non-diagonal mass matrix and kinetic terms, the physical mass eigenstates are linear combinations of the hatted fields (App. B). Setting for simplicity the kinetic mixing angle χ to zero, the transformation to the mass eigenstates Z_1 and Z_2 takes the simple form

$$\begin{pmatrix} Z_1 \\ Z_2 \end{pmatrix} = \begin{pmatrix} \cos\theta & \sin\theta \\ -\sin\theta & \cos\theta \end{pmatrix} \begin{pmatrix} \hat{Z} \\ \hat{Z}' \end{pmatrix}, \quad \tan 2\theta = \frac{2\,\delta\hat{M}^2}{\hat{M}_Z^2 - \hat{M}_{Z'}^2} \,, \tag{3.12}$$

with the Z–Z' mixing angle θ, modifying the couplings of the gauge bosons to fermions. Using a modified version of GAPP [135,136] to fit our model with an arbitrary scalar sector we obtain the 95% C.L. limit $|g' \sin\theta| \lesssim 10^{-4}$ (see Fig. 3.2) from electroweak precision data. Constraints for the mass $M_{Z'}$ are obtained from collider searches, as the gauge boson of $U(1)_{B+3\overline{L}}$ couples directly to first-generation particles. LEP-2 searches for new physics give a stronger limit than Tevatron, namely $M_{Z'}/g' \gtrsim 13.5\,\mathrm{TeV}$ at 95% C.L. [66,67], because the Z' couples strongly to the electron ($Y'(e) = 3$); this translates into a bound on the VEV of $v_S > 2.3\,\mathrm{TeV}$. Since v_S is also connected to the seesaw scale via $\langle S\rangle \sim \varepsilon\mathcal{M}_R$ (Eq. (3.7)), one could also consider $v_S \sim 10^{15}\,\mathrm{GeV}$, which would make Z' and s pretty much impossible to observe. It is therefore more interesting to consider the low-energy end of the seesaw scale, which can lead to observable effects.

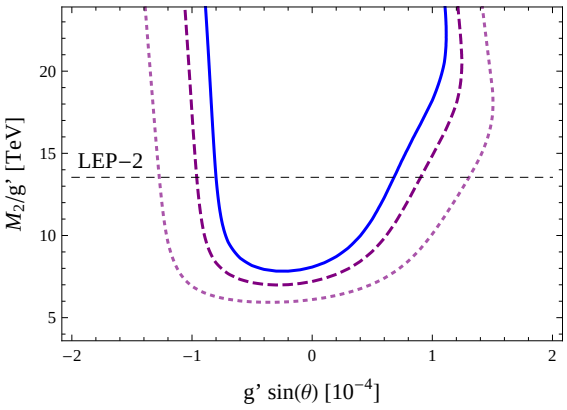

Figure 3.2: χ^2 contours in the M_2–sin(θ) plane, corresponding to 90%, 95%, and 99% C.L. The horizontal dashed line is the 95% C.L. lower limit from LEP-2 [66, 67].

We note that the non-universal lepton coupling of $B + 3\overline{L}$ also gives rise to non-standard neutrino interactions (NSIs), which are usually parametrized by the non-renormalizable effective Lagrangian

$$\mathcal{L}_{\text{NSI}}^{\text{eff}} = -2\sqrt{2}G_F\varepsilon_{\alpha\beta}^{fP}\left[\bar{f}\gamma^\mu P f\right]\left[\bar{\nu}_\alpha\gamma_\mu P_L\nu_\beta\right], \tag{3.13}$$

in our case obtained upon integrating out the heavy gauge boson Z'. Without going into details, we can estimate

$$\varepsilon_{\alpha\beta} \sim \frac{v_{EW}^2}{(M_{Z'}/g')^2}\,\text{diag}(1,-1,-1) = \frac{v_{EW}^2}{(M_{Z'}/g')^2}\,\text{diag}(2,0,0) + \frac{v_{EW}^2}{(M_{Z'}/g')^2}\,\text{diag}(1,1,1)\,. \tag{3.14}$$

The magnitude is very small ($\varepsilon \sim 10^{-4}$) and since the term proportional to the identity matrix does not affect oscillations, we actually only induce ε_{ee}, i.e. modify the usual matter potential, which is hard to measure.

In the following we will ignore any Z–Z' mixing, be it mass mixing (not induced at tree-level in our minimal model) or kinetic mixing; with $\mathcal{L}_{\text{mix}} = 0$ we can omit all the hats of the parameters in Eq. (3.11). See App. B for a more detailed discussion of Z–Z' mixing and relevant references.

3.2 Neutrino Hierarchies: Inverted Spectrum

In the previous section we have found a way to connect the normal neutrino hierarchy to an abelian gauge symmetry. For this, the $\mathcal{G}$ subgroup $U(1)_{B+3(L_e-L_\mu-L_\tau)}$ was spontaneously broken, leading to an approximately L_e symmetric neutrino mass matrix $\mathcal{M}_\nu$ after seesaw. We want to repeat this procedure to generate an *inverted* neutrino spectrum, i.e. an approximately $\overline{L} \equiv L_e - L_\mu - L_\tau$ symmetric neutrino mass matrix

$$\mathcal{M}_\nu^{\overline{L}} \sim \begin{pmatrix} 0 & \times & \times \\ \times & 0 & 0 \\ \times & 0 & 0 \end{pmatrix}. \tag{3.15}$$

This appears as a trivial exercise after the work of Sec. 3.1, but proves to be more difficult. We have already learned that an $\overline{L}$ symmetric $\mathcal{M}_R$ will not lead to an $\overline{L}$ symmetric $\mathcal{M}_\nu$

after seesaw, but rather an L_e symmetric one. Turning this around, it seems to be a good idea to impose an L_e symmetry on $\mathcal{M}_R$—better yet an anomaly-free $U(1)_{B-3L_e}$—hoping for an $\overline{L}$ symmetric $\mathcal{M}_\nu$ after the seesaw dust has settled. This fails for the same reason that it works in Sec. 3.1: $\mathcal{M}_R^{\overline{L}}$ has rank 2, so spontaneous symmetry breaking will give a mass to the third ν_R much smaller than $\mathcal{M}_R^{\overline{L}}$. This small mass will dominate in the seesaw formula $\mathcal{M}_\nu \sim \mathcal{M}_R^{-1}$, making *one* of the active neutrinos much heavier than the others. This is good for NH but terrible for IH, which rather requires *two* almost degenerate massive neutrinos (as can be seen from Fig. 1.1). A different approach is therefore needed to generate inverted hierarchy from an abelian gauge symmetry.

3.2.1 Three Right-Handed Neutrinos and a $\mathbb{Z}_2$ Symmetry

The reason for the different approximate symmetries in $\mathcal{M}_R$ and $\mathcal{M}_R^{-1}$ is the occurring vanishing eigenvalue of $\mathcal{M}_R$ in the unbroken case. To solve this problem, we will decouple the zero mode, i.e. forbid a coupling of the "massless" ν_R to the active neutrinos. The massless eigenvector of the matrix $\mathcal{M}_R^{\overline{L}}$ (3.15) is a linear combination of $\nu_{R,2}$ and $\nu_{R,3}$. We can, without loss of generality, choose to decouple $\nu_{R,3}$ from the other ν_R, which just corresponds to an unphysical rotation in $\nu_{R,2}$–$\nu_{R,3}$ space. The decoupling is accomplished with an additional $\mathbb{Z}_2$ symmetry under which $\nu_{R,3}$ transforms as $\nu_{R,3} \to -\nu_{R,3}$ while all other fields are even.[3] The only allowed interactions for $\nu_{R,3}$ are then

$$\begin{aligned}\mathcal{L}_{\nu_{R,3}} &= i\overline{\nu}_{R,3}\gamma^\mu\left(\partial_\mu - i(-3)g'Z'_\mu\right)\nu_{R,3} - Y_\chi S\,\overline{\nu}^c_{R,3}\nu_{R,3} + \text{h.c.} \\ &= \frac{i}{2}\chi^T\mathcal{C}\gamma^\mu\partial_\mu\chi - \frac{3}{2}g'Z'_\mu\chi^T\mathcal{C}\gamma^\mu\gamma_5\chi - \underbrace{Y_\chi\frac{v_S}{\sqrt{2}}}_{M_\chi/2}\chi^T\mathcal{C}\chi\left(1+\frac{s}{v_S}\right),\end{aligned} \tag{3.16}$$

making it massive and stable after $B+3\overline{L}$ breaking. In the last line we replaced the right-handed Dirac fermion $\nu_{R,3}$ by a Majorana fermion $\chi = \nu_{R,3} + \nu^c_{R,3}$ and switched to unitary gauge, in complete analogy to Sec. 2.2. The stable Majorana fermion χ is therefore a candidate for dark matter, to be further examined in Sec. 3.2.3. Note that the stability arises accidentally, as the $\mathbb{Z}_2$ was only introduced to implement an inverted hierarchy for the active neutrinos.

Back to the neutrinos: The left-handed neutrinos now couple only to $\nu_{R,1}$ and $\nu_{R,2}$, so at most *two* active neutrinos acquire mass at tree level [137]. The $B+3\overline{L}$ symmetry is broken in $\mathcal{M}_R$ by the parameters A and B, so with the usual seesaw mechanism we find

$$\mathcal{M}_\nu \simeq -\begin{pmatrix} a & 0 \\ 0 & b \\ 0 & c \end{pmatrix}\begin{pmatrix} A & X \\ X & B \end{pmatrix}^{-1}\begin{pmatrix} a & 0 & 0 \\ 0 & b & c \end{pmatrix} = \frac{1}{X^2-AB}\begin{pmatrix} a^2B & -abX & -acX \\ \cdot & b^2A & bcA \\ \cdot & \cdot & c^2A \end{pmatrix}, \tag{3.17}$$

which features an interesting structure [128,138]: The decoupling of $\nu_{R,3}$ results as intended in an invertible $\mathcal{M}_R^{2\times2}$, so $\mathcal{M}_\nu$ now conserves $L_e - L_\mu - L_\tau$ in the limit $A, B \to 0$. $\mathcal{M}_\nu$ is hence a good mass matrix for IH, with two degenerate massive neutrinos and a massless

[3] This can also be interpreted as an exchange symmetry $\nu_{R,2} \leftrightarrow \nu_{R,3}$ by using the basis $\Psi_1 \sim \nu_{R,2} + \nu_{R,3}$, $\Psi_2 \sim \nu_{R,2} - \nu_{R,3}$.

$\nu_3 = s_{23}\nu_\mu + c_{23}\nu_\tau$ at leading order. This model also gives a simple explicit realization of "scaling" [139,140], seeing as the second and third column of $\mathcal{M}_\nu$ are proportional. Therefore we have an inverted hierarchy solution with $\theta_{13} = 0$, whereas the atmospheric mixing angle is once again large but not maximal, also due to the contributions of the charged leptons. At 2-loop level radiative corrections will induce a nonzero θ_{13}, but of practically irrelevant magnitude [141]. The solar mixing angle becomes *maximal* for $A, B \to 0$, so the breaking scale $\langle S \rangle$ needs to be close to the bare mass term X to lower θ_{12}.

In any case, a vanishing reactor angle θ_{13} is by now excluded (see Tab. 1.2) and requires a modification of our model. As it turns out, θ_{13} and the mass of the lightest neutrino are linked [139,140], so we simply need to make ν_3 massive; one solution would involve breaking the $\mathbb{Z}_2$ in order to couple $\nu_{R,3}$ to the active neutrinos and generate a nonzero θ_{13}, also rendering the DM candidate χ unstable, with a short lifetime compared to the age of the Universe (estimated in our paper [3]). Solutions along this route are bothersome and typically involve the introduction of additional scalars if IH is to be maintained, not to be discussed further. In the next section we will rather show that a slight extension of the fermion sector can easily generate a non-vanishing reactor angle while retaining a simple scalar sector and the exact $\mathbb{Z}_2$ symmetry—leading to IH.

3.2.2 Five Right-Handed Neutrinos and a $\mathbb{Z}_2$ Symmetry

Since the extension by scalars is cumbersome, we seek out a different solution to generate $\theta_{13} \neq 0$. Seeing as the vanishing reactor angle is linked to the vanishing neutrino mass m_3 [139,140], we should try to make all three active neutrinos massive. In the type-I seesaw mechanism employed in this thesis, this simply requires the introduction of more right-handed neutrinos $\nu_{R,j}$; these need to carry lepton numbers, so we can only add them in vector-like pairs, otherwise they would introduce $U(1)_{B+3\overline{L}}$ gauge anomalies (see Sec. 1.5). The simplest possibilities is then to introduce two more RHNs to our $U(1)_{B+3\overline{L}}$ model, $\nu_{R,4} \sim +3$ and $\nu_{R,5} \sim -3$. The full 5×5 matrix $\mathcal{M}_R$ would, of course, again be *singular* in the exact $\overline{L}$ limit, so we still have to introduce our $\mathbb{Z}_2$ to decouple one of the right-handed neutrinos ($\chi \equiv N_3$) and obtain an invertible $\mathcal{M}_R$—leading to an approximately $\overline{L}$ symmetric $\mathcal{M}_\nu$. χ will again be our dark matter candidate, to be discussed in Sec. 3.2.3.

After symmetry breaking with the scalars $H \sim (\mathbf{1}, \mathbf{2}, +1)(0)$ and $S \sim (\mathbf{1}, \mathbf{1}, 0)(+6)$ we obtain the mass matrix for the active neutrinos via the seesaw mechanism

$$\mathcal{M}_\nu \simeq -\begin{pmatrix} a & b & 0 & 0 \\ 0 & 0 & c & d \\ 0 & 0 & e & f \end{pmatrix} \begin{pmatrix} \mathcal{A} & \mathcal{X} \\ \mathcal{X}^T & \mathcal{B} \end{pmatrix}^{-1} \begin{pmatrix} a & 0 & 0 \\ b & 0 & 0 \\ 0 & c & e \\ 0 & d & f \end{pmatrix}, \tag{3.18}$$

where $\mathcal{X}$ is an arbitrary 2×2 matrix (the gauge invariant mass terms for the RHNs) and $\mathcal{A}$, $\mathcal{B}$ are symmetric 2×2 matrices generated by spontaneous $B+3\overline{L}$ breaking. For $cf - ed \neq 0$ there is no massless neutrino $\alpha\,\nu_\mu + \beta\,\nu_\tau$, so we have $\theta_{13} \neq 0$ in general. The solar mixing angle becomes maximal for $\mathcal{A}, \mathcal{B} \to 0$, so the breaking scale needs to be close to the bare mass terms to lower θ_{12}. A large θ_{13} in agreement with recent results also forbids too low a breaking scale, meaning that the breaking parameter should be at least $\varepsilon = \langle S \rangle / |\mathcal{X}| \simeq 0.1$ in our minimal model. For the scatter plots in Fig. 3.3 we generated random Yukawa couplings $|(m_D)_{ij}| \leq 1$,

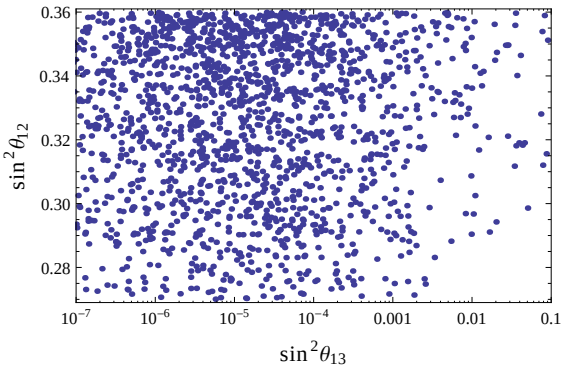

Figure 3.3: Scatter plot using the neutrino mass matrix (3.18) ($\varepsilon = 0.1$) with five RHNs and a $\mathbb{Z}_2$, which leads to IH. The accepted values of the mixing parameters satisfy the 3σ bounds from Ref. [131], except for θ_{23}, because it can be arbitrarily adjusted by the charged-lepton contribution.

$|(\mathcal{A})_{ij}|, |(\mathcal{B})_{ij}| \leq \varepsilon$ and $|(\mathcal{X})_{ij}| > 1$. Except for the approximate $\overline{L}$ symmetry in the limit $\mathcal{A}_{ij}, \mathcal{B}_{ij} \ll \mathcal{X}_{mn}$ (and the corresponding inverted hierarchy) there is no further structure in $\mathcal{M}_\nu$, so we refrain from any analytical discussion. Since IH requires $m_{ee} \gtrsim 10^{-2}\,\text{eV}$, it can in principle be completely probed in $0\nu2\beta$ experiments.

This accomplishes our goal to impose the inverted neutrino hierarchy by means of an abelian gauge symmetry. Surprisingly, it is the same $U(1)' = U(1)_{B+3\overline{L}}$ that lead to NH in Sec. 3.1, albeit accompanied not only by two more RHNs, but also a $\mathbb{Z}_2$ symmetry. This $\mathbb{Z}_2$ symmetry was required in the neutrino sector in order to obtain IH solutions, but accidentally stabilizes one of the new fermions. The rest of this section is devoted to a discussion of this naturally arising DM candidate.

3.2.3 Dark Matter

As we have seen above, our model for inverted neutrino hierarchy leads to a stable "right-handed neutrino" χ which interacts with the Z' boson and the physical scalars ϕ_i via the Lagrangian from Eq. (3.16). The measured relic density $\Omega_\chi h^2 \simeq 0.1$ (Eq. (1.26)) can be obtained around either of the scalar s-channel resonances $M_\chi \simeq m_i/2$, but for the ϕ_1-resonance one needs a rather large scalar-mixing angle α. Choosing parameters that make the model testable at LHC and direct DM detection experiments—$M_\chi \sim 10$–$100\,\text{GeV}$, $m_2 \sim 100\,\text{GeV}$—can lead to viable DM relic abundance in complete analogy to Refs. [142, 143], where a $\mathbb{Z}_2$ symmetry is added to the minimal $B-L$ model (Sec. 2.2) to make one of the RHNs stable. We stress however that the $\mathbb{Z}_2$ in our model was not introduced to make a particle stable, but to generate the right flavor symmetry in the neutrino mass matrix. The stability of χ is in that sense just a welcome accident.[4] We show the relic abundance of χ as a function of its mass and the h–s mixing angle α in Fig. 3.4, as calculated with a modified version of microMEGAs [144–146]. There is no difference between the $B+3\overline{L}$ model and the $B-L$ model in the region $M_\chi \ll M_{Z'}$ of parameter space, because the Z' plays a sub-dominant role for the properties of the scalars, so we refer to Refs. [142, 143] for exact formulae of the relevant cross sections and discussions of direct detection signals. Additional work on $B-L$ in connection with dark matter can be found in Refs. [147–149].

[4] Note that we need an exact $\mathbb{Z}_2$ for stable DM, while a valid IH solution could also work with a broken $\mathbb{Z}_2$. This would however necessitate a more complicated model, so Occam's razor suggests an exact $\mathbb{Z}_2$.

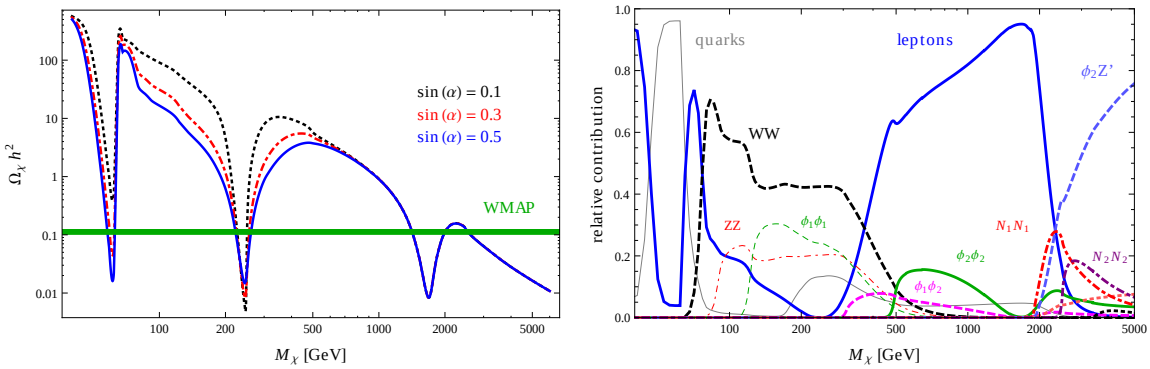

Figure 3.4: Left: Relic density of χ for the parameters $m_1 = 125\,\text{GeV}$, $m_2 = 500\,\text{GeV}$, $v_S = 2.3\,\text{TeV}$, $g' = 0.25$, $N_1 = 1.9\,\text{TeV}$, $N_2 = 2.5\,\text{TeV}$, and $\sin\alpha = 0.5$ (blue), 0.3 (red) and 0.1 (black). This puts the ϕ_1, ϕ_2 and Z' resonances at $\sim 60\,\text{GeV}$, 250 GeV and 1.7 TeV, respectively. The green band shows the 3σ range measured by WMAP. Right: Relative contribution to the relic density by the processes $\chi\chi \to q\overline{q}$ (sum over all quarks), leptons (including neutrinos), ZZ, etc., for $\sin\alpha = 0.3$.

Values around $M_\chi \sim 100\,\text{GeV}$ are an interesting limiting case for collider searches. However, since χ, Z', and ϕ_2 all obtain their masses from $B + 3\overline{L}$ breaking

$$M_{Z'} = 6|g' v_S|\,, \qquad m_2 \simeq m_s \simeq \sqrt{2\lambda_2} v_S\,, \qquad M_\chi = \sqrt{2} Y_\chi v_S\,, \tag{3.19}$$

we would naturally expect their masses to be of similar order:

$$M_{Z'} \sim m_2 \sim M_\chi\,. \tag{3.20}$$

To satisfy collider constraints one needs the scale for these masses to be above 1–10 TeV, but it can, of course, be even higher. A valid relic density can be obtained yet again around the ϕ_2 resonance, since we expect χ and ϕ_2 to have similar masses anyway. The important annihilation channels are then $\chi\chi \to$ leptons, WW, ZZ and $\phi_1\phi_1$. The latter three have a fixed ratio at the resonance, because one can calculate for $m_2 \gg m_1, M_Z$

$$\Gamma(\phi_2 \to W^+W^-) \simeq 2\Gamma(\phi_2 \to ZZ) \simeq 2\Gamma(\phi_2 \to \phi_1\phi_1) \simeq \frac{m_2^3}{16\pi v^2} \sin^2\alpha\,. \tag{3.21}$$

For $M_\chi \simeq m_2/2 > m_t$ there is, of course, the additional important decay into top quarks. However, for a DM candidate this heavy, we also have a Z' resonance $M_\chi \simeq M_{Z'}/2$ independent of the mixing angle α. Due to the different coupling of our Z' compared to $B - L$, this Z' resonance is particularly interesting to distinguish the models. The interactions between fermions and Z' are given by

$$\begin{aligned}\mathcal{L} \supset\; g' Z'_\mu \Big(&-\frac{3}{2}\overline{\chi}\gamma^\mu\gamma_5\chi + \frac{1}{3}\sum_q \overline{q}\gamma^\mu q - 3\,\overline{e}\gamma^\mu e + 3\,\overline{\tau}\gamma^\mu\tau \\ &+ \frac{3}{2}\overline{\nu}_e\gamma^\mu(-\gamma_5)\nu_e - \frac{3}{2}\overline{\nu}_\tau\gamma^\mu(-\gamma_5)\nu_\tau + \frac{3}{2}\overline{N}_1\gamma^\mu(+\gamma_5)N_1 + \ldots\Big)\,,\end{aligned} \tag{3.22}$$

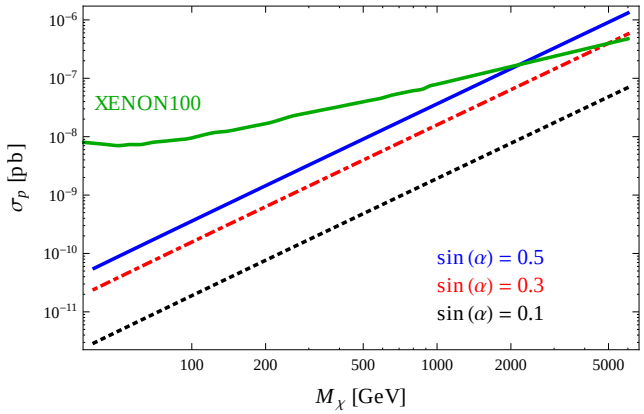

Figure 3.5: Spin-independent cross section of χ with a proton with the same parameters as in Fig. 3.4. Also shown is the XENON100 90% C.L. exclusion from Ref. [151].

where χ and the neutrinos are written as Majorana fermions. The structure of the effective operators $\overline{\chi}\gamma^\mu\gamma_5\chi\,\overline{f}\gamma_\mu f$ upon integrating out Z' leads to spin-independent and spin-dependent interactions in the non-relativistic limit, suppressed by v^2 (velocity) and q^2 (momentum transfer), respectively, as discussed in Ref. [150].

Around the Z' resonance, the relevant processes $\chi\chi \to Z' \to f\overline{f}$ lead to the thermally averaged cross section $\langle\sigma v\rangle \simeq a + bv^2$ with $a = 0$ and

$$b \simeq \frac{2g'^4}{3\pi}\,\frac{M_\chi^2}{(M_{Z'}^2 - 4M_\chi^2)^2 + \Gamma_{Z'}^2 M_{Z'}^2}\sum_f Y'^2_f Y'^2_\chi\,, \tag{3.23}$$

where we neglected the fermion masses for simplicity. This can be used to calculate the freeze-out temperature and the relic density $\Omega_\chi h^2 \sim 1/b$ [142, 143] of χ. Due to the larger coupling of Z' to leptons compared to $B - L$, the annihilation channels around the Z' resonance are mainly $\ell\overline{\ell}$, $\nu\overline{\nu}$, and also $N_i N_i$ if $M_{N_i} \lesssim M_{Z'}/2$. At this point it matters whether we take χ from Sec. 3.2.1 or Sec. 3.2.2, because the models differ in the number of heavy neutrinos. However, additional RHNs do not change the discussion qualitatively, so we will perform our calculations with $n_N = 3$ (Sec. 3.2.1) for simplicity, assuming any additional N_i to be heavy enough to be negligible. In Fig. 3.4 we already showed the relic density of χ and the contributing processes around the Z' resonance.

While it is clear from Fig. 3.4 that the Z' channel can lead to the proper relic density (even for $\sin\alpha = 0$), direct detection signals from Z' interactions are difficult to measure due to the Lorentz structure of the effective operator $\overline{\chi}\gamma^\mu\gamma_5\chi\,\overline{f}\gamma_\mu f$. Since direct detection occurs via t-channel Z' exchange, there is no resonance boost like in the annihilation case. The spin-dependent operators $\overline{\chi}\gamma^\mu\gamma_5\chi\,\overline{f}\gamma_\mu\gamma_5 f$—which do not suffer from q^2 or v^2 suppression—can only be obtained via electroweak loops or Z–Z' mixing, which once again suppresses them. Correspondingly, direct detection experiments will not be sensitive to Z' exchange, so the cross section will be dominated by the scalar-induced operator $\overline{\chi}\chi\,\overline{q}q$, which gives spin-independent cross sections proportional to $\sin^2 2\alpha\, M_\chi^2/v_S^2$. We show the cross sections for $\chi p \to \chi p$ in Fig. 3.5 (as calculated with microMEGAs) for the same parameters as in Fig. 3.4. The observed relic density can be obtained, for example, at the ϕ_2 resonance with $M_\chi \simeq 225\,\text{GeV}$, which gives a cross section $\sigma_p/\sin^2 2\alpha \simeq 2.5 \times 10^{-9}\,\text{pb}$. This evades current XENON100 bounds [151] but can be probed in future experiments like XENON1T [142, 143].

We note that a supersymmetric extension of this model might result in $\alpha \ll 1$—making the Z' resonance crucial for relic abundance—similar to a supersymmetric extension of the $B-L$ model of Ref. [142,143] discussed in Ref. [149].

To summarize: The inverted hierarchy discussed in this section is harder to realize than the normal hierarchy of Sec. 3.1. Both are connected to the abelian gauge symmetry $U(1)_{B+3\overline{L}}$, but IH requires additional RHNs and a $\mathbb{Z}_2$ symmetry to decouple one of them. On the plus side, we find a dark matter candidate, coupled to the SM via the two new bosons Z' and s.

3.3 Neutrino Hierarchies: Quasi-Degenerate Spectrum

In the last two sections we have shown how the approximate symmetry structures behind normal and inverted hierarchy (cf. Eq. (3.3)) can be motivated and enforced by an abelian gauge symmetry, in both cases $U(1)_{B+3\overline{L}}$ (accompanied by a $\mathbb{Z}_2$ for IH). As already stated in the introduction to this chapter, a different approximate symmetry arises for a quasi-degenerate neutrino spectrum, namely $L_\mu - L_\tau$:

$$\mathcal{M}_\nu^{L_\mu - L_\tau} \sim \begin{pmatrix} \times & 0 & 0 \\ 0 & 0 & \times \\ 0 & \times & 0 \end{pmatrix}. \tag{3.24}$$

It is again our goal to enforce this structure, and hence QD, by means of a $U(1)' \subset \mathcal{G}$ subgroup, similar to the previous two sections. This turns out to be very straightforward, because the matrix $\mathcal{M}_\nu^{L_\mu - L_\tau}$ is invertible (otherwise it could hardly work as a symmetry for QD, i.e. $m_1 \simeq m_2 \simeq m_3 \neq 0$). Consequently, an $L_\mu - L_\tau$ symmetric $\mathcal{M}_\nu$ can be obtained from an $L_\mu - L_\tau$ symmetric $\mathcal{M}_R$ via seesaw, without even the need to break the symmetry. This makes it an easy symmetry to discuss; furthermore, $L_\mu - L_\tau$ is already an $U(1)'$ subgroup of $\mathcal{G}$, and can hence be promoted to a *gauge* symmetry without any effort. In fact, it is not even necessary to introduce right-handed neutrinos to the SM to do this, as $U(1)_{L_\mu - L_\tau}$ is already anomaly-free with the SM particle content from Tab. 1.1, as recognized long ago [52–54]. This makes $L_\mu - L_\tau$ an *especially* well-motivated gauge group extension of the SM, and has consequently been discussed at length in the literature (see references in Ref. [4] and the diploma thesis "Phenomenology of a gauged $L_\mu - L_\tau$ symmetry" [152]).

3.3.1 Neutrino Masses

Let us briefly discuss a simple $L_\mu - L_\tau$ model to illustrate the possible effects. An unbroken $U(1)_{L_\mu - L_\tau}$ gauge symmetry only allows for the following Majorana mass matrix for the RHNs

$$\mathcal{M}_R^{L_\mu - L_\tau} = \begin{pmatrix} X & 0 & 0 \\ 0 & 0 & Y \\ 0 & Y & 0 \end{pmatrix}. \tag{3.25}$$

Since electron, muon, and tauon all carry different charges under our $U(1)'$, all leptonic Yukawa couplings with the SM Higgs doublet—and hence all Dirac mass matrices—are diagonal *by symmetry*: $M_e = \mathrm{diag}(m_e, m_\mu, m_\tau)$, $m_D = \mathrm{diag}(m_{\nu_e}, m_{\nu_\mu}, m_{\nu_\tau})$, in the notation of

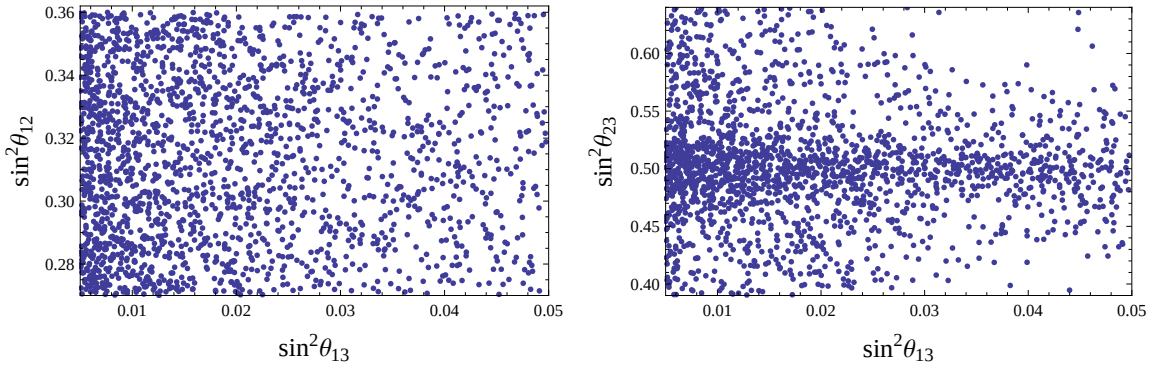

Figure 3.6: Scatter plots for $L_\mu - L_\tau$, spontaneously broken by two scalars with vacuum expectation values $\langle S_j\rangle/\mathcal{M}_R \sim 0.02$.

Sec. 1.1. Invoking the seesaw mechanism in the form of $X, Y \gg m_{\nu_i}$ results in the $L_\mu - L_\tau$ symmetric low-energy Majorana mass matrix for the active neutrinos

$$\mathcal{M}_\nu^{L_\mu - L_\tau} \simeq -m_D^T \left(\mathcal{M}_R^{L_\mu - L_\tau}\right)^{-1} m_D = -\begin{pmatrix} \frac{m_{\nu_e}^2}{X} & 0 & 0 \\ 0 & 0 & \frac{m_{\nu_\mu} m_{\nu_\tau}}{Y} \\ 0 & \frac{m_{\nu_\mu} m_{\nu_\tau}}{Y} & 0 \end{pmatrix}. \tag{3.26}$$

We stress here that X and Y are both allowed by the $U(1)'$ symmetry and hence expected to be of similar order, so we assume $X \simeq Y$ below. The same holds for the m_D entries m_{ν_μ}, m_{ν_τ}, and m_{ν_e}. The eigenvalues of $\mathcal{M}_\nu^{L_\mu - L_\tau}$, $-m_{\nu_e}^2/X$ and $\pm m_{\nu_\mu} m_{\nu_\tau}/Y$, are therefore naturally of similar magnitude, i.e. there is at most a mild hierarchy between the neutrino masses.[5] The atmospheric mixing angle θ_{23} associated with this mass matrix is maximal, i.e. $\sin^2(\theta_{23}) = 1/2$, while the other two mixing angles θ_{13} and θ_{12} are zero and will be induced by breaking the $U(1)_{L_\mu - L_\tau}$ symmetry. The two degenerate neutrino masses $|m_{\nu_\mu} m_{\nu_\tau}/Y|$ will also be split by the breaking.

In order to break the symmetry spontaneously, we introduce two SM-singlet scalars, $S_1 \sim +1$ and $S_2 \sim +2$, instead of just one as in the sections above. This is convenient because the VEVs $\langle S_j\rangle$ will then fill *all* the zeros in $\mathcal{M}_R^{L_\mu - L_\tau}$ of Eq. (3.25), and consequently *all* zeros in $\mathcal{M}_\nu^{L_\mu - L_\tau}$ after seesaw, with entries suppressed by $\varepsilon \equiv \langle S_j\rangle/X \ll 1$. Note that the trilinear coupling $\mu S_1^2 S_2^*$ in the scalar potential will unavoidably induce an S_2 VEV if $\langle S_1\rangle \neq 0$—roughly $\langle S_2\rangle \sim \mu\langle S_1\rangle^2/m_{S_2}^4$—and hence no dangerous Goldstone bosons arise. To generate viable mixing angles and mass differences, only small perturbations $\varepsilon = \mathcal{O}(10^{-2})$ are necessary (see Fig. 3.6), so the $L_\mu - L_\tau$ breaking scale $\langle S_j\rangle$ should be roughly 100 times below the seesaw scale $\mathcal{M}_R^{L_\mu - L_\tau}$.

A model with just one SM-singlet scalar will be discussed in Sec. 3.4, giving rise to two vanishing minors in $\mathcal{M}_\nu$, and hence a relation between neutrino mixing parameters beyond our approximate $L_\mu - L_\tau$ symmetry. Using one SM-singlet scalar and one additional $SU(2)_L$

[5] Note that *positive* masses can be obtained by minor phase shifts of the fields; in particular, one of the Majorana phases $\varphi_{1,2}$ in the PMNS matrix (1.12) is π, while the other vanishes.

doublet to break $SU(2)_L \times U(1)_Y \times U(1)_{L_\mu - L_\tau} \to U(1)_{\text{EM}}$ gives rise to a rich phenomenology, as discussed in our paper "Gauged $L_\mu - L_\tau$ symmetry at the electroweak scale" [4] (in collaboration with W. Rodejohann). The texture zeros in $\mathcal{M}_\nu$ are then filled with entries from $\Delta\mathcal{M}_R$ *and* Δm_D. This gives rise to specific lepton flavor violating signatures—$\tau \to eX$ and $\mu \to eX$, but not $\tau \to \mu X$—and Z–Z' mixing testable at the LHC. Also discussed in Ref. [4] is an embedding of $U(1)_{L_\mu - L_\tau}$ into a non-abelian $SU(2)$, in an effort to enforce the required degeneracy in the neutrino mass matrices, e.g. $X = Y$ in Eq. (3.25). Since a discussion of this model would take us too far off track, we have to refer the interested reader to our paper for details.

Let this suffice as a reminder of the neutrino phenomenology of $L_\mu - L_\tau$. Experimentally, we expect large $0\nu2\beta$ rates, close-to maximal θ_{23}, and a large neutrino-mass contribution in cosmology, i.e. measurable values for $\sum_j m_j$. Additional interesting effects arise from the Z' discussed in the next subsection.

3.3.2 Gauge Boson

Of all the $U(1)'$ symmetries in this chapter, $L_\mu - L_\tau$ is the only one that requires a modified discussion of the gauge boson phenomenology. This is because the Z' of $L_\mu - L_\tau$ couples neither to quarks nor to electrons, invalidating all limits on $M_{Z'}$ and g' mentioned in Sec. 2.1.1. In absence of Z–Z' mixing, limits arise only from experiments with *muons*, seeing as tauons are experimentally more difficult to handle. The prime observable here is the muon's anomalous magnetic moment $a_\mu \equiv (g_\mu - 2)/2$, to which the Z' contributes at one-loop level. Restricting ourselves to gauge boson masses $M_{Z'} \gg m_\mu$,[6] the contribution takes the simple form [154]

$$\Delta a_\mu = \frac{m_\mu^2}{12\pi^2}\frac{g'^2}{M_{Z'}^2} \simeq 290 \times 10^{-11} \left(\frac{180\,\text{GeV}}{M_{Z'}/g'}\right)^2 . \tag{3.27}$$

As it so happens, this contribution can *resolve* the longstanding $\sim 3\sigma$ deviation between experiment and SM prediction $a_\mu^{\text{exp}} - a_\mu^{\text{SM}} = 289(80) \times 10^{-11}$ [16], where we combined the errors in quadrature. The $U(1)_{L_\mu - L_\tau}$ gauge boson is therefore not only allowed to be lighter than TeV, but is even strongly preferred to sit around the electroweak scale! Hadronic contributions to a_μ^{SM} are however notoriously hard to calculate, resulting in a sort-of-systematic error not taken into account here. The $U(1)_{L_\mu - L_\tau}$-breaking VEV(s) can now be fixed by Δa_μ close to the electroweak scale: $M_{Z'}/g' \propto \langle S \rangle \sim 200\,\text{GeV}$. Together with our knowledge from above about the neutrino masses, we can actually *predict* the seesaw scale to be roughly $\mathcal{M}_R = \mathcal{O}(10)\,\text{TeV}$ in this model. Since this is much too low for standard thermal leptogenesis, as discussed in Sec. 2.2.2, the modified version of *resonant* leptogenesis [84] has to be employed, which requires the RHNs to be quasi-degenerate. While this should presumably work nicely, seeing as we expect and need quasi-degenerate neutrinos anyways in our model, a discussion goes beyond the scope of this thesis.

Let us briefly mention collider phenomenology; while certainly more challenging than the search for gauge bosons *with* couplings to first-generation particles, there are still interesting signatures. As noted long ago [155–157], the Z' can be radiated off final state muons (or tauons), with subsequent decay $Z' \to \mu\mu$, $\tau\tau$. Correspondingly, the Breit–Wigner peak of

[6] The long-range limit of $U(1)_{L_\mu - L_\tau}$ has been studied by us in Refs. [152, 153].

the $U(1)_{L_\mu - L_\tau}$ gauge boson could be discovered in the invariant-mass distribution of lepton pairs in the final states 4μ, 4τ, or $2\mu 2\tau$. A recent reevaluation of the discovery reach at the LHC can be found in Ref. [158].

3.4 Texture Zeros and Vanishing Minors

Time for a slight change of topics. In the previous sections, we have taken the approach to identify approximate symmetries in the neutrino mass hierarchies and promote them to gauge symmetries. In effect, we imposed a structure on $\mathcal{M}_R$ and introduced small perturbations $\Delta\mathcal{M}_R \sim \langle S\rangle$ by breaking the $U(1)'$, which then trickle down to $\mathcal{M}_\nu$ via seesaw. A more extreme approach to impose structure on the neutrino mass matrix are texture zeros and vanishing minors. We start with an example to illustrate both the idea and the novel approach of our paper [5]: Let us consider the $U(1)'$ subgroup of $U(1)_{B-L} \times U(1)_{L_e - L_\mu} \times U(1)_{L_\mu - L_\tau}$ generated by

$$Y' = (B-L) + 2(L_e - L_\mu) + 2(L_\mu - L_\tau) = B + L_e - L_\mu - 3L_\tau \,, \tag{3.28}$$

which is, of course, anomaly free. Since electron, muon, and tauon carry different charges under this $U(1)'$ gauge group, the Dirac mass matrix for the charged leptons is automatically diagonal, as is the Dirac mass matrix of the neutrinos m_D. For the right-handed neutrinos, we can write down only one Majorana mass term, namely $M\overline{\nu}^c_{R,1}\nu_{R,2}$, which means that all entries of $\mathcal{M}_R$ are zero except for $(\mathcal{M}_R)_{12} = (\mathcal{M}_R)_{21}$. Breaking the $U(1)'$ with an SM-singlet scalar S of charge $Y'(S) = 2$ generates, however, more Majorana mass terms:

$$\mathcal{M}_R = M \begin{pmatrix} 0 & \times & 0 \\ \times & 0 & 0 \\ 0 & 0 & 0 \end{pmatrix} + \langle S\rangle \begin{pmatrix} \times & 0 & \times \\ 0 & \times & 0 \\ \times & 0 & 0 \end{pmatrix} \sim \begin{pmatrix} \times & \times & \times \\ \times & \times & 0 \\ \times & 0 & 0 \end{pmatrix} , \tag{3.29}$$

where $\times$ again just denotes some nonzero entry. Assuming both M and $\langle S\rangle$ to be much larger than the electroweak scale, we can use the seesaw relation (2.16) to calculate the low-energy neutrino mass matrix

$$\mathcal{M}_\nu \simeq -m_D \mathcal{M}_R^{-1} m_D \sim \begin{pmatrix} \times & \times & \times \\ \times & \times & 0 \\ \times & 0 & 0 \end{pmatrix}^{-1} \sim \begin{pmatrix} 0 & 0 & \times \\ 0 & \times & \times \\ \times & \times & \times \end{pmatrix} , \tag{3.30}$$

using the fact that m_D is diagonal. Writing $\mathcal{M}_\nu = U^*_{\text{PMNS}}\,\text{diag}(m_1, m_2, m_3)\,U^\dagger_{\text{PMNS}}$ in the usual parametrization (2.17), we see that the two texture zeros $(\mathcal{M}_\nu)_{ee} = (\mathcal{M}_\nu)_{e\mu} = 0$ imposed by our symmetry lead to the relations

$$m_1 \cos^2\theta_{12}\cos^2\theta_{13} + m_2 \sin^2\theta_{12}\cos^2\theta_{13} e^{-i\varphi_1} + m_3 \sin^2\theta_{13} e^{2i\delta - i\varphi_2} = 0 \,, \tag{3.31}$$

$$\begin{aligned} &m_1 \cos\theta_{12}\left(\cos\theta_{23}\sin\theta_{12} + e^{-i\delta}\cos\theta_{12}\sin\theta_{23}\sin\theta_{13}\right) \\ &\quad + m_2 \sin\theta_{12}\left(\sin\theta_{12}\sin\theta_{23}\sin\theta_{13} - e^{i\delta}\cos\theta_{12}\cos\theta_{23}\right) e^{-i\varphi_1 - i\delta} \\ &\quad - m_3 \sin\theta_{23}\sin\theta_{13} e^{i\delta - i\varphi_2} = 0 \,. \end{aligned} \tag{3.32}$$

Using data from neutrino oscillation experiments for θ_{ij} and the mass-squared differences $\Delta m^2_{31,21}$ (see Tab. 1.2), one can solve the two complex equations above to obtain the remaining unknowns: the three CP-violating phases δ, φ_1, and φ_2, as well as the lightest neutrino mass m_1. In this example, one finds $m_1 \simeq 3.9\,\text{meV}$, normal hierarchy, and a vanishing rate of neutrinoless double beta decay, because $(\mathcal{M}_\nu)_{ee} = 0$ [159].

The above example nicely illustrates the approach of this section: We take $U(1)'$ subgroups of our maximal anomaly-free group $\mathcal{G}$ that lead to diagonal Dirac matrices. Breaking the $U(1)'$ spontaneously with SM-singlet scalars of appropriate charge will lead to texture zeros in $\mathcal{M}_R$, which translate into vanishing minors of $\mathcal{M}_\nu \sim \mathcal{M}_R^{-1}$—to be defined below—and give rise to testable relations among the neutrino mixing parameters. After identifying the seven currently allowed two-zero textures in $\mathcal{M}_R \sim \mathcal{M}_\nu^{-1}$, we will show how five of them can be realized via $U(1)'$ symmetries in the simplest possible way, using only one SM-singlet scalar to break the $U(1)'$; the remaining two viable two-zero textures in $\mathcal{M}_R$ can be realized in a model with two scalars.

The idea of imposing texture zeros [160–163] or vanishing minors [164,165] is, of course, not new; typically, discrete $\mathbb{Z}_N$ symmetries are used to forbid the mass-matrix entries, employing a vast number of additional scalars [166]. However, it is not completely clear that discrete global symmetries would survive quantum gravity effects [167], and moreover the spontaneous breaking of discrete symmetries may suffer from the domain wall problem. In this sense, it might be more convincing to adopt gauge symmetries instead of discrete ones, especially considering our motivation for these symmetries in Sec. 1.5. Furthermore, the new $U(1)'$ gauge boson can be expected to have some impact on the LHC phenomenology and therefore provide better testability.

3.4.1 Classification and Current Status

It is easy to prove that Majorana neutrino mass matrices with three or more independent texture zeros in $\mathcal{M}_\nu$ or $\mathcal{M}_\nu^{-1}$ are incompatible with current data. We will therefore only study two-zero textures,[7] listed here in the common notation [161]:

$$\boldsymbol{A}_1: \begin{pmatrix} 0 & 0 & \times \\ 0 & \times & \times \\ \times & \times & \times \end{pmatrix}, \quad \boldsymbol{A}_2: \begin{pmatrix} 0 & \times & 0 \\ \times & \times & \times \\ 0 & \times & \times \end{pmatrix}; \tag{3.33}$$

$$\boldsymbol{B}_1: \begin{pmatrix} \times & \times & 0 \\ \times & 0 & \times \\ 0 & \times & \times \end{pmatrix}, \quad \boldsymbol{B}_2: \begin{pmatrix} \times & 0 & \times \\ 0 & \times & \times \\ \times & \times & 0 \end{pmatrix}, \tag{3.34}$$

$$\boldsymbol{B}_3: \begin{pmatrix} \times & 0 & \times \\ 0 & 0 & \times \\ \times & \times & \times \end{pmatrix}, \quad \boldsymbol{B}_4: \begin{pmatrix} \times & \times & 0 \\ \times & \times & \times \\ 0 & \times & 0 \end{pmatrix}; \tag{3.35}$$

[7] Imposing only one zero [168] or vanishing minor [169] severely reduces the predictivity of the model and will not be studied here. Our $U(1)'$ approach can, however, also be useful in these cases.

pattern of M	$\boldsymbol{A}_1$	$\boldsymbol{A}_2$	$\boldsymbol{B}_3$	$\boldsymbol{B}_4$	$\boldsymbol{D}_1$	$\boldsymbol{D}_2$	$\boldsymbol{F}_j$
pattern of M^{-1}	$\boldsymbol{D}_2$	$\boldsymbol{D}_1$	$\boldsymbol{B}_4$	$\boldsymbol{B}_3$	$\boldsymbol{A}_2$	$\boldsymbol{A}_1$	$\boldsymbol{F}_j$

Table 3.1: Two-texture zeros of a non-singular symmetric 3×3 matrix M that lead to two texture zeros in the inverse matrix M^{-1}.

$$\boldsymbol{C}: \begin{pmatrix} \times & \times & \times \\ \times & 0 & \times \\ \times & \times & 0 \end{pmatrix}; \quad \boldsymbol{D}_1: \begin{pmatrix} \times & \times & \times \\ \times & 0 & 0 \\ \times & 0 & \times \end{pmatrix}, \quad \boldsymbol{D}_2: \begin{pmatrix} \times & \times & \times \\ \times & \times & 0 \\ \times & 0 & 0 \end{pmatrix}; \tag{3.36}$$

$$\boldsymbol{E}_1: \begin{pmatrix} 0 & \times & \times \\ \times & 0 & \times \\ \times & \times & \times \end{pmatrix}, \quad \boldsymbol{E}_2: \begin{pmatrix} 0 & \times & \times \\ \times & \times & \times \\ \times & \times & 0 \end{pmatrix}, \quad \boldsymbol{E}_3: \begin{pmatrix} 0 & \times & \times \\ \times & \times & 0 \\ \times & 0 & \times \end{pmatrix}; \tag{3.37}$$

$$\boldsymbol{F}_1: \begin{pmatrix} \times & 0 & 0 \\ 0 & \times & \times \\ 0 & \times & \times \end{pmatrix}, \quad \boldsymbol{F}_2: \begin{pmatrix} \times & 0 & \times \\ 0 & \times & 0 \\ \times & 0 & \times \end{pmatrix}, \quad \boldsymbol{F}_3: \begin{pmatrix} \times & \times & 0 \\ \times & \times & 0 \\ 0 & 0 & \times \end{pmatrix}. \tag{3.38}$$

In all cases, the symbol $\times$ denotes a non-vanishing entry. In some cases—listed in Tab. 3.1—the texture zeros propagate to the inverse matrix, but in any case, two-zero textures of M lead to two *vanishing minors* in M^{-1}. We define the minor (i, j) of an $n \times n$ matrix A as the determinant of the $(n-1)\times(n-1)$ matrix obtained from A by removing the i-th row and j-th column. This is a useful convention, because now the texture zeros $M_{ij} = 0 = M_{nm}$ result in the vanishing minors (i, j) and (n, m) of M^{-1}. We can therefore classify vanishing minors in $\mathcal{M}_\nu$ as texture zeros in $\mathcal{M}_\nu^{-1}$ and vice versa. Since our leptonic Dirac mass matrices are diagonal on symmetry grounds, the texture-zero structure of $\mathcal{M}_R$ and $\mathcal{M}_\nu^{-1} \simeq -m_D^{-1}\mathcal{M}_R m_D^{-1}$ is identical, only the magnitude of the nonzero entries is different. We can therefore classify the vanishing minors of $\mathcal{M}_\nu$ as texture zeros in $\mathcal{M}_\nu^{-1}$ or texture zeros in $\mathcal{M}_R$. Two-zero texture patterns $\boldsymbol{P}_i$ in $\mathcal{M}_\nu$ ($\mathcal{M}_R$) will be denoted with an index ν (R), i.e. as $\boldsymbol{P}_i^\nu$ ($\boldsymbol{P}_i^R$), to avoid confusion between the patterns.

The analysis of texture zeros in $\mathcal{M}_\nu$ has been recently performed in Ref. [159], with the result that seven patterns of $\mathcal{M}_\nu$ with two independent zeros are consistent with the latest global fit of neutrino oscillation data at the 3σ level, namely $\boldsymbol{A}_1^\nu$, $\boldsymbol{A}_2^\nu$, $\boldsymbol{B}_1^\nu$, $\boldsymbol{B}_2^\nu$, $\boldsymbol{B}_3^\nu$, $\boldsymbol{B}_4^\nu$, and $\boldsymbol{C}^\nu$.[8] Of the seven patterns, $\boldsymbol{A}_2^\nu$, $\boldsymbol{A}_1^\nu$, $\boldsymbol{B}_4^\nu$, and $\boldsymbol{B}_3^\nu$ translate into the following two-zero textures in $\mathcal{M}_R$ (or $\mathcal{M}_\nu^{-1}$)

$$\begin{aligned} \boldsymbol{D}_1^R: \begin{pmatrix} \times & \times & \times \\ \times & 0 & 0 \\ \times & 0 & \times \end{pmatrix}, \quad & \boldsymbol{D}_2^R: \begin{pmatrix} \times & \times & \times \\ \times & \times & 0 \\ \times & 0 & 0 \end{pmatrix}, \\ \boldsymbol{B}_3^R: \begin{pmatrix} \times & 0 & \times \\ 0 & 0 & \times \\ \times & \times & \times \end{pmatrix}, \quad & \boldsymbol{B}_4^R: \begin{pmatrix} \times & \times & 0 \\ \times & \times & \times \\ 0 & \times & 0 \end{pmatrix}, \end{aligned} \tag{3.39}$$

[8] The Planck limit on the sum of neutrino masses (Sec. 1.1.2) gives additional constraints, especially on pattern $\boldsymbol{C}^\nu$ [170]. Since this limit depends strongly on the combined datasets, we will not use it here.

respectively, while the other patterns $\boldsymbol{B}_1^\nu$, $\boldsymbol{B}_2^\nu$, and $\boldsymbol{C}^\nu$ do not lead to texture zeros in $\mathcal{M}_R$. Correspondingly, there might be additional allowed zeros in $\mathcal{M}_R$ that do not give zeros in $\mathcal{M}_\nu$ and are therefore invisible in the analysis of Ref. [159]. Using the current values for the mixing angles and mass-squared differences from Tab. 1.2, we checked that the following three patterns of $\mathcal{M}_R$

$$\boldsymbol{B}_1^R : \begin{pmatrix} \times & \times & 0 \\ \times & 0 & \times \\ 0 & \times & \times \end{pmatrix}, \qquad \boldsymbol{B}_2^R : \begin{pmatrix} \times & 0 & \times \\ 0 & \times & \times \\ \times & \times & 0 \end{pmatrix}, \qquad \boldsymbol{C}^R : \begin{pmatrix} \times & \times & \times \\ \times & 0 & \times \\ \times & \times & 0 \end{pmatrix}, \tag{3.40}$$

are indeed also allowed at the 3σ level. Consequently, we have seven allowed two-zero textures in $\mathcal{M}_R$ in analogy to $\mathcal{M}_\nu$. For convenience we list the allowed two-zero textures in $\mathcal{M}_\nu$ and $\mathcal{M}_R$ in terms of the notation defined above:

$$\begin{aligned} \mathcal{M}_\nu : &\qquad \boldsymbol{A}_1^\nu\,, \boldsymbol{A}_2^\nu\,, \boldsymbol{B}_1^\nu\,, \boldsymbol{B}_2^\nu\,, \boldsymbol{B}_3^\nu\,, \boldsymbol{B}_4^\nu\,, \boldsymbol{C}^\nu\,, \\ \mathcal{M}_R : &\qquad \boldsymbol{D}_1^R\,, \boldsymbol{D}_2^R\,, \boldsymbol{B}_1^R\,, \boldsymbol{B}_2^R\,, \boldsymbol{B}_3^R\,, \boldsymbol{B}_4^R\,, \boldsymbol{C}^R\,. \end{aligned} \tag{3.41}$$

The patterns $\boldsymbol{B}_i^R$ admit normal as well as inverted hierarchy solutions, while $\boldsymbol{D}_i^R$ and $\boldsymbol{C}^R$ require normal ordering. To illustrate how well the different textures perform, we filled the non-vanishing entries in $\mathcal{M}_R$ with random complex numbers of magnitude ≤ 1 and checked if the resulting neutrino mass matrix has parameters θ_{ij}, $\Delta m^2_{21}/\Delta m^2_{31}$ in the allowed 3σ range.[9] From the patterns $\boldsymbol{D}_i^R$, $\mathcal{O}(10^6)$ out of 10^9 random matrices were compatible with data, $\boldsymbol{C}^R$ gave $\mathcal{O}(10^4)$ valid matrices and the $\boldsymbol{B}_i$ patterns $\mathcal{O}(10^2)$.[10] A more detailed analysis of fine-tuning in $\mathcal{M}_\nu$ texture zeros was recently performed in Ref. [171], where the least fine-tuned patterns were identified as $\boldsymbol{A}_i^\nu$ (which is our $\boldsymbol{D}_j^R$). Since the $\mathcal{M}_R$ textures of Eq. (3.40) do not lead to texture zeros in $\mathcal{M}_\nu$, they were not considered in the analysis of Ref. [171]. However, the counting of valid random matrices suggests a similar conclusion, i.e. the patterns $\boldsymbol{B}_i^R$ and $\boldsymbol{C}^R$ can be considered less natural than $\boldsymbol{D}_i^R$, at least for normal hierarchy. Should the mass ordering of neutrinos turn out to be inverted, we would just have the $\boldsymbol{B}_i^R$ textures, with similar performance.

3.4.2 Realization via Flavor Symmetries

For each of the valid two-zero patterns from Eq. (3.41) one can solve the two resulting complex equations to obtain the CP phases and neutrino masses either numerically or analytically. Dedicated analyses of this sort can be found in Refs. [164, 165], we will not discuss the implications of the texture zeros on the neutrino mixing parameters any further in this thesis. We will rather show that all of the allowed patterns for $\mathcal{M}_R$ (3.41) can be derived by family non-universal $U(1)'$ gauge symmetries with at most two new SM-singlet scalars. We employ $U(1)'$ subgroups of our well-motivated gauge group $\mathcal{G} = U(1)_{B-L} \times U(1)_{L_e-L_\mu} \times U(1)_{L_\mu-L_\tau}$; as already pointed out in Sec. 1.5, every such $U(1)'$ subgroup is generated by a linear combination of $\mathcal{G}$ generators, i.e. by $Y' = \alpha(B-L) + \beta(L_e - L_\mu) + \gamma(L_\mu - L_\tau)$. It turns

[9] In our publication [5] this was not done with the values from Tab. 1.2, but with older data; the qualitative results of this paragraph remain valid.

[10] The exact numbers (#NH, #IH) of valid matrices for 10^9 random tries were: $(2.9 \times 10^6, 0)$ for $\boldsymbol{D}_1^R$, $(2.8 \times 10^6, 0)$ for $\boldsymbol{D}_2^R$, $(7961, 0)$ for $\boldsymbol{C}^R$, $(950, 54)$ for $\boldsymbol{B}_1^R$, $(335, 78)$ for $\boldsymbol{B}_2^R$, $(543, 50)$ for $\boldsymbol{B}_3^R$ and $(215, 80)$ for $\boldsymbol{B}_4^R$.

out to be convenient to distinguish the two cases $\alpha = 0$ and $\alpha \neq 0$, which we can parametrize as

$$Y' = y_e L_e + y_\mu L_\mu - (y_e + y_\mu) L_\tau \tag{3.42}$$

and

$$Y' = B - x_e L_e - x_\mu L_\mu - (3 - x_e - x_\mu) L_\tau \,, \tag{3.43}$$

respectively. Due to the insignificant overall normalization of $U(1)'$ generators it is sufficient to consider these two two-parameter subgroups of $\mathcal{G}$. $Y' = y_e L_e + y_\mu L_\mu - (y_e + y_\mu) L_\tau$ could be similarly split into $y_e = 0$ ($Y' = L_\mu - L_\tau$) and $y_e \neq 0$ ($Y' = L_e + y_\mu L_\mu - (1 + y_\mu) L_\tau$), which however barely simplifies matters.

To make the connection between texture zeros and symmetries, we list the charge-matrices of $Y'(\overline{\nu}^c_{R,i} \nu_{R,j})$ for the two cases:

$$\begin{pmatrix} 2y_e & y_e + y_\mu & -y_\mu \\ y_e + y_\mu & 2y_\mu & -y_e \\ -y_\mu & -y_e & -2(y_e + y_\mu) \end{pmatrix}, \quad \begin{pmatrix} -2x_e & -x_e - x_\mu & x_\mu - 3 \\ -x_e - x_\mu & -2x_\mu & x_e - 3 \\ x_\mu - 3 & x_e - 3 & 2x_e + 2x_\mu - 6 \end{pmatrix}. \tag{3.44}$$

If the parameters y_j (x_j) are so that an entry $Y'(\overline{\nu}^c_{R,i} \nu_{R,j})$ is zero, the symmetry-conserving mass term $M \overline{\nu}^c_{R,i} \nu_{R,j}$ can be included in the Lagrangian. If not zero, the fermion bilinear $\overline{\nu}^c_{R,i} \nu_{R,j}$ can still be coupled to a scalar S of appropriate $U(1)'$ charge. The VEV of S then generates a nonzero entry $(\mathcal{M}_R)_{ij}$. Every entry in $\mathcal{M}_R$ can thus be filled with at most six scalars, but our goal here is to keep some entries zero, and also to use as few scalars as possible for simplicity. With a little time and combinatorics, one can systematically look for successful patterns. We note that the family non-universality—resulting in convenient diagonal Dirac matrices—requires $y_e \neq y_\mu$, $y_e \neq -2y_\mu$, $y_\mu \neq -2y_e$, $x_e \neq x_\mu$, $x_e \neq 3 - 2x_\mu$ and $x_\mu \neq 3 - 2x_e$. An example has already been provided at the beginning of this section, but let us consider one more: Imposing an exact $L_\alpha - L_\beta$ symmetry results in 4 zeros and two independent symmetry conserving entries (with scale $M_{L_\alpha - L_\beta}$). A scalar with $L_\alpha - L_\beta$ charge ± 1 or ± 2 will fill two of those zeros after acquiring a VEV. Matching this to Eq. (3.39) and Eq. (3.40) shows that only the $L_\mu - L_\tau$ symmetry, with a scalar S whose charge is ± 1, can lead to a valid pattern, namely $\boldsymbol{C}^R$:

$$\mathcal{M}_R = M_{L_\mu - L_\tau} \begin{pmatrix} \times & 0 & 0 \\ 0 & 0 & \times \\ 0 & \times & 0 \end{pmatrix} + \langle S \rangle \begin{pmatrix} 0 & \times & \times \\ \times & 0 & 0 \\ \times & 0 & 0 \end{pmatrix} \sim \begin{pmatrix} \times & \times & \times \\ \times & 0 & \times \\ \times & \times & 0 \end{pmatrix}. \tag{3.45}$$

The remaining zeros in this case will be filled by effective operators $S^2 \overline{\nu}^c_{R,i} \nu_{R,j} / \Lambda$, suppressed by a new-physics scale Λ. In order for us to talk about texture "zeros," we require $\Lambda \gg M_{L_\mu - L_\tau}, \langle S \rangle$. Furthermore, the charged-lepton mass matrix will also receive off-diagonal elements suppressed by Λ^n, which introduces a contribution U^{e_L} to the lepton mixing matrix $U_{\text{PMNS}} = U^{e_L} (U^{\nu_L})^\dagger$ (see Sec. 1.1). Correspondingly, the predictivity of the texture-zero approach goes down the drain if we allow for a low Λ, but the perturbations could on the other hand be used to alleviate any tension between the predicted and observed values. Since all

symmetry generator Y'	$\lvert Y'(S)\rvert$	$v_S = \sqrt{2}\,\lvert\langle S\rangle\rvert$	$\mathcal{M}_R$	$\mathcal{M}_\nu$
$L_\mu - L_\tau$	1	$\geq 160\,\text{GeV}$	$\boldsymbol{C}^R$	–
$B - L_e + L_\mu - 3L_\tau$	2	$\geq 3.5\,\text{TeV}$	$\boldsymbol{B}_4^R$	$\boldsymbol{B}_3^\nu$
$B - L_e - 3L_\mu + L_\tau$	2	$\geq 4.8\,\text{TeV}$	$\boldsymbol{B}_3^R$	$\boldsymbol{B}_4^\nu$
$B + L_e - L_\mu - 3L_\tau$	2	$\geq 3.5\,\text{TeV}$	$\boldsymbol{D}_2^R$	$\boldsymbol{A}_1^\nu$
$B + L_e - 3L_\mu - L_\tau$	2	$\geq 3.5\,\text{TeV}$	$\boldsymbol{D}_1^R$	$\boldsymbol{A}_2^\nu$

Table 3.2: Anomaly-free $U(1)'$ gauge symmetries that lead to the allowed two-zero textures in the right-handed Majorana mass matrix $\mathcal{M}_R$ with the addition of just one SM-singlet scalar S. Some of the texture zeros propagate to $\mathcal{M}_\nu \simeq -m_D \mathcal{M}_R^{-1} m_D$ after seesaw. Classification of the two-zero textures according to Sec. 3.4.1.

the $U(1)'$ models we employ here are anomaly-free, our models are renormalizable and can be valid up to the Planck scale (assuming this is where quantum gravity takes over). Potential Landau poles below M_{Pl} can be avoided with small enough gauge coupling g', irrelevant to the neutrino masses. In the following, we will therefore always assume these higher-dimensional operators to be sufficiently suppressed.

Back to the possible flavor symmetries that give two vanishing minors in $\mathcal{M}_\nu$. In the case of $y_e \neq 0$, $y_\mu \neq 0$ and $y_e \neq -y_\mu$, we need at least *three* SM-singlet scalars with VEVs in order to construct the allowed patterns of two-zero textures. All seven viable $\mathcal{M}_R$ patterns can be realized, but each with at least two different $U(1)'$ symmetries, so there is no unique symmetry behind each texture. Since the three required scalars make the models somewhat complicated, we will not discuss them any further. A list of $U(1)'$ symmetries with their two-zero textures can be found in our paper [5].

Going to the $B - x_e L_e - x_\mu L_\mu - (3 - x_e - x_\mu) L_\tau$ symmetry allows for a lot more patterns; there are many assignments for x_e and x_μ that give one or even no zeros and can therefore easily produce consistent phenomenology. Of interest here are the assignments that lead to valid two-zero textures with just one scalar, a complete list is given in Tab. 3.2 (see also the example at the beginning of this section). We see that only the patterns $\boldsymbol{D}_1^R$, $\boldsymbol{D}_2^R$, $\boldsymbol{B}_3^R$, $\boldsymbol{B}_4^R$ and $\boldsymbol{C}^R$ can be obtained in this highly economic way. The charge assignments are summarized in Tab. 3.2 together with the lower bounds on the $U(1)'$ breaking scale, $|M_{Z'}/g'| = |Y'(S)\, v_S| = \sqrt{2}\,|Y'(S)\,\langle S\rangle|$, as determined by the anomalous magnetic moment of the muon [4] or LEP-2 measurements [66, 67]. The discussion of the scalar sector can be taken directly from Sec. 2.2.1.

If we extend the scalar sector by two SM singlet scalars instead of just one, we can construct the remaining two valid patterns of $\mathcal{M}_R$ listed in Eq. (3.40), by using for example $B - L_e - 5L_\mu + 3L_\tau$ for $\boldsymbol{B}_2^R$ and $B - L_e + 3L_\mu - 5L_\tau$ for $\boldsymbol{B}_1^R$, respectively. In both cases we need scalars with charge $|Y'(S_1)| = 2$ and $|Y'(S_2)| = 10$. Since there is no unique symmetry behind the patterns $\boldsymbol{B}_{1,2}^R$, we will not discuss them any further. Tab. 3.3 provides a complete list of the $B - x_e L_e - x_\mu L_\mu - (3 - x_e - x_\mu) L_\tau$ charge assignments that yield the allowed two-zero textures in $\mathcal{M}_R$ with two scalars. Some of the solutions do not allow for flavor-symmetric mass terms, which means there are only the two breaking scales $\langle S_1\rangle$ and $\langle S_2\rangle$ that determine $\mathcal{M}_R$. As

$\mathcal{M}_R$	symmetry generator Y'	$\lvert Y'(S_i)\rvert$
$\boldsymbol{D}_1^R$	$B - aL_e - 3L_\mu + aL_\tau$, $a \notin \{-9,-3,0,1,3\}$	$2\lvert a\rvert,\ \lvert 3+a\rvert$
	$B - 2L_\mu - L_\tau$	$1,\ 2$
	$B + \frac{3}{2}L_e - \frac{9}{2}L_\mu$	$3,\ \frac{3}{2}$
	$B + \frac{9}{7}L_e - \frac{27}{7}L_\mu - \frac{3}{7}L_\tau$	$\frac{18}{7},\ \frac{6}{7}$
	$B + \frac{1}{3}L_e - \frac{7}{3}L_\mu - L_\tau$	$2,\ \frac{2}{3}$
$\boldsymbol{D}_2^R$	$\boldsymbol{D}_1^R$ with $L_\mu \leftrightarrow L_\tau$	
$\boldsymbol{B}_3^R$	$\boldsymbol{D}_1^R$ with $L_e \leftrightarrow L_\tau$	
$\boldsymbol{B}_4^R$	$\boldsymbol{B}_3^R$ with $L_\mu \leftrightarrow L_\tau$	
$\boldsymbol{B}_1^R$	$B + 3L_\mu - 6L_\tau$	$3,\ 12$
	$B - 2L_\mu - L_\tau$	$2,\ 3$
	$B - \frac{9}{2}L_\mu + \frac{3}{2}L_\tau$	$3,\ \frac{9}{2}$
	$B - 6L_e + 3L_\mu$	$3,\ 12$
	$B + \frac{3}{2}L_e - \frac{9}{2}L_\mu$	$3,\ \frac{9}{2}$
	$B - L_e - 2L_\mu$	$2,\ 3$
	$B - L_e + 3L_\mu - 5L_\tau$	$2,\ 10$
	$B - 5L_e + 3L_\mu - L_\tau$	$2,\ 10$
$\boldsymbol{B}_2^R$	$\boldsymbol{B}_1^R$ with $L_\mu \leftrightarrow L_\tau$	
$\boldsymbol{C}^R$	$B + 3L_e - aL_\mu - (6-a)L_\tau$, $a \notin \{-3,0,1,3,5,6,9\}$	$5,\ \lvert 3-a\rvert$
	$B - 6L_\mu + 3L_\tau$	$3,\ 6$
	$B - 3L_e \pm 9L_\mu \mp 9L_\tau$	$6,\ 12$

Table 3.3: $Y' = B - x_e L_e - x_\mu L_\mu - (3 - x_e - x_\mu)L_\tau$ charge assignments that lead to viable two-zero textures in the right-handed Majorana neutrino mass matrix $\mathcal{M}_R \sim \mathcal{M}_\nu^{-1}$ after breaking the $U(1)'$ with *two* SM-singlet scalars S_i of appropriate charge $Y'(S_i)$.

can be seen in Tab. 3.3, all patterns that already work with just one scalar (Tab. 3.2) have infinitely many realizations once another scalar is introduced. Since the patterns $\boldsymbol{D}_1^R$, $\boldsymbol{D}_2^R$, $\boldsymbol{B}_3^R$ and $\boldsymbol{B}_4^R$ are related by $L_\alpha \leftrightarrow L_\beta$ operations, we do not list them explicitly. Let us make a brief comment on the scalar potential of these two-scalar models: If the charges $Y'(S_1)$ and $Y'(S_2)$ are vastly different and make it impossible to write down $U(1)'$ invariant terms of the form $S_1^n S_2^m$ or $S_1^n (S_2^*)^m$ with $n + m \leq 4$, the scalar potential will enjoy an additional accidental global $U(1)$ symmetry, and the two VEVs $\langle S_{1,2}\rangle$ will generate a massless Goldstone boson. This is potentially problematic, but can be cured by introducing yet more scalars that connect S_1 to S_2 and break the accidental global $U(1)$ symmetry of the potential. We refrain from a more detailed discussion, and merely emphasize that the models from Tab. 3.2 are infinitely simpler, seeing as they only require one scalar beyond the SM.

Having shown that we can construct two-zero patterns via various broken flavor symmetries, we will now briefly comment on the involved scales. The allowed two-zero textures of $\mathcal{M}_\nu^{-1}$

typically have non-vanishing entries of similar magnitude, which means that the symmetry breaking scales need to be comparable to the flavor symmetric mass terms, i.e. $\langle S\rangle \sim \mathcal{M}_R$. To illustrate this point, we present a particularly cute solution with non-vanishing elements of similar order:

$$\mathcal{M}_R = M_0 \begin{pmatrix} -2 & -2 & 3 \\ -2 & 1 & 0 \\ 3 & 0 & 0 \end{pmatrix} \qquad \Rightarrow \qquad \mathcal{M}_\nu = m_0 \begin{pmatrix} 0 & 0 & 1 \\ 0 & 3 & 2 \\ 1 & 2 & 2 \end{pmatrix}, \tag{3.46}$$

where we assumed $m_D = i\sqrt{m_0 M_0}\mathbb{1}$. This mass matrix leads to normal hierarchy and the mixing parameters take the form

$$\sin^2\theta_{12} \simeq \frac{1}{3}\,, \qquad \sin^2\theta_{13} = \frac{1}{3} - \frac{5}{6\sqrt{7}} \simeq 0.018\,, \tag{3.47}$$

$$\sin^2\theta_{23} \simeq \frac{1}{3} + \frac{2}{3\sqrt{7}} \simeq 0.59\,, \qquad \frac{\Delta m^2_{21}}{\Delta m^2_{31}} = \frac{1}{2} - \frac{5}{4\sqrt{7}} \simeq 0.027\,, \tag{3.48}$$

which fall in the 3σ range of Tab. 1.2. It should be clear that the overall seesaw scale M_0 is a free parameter in our models, as a change in M_0 can be compensated by a change in m_D. Thus, the predicted scaling $\langle S\rangle \sim \mathcal{M}_R$ can sit anywhere from 10^{15} GeV to 1 TeV, the latter being obviously more interesting for collider phenomenology.

While there is no hierarchy in $\mathcal{M}_\nu$ in the case of two-zero textures, some hierarchy among the $\mathcal{M}_R$ entries is present if the elements of $m_D = \mathrm{diag}(a,b,c)$, are hierarchical.[11] Taking for example our model for $\boldsymbol{D}_1^R$, i.e. $B + L_e - 3L_\mu - L_\tau$, we find numerically the following typical hierarchy among the nonzero elements:

$$S_{11}/a^2 \sim S_{12}/ab \sim M_{13}/ac > S_{33}/c^2\,. \tag{3.49}$$

Here and in the following, M_{ij} denotes an $\mathcal{M}_R$ entry allowed by the imposed flavor symmetry and $S_{ij} = \lambda_{ij}\langle S\rangle$ a symmetry breaking entry. The hierarchy is very mild, but we can easily make $M_{ij} \gg S_{ij}$ by imposing $a, b \ll c$. The same qualitative result holds for $\boldsymbol{D}_2^R$. An analogous analysis of $\boldsymbol{B}_3^R$ $(B - L_e - 3L_\mu + L_\tau)$ gives

$$S_{11}/a^2 \gtrsim S_{23}/bc > S_{33}/c^2 \gg M_{13}/ac\,, \tag{3.50}$$

the ratio of largest to smallest non-vanishing entry being ~ 15. Here we cannot make $M_{ij} \gg S_{ij}$, but are drawn to the scaling $M_{ij} \sim S_{ij}$ (similar for $\boldsymbol{B}_4^R$). The same can be said for case $\boldsymbol{C}^R$ $(L_\mu - L_\tau)$, with the typical relations

$$M_{11}/a^2 \sim S_{13}/ac \sim M_{23}/bc > S_{12}/ab\,. \tag{3.51}$$

However, for $\boldsymbol{C}^R$ there are also solutions that naturally suggest $M_{ij} > S_{ij}$.

The above examples show that the hierarchy among the m_D entries reflects the hierarchy among the $\mathcal{M}_R$ entries. Similar analyses can be performed for the other patters, but the

[11] Note that our symmetries do not constrain the values of Yukawa couplings. In particular, we cannot explain the hierarchy of the charged lepton masses in this framework, but have to put in the right Yukawa couplings by hand. An extension of our model by a Frogatt–Nielsen-type mechanism [172] to explain the hierarchy may be possible, but goes beyond the scope of this thesis.

analysis will not change the conclusion that the $\mathcal{M}_R$ patterns given in Eq. (3.41) are consistent with the most recent data within one standard deviation.

Having discussed texture-zero realizations via continuous symmetries $U(1)'$, let us mention another possibility: discrete subgroups $\mathbb{Z}_n$ of our gauge symmetries $U(1)'$. Such discrete gauge symmetries are yet another way to evade the quantum gravitational breaking of discrete symmetries [173], hence it may be interesting to explore discrete subgroups of the discussed $U(1)'$ gauge symmetries and see whether or not they are useful to derive the allowed two-zero textures. Taking the $B - L_e + L_\mu - 3L_\tau$ symmetry as an example, we find that its $\mathbb{Z}_5$ subgroup with a scalar with charge 3 leads to the same phenomenology as the overlying $U(1)'$. Similar discussions hold for the other symmetries that work with just one scalar. Something new happens however for the two patterns $\boldsymbol{B}^R_{1,2}$ that required two scalars in the above $U(1)'$ approach. For instance, the charge matrices of the $B - L_e - 5L_\mu + 3L_\tau$ symmetry and its $\mathbb{Z}_5$ subgroup are given by

$$Y'(\overline{\nu}^c_{R,i}\nu_{R,j}) = \begin{pmatrix} -2 & -6 & 2 \\ -6 & -10 & -2 \\ 2 & -2 & 6 \end{pmatrix}, \qquad \begin{pmatrix} -2 & -1 & 2 \\ -1 & 0 & -2 \\ 2 & -2 & 1 \end{pmatrix} \bmod 5\,, \tag{3.52}$$

respectively, and we see that instead of two scalars with $|Y'(S_1)| = 10$ and $|Y'(S_2)| = 2$ for the $U(1)'$ case (Tab. 3.3), we only need one scalar with charge 2 in the $\mathbb{Z}_5$ case to obtain the same pattern $\boldsymbol{B}^R_2$. Notice that the family non-universality is preserved even for the $\mathbb{Z}_5$ case, and thus the Dirac mass matrices remain diagonal. In that sense, we can conclude that all viable two-zero textures in $\mathcal{M}_R$ can be obtained from a $U(1)'$ gauge symmetry, be it continuous or discrete, with just one additional complex scalar.

Before we conclude this section, let us make one more remark about our specific realization of texture zeros, concerning the opportunities at colliders. The LHC phenomenology of the $B - \sum_\alpha x_\alpha L_\alpha$ gauge boson Z' is similar to that of the $B - L$ gauge boson (Sec. 2.1.1), so we will not discuss it here. We do however note that the LHC has the potential to differentiate between the different classes of two-zero textures in our model. The reason for the naming scheme of the two-zero textures in Sec. 3.4.1 is the similar phenomenology at neutrino oscillation experiments; for example, the patterns $\boldsymbol{A}^\nu_1$ and $\boldsymbol{A}^\nu_2$ lead to almost identical predictions for the oscillation parameters and are therefore very hard to distinguish using only neutrino data. In our framework, however, these patterns are imposed by the gauge symmetries $B + L_e - L_\mu - 3L_\tau$ and $B + L_e - 3L_\mu - L_\tau$, respectively, which are much easier to separate. One just needs to look at the flavor ratios of the final state $Z' \to \ell\ell$ to verify or exclude the different $B - \sum_\alpha x_\alpha L_\alpha$ models.

3.4.3 Summary of Texture Zeros

Setting entries in $\mathcal{M}_\nu$ or $\mathcal{M}_\nu^{-1}$ to zero in the flavor basis results in testable relations among the neutrino mixing parameters. The study of such texture-zero patterns would not be particularly useful without a means to *impose* these vanishing entries. A novel framework to do exactly this was presented in this section, using simple $U(1)'$ gauge symmetries.

We presented numerous examples of anomaly-free gauge symmetries that lead to two-zero textures in $\mathcal{M}_R$ and therefore to testable predictions for neutrino parameters. We showed that all viable patterns of $\mathcal{M}_R$ ($\boldsymbol{D}^R_{1,2}$, $\boldsymbol{B}^R_{1,2,3,4}$, $\boldsymbol{C}^R$) can be implemented by a family non-universal

$U(1)'$ gauge symmetry with at most two new scalars, making these models very simple and possibly distinguishable at collider experiments. Using instead discrete gauge subgroups $\mathbb{Z}_N \subset U(1)'$ reduces the number of necessary new scalars to one. As a side product, we also see that four of the seven allowed two-zero textures of $\mathcal{M}_\nu$ can have this origin (including the "least fine-tuned" patterns $\boldsymbol{A}_i^\nu$). The remaining three two-zero textures of $\mathcal{M}_\nu$, namely $\boldsymbol{C}^\nu$, $\boldsymbol{B}_1^\nu$ and $\boldsymbol{B}_2^\nu$, cannot be explained in this simple framework.

Compared to other texture-zero models, our approach requires only a modicum of new particles; the most natural two-zero textures in $\mathcal{M}_R \sim \mathcal{M}_\nu^{-1}$ even work with a single complex scalar that breaks the $U(1)'$ (see Tab. 3.2). Simplicity aside, the $U(1)'$ approach to texture zeros also provides a new handle to distinguish closely related patterns by means of the underlying symmetry. The leptonic branching ratios of a future Z' resonance could then provide information about neutrino mixing. This is a particularly strong example of the connection between neutrinos and abelian gauge symmetries that underlies this thesis.

3.5 Conclusion

After a careful survey of the *unflavored* part $U(1)_{B-L}$ of our well-motivated abelian gauge group extension

$$\mathcal{G} = U(1)_{B-L} \times U(1)_{L_e-L_\mu} \times U(1)_{L_\mu-L_\tau} \tag{3.53}$$

in chapter 2, we turned on the flavor in this chapter. Seeing as two-thirds of $\mathcal{G}$ contain flavor information, it is no surprise that we find a rich connection between $U(1)' \subset \mathcal{G}$ subgroups and the distinct leptonic mixing pattern reviewed in Sec. 1.1.

The idea is simple: $U(1)' \subset \mathcal{G}$ subgroups allow *at least* for diagonal Dirac mass matrices for the charged leptons (M_e) and neutrinos (m_D), and typically allow for some entries in the right-handed neutrino Majorana mass matrix $\mathcal{M}_R$. Breaking the $U(1)'$ in the most economic way by a simple SM-singlet scalar can generate more entries in $\mathcal{M}_R$, which is then used in the seesaw mechanism to give mass to the active neutrinos $\mathcal{M}_\nu \simeq -m_D^T \mathcal{M}_R^{-1} m_D$. If the $\mathcal{M}_R$ entries generated by the $U(1)'$ breakdown are much smaller than the "$U(1)'$ symmetric" mass terms—or if some entries in $\mathcal{M}_R$ are still zero after symmetry breaking—we effectively impose a structure on $\mathcal{M}_R$ that trickles down to a structure in $\mathcal{M}_\nu$ (because m_D is often diagonal by symmetry). We have explored the various $\mathcal{M}_\nu$ structures allowed and motivated by current data, and their associated $U(1)' \subset \mathcal{G}$ symmetries.

Depending on the ordering of neutrino masses, $\mathcal{M}_\nu$ exhibits a different approximate lepton number symmetry: L_e for normal hierarchy and $\overline{L} = L_e - L_\mu - L_\tau$ for inverted hierarchy. We have shown that *both* can be realized by imposing a $U(1)_{B+3\overline{L}} \subset \mathcal{G}$ gauge symmetry, surprising as this might seem. In the vanilla framework, the $U(1)_{B+3\overline{L}}$ leads to an approximately L_e symmetric $\mathcal{M}_\nu$, and hence enforces normal hierarchy (with large θ_{23} and θ_{12}, and small θ_{13} and m_{ee}). Decoupling one of the RHNs with an additional $\mathbb{Z}_2$ symmetry leads on the other hand to an approximately $\overline{L}$ symmetric $\mathcal{M}_\nu$, and hence inverted hierarchy (with tiny θ_{13} but large m_{ee}). The latter has the interesting feature of a stable dark matter candidate, coupled to the SM via the new gauge boson Z' and the Higgs portal. The measured relic density can be obtained using any of the boson resonances, and the model is testable in future experiments. Besides normal and inverted hierarchy, quasi-degenerate neutrinos actually display an $L_\mu - L_\tau$

symmetry in their mass matrix, comparably easy to promote to a gauge symmetry, even possible in the SM. This $U(1)_{L_\mu - L_\tau}$ is well studied, and leads to many interesting effects, briefly reviewed above. Most importantly, the bounds on the Z' boson are very weak, as it does not couple to electrons or protons; the strongest constraint comes from the muon's magnetic moment, and the Z' can actually be employed to fix the long-standing discrepancy between the measured value and the theoretical prediction, hinting at a low $U(1)'$ breaking scale around 200 GeV. For neutrinos, we expect close-to maximal θ_{23} and, of course, large neutrino masses measurable in $0\nu2\beta$ experiments, KATRIN, and cosmology.

Beyond the three *approximate* lepton-number symmetries for the neutrino mass matrix, it is possible to use the $U(1)'$-induced structure in $\mathcal{M}_R$ and $\mathcal{M}_\nu$ to enforce testable relations among the neutrino mixing parameters. In our case this is done by imposing two texture zeros in $\mathcal{M}_R$ by a suitable choice of $U(1)' \subset \mathcal{G}$ and charge Y' of the scalar breaking the symmetry. These two zeros then lead to two (complex) constraints on the entries in the low-energy neutrino mass matrix $\mathcal{M}_\nu \simeq -m_D^T \mathcal{M}_R^{-1} m_D = U_{\text{PMNS}}^* \text{diag}(m_1, m_2, m_3) U_{\text{PMNS}}^\dagger$, and hence to *four* constraints on the nine parameters m_j, θ_{ij}, δ, φ_1, and φ_2, to be checked against the observed values. We showed that five out of the seven currently viable two-zero textures in $\mathcal{M}_R$ can be obtained with $U(1)' \subset \mathcal{G}$ symmetries in the simplest possible manner, i.e. broken only by one SM-singlet scalar, while the other viable patterns require two scalars. Improved precision of the neutrino parameters and a determination of the mass scale can test the predictions of the texture-zero ansatz.

Many phenomenological aspects of the models in this chapter are similar to previously discussed $B - L$ analyses ($L_\mu - L_\tau$ aside). However, the fact that our modified gauge group includes flavor information makes it possible to provide predictions on neutrino mixing and their mass spectrum, which is impossible in theories based on $B - L$. Such "flavored $B - L$" scenarios thus offer an interesting framework for connecting neutrinos and abelian gauge symmetries. It bears repeating that abelian gauge groups offer a way to understand leptonic mixing in a simple and *testable* manner, to be contrasted with the more common approach using global non-abelian discrete symmetries.

The zoo of possible local abelian flavor symmetries $U(1)'$ presented in this chapter will shrink significantly following the experimental determination of the neutrino mass hierarchy and/or the neutrino mass scale. Complementary constraints arise from searches for lepton non-universality, a generic prediction of all our models. $L_\mu - L_\tau$ is particularly interesting, as experimental data already hints at a low scale testable at the LHC.

Chapter 4

Dark Symmetries

So far in this thesis, we have been concerned with abelian gauge group extensions that are subgroups of

$$\mathcal{G} = U(1)_{B-L} \times U(1)_{L_e-L_\mu} \times U(1)_{L_\mu-L_\tau} \,, \tag{4.1}$$

following our motivation for $\mathcal{G}$ from Sec. 1.5. In all cases, the new gauge groups have been intimately connected to neutrinos, either concerning their mass hierarchies, their mixing, or their very nature, Dirac or Majorana. In this chapter we will show that neutrino physics can even be influenced by an additional $U(1)'$ if none of the SM fermions are charged under it. In our framework, the connection is realized through the mixing of active neutrinos with states that carry charge of the spontaneously broken $U(1)'$, but are otherwise sterile. Such sterile neutrinos can resolve several long-standing anomalies in neutrino experiments, should they be light—of order eV—and sufficiently mixed. The mechanism presented here provides a motivation for the lightness of these sterile states by putting them in the same seesaw mechanism that generates the small masses for the active neutrinos. A consistent implementation requires the addition of anomaly-canceling fermions, which are automatically stable and form WIMP DM—allowing us to identify $U(1)' \equiv U(1)_{\text{DM}}$.

This chapter follows closely our paper "Exotic charges, multicomponent dark matter and light sterile neutrinos" [8] (in collaboration with H. Zhang).

4.1 Light Sterile Neutrinos

The majority of neutrino oscillation data, as collected by various experiments in different parameter regions, seems to be consistent with three massive active neutrinos, following the arguments from Sec. 1.1. However, a couple of experimental results challenge this simple paradigm and hint towards even more new physics in the neutrino sector, namely the presence of *sterile neutrinos* at the eV scale, which do not participate in the weak interactions but mix with active neutrinos with a mixing angle $\theta_s \sim \mathcal{O}(0.1)$ [174, 175].

Specifically, the LSND [176] and MiniBooNE [177, 178] short-baseline experiments have probed the appearance channel $\overline{\nu}_\mu \to \overline{\nu}_e$ (also $\nu_\mu \to \nu_e$ in MiniBooNE), with source–detector distances L and neutrino energies E sensitive to Δm^2 regions around eV^2. Since this is far above the established active-neutrino mass-squared differences (Tab. 1.2), the observed events hint at the existence of a new neutrino ν_s which mixes with electron and muon neutrinos. Seeing as the invisible Z width is well described by just three light neutrinos [16], the new state has to be *sterile* under $SU(2)_L \times U(1)_Y$. Adding *two* sterile neutrinos with

	Δm^2_{41} [eV^2]	$\lvert U_{e4}\rvert^2$	$\lvert U_{\mu 4}\rvert^2$	Δm^2_{51} [eV^2]	$\lvert U_{e5}\rvert^2$	$\lvert U_{\mu 5}\rvert^2$
$3+1$	1.6	0.033	0.012	–	–	–
$3+2$	1.9	0.03	0.012	4.1	0.013	0.0065

Table 4.1: Results of a global fit to short-baseline data with n additional sterile neutrinos ($3+n$) [179].

eV masses (dubbed $3+2$ scheme compared to the previous $3+1$ scheme) even allows for CP violation, a convenient ingredient to resolve discrepancies between the neutrino mode $\nu_\mu \to \nu_s \to \nu_e$ and its anti-neutrino counterpart. Other than LSND and MiniBooNE, there is also the gallium anomaly, a lower-than-expected flux of electron neutrinos (ν_e disappearance) in gallium-target neutrino experiments, which can be resolved by additional sterile neutrinos. Furthermore, recent re-evaluations of reactor anti-neutrino fluxes indicate that previous reactor-neutrino experiments had observed a flux deficit ($\overline{\nu}_e$ disappearance) as well. An up-to-date global fit to the relevant short-baseline neutrino data can be found in Ref. [179], the results for the $3+1$ and $3+2$ scheme are collected in Tab. 4.1; different combinations of datasets yield improved fits and different numerical values for the mixing parameters, but the overall qualitative picture relevant for this chapter remains. While no individual experiment has provided a 5σ discovery for sterile neutrinos yet—and there are some inconsistencies in the data we have not addressed—the described ~ 2–3σ hints have generated a great deal of interest, with numerous experiments planned to clarify the situation [21]. Let us also mention that the light-element abundances from precision cosmology and BBN seem to favor extra radiation in the Universe, which could be interpreted with the help of one additional sterile neutrino, albeit with a mass *below* eV [180, 181]. As it is, cosmology apparently disfavors the sterile-neutrino parameter space of interest for short-baseline oscillations, depending strongly, however, on the combined datasets [182] and underlying cosmology [183]. We will comment on this in due time. Length constraints do not allow us to elaborate further on the experimental status, but an exhaustive overview of light sterile neutrinos, covering both experiment and theory, can be found in the topical white paper in Ref. [21].

Taking these exciting hints for eV-sterile neutrinos seriously not only spawns new experimental efforts to accumulate more data, but also begs for theoretical explanations and guidance from model building. Note that we have encountered sterile neutrinos many times in the previous chapters of this thesis, albeit under a different name: The right-handed neutrinos of the seesaw mechanism (Sec. 2.2.1) are actually nothing but sterile neutrinos, as they are SM singlets that mix with the active neutrinos. This mixing is of order $\theta_s \sim m_D/\mathcal{M}_R$, too small in the natural seesaw limit $m_D \ll \mathcal{M}_R$ to explain the above-mentioned anomalies. One can however push the seesaw mechanism to a regime where it does work: Taking the scales $m_D \sim 0.1\,\text{eV}$ and $\mathcal{M}_R \sim 1\,\text{eV}$ can give active (sterile) neutrino masses $m_\nu \sim 10^{-2}\,\text{eV}$ ($m_s \sim 1\,\text{eV}$) with mixing $\theta_s \sim 0.1$ [184], in the right range to accommodate the experimental data. The successful generation of two active-neutrino masses via seesaw requires at least two RHNs, so an eV seesaw predicts either more than one light sterile neutrino, or a huge hierarchy in sterile-neutrino masses, i.e. in $\mathcal{M}_R$. The latter is a rather unnatural solution, while the former is incapable to accommodate just one sterile neutrino, i.e. the $3+1$ scheme, and can in any case no longer explain the BAU via leptogenesis.

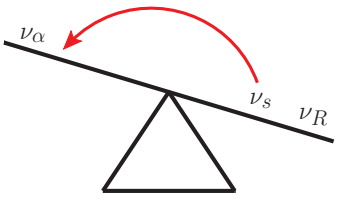

Figure 4.1: The goal of this chapter: to put a sterile neutrino ν_s on the light side of the seesaw.

A more natural explanation for the small sterile neutrino mass scale $\mathcal{O}(\text{eV})$ is hence desirable. Seeing as the seesaw mechanism is one of the most popular theoretical attempts to understand the smallness of *active* neutrino masses, an obvious ansatz is to use the same seesaw mechanism to suppress *sterile* neutrino masses, i.e. to put the sterile neutrinos on the same side of the seesaw as the active neutrinos (Fig. 4.1). To this end, the RHN content has to be extended compared to that in the simplest type-I seesaw mechanism, and a specific flavor structure, i.e. the minimal extended seesaw (MES), has to be employed in order to let the sterile neutrino mass couplings mimic the ones of the active neutrinos [185, 186]. Explicitly, in the MES model, the SM fermion content from Tab. 1.1 is extended by adding three RHNs $\nu_{R,i}$, $i = 1, 2, 3$, together with one singlet fermion S, and the full Majorana mass matrix for the neutral fermions in the basis $(\nu_e, \nu_\mu, \nu_\tau, \nu^c_{R,1}, \nu^c_{R,2}, \nu^c_{R,3}, S^c)$ is *assumed* to be

$$\mathcal{M}_{\text{MES}} = \begin{pmatrix} 0 & m_D & 0 \\ m_D^T & \mathcal{M}_R & m_S \\ 0 & m_S^T & 0 \end{pmatrix} . \tag{4.2}$$

To clear up potential confusion right away: All the fields $\nu_{R,j}$ and S_j introduced in this chapter are just right-handed fermions, sometimes referred to as singlets. We denote the S_j with a different symbol than $\nu_{R,i}$ to emphasize that they are not the usual right-handed neutrinos from the seesaw mechanism, because they carry additional (hidden) quantum numbers and do therefore not partner up with the active neutrinos in the same way.

Let us briefly show how the MES structure can indeed lead to naturally light sterile and active neutrinos, for a longer discussion see Ref. [186].[1] The bare mass term $\mathcal{M}_R$ in $\mathcal{M}_{\text{MES}}$ is unrestricted and can be large, as in the canonical seesaw case (Sec. 2.2.1). We will consider this possibility here by setting $\mathcal{M}_R \gg m_D, m_S$, which leads to the effective low-energy neutrino mass matrix

$$\mathcal{M}_\nu^{4\times 4} \simeq -\begin{pmatrix} m_D \mathcal{M}_R^{-1} m_D^T & m_D \mathcal{M}_R^{-1} m_S \\ m_S^T \mathcal{M}_R^{-1} m_D^T & m_S^T \mathcal{M}_R^{-1} m_S \end{pmatrix} , \tag{4.3}$$

for (ν_L, S_1^c).[2] Such a mass matrix can be diagonalized by means of a unitary transformation as $\mathcal{M}_\nu^{4\times 4} = V\, \text{diag}(m_1, m_2, m_3, m_4)\, V^T$. Phenomenologically, the most interesting situation arises for $m_S \gg m_D$, since the hierarchical structure of $\mathcal{M}_\nu^{4\times 4}$ allows us to apply the seesaw expansion once more, and arrive at the sterile neutrino mass

$$m_4 \simeq -m_S^T \mathcal{M}_R^{-1} m_S \tag{4.4}$$

[1] In the MES framework, the $\nu_e \leftrightarrow S$ conversion has previously been used to solve the solar neutrino anomaly, see Refs. [187, 188].

[2] On a more fundamental level, one can integrate out the heavy right-handed neutrinos ν_R at energies $E \ll \mathcal{M}_R$ to generate the effective dimension-five Weinberg operators $(m_D)_{ij}(m_D)_{kj}\overline{L}_i \tilde{H} H^\dagger \tilde{L}_k / (\langle H \rangle^2 (\mathcal{M}_R)_{jj})$, $w_i^2\, \phi^2 \overline{S}_1 S_1^c / (\mathcal{M}_R)_{ii}$ and $(m_D)_{ij} w_j\, \overline{L}_i \tilde{H} S_1 \phi^\dagger / (\langle H \rangle (\mathcal{M}_R)_{jj})$, which were the starting point in Refs. [189–191].

together with the mass matrix for the three active neutrinos

$$\begin{aligned}\mathcal{M}_\nu^{3\times3} &\simeq -m_D\mathcal{M}_R^{-1}m_D^T + m_D\mathcal{M}_R^{-1}m_S\,(m_S^T\mathcal{M}_R^{-1}m_S)^{-1}m_S^T\mathcal{M}_R^{-1}m_D^T \\ &= U\,\mathrm{diag}(m_1,m_2,m_3)\,U^T,\end{aligned} \tag{4.5}$$

diagonalized by U. The 4×4 unitary mixing matrix V is approximately given by

$$V \simeq \begin{pmatrix}(1-\frac{1}{2}RR^\dagger)U & R \\ -R^\dagger U & 1-\frac{1}{2}R^\dagger R\end{pmatrix}, \tag{4.6}$$

with the active–sterile mixing vector

$$R = m_D\mathcal{M}_R^{-1}m_S\,(m_S^T\mathcal{M}_R^{-1}m_S)^{-1} = \mathcal{O}(m_D/m_S)\,. \tag{4.7}$$

As a rough numerical estimate, for $m_D \simeq 10^2\,\mathrm{GeV}$, $m_S \simeq 5\times10^2\,\mathrm{GeV}$ and $\mathcal{M}_R \simeq 2\times10^{14}\,\mathrm{GeV}$, one obtains the active-neutrino mass scale $m_\nu \simeq 0.05\,\mathrm{eV}$, the sterile-neutrino mass scale $m_s \simeq 1.3\,\mathrm{eV}$ together with mixing $|R| \simeq 0.2$. This is in good agreement with the global-fit data for the $3+1$ scheme [175], i.e. $|R_1| \simeq 0.15$ and $\Delta m_{41}^2 \simeq 1.8\,\mathrm{eV}^2$.

Let us briefly comment on a generalization of the MES structure (4.2), promoting m_D, m_S and $\mathcal{M}_R$ to matrices of dimension $n(\nu_L)\times n(\nu_R)$, $n(\nu_R)\times n(S)$ and $n(\nu_R)\times n(\nu_R)$, respectively. In other words, we take $n(\nu_L)$ active, left-handed neutrinos, $n(S)$ will-be sterile neutrinos and $n(\nu_R)$ heavy RHNs. As far as the mass matrices are concerned, the $n(S)$ fermions S^c behave just like the SM neutrinos ν_L—per construction—so we can use the standard argument to determine the number of massless states as $n(\nu_L)+n(S)-n(\nu_R)$ [137]. Global fits using neutrino oscillations with $n(\nu_L)+n(S)$ light neutrinos are only sensitive to mass-squared differences, so one light neutrino is always allowed to be massless. Consequently, we need at least $2+n(S)$ heavy RHNs $\nu_{R,i}$ if we want $n(S)$ light sterile neutrinos—dubbed $3+n(S)$ scheme. The minimal case—which lends the MES scheme its name—is then $n(S)=1$ and $n(\nu_R)=3$. This case will be discussed in the main part of this chapter, but we will also comment on the extensions described in this paragraph.

The MES structure defined in Eq. (4.2) successfully puts some sterile neutrinos on the light side of the seesaw (Fig. 4.1), leading to sterile neutrinos with small masses and potentially large mixing with the active neutrinos. The main application for such light sterile neutrinos is, of course, the solution of the reactor anomaly [21], but the framework presented here is flexible enough to be of general interest. Our discussion so far is however vastly insufficient: The actual MES pattern—meaning the zeros in the upper and lower right corners of $\mathcal{M}_{\mathrm{MES}}$—has to be enforced and motivated by some symmetry! This is the actual challenge of this chapter: to make a sterile neutrino light *consistently*, i.e. without relying on the magic occurrence of a pattern such as Eq. (4.2). The MES structure can be obtained with discrete flavor symmetries under which the RHNs and S carry different charges [186], but with the same uncomfortable complexity as all models with discrete non-abelian symmetries (cf. Ref. [20]). Following the theme of this thesis, we will show that the MES structure can also be obtained in models with abelian symmetries. For example, one may introduce an extra $U(1)'$ symmetry under which all SM particles and the three RHNs $\nu_{R,i}$ are neutral. One may then write down a bare Majorana mass matrix $\mathcal{M}_R$ for ν_R, which is unprotected by the electroweak or $U(1)'$ scale. The right-handed singlet S on the other hand carries a $U(1)'$ charge Y', and we further

introduce an SM singlet scalar ϕ with charge $-Y'$. The gauge invariant coupling $\overline{S^c}\nu_R\phi$ then generates the m_S matrix in Eq. (4.2) after ϕ acquires a VEV, while the Majorana mass for S (i.e. $\overline{S^c}S$) and a coupling to the active ν_L are still forbidden by the $U(1)'$ symmetry at the renormalizable level. Such a simple realization of MES suffers, however, from the problem of triangle anomalies, and can therefore only work as a global $U(1)'$ symmetry, whose spontaneous breaking would result in a massless Goldstone boson. This might not be disastrous, but more interesting phenomenology arises when the $U(1)'$ is promoted to a *local* symmetry. Consequently, one has to extend the model by additional chiral fermions so as to cancel the arising gauge anomalies. Along these lines, possible model constructions for sterile neutrinos in the $U(1)'$ framework have already been discussed in Refs. [189–191], using an effective field theory approach.

In the rest of this chapter we will work in the seesaw framework and discuss minimal renormalizable and anomaly-free $U(1)'$ symmetries which are spontaneously broken by just one additional scalar and reproduce the MES structure (4.2) accounting for the $3+1$ or $3+2$ scheme of light sterile neutrinos. In particular, we will show that the additional singlet fermions employed for the anomaly cancellation (Sec. 4.2) turn out to be stable—due to accidental remaining $\mathbb{Z}_N$ symmetries—and thus form DM. In Sec. 4.3 we discuss in some detail the phenomenology of a specific example with one light sterile neutrino ($3+1$ scheme) and three stable DM candidates, with a focus on the novel effects inherent in our model. We briefly discuss other interesting examples of this framework in Sec. 4.4, including an extension to the $3+2$ case. Finally, we summarize this chapter in Sec. 4.5.

4.2 Exotic Charges

As already mentioned in the introduction, adding just one extra right-handed singlet S to the three RHNs ν_R results in triangle anomalies if only S is charged under the extra $U(1)'$ symmetry. Instead of treating $U(1)'$ as a global symmetry, we gauge the $U(1)'$ in the rest of this work, and accordingly introduce additional singlet chiral fermions to cancel the anomalies. As we will see below, these new states need to decouple from the neutrino sector in order not to spoil the MES structure (4.2) and automatically lead to DM candidates without the need for additional discrete stabilizing symmetries. This is somewhat similar to Sec. 3.2, where one singlet had to be decoupled in order to obtain the desired structure behind inverted neutrino ordering. Here, however, we do not decouple the unwanted fermions by introducing an additional $\mathbb{Z}_2$ symmetry, but rather select the field content in such a way that an exploitable $\mathbb{Z}_N \subset U(1)'$ subgroup remains automatically.

For a gauged $U(1)'$ symmetry under which all SM particles are singlets, there are no mixed triangle anomalies (cf. Sec. 1.5), so anomaly freedom reduces to the two equations

$$\sum_f Y'(f) = 0 \text{ and } \sum_f (Y'(f))^3 = 0\,, \tag{4.8}$$

where f stands for our new right-handed fermions. In order to cancel the contribution from the will-be sterile neutrino $S \equiv S_1$, more $U(1)'$ charged chiral fermions $S_{i\geq 2}$ have to be introduced. The solutions of Eq. (4.8) for $n = 2$ are simply given by $Y'(S_1) = -Y'(S_2)$. In this case, a bare mass term $m\overline{S_1^c}S_2$—unconstrained by any symmetry—can be constructed,

	$\nu_{R,1}$	$\nu_{R,2}$	$\nu_{R,3}$	S_1	S_2	S_3	S_4	S_5	S_6	S_7	ϕ
Y'	0	0	0	11	-5	-6	1	-12	2	9	11

Table 4.2: $U(1)'$ charge assignments of the right-handed fermions and the scalar ϕ leading to the 3+1 MES scheme.

which spoils the desired MES structure for light sterile neutrinos unless we make m very small. There is no integer solution for $n = 3$ according to the famous Fermat theorem, and it can be shown more generally that Eq. (4.8) with $n = 3$ only has solutions with one Y' being zero, effectively reducing it to the case with $n = 2$. In the case of $n = 4$, it is easy to prove that there is no phenomenologically interesting solution since two of the S_i must have $U(1)'$ charges of opposite sign and equal magnitude, inducing an unconstrained bare mass term as in the case of $n = 2$.

For $n \geq 5$ however, there exist interesting non-trivial anomaly-free charge assignments—dubbed *exotic charges* hereafter—for example the set (10, 4, -9, 2, -7) for $n = 5$ [189–192]. In order to make all new fermions massive at tree level with just *one* scalar ϕ, even more chiral singlets have to be introduced. For the 3+1 scheme discussed in the main text, we add *seven* singlet fermions S_i to the model (the 3+2 scheme discussed in Sec. 4.4 needs six). The charges of all the ten right-handed fermions discussed in the following are listed in Tab. 4.2; they are by no means unique, but serve as a simple illustration of this framework. We further stress that *at least* three $U(1)'$ singlet RHNs $\nu_{R,i}$ are needed in order to explain the observed light neutrino mass-squared differences Δm^2_{21}, Δm^2_{31} and Δm^2_{41}—as already mentioned in the introduction—resulting in one massless active neutrino. This is however not a hard prediction of the MES scheme; adding a fourth ν_R (or even more) to the model makes all light neutrinos massive and does not qualitatively change or complicate the discussion below. Other interesting charge assignments with similar overall phenomenology are presented in Sec. 4.4.

In the scalar sector, we adopt only one SM-singlet scalar ϕ with $U(1)'$ charge 11. With the particle content from Tabs. 1.1 and 4.2 we can then write down the following renormalizable couplings relevant for the neutrino masses

$$\begin{aligned} -\mathcal{L}_m = (m_D)_{ij}\overline{\nu}_{L,i}\nu_{R,j} + \frac{1}{2}(\mathcal{M}_R)_{ij}\overline{\nu}^c_{R,i}\nu_{R,j} + w_i\phi^\dagger\,\overline{S}^c_1\nu_{R,i} \\ + y_1\phi\,\overline{S}^c_3 S_2 + y_2\phi\,\overline{S}^c_4 S_5 + y_3\phi^\dagger\,\overline{S}^c_6 S_7 + \text{h.c.}, \end{aligned} \tag{4.9}$$

where appropriate sums over i and j are understood. The m_D terms stem from EWSB using the usual SM Higgs doublet H (see previous chapters), while w_i and y_i are Yukawa couplings. Absorbing phases into the S_j we can take y_j and one of the w_j to be real, while $\mathcal{M}_R$ can taken to be real and diagonal as well. Once ϕ acquires a VEV, all the neutral fermions in Eq. (4.9) acquire masses, encoded in the full 13×13 mass matrix for the neutral fermions

$$\mathcal{M} = \begin{pmatrix} (\mathcal{M}_{\text{MES}})_{7\times 7} & 0 \\ 0 & (\mathcal{M}_S)_{6\times 6} \end{pmatrix}, \tag{4.10}$$

written in the basis

$$\nu = (\nu_{L,1}, \nu_{L,2}, \nu_{L,3}, \nu^c_{R,1}, \nu^c_{R,2}, \nu^c_{R,3}, S^c_1, S^c_2, S^c_3, S^c_4, S^c_5, S^c_6, S^c_7)\,. \tag{4.11}$$

Here, the matrix $\mathcal{M}_{\text{MES}}$ successfully reproduces the MES structure from Eq. (4.2) with $m_S = w_j\langle\phi\rangle$, and $\mathcal{M}_S$ denotes the mass matrix of $S_{2\text{–}7}$, explicitly given as

$$\mathcal{M}_S = \begin{pmatrix} 0 & y_1\langle\phi\rangle & 0 & 0 & 0 & 0 \\ y_1\langle\phi\rangle & 0 & 0 & 0 & 0 & 0 \\ 0 & 0 & 0 & y_2\langle\phi\rangle & 0 & 0 \\ 0 & 0 & y_2\langle\phi\rangle & 0 & 0 & 0 \\ 0 & 0 & 0 & 0 & 0 & y_3\langle\phi\rangle \\ 0 & 0 & 0 & 0 & y_3\langle\phi\rangle & 0 \end{pmatrix}. \tag{4.12}$$

Obviously $S_{2\text{–}7}$ decouple from the neutrino sector and can no longer be interpreted as right-handed neutrinos, because they do not mix with the SM neutrinos. $S_{2\text{–}7}$ can actually be paired together to form three (stable) Dirac fermions $\Psi_{1,2,3}$, to be discussed in Sec. 4.3. It should be appreciated that the entire structure of $\mathcal{M}$—the $\mathcal{M}_{\text{MES}}$ submatrix, the texture zeros that decouple $S_{2\text{–}7}$, and the convenient block form in $\mathcal{M}_S$—is deeply encoded in the anomaly-free exotic charges of Tab. 4.2.

The mass term m_S of the MES pattern is generated spontaneously in our model, just like the Dirac mass term m_D. For Yukawa couplings of order one, the observed large active–sterile mixing implies the scaling $m_S/m_D \sim \langle\phi\rangle/\langle H\rangle \sim 5\text{–}10$. The new physics scale around TeV is hence not tuned to make LHC phenomenology most interesting, but comes directly from the neutrino sector. Actually—even though we obtain the magic TeV scale—the LHC implications of our model are rather boring, as we only expect small mixing effects in the Higgs and Z-boson interactions, to be discussed in the next subsection.

Let us briefly comment on thermal leptogenesis in our framework. In principle, the additional singlet fermions may spoil the ordinary picture of leptogenesis (Sec. 2.2.2) since the RHNs might predominately decay to sterile neutrinos instead of active neutrinos. This drawback can be easily circumvented here by choosing the coupling of the lightest RHN $\nu_{R,1}$ to the new states to be small, i.e. $w_1 \ll w_{2,3}$. This will not modify the desired MES structure in the neutrino sector, but sufficiently increase the branching ratio of $\nu_{R,1}$ into SM particles, so standard thermal leptogenesis ensues.

Before delving into the dark matter phenomenology of our model, let us make note of a theoretical constraint: An inherent problem in any gauge theory involving abelian factors is the occurrence of a Landau pole, i.e. a scale at which the gauge coupling becomes so large that our perturbative calculations break down. In our model, the one-loop beta function β of the $U(1)'$ gauge coupling g' takes the form

$$\frac{\mathrm{d}}{\mathrm{d}\ln\mu} g' = \beta = \frac{g'^3}{16\pi^2} b = \frac{g'^3}{16\pi^2} \left[\frac{2}{3} \sum_j (Y'(S_j))^2 + \frac{1}{3} (Y'(\phi))^2 \right], \tag{4.13}$$

so the Landau pole of g' appears around the scale

$$\Lambda_L \simeq \Lambda' \exp\left(\frac{8\pi^2}{b\,(g'(\Lambda'))^2} \right), \tag{4.14}$$

where Λ' characterizes the $U(1)'$ breaking scale. Inserting the $U(1)'$ charges given in Tab. 4.2 we find $b = 315$, whereas for the $3 + 2$ scheme from Tab. 4.3 (which will be discussed later

on in Sec. 4.4) we have $b = 75$. For $\Lambda' \simeq 1\,\text{TeV}$ and $\Lambda_L \gtrsim M_{\text{Pl}} \simeq 10^{19}\,\text{GeV}$, one obtains the constraints $g'(\Lambda') \lesssim 0.08$ for the $3+1$ case and $g'(\Lambda') \lesssim 0.17$ for $3+2$ case. Alternatively, if we take the cutoff scale of the model to be the RHN mass scale, i.e. $\Lambda_L \gtrsim M_R \sim 10^{14}\,\text{GeV}$, these bounds relax to $g'(\Lambda') \lesssim 0.1$ and $g'(\Lambda') \lesssim 0.2$ for $3+1$ and $3+2$, respectively. These upper bounds are stricter than the naive perturbativity bound $g'^2/4\pi \lesssim \mathcal{O}(1)/\max(Y')^2$.

4.3 Dark Matter

Having succeeded in implementing the MES scheme for one light sterile neutrino by means of a simple abelian gauge symmetry $U(1)'$, we turn to a discussion of the new stable fermions predicted by our model, with an emphasis on the novel effects in our framework. A brief overview of the boson sector is in order to establish possible connections between the SM and DM sectors. With the introduction of just one SM-singlet complex scalar, the scalar potential W is identical to that of Sec. 2.2.3—minor renaming aside—repeated here for convenience:

$$W = -\mu_H^2|H|^2 + \lambda_H|H|^4 - \mu_\phi^2|\phi|^2 + \lambda_\phi|\phi|^4 + \delta\,|H|^2|\phi|^2\,. \tag{4.15}$$

ϕ can be decomposed as

$$\phi = (\text{Re}\,\phi + i\,\text{Im}\,\phi)/\sqrt{2} \equiv (\langle \text{Re}\,\phi\rangle + \varphi + i\,\text{Im}\,\phi)/\sqrt{2}\,, \tag{4.16}$$

$\text{Im}\,\phi$ being absorbed by the Z' boson after symmetry breaking and in unitary gauge, giving it a mass $M_{Z'} = |11g'\langle\phi\rangle|$. Due to the δ term in the scalar potential, we have a generic mixing between the remaining real scalar field φ and the neutral SM-Higgs h contained in H:

$$\begin{pmatrix} h_1 \\ h_2 \end{pmatrix} = \begin{pmatrix} \cos\theta & -\sin\theta \\ \sin\theta & \cos\theta \end{pmatrix} \begin{pmatrix} h \\ \varphi \end{pmatrix}, \tag{4.17}$$

where h_1 and h_2 are the physical mass eigenstates, and the mixing angle θ is given by

$$\sin 2\theta = \frac{\delta\langle\phi\rangle\langle H\rangle}{\sqrt{\left(\lambda_\phi\langle\phi\rangle^2 - \lambda_H\langle H\rangle^2\right)^2 + \left(\delta\langle H\rangle\langle\phi\rangle\right)^2}}\,. \tag{4.18}$$

A nonzero δ—and hence θ—opens the well-known Higgs portal [193] for the DM production/annihilation, which will be discussed below.

The Higgs portal $|\phi|^2|H|^2$ aside, there is one more renormalizable gauge-invariant operator that will induce a coupling between the SM and DM sectors, namely the kinetic-mixing operator $\sin\xi\, F_Y^{\mu\nu}F'_{\mu\nu}$ (see App. B). This off-diagonal kinetic term involving the hypercharge and $U(1)'$ field strength tensors will induce a coupling of the physical Z' boson to the hypercharge current. The relevant phenomenology of the resulting interaction between the SM and DM particles can be found for example in Refs. [194–196].

As we mentioned before, the singlet fermions $S_{2\text{–}7}$ in our model are DM candidates. To see this more clearly, we write down the full Lagrangian for the right-handed singlets S_2 and S_3:

$$\mathcal{L}_{S_{2,3}} = i\overline{S}_2\gamma^\mu(\partial_\mu - i(-5g')Z'_\mu)S_2 + i\overline{S}_3\gamma^\mu(\partial_\mu - i(-6g')Z'_\mu)S_3 + y_1(\phi\,\overline{S}_3^c S_2 + \text{h.c.})\,. \tag{4.19}$$

By defining the Dirac field $\Psi_1 \equiv S_2 + S_3^c$, the above Lagrangian can be rewritten in unitary gauge as

$$\begin{aligned}\mathcal{L}_{S_{2,3}} &= i\overline{\Psi}_1\gamma^\mu\partial_\mu\Psi_1 - M_1\overline{\Psi}_1\Psi_1 \\ &\quad + g' Z'_\mu \overline{\Psi}_1\gamma^\mu \left(\frac{(-5)-(-6)}{2} + \frac{(-5)+(-6)}{2}\gamma_5\right)\Psi_1 + \frac{y_1}{\sqrt{2}}\varphi\,\overline{\Psi}_1\Psi_1\,.\end{aligned} \tag{4.20}$$

After spontaneous symmetry breaking, Ψ_1 acquires a Dirac mass $M_1 \equiv -y_1\langle \mathrm{Re}\,\phi\rangle/\sqrt{2}$. Similarly, we can define $\Psi_2 \equiv S_4 + S_5^c$ and $\Psi_3 \equiv S_6 + S_7^c$ for $S_{4,5}$ and $S_{6,7}$, and obtain altogether the DM Lagrangian

$$\begin{aligned}\mathcal{L}_{\mathrm{DM}} = \sum_{j=1,2,3}\Bigg[&i\overline{\Psi}_j\gamma^\mu\partial_\mu\Psi_j - M_j\overline{\Psi}_j\Psi_j - \frac{M_j}{\langle \mathrm{Re}(\phi)\rangle}\,\varphi\;\overline{\Psi}_j\Psi_j \\ &+\frac{g'}{2}Z'_\mu\overline{\Psi}_j\gamma^\mu\left[(Y'_{2j} - Y'_{2j+1}) + (Y'_{2j} + Y'_{2j+1})\gamma_5\right]\Psi_j\Bigg]\,,\end{aligned} \tag{4.21}$$

where we defined $Y'_j \equiv Y'(S_j)$. The stability of these fields will be discussed below, but let us first take a look at the interactions involving the will-be sterile neutrino S_1, given by the Lagrangian

$$\mathcal{L}_{S_1} = i\overline{S}_1\gamma^\mu(\partial_\mu - i(11g')Z'_\mu)S_1 + \left(w_i\phi^\dagger\;\overline{S}_1^c\nu_{R,i} + \mathrm{h.c.}\right). \tag{4.22}$$

The important part is the Z' interaction, as it allows for the annihilation $\Psi_i\Psi_i \to Z' \to S_1S_1$. Since the physical sterile neutrino $\nu_s \equiv \nu_4$ consists mainly of S_1, but contains a not-too-small part of the active neutrinos $\nu_{e,\mu,\tau}$, this process connects the DM to the SM sector. Specifically, this "neutrino portal" takes the form

$$\begin{aligned}\mathcal{L}_{\nu\text{-portal}} = \frac{g'}{2}Z'_\mu\Bigg[&\overline{\Psi}_1\gamma^\mu(1-11\gamma_5)\Psi_1 + \overline{\Psi}_2\gamma^\mu(13-11\gamma_5)\Psi_2 + \overline{\Psi}_3\gamma^\mu(-7+11\gamma_5)\Psi_3 \\ &+ 11\sum_{i,j=1}^{4} V_{4i}^* V_{4j}\;\left(\overline{\nu}_i\gamma^\mu\gamma_5\nu_j + \overline{\nu}_i\gamma^\mu\nu_j\right)\Bigg],\end{aligned} \tag{4.23}$$

where the four light mass eigenstates ν_j are written as Majorana spinors and the unitary matrix V is defined in Eq. (4.6).

We further note that the heavier dark matter particles can also convert to the lighter ones, i.e. $\Psi_i\Psi_i \to \Psi_j\Psi_j$ via the s-channel exchange of the bosons Z' or ϕ. Moreover, Ψ_i may also annihilate to Z' and ϕ, which can enhance the total annihilation cross section significantly.

The model content and relevant scales are illustrated in Fig. 4.2. The (self-interacting) DM sector couples to the SM just like all models with a dark symmetry $U(1)_{\mathrm{DM}}$, namely through scalar mixing (Higgs portal, parametrized through δ) and vector mixing (kinetic-mixing portal, parametrized through ξ). However, due to the gauge interactions of the DM with the sterile neutrinos, a new portal through fermion mixing (neutrino portal) opens up in our model. Since this portal is not often discussed in the literature (see however Refs. [197–199]), we will focus on it in the remainder of this chapter.

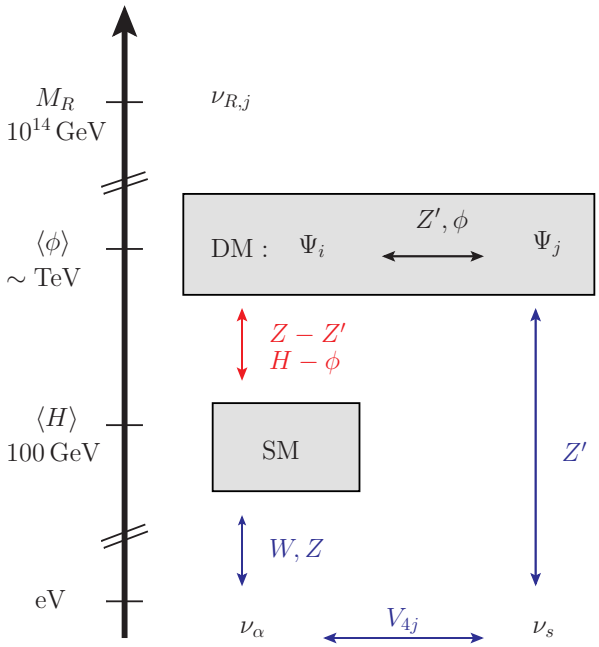

Figure 4.2: Visualization of the different scales in our framework, as well as the relevant interaction channels. The red connection between the DM and SM sectors represents the well-known kinetic-mixing and Higgs portals (based on vector and scalar mixing respectively), while the blue interactions are relevant for the neutrino portal (based on fermion mixing). Interactions with the $\nu_{R,j}$ are highly suppressed and not shown.

Stability

It is fairly obvious that the Ψ_i fields in Eq. (4.21) are stable, since there exists an accidental global $U(1)^3$ symmetry shifting the phases of Ψ_i, similar to baryon and lepton number in the SM (see Sec. 1.4). The occurrence of several stable DM particles, i.e. multicomponent DM, results in numerous interesting effects—see Refs. [200, 201] for some early work. The underlying reason for the stability in our case is the remaining exact $\mathbb{Z}_{11}$ symmetry after the spontaneous breakdown of the $U(1)'$. The Ψ_j form representations under this discrete gauge group with charges 6, 1 and 2 (modulo 11), which stabilizes at least the lightest of them, even when higher-dimensional operators are considered.

While our model is renormalizable, we expect it to be only valid up to a certain cutoff scale Λ, either because quantum gravity takes over, or because sooner or later we will hit the $U(1)'$ Landau pole—as discussed at the end of Sec. 4.2. At the cutoff scale, higher-dimensional operators might be generated, and in our models these will always include $\phi^2\overline{S}_1 S_1^c/\Lambda$ and the Weinberg operator for ν_L-Majorana masses (Eq. (1.18)). Taking $\Lambda \sim M_{\rm Pl}$ does not destroy the discussed MES structure if $\langle\phi\rangle \lesssim 10\,\text{TeV}$. For the charge assignment here, there are also dimension-six operators like $\overline{S}_2^c S_4 \overline{S}_6 S_3^c/\Lambda^2$, which break the global $U(1)^3$ to a $U(1)$ symmetry, so only one stable Dirac fermion survives. However, since these operators are highly suppressed for $\Lambda \sim M_{\rm Pl}$, the resulting lifetimes are typically longer than the age of the Universe, and thus we will not include them in our discussions below, but take all three Ψ_j to be independently stable.

4.3.1 Relic Density and Thermal History

We will now discuss the interplay of the three portals (Higgs, kinetic-mixing, and neutrino portal) and identify some valid regions in the parameter space where the correct relic density

(Eq. (1.26)) for Ψ_j can be obtained. Note that the mixing parameters δ and ξ are the only new physics parameters we assume to be small in this chapter, all other couplings are somewhat "natural." We restrict ourselves to small mixing parameters solely for simplicity, as larger values lead to very constrained effects, see Refs. [193–196, 202].

We only consider freeze-out scenarios. Also note that we always end up with a thermalized sterile neutrino at the epoch of neutrino decoupling, so the usual cosmological bounds on $N_{\rm eff}$ and $\sum m_\nu$ hold [21] (see Ch. 1). This is to be expected in models with light sterile neutrinos, and can be solved on the astrophysics side—as the limits strongly depend on the used datasets [182] and, of course, the underlying cosmology [183]—or by choosing a smaller-than-eV mass for the sterile neutrino.

Case A: $\delta, \xi = 0$. To check the validity of the neutrino portal, we first turn off the Higgs and kinetic-mixing portals by setting $\delta = \xi = 0$ (or at least small enough to be negligible). In this case, the only connection between the new physics sector and the SM comes from active–sterile mixing, or, at a more fundamental level, from the exchange of heavy RHNs. Integrating out the ν_R yields for example the operator $LHS_1\phi/M_R$ (using order one Yukawa couplings), which gives a rough scattering rate for $LH \leftrightarrow S_1\phi$ around $\sim T^3/M_R^2$—to be compared to the expansion rate in the early Universe $\sim \sqrt{g_*}T^2/M_{\rm Pl}$—which puts all particles in equilibrium above $T \gtrsim 10^{10}\,\text{GeV}$. Below that temperature, the two sectors SM and DM (the latter consisting of Z', ϕ and S_j) evolve independently, while the temperature decreases due to expansion of the Universe in both sectors. Nothing really happens until $T \sim$ TeV, when the Ψ_j freeze-out occurs. For simplicity we will ignore the multicomponent structure of the Ψ_j in this qualitative discussion, but will come back to it later on. For now, we assume that the heavier Ψ_j annihilate sufficiently fast into the lightest Ψ_j, which then becomes our DM. This can be accomplished via the mass spectrum of the Ψ_j and ϕ, see Fig. 4.3 for illustrations. To deplete the abundance of the remaining Ψ_j fast enough, we can make use of the neutrino portal, i.e. the annihilation of the lightest Ψ_j into ν_s around the Z' resonance.

After freeze-out, we then have overall three decoupled sectors—SM, Ψ_j and ν_s—all with different temperatures. Above active-neutrino decoupling, the Universe was radiation dominated, so only the temperature of ν_s and the relativistic degrees of freedom in the SM sector are of interest and will be calculated now. Using conservation of entropy in the two sectors SM and DM, we have the equalities

$$g_*^{\rm SM} T^3 a^3\Big|_{t_{\rm sep}} = g_*^{\rm SM} T_{\rm SM}^3 a^3\Big|_{t_{\rm f}} \text{ and } g_*^{\rm DM} T^3 a^3\Big|_{t_{\rm sep}} = g_*^{\rm DM} T_{\rm DM}^3 a^3\Big|_{t_{\rm f}}, \tag{4.24}$$

where g_*^X denotes the effective number of relativistic degrees of freedom in sector X, a the scale factor, $t_{\rm sep}$ the time when the two sectors just separated from equilibrium (i.e. at temperatures around $10^{10}\,\text{GeV}$), and t_f the final time we are interested in, namely close to active-neutrino decoupling (e.g. when $T_{\rm SM} \sim 10\,\text{MeV}$). At t_f, the SM sector consists of photons, electrons and neutrinos, while the DM sector only has the relativistic $S_1 \sim \nu_s$, so we find

$$T_{\nu_s}/T_{\rm SM}\Big|_{t_{\rm f}} = \left(\frac{g_*^{\rm DM}(t_{\rm sep})}{g_*^{\rm DM}(t_f)}\frac{g_*^{\rm SM}(t_f)}{g_*^{\rm SM}(t_{\rm sep})}\right)^{1/3} = \left(\frac{65/4}{7/4}\frac{43/4}{427/4}\right)^{1/3} \simeq 0.98\,. \tag{4.25}$$

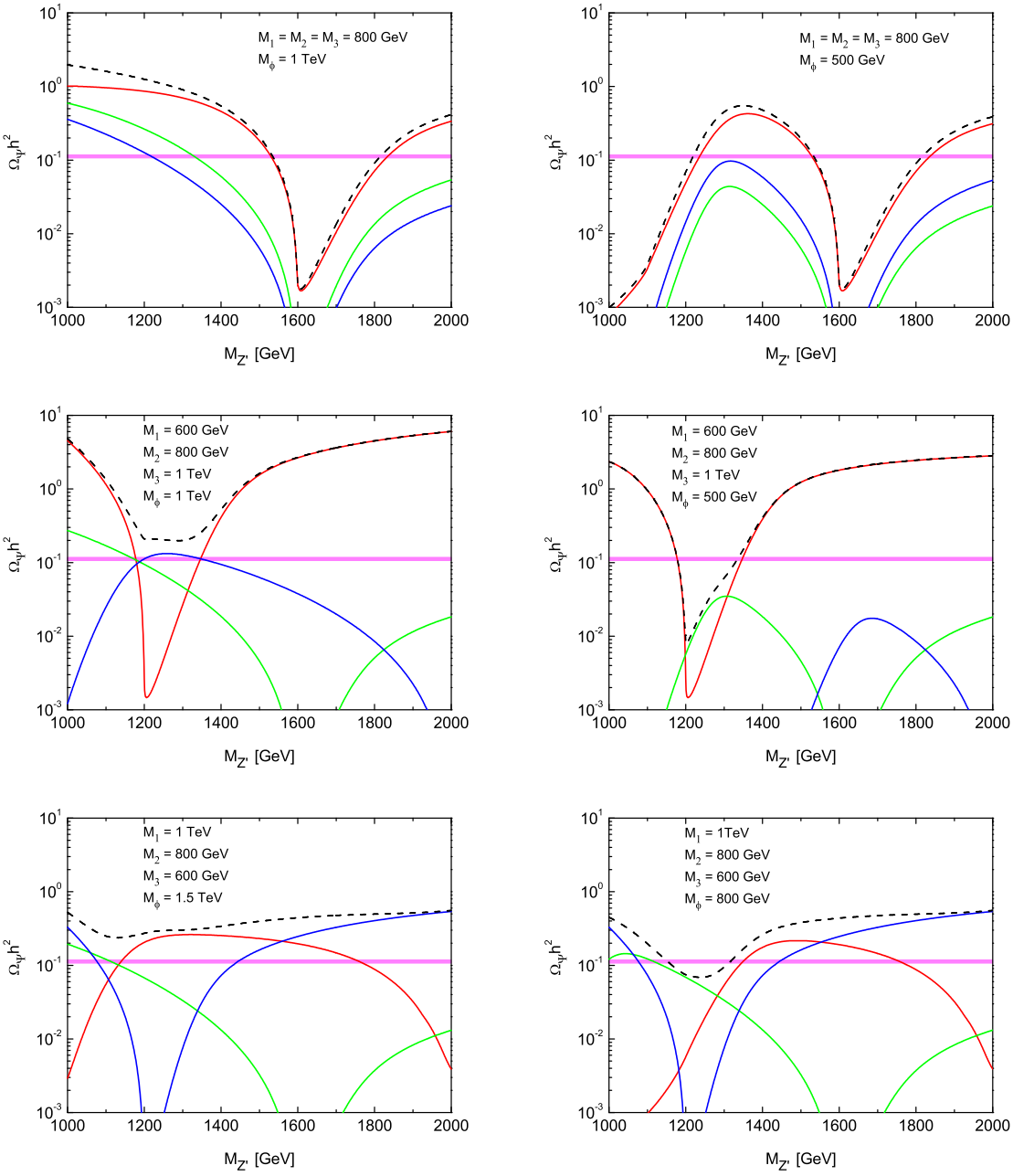

Figure 4.3: Relic density $\Omega_\Psi h^2$ versus the Z' mass $M_{Z'}$ for degenerate (top panels) and hierarchical (middle and bottom panels) DM masses. The VEV is fixed to $\langle\phi\rangle = 1.5\,\text{TeV}$, the scalar mass is indicated in the plot. The red, green and blue lines show the relic density of Ψ_1, Ψ_2, and Ψ_3, respectively, while the black dashed line gives the full $\Omega_\Psi h^2 \equiv \sum_j \Omega_{\Psi_j} h^2$. The horizontal pink band represents the observed relic density from Eq. (1.26) (1σ range).

Ignoring active–sterile oscillations, this would make the sterile neutrinos slightly colder than the active ones at decoupling, alleviating cosmological constraints to some degree (the one sterile neutrino effectively contributes only $\Delta N_{\text{eff}} = (T_{\nu_s}/T_{\text{SM}})^4 \simeq 0.92$ additional neutrinos to the energy density). However, for the sterile neutrino parameters relevant for the short-baseline anomalies, i.e. $m_s \sim$ eV, $\theta_s \sim 0.1$, active–sterile oscillations will become effective around $T \sim 100\,\text{MeV}$–$1\,\text{MeV}$ [22, 203], once again connecting the SM bath and ν_s and thus thermalizing the sterile neutrino at neutrino decoupling. Note that the usual discussions of active–sterile oscillations at these temperatures are not readily applicable, as our model starts with abundant ν_s and self-interactions mediated by Z' (freezing out around $T_{\text{DM}} \sim 10\,\text{MeV}$). In any case, the cosmological bound on relativistic degrees of freedom is expected to be approximately valid in our model.

Case B: $\delta \neq 0$. Let us open the Higgs portal. The thermal evolution is similar to case A, but values $\delta \gtrsim 10^{-7}$ will put ϕ in equilibrium with the SM at temperatures below $T \sim 10\,\text{TeV}$, because the scattering rate $hh \leftrightarrow \phi\phi$ goes with $\delta^2 T/4\pi$ [196]. ϕ and the rest of the DM sector (Z', Ψ_j and ν_s) are in equilibrium through $U(1)'$ gauge interactions (for not too small gauge coupling g'), so SM and DM are in equilibrium around DM freeze-out. For the freeze-out we can again use the neutrino portal, i.e. resonant annihilation $\Psi\Psi \to Z' \to \nu_s\nu_s$. As ϕ and Z' go out of equilibrium around the same time, the connection between the SM sector and ν_s is severed and the two evolve independently for a while, until they are reconnected around $T \sim 10\,\text{MeV}$ by active–sterile neutrino oscillations.

In a different region of parameter space, we can make use of the resonant annihilation of DM into SM particles via scalars, i.e. the Higgs portal in the way it is intended. The discussion is then completely analogous to other $U(1)_{\text{DM}}$ models, so we refer the interested reader to Ref. [202] for a recent evaluation.

Case C: $\xi \neq 0$. A very similar discussion can be made for an open kinetic-mixing portal. Again small values $\xi \gtrsim 10^{-7}$ suffice to reach thermal equilibrium of the SM and DM sectors, e.g. through scattering $Zh \leftrightarrow Z'h$. The thermal evolution then closely resembles that of case B, with some minor differences: The Z'–Z mixing couples ν_s to the SM, so Z' interactions keep ν_s thermalized a while longer before it decouples and finally reconnects with the SM. Furthermore, the DM annihilation around the Z' resonance contains a small branching ratio into SM particles.

The above discussion of the cases A, B, and C gives a qualitative overview over the behavior of the sterile neutrino and the DM particles. In all cases, the SM and DM sectors are in equilibrium at some point—creating DM particles, which then freeze out. Even ignoring the Higgs and kinetic-mixing portals, we can use the neutrino portal to get the correct relic density for Ψ. This reheats the sterile neutrinos, but since they invariably re-equilibrate with the active neutrinos—before active-neutrino decoupling—this does not lead to new effects. Knowing that Ψ will have a similar temperature as the SM sector before freeze-out, and that the final-state sterile neutrinos will re-equilibrate with the active neutrinos anyway, the most interesting part left to discuss is then the annihilation $\Psi\Psi \to \nu_s\nu_s$. For this we again ignore the effects of the Higgs and kinetic-mixing portals for simplicity. We are mainly concerned

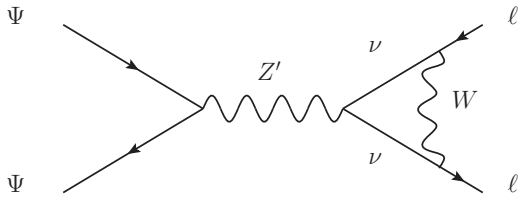

Figure 4.4: Coupling of our DM particles to leptons via loops of active/sterile neutrinos, as relevant for DM detection.

with the multicomponent aspect of our DM, i.e. whether the correct relic density can be obtained for an arbitrary mass spectrum, and which Ψ will be most abundant.

In order to illustrate the feasibility of the DM candidates via the neutrino portal, we implement the model in micrOMEGAs [144–146] and evaluate the relic density of DM particles Ψ_i. The scalar VEV is taken to be $\langle\phi\rangle = 1.5\,\text{TeV}$ as an example. The gauge coupling g' is therefore obtained from the relation of Z' mass and $\langle\phi\rangle$. As shown in the upper panels of Fig. 4.3, a resonance appears at $M_\Psi \simeq M_{Z'}/2$, and the relic density $\Omega_\Psi h^2 \simeq 0.1$ (Eq. (1.26)) measured by WMAP [36] and Planck [23] can be obtained. In the degenerate case (i.e. $M_1 \simeq M_2 \simeq M_3$), the Ψ_1 contribution to $\Omega_\Psi h^2$ is dominating because it has the smallest Z' coupling. Moreover, in case of a small scalar mass, e.g. $M_\phi = 500\,\text{GeV}$, a new channel $\Psi\Psi \to Z'\phi$ opens up for light Z', which is observed from the upper-right panel of Fig. 4.3. For the case of non-degenerate spectrum (i.e. $M_1 \neq M_2 \neq M_3$), the most significant contribution to the relic density may come from either Ψ_1, Ψ_2 or Ψ_3, depending on the specific fermion spectrum as well as the scalar and vector masses. As can be seen in the middle and lower panels of Fig. 4.3, the Ψ_1 contribution to the relic density typically dominates, but there exist model parameters that make Ψ_2 or Ψ_3 the main DM particle.

4.3.2 Direct and Indirect Detection

The neutrino portal discussed so far does not lead to any direct detection signals, because the cross sections are highly suppressed. Loop processes connecting Ψ to SM fermions, e.g. as in Fig. 4.4, vanish in case of degenerate active–sterile masses, so these amplitudes are suppressed by tiny factors like $\Delta m^2_{41}/\mathcal{O}(100\,\text{GeV})^2 \sim 10^{-22}$.

Indirect detection might naively be more fruitful, because the annihilation of the Ψ_j in the Galactic Center or halo leads to two back-to-back neutrinos with energies $\simeq M_j$ (whichever Ψ_j is sufficiently abundant), which is an ideal signal for neutrino telescopes like IceCube.[3] However, since we considered Ψ_j to be a thermal relic, the self-annihilation cross section is already set by the relic density, which is too small to be probed [204]—even though the branching ratio into neutrinos is $\simeq 100\%$, so the signal is as clear as it gets.

Direct and indirect detection measurements are, of course, sensitive to the Higgs and kinetic-mixing portal parameters δ and ξ, as discussed in the literature; Ref. [199], for example, discusses the Higgs portal in a framework similar to the neutrino portal.

[3] The DM–nucleon cross section in our model is too small to efficiently capture DM inside the Sun or Earth, so we have to rely on astrophysical objects with high DM density.

	$\nu_{R,1}$	$\nu_{R,2}$	$\nu_{R,3}$	$\nu_{R,4}$	S_1	S_2	S_3	S_4	S_5	S_6	ϕ
Y'	0	0	0	0	-5	-5	-1	6	2	3	5

Table 4.3: Exotic $U(1)'$ charge assignments of the right-handed fermions and the scalar ϕ to obtain the $3+2$ MES scheme.

4.4 Model Variations

Having focused on one specific example using the charges from Tab. 4.2, we will now briefly present other charge assignments with interesting phenomenology. In all cases we only introduce one additional scalar ϕ, so the results concerning scalar and vector interactions remain unchanged—different numerical values for the charges aside. Only the sterile neutrino and dark matter sector will be slightly modified.

More Light Sterile Neutrinos

The introduction of $n \geq 2$ light sterile neutrinos ($3+n$ scheme) increases the number of new parameters and most importantly allows for CP-violation in the effective oscillation analysis [205]. This feature can significantly improve the fit to neutrino oscillation data and has been studied extensively [174, 175, 206]. Note that the tension with the standard model of cosmology typically worsens, depending on the used data sets [182].

We can easily modify the above $U(1)'$ framework to accommodate the $3+2$ MES scheme by choosing different charges for the singlets; we also need at least one more neutral $\nu_{R,4}$ to generate the necessary light mass squared differences. Now we have to find charges that treat two of the S_i the same (without loss of generality S_1 and S_2), i.e. $Y'(S_1) = Y'(S_2)$, so these will become our two light sterile neutrinos after coupling them to a scalar ϕ. We can once again find exotic charges in such a way that the decoupled S_j become massive by coupling to the same scalar, the magic number for this to happen seems to be six. See Tab. 4.3 for a valid anomaly-free charge assignment with the desired properties—previously used in Ref. [189]. After breaking the $U(1)'$ and the electroweak symmetry, the 13×13 mass matrix for the neutral fermions takes the desired form

$$\mathcal{M} = \begin{pmatrix} (\mathcal{M}_{\text{MES}})_{9\times 9} & 0 \\ 0 & (\mathcal{M}_S)_{4\times 4} \end{pmatrix}, \tag{4.26}$$

where the 9×9 matrix $\mathcal{M}_{\text{MES}}$ in the basis $(\nu_e, \nu_\mu, \nu_\tau, \nu^c_{R,1}, \nu^c_{R,2}, \nu^c_{R,3}, \nu^c_{R,4}, S^c_1, S^c_2)$ is the obvious extension of the MES structure from Eq. (4.2) for the $3+2$ scheme, while $\mathcal{M}_S$ denotes the simple mass matrix of $S_{3\text{–}6}$,

$$\mathcal{M}_S = \begin{pmatrix} 0 & y_1\langle\phi\rangle & 0 & 0 \\ y_1\langle\phi\rangle & 0 & 0 & 0 \\ 0 & 0 & 0 & y_2\langle\phi\rangle \\ 0 & 0 & y_2\langle\phi\rangle & 0 \end{pmatrix}, \tag{4.27}$$

resulting in two Dirac fermions, decoupled from the neutrino sector.

Compared to the $3+1$ scheme discussed so far, the scalar sector is identical, whereas the dark matter sector is slightly modified because we have only two stable Dirac fermions—protected by the remaining discrete gauge group $\mathbb{Z}_5$—instead of three, but two light sterile neutrinos instead of one. This does not influence the qualitative behavior significantly.

The expressions from Sec. 4.1 for the neutrino masses go through in the same manner, we still have

$$\mathcal{M}_\nu^{3\times3} \simeq -m_D \mathcal{M}_R^{-1} m_D^T + m_D \mathcal{M}_R^{-1} m_S \left(m_S^T \mathcal{M}_R^{-1} m_S\right)^{-1} m_S^T \mathcal{M}_R^{-1} m_D^T \tag{4.28}$$

and

$$\mathcal{M}_{\nu_s}^{2\times2} \simeq -m_S^T \mathcal{M}_R^{-1} m_S \tag{4.29}$$

for the masses, where we assumed $m_D \ll m_S \ll \mathcal{M}_R$, and m_D, m_S, and $\mathcal{M}_R$ are 3×4, 4×2, and 4×4 matrices, respectively. The active–sterile mixing is again $\mathcal{O}(m_D/m_S)$, so the required values $\mathcal{O}(0.1)$ put the $U(1)'$ breaking scale naturally in the TeV range.

Let us briefly comment on the thermal evolution of the universe in this model. Seeing as the number of degrees of freedom is smaller (larger) at t_{sep} (t_f) compared to the $3+1$ scheme of Sec. 4.3.1, the sterile neutrino bath is colder than the SM bath (prior to neutrino decoupling) by a factor of $\simeq 0.75$. Without active–sterile neutrino oscillations, this would mean that the two sterile neutrinos effectively only contribute $\Delta N_{\text{eff}} \simeq 0.6$ additional neutrino species to the energy density, alleviating cosmological bounds. It is, of course, to be expected that active–sterile oscillations before neutrino decoupling generate thermal equilibrium among the neutrinos, giving rise to the usual constraints.

For completeness, we also give an assignment for the $3+3$ case, which has been fitted to the neutrino anomalies in Ref. [207]. To make at least five light neutrinos massive, we need five ν_R. A possible charge assignment for nine S_j is then $(7,7,7,2,-9,-1,-6,-4,-3)$, with one scalar $\phi \sim 7$. This leads to three light sterile neutrinos and three stable Dirac DM particles—protected by the remaining discrete gauge group $\mathbb{Z}_7$.

Majorana Dark Matter

Having focused on Dirac DM in the main text for no particular reason, we will now give an example with Majorana DM. For the $3+1$ MES scheme, we take the exotic charges $(6,-3,-3,2,-8,-1,7)$ for the S_i and one scalar with charge $Y'(\phi) = 6$. The VEV of ϕ breaks $U(1)' \to \mathbb{Z}_6$, S_1 will again become the sterile neutrino, while S_2 and S_3 share the most general Majorana mass matrix—which we can take to be diagonal without loss of generality—resulting in two Majorana fermions $\Psi_{1,2}$. (S_4, S_5, S_6, S_7) share the mass matrix

$$\mathcal{M}_S = \begin{pmatrix} 0 & y_1\langle\phi\rangle & 0 & 0 \\ y_1\langle\phi\rangle & 0 & 0 & 0 \\ 0 & 0 & 0 & y_2\langle\phi\rangle \\ 0 & 0 & y_2\langle\phi\rangle & 0 \end{pmatrix}, \tag{4.30}$$

resulting in two Dirac fermions $\Psi_{3,4}$; all Ψ_j are decoupled from the neutrino sector. These particles form representations $\Psi_{1,2} \sim 3 \sim (1,0)$, $\Psi_3 \sim 2 \sim (0,2)$, and $\Psi_4 \sim 1 \sim (1,1)$ under $\mathbb{Z}_6 \cong \mathbb{Z}_2 \times \mathbb{Z}_3$, so depending on the mass spectrum, we can obtain a stable Majorana fermion.

Unstable Dark Matter

The charges for the S_i and ϕ discussed so far have been chosen in such a way that the spontaneous breaking of $U(1)'$ leaves a nontrivial $\mathbb{Z}_N$ that stabilizes the DM candidates. This is, of course, not a generic feature of exotic charges, but just a convenient choice to obtain exactly stable particles. Let us briefly comment on unstable DM candidates: Taking $(1, -10, 9, -7, 6, -11, 12)$ for the $3+1$ scheme with a scalar $\phi \sim 1$ gives three Dirac DM candidates—$\Psi_1 = S_2 + S_3^c$, $\Psi_2 = S_4 + S_5^c$, and $\Psi_3 = S_6 + S_7^c$—which are independently stable due to an accidental global $U(1)^3$ symmetry. However, with this charge assignment, there is no leftover $\mathbb{Z}_N$ symmetry protecting this stability. We can study higher-dimensional operators similar to the discussion in Sec. 4.3. For the charge assignment here, there are already dimension-five operators

$$\phi^2 \overline{S}_3 S_4^c / \Lambda \,, \qquad \phi^2 \overline{S}_3^c S_6 / \Lambda \,, \qquad \phi^2 \overline{S}_2 S_7^c / \Lambda \,, \tag{4.31}$$

which break the global $U(1)^3$ to a $U(1)$ symmetry, so only one stable Dirac fermion survives. Even this stability is not exact, as there are operators like $\phi^6 \overline{S}_5^c \nu_R / \Lambda^5$ which break the global $U(1)$ and lead to DM decay. In this particular example—and for $\Lambda \sim M_{\rm Pl}$—the decay would be suppressed enough to still allow for valid DM, but in principle there are charge assignments with decaying DM, or even no DM candidate at all.

More Less-Exotic Charges

As was shown in Ref. [192], the $U(1)'$ anomalies from S_1 can always be canceled by a (typically large) number of fermions with basic charges -2 and $+1$, instead of the small set of exotic charges used so far. For example, the anomaly of $S_1 \sim 4$ can be canceled with ten copies of S^{-2} and sixteen copies of S^{+1}, i.e. one effectively trades the large charge magnitude of a small number of fermions with the small charge magnitude of a large number of fermions. Since this approach might be seen as less exotic—sacrificing however the small number of particles and parameters employed so far—we will comment on it in our framework. Seeing as the number of fermions S_j^{-2} with charge -2 is not equal to the number of fermions S_j^{+1} with charge $+1$ [192], it does not suffice to introduce just one more scalar $\phi_2 \sim 1$ to make them massive, we need at least two, e.g. $\phi_2 \sim 1$ and $\phi_3 \sim 2$. For all choices, there will be a coupling of either S^{+1} or S^{-2} to the RHNs ν_R, for example $\phi_3 \overline{\nu}_R^c S^{-2}$. Consequently, there is no way of making the anomaly-canceling fermions massive without modifying the MES structure in Eq. (4.2). As our motivation was a consistent realization of this structure, we will not discuss these less-exotic charges any further.

4.5 Conclusion

Should light sterile neutrinos exist, as hinted at by experiments, the origin of their mass demands a theoretical explanation. Generating small sterile neutrino masses via the same seesaw mechanism that suppresses active neutrino masses requires a specific structure in the neutral fermion mass matrix. We showed how this so-called MES structure can be obtained in a simple way from a new spontaneously broken abelian gauge symmetry $U(1)'$, under which the "sterile" neutrino is charged. Heavily mixed eV-scale steriles then hint at a $U(1)'$

breaking scale around TeV. Additional anomaly-canceling fermions need to carry exotic $U(1)'$ charges in order to not spoil the MES structure, which coincidentally stabilizes one or more of them—all without the need for any discrete symmetries. The main connection between this multicomponent dark matter sector and the SM is the active–sterile mixing (neutrino portal). We discussed how the dark matter annihilation almost exclusively into sterile neutrinos can be used to obtain the measured relic density, and also the interplay with the other two portals (Higgs and kinetic-mixing portals).

It should be kept in mind that the SM fermion content forms a chiral set (i.e. has exotic charges) of the gauge group $SU(3)_C \times SU(2)_L \times U(1)_Y$ (Tab. 1.1), so it is a reasonable assumption that a possible hidden sector also has a chiral structure. The simplest example of a chiral hidden sector is then a $U(1)'$ with exotic charges, as discussed in this chapter. We focused on a few specific examples, but the presented framework of exotic charges obviously provides a rich playground for model building, depending on the used charges and number of new particles. Worthwhile extensions with $U(1)'$-charged SM fermions, e.g. $(B-L)$-type symmetries similar to Ch. 2, can be obtained with slightly more complicated scalar sectors and will be discussed elsewhere. See for example Refs. [208, 209] for a model with an MES sterile neutrino coupled to a gauged baryon-number symmetry.

In the greater context of this thesis, we showed in this chapter that the connection between neutrinos and abelian gauge symmetries is not limited to the groups $U(1)_{B-L} \times U(1)_{L_e-L_\mu} \times U(1)_{L_\mu-L_\tau}$ motivated by the SM (see Sec. 1.5), but extends also to "dark" symmetries $U(1)_{\mathrm{DM}}$. The singlet-structure of the neutrinos under the unbroken $SU(3)_C \times U(1)_Y$ allows for mixing with singlet-like fermions from a dark sector, the details of which depend on symmetries such as $U(1)_{\mathrm{DM}}$. Compared to the previous chapters, it is now the *sterile* neutrinos that are possibly connected to new symmetries, opening a window into beyond-the-SM physics by studying these most-elusive of particles.

Chapter 5

Summary and Outlook

Experiments have by now firmly established the existence of neutrino oscillations and lepton flavor mixing, indicating that the Standard Model of particle physics has to be extended to include neutrino masses. Neutrinos are not only the first conclusive sign for physics beyond the SM, they even pave the way for more; in this thesis, we discussed the intimate connection between neutrinos and *abelian gauge symmetries*. The motivation stems directly from the SM, which has the global abelian symmetry $\mathcal{G} = U(1)_{B-L} \times U(1)_{L_e-L_\mu} \times U(1)_{L_\mu-L_\tau}$. Following the great success of the gauge principle in the SM, we can promote this *global* symmetry group to a *local* symmetry group just by introducing three right-handed neutrinos, resulting automatically in *massive neutrinos*. The link between neutrinos and $U(1)'$ is deeper still, as even new abelian symmetries $U(1)_{\mathrm{DM}}$ in the dark matter sector—well-motivated in their own right—can severely affect the behavior of neutrinos, which have the right quantum numbers to act as mediators between the two realms. Putting it all together, we were inclined to study the abelian gauge group extension of the SM (plus right-handed neutrinos, possibly with dark matter) by

$$G_{\mathrm{local}} = \overbrace{\underbrace{U(1)_{B-L}}_{\text{chapter 2}} \times U(1)_{L_e-L_\mu} \times U(1)_{L_\mu-L_\tau}}^{\text{chapter 3}} \times \underbrace{U(1)_{\mathrm{DM}}}_{\text{chapter 4}} \,. \tag{5.1}$$

For simplicity we were only concerned with $U(1)'$ subgroups of G_{local} in the various chapters of this thesis, as indicated above, generated by specific linear combinations of the generators $B - L$, $L_e - L_\mu$, etc. These have the advantage of a simple symmetry-breaking sector—often just one complex scalar in addition to the familiar Higgs doublet—and only few new parameters overall.

In chapter 2 we studied the various realizations of $U(1)_{B-L}$, the unflavored subgroup of G_{local}, both unbroken and spontaneously broken. The abelian symmetry $B - L$ is closely connected to the *nature* of neutrinos, i.e. whether they are Dirac or Majorana particles. The latter arise from breaking the symmetry by *two* units, enabling the famous seesaw mechanism for small Majorana neutrino masses—accompanied by the signature neutrinoless double beta decay—as well as a simple thermal leptogenesis solution for the matter–antimatter asymmetry of the Universe. While phenomenologically interesting, this "Majorana $B - L$" is not the only possible fate of a local $U(1)_{B-L}$. Indeed, the symmetry does actually not have to be broken at all to be consistent with observations, as the $B - L$ gauge boson Z' can either be weakly coupled or acquire a gauge-invariant Stückelberg mass. Neutrinos are then Dirac particles just like the other known fermions, and even the baryon asymmetry can be explained by a leptogenesis mechanism that makes use of the non-thermalization of the right-handed

neutrino partners. Since the Z' mass is a free parameter disconnected from other scales, the unbroken $B-L$ scenario can be probed at every accessible distance, from long-range astrophysics to short-range colliders—potentially proving the existence of a conserved quantum number besides electric charge and color.

Even if $B-L$ is broken, it does not have to be broken by two units: The original-research part of chapter 2 focused on breaking $B-L$ by *four* units, making neutrinos Dirac particles but still allowing for lepton-number-violating processes. We proposed neutrinoless quadruple beta decay ($0\nu4\beta$) as the signature process of the dominant $\Delta L = 4$ interactions—analogous to neutrinoless double beta decay ($0\nu2\beta$) for $\Delta L = 2$—with the prime candidate being $^{150}\mathrm{Nd} \to {}^{150}\mathrm{Gd} + 4\,e^-$. This nuclear decay would emit four electrons with summed total-energy peak at the Q value 2.079 MeV, competing with the already observed double beta decay ($2\nu2\beta$) $^{150}\mathrm{Nd} \to {}^{150}\mathrm{Sm} + 2\,e^- + 2\,\nu$. The expected rates for this $0\nu4\beta$ decay in our simplest model are unobservably small, but existing experiments could put a first limit on this $\Delta(B-L) = 4$ process. We have furthermore shown that the $\Delta(B-L) = 4$ interactions of our model can give rise to a new kind of leptogenesis mechanism with Dirac neutrinos, exciting in its own right. Compared to the old mechanism, our scenario *requires* the thermalization of the right-handed neutrino partners ν_R with the rest of the SM in the early Universe in order to translate a ν_R asymmetry to the baryons. The necessary thermalization manifests itself in a contribution to the effective number of neutrinos $N_{\mathrm{eff}} > 3.14$, providing a handle to test this leptogenesis mechanism. The abelian gauge symmetry $U(1)_{B-L}$ is hence not only linked to the neutrino nature, but also to the origin of matter, making it an important window to physics beyond the SM.

After elucidating the connection between abelian gauge symmetries (namely $B-L$) and the *nature* of neutrinos, we studied the connection of $U(1)'$ to the neutrino *mass hierarchies* and *mixing angles* in chapter 3, using "flavored" $U(1)'$ subgroups of $U(1)_{B-L} \times U(1)_{L_e-L_\mu} \times U(1)_{L_\mu-L_\tau}$ with a minimal scalar sector. Such $U(1)'$ symmetries basically enforce a structure in the Majorana mass matrix of the right-handed neutrinos $\mathcal{M}_R$, slightly perturbed by spontaneous $U(1)'$ symmetry breaking; this structure then trickles down to the active-neutrino Majorana mass matrix $\mathcal{M}_\nu \simeq -m_D^T \mathcal{M}_R^{-1} m_D$ via the seesaw mechanism and can shed light on the peculiar observed pattern. We have shown in particular that $U(1)_{B+3(L_e-L_\mu-L_\tau)}$ is a good symmetry for neutrinos with normal hierarchy, as it leads to an approximately L_e-symmetric neutrino mass matrix $\mathcal{M}_\nu$, giving rise to large neutrino mixing angles and small $0\nu2\beta$ rates. Inverted hierarchy, which requires an approximate $L_e - L_\mu - L_\tau$ symmetry in $\mathcal{M}_\nu$, can on the other hand be obtained by augmenting the local $U(1)_{B+3(L_e-L_\mu-L_\tau)}$ with a $\mathbb{Z}_2$ symmetry. This effectively decouples one of the right-handed neutrinos and turns it into a dark matter candidate, which is coupled to visible matter by the new gauge boson Z'_μ and scalar s. The observed density of dark matter requires a resonantly enhanced annihilation cross section, mediated by either Z' or s.

For quasi-degenerate neutrinos, the abelian symmetry of interest is $U(1)_{L_\mu-L_\tau}$. Acting only on particles of the second and third generation, the constraints on the associated gauge boson are rather weak, allowing for a breaking scale below TeV. Not only can this symmetry provide an explanation for the close-to-maximal atmospheric mixing angle θ_{23} and the small reactor angle θ_{13}, it also nicely solves the longstanding anomaly concerning the muon's magnetic moment; the required values $M_{Z'}/g' \simeq 200\,\mathrm{GeV}$ make the model testable at the LHC. We furthermore discussed texture zeros and vanishing minors in $\mathcal{M}_\nu$ as extreme examples of

$U(1)'$-induced structures, giving rise to falsifiable relations among the neutrino mixing angles and masses. Many of the allowed two-zero textures can be realized in a highly economic way, using only one complex scalar to break the $U(1)'$, and the predicted gauge boson Z' can even provide a new handle to distinguish various patterns. All in all, flavored abelian gauge symmetries make for an economic and testable framework to understand lepton mixing, and should be embraced as an alternative to the increasingly complicated approach of discrete non-abelian global symmetries.

In the last chapter (4), we pointed out that a connection between neutrinos and abelian gauge symmetries can arise even if the symmetry does not act on SM particles. Motivated by experimental hints for sterile neutrinos with eV masses, we constructed a simple model that explains the small sterile-neutrino masses by the very same seesaw mechanism that underlies the active-neutrino masses. The required structure in the neutral-fermion mass matrix is enforced by an abelian gauge symmetry $U(1)'$, acting only on new SM singlets. Anomaly cancellation makes necessary the introduction of fermions which decouple from the SM and consequently make up automatically stable multicomponent dark matter. Since both the sterile neutrinos and the DM fermions are charged under $U(1)' = U(1)_{\mathrm{DM}}$, active–sterile mixing connects the active neutrinos to the gauge symmetry. The existence of light sterile neutrinos could therefore hint at a new abelian gauge symmetry connected to dark matter.

Some topics thematically adjacent to the main part have been placed in the appendices in order to form a more coherent structure. These appendices do nevertheless contain interesting original work, so let us summarize them as well: In appendix B we extended the known framework of Z–Z' mixing to *three* gauge bosons, including the unavoidable kinetic mixing. This is obviously of interest following our motivation of a multitude of abelian groups (Eq. (5.1)) and can lead to intricate couplings between the gauge bosons, dark matter, and neutrinos.

Kinetic mixing is but one oddity of abelian groups, the Stückelberg mass mechanism another: Abelian gauge symmetries are special in the sense that they permit a *massive* gauge boson without symmetry breaking, a fact that we employed in appendix A to motivate a massive photon. Although experimentally constrained to be very light, a massive photon can conceivably decay into the lightest neutrino—connecting yet again neutrinos and abelian gauge symmetries—or particles beyond the SM. We have provided the first lower bound on the lifetime of the photon using the well-measured black-body spectrum of the cosmic microwave background: a mere three years in the photon's rest frame.

With all of the above, we could hopefully convince the reader of the claimed connection between neutrinos and abelian gauge symmetries. As far as possible future improvements of our results go, some work has already been laid out for us. Following our motivation, a discussion of the full gauged symmetry group $\mathcal{G}$ and its breakdown to one of the viable $U(1)'$ subgroups presented here should be a worthwhile endeavor. Such a top-down approach will typically be more restrictive than our bottom-up framework, making it more predictive and testable. As we have seen in this thesis, some symmetries work well with very high breaking scales, e.g. Majorana $B - L$, while others sit comfortably around the electroweak scale ($L_\mu - L_\tau$ and DM symmetries), a feature that should be addressed by the scalar sector behind the breaking $\mathcal{G} \to$ nothing. Going even further up the ladder, an embedding of the flavored part $U(1)_{L_e - L_\mu} \times U(1)_{L_\mu - L_\tau}$ into the non-abelian $SU(3)_\ell$ is possible and replaces the somewhat arbitrary $U(1)^2$ by a factor that explains why there are three generations.

This comes at the prize of a more elaborate scalar sector to generate the charged-lepton mass hierarchies. A more ambitious extension of the above framework could take the quark families into account, too, i.e. look for an explanation of the quark mixing by means of a gauged $U(1)'$ symmetry. This would basically constitute a renormalizable realization of the Froggatt–Nielsen mechanism, with accompanying bosonic and fermionic mediators. A challenging approach for sure, but certainly one with rich phenomenology to explore.

Going back to the bottom-up approach, there are actually still several issues that deserve attention before we put more new physics on top. We have been careful to address the matter–antimatter asymmetry over the entire $B - L$ landscape, but have rarely commented on this issue in the later chapters. For the flavored symmetries employed in chapter 3, the impact on leptogenesis should be clarified, especially in low-scale models such as $L_\mu - L_\tau$. The additional constraints coming from successful baryogenesis can then further increase the testability of our $U(1)'$ approach to lepton mixing. Furthermore, the family non-universal structure of these gauge symmetries can manifest itself not only at the LHC in different ratios of leptonic final states, but also at low energies as loop-induced lepton flavor violation. The prospects to distinguish the different motivated $U(1)'$ groups in this way should be studied in order to make use of the high precision in existing experiments looking for decays such as $\mu \to e\gamma$. A quite different kind of limit not covered in this thesis comes from the scalar sector of our models; it has been shown that the introduction of an additional complex scalar to the Standard Model can solve the meta-stability issue, stabilizing the vacuum up to the Planck scale. While not a problem of immediate concern, any guidance on the parameters of our models is welcome and should be used. In the same vein, renormalization-group running of high-scale parameters are obviously of interest in all models that make use of precise data.

Switching topics, the newly introduced framework of lepton-number-violating Dirac neutrinos provides the theoretical motivation to continue the search for LNV even if neutrinos turn out to be of Dirac type. We have seen that the dominant $\Delta L = 4$ processes are inherently challenging to probe experimentally due to the large number of involved particles, so the main task of future work is to find clean signatures, as well as to provide testable models. The simplest models for LNV Dirac neutrinos presented here employ a gauged $B-L$ symmetry, which lends itself to an embedding into a left–right symmetric framework. Such an extension will significantly increase the intriguing $\Delta L = 4$ cross sections and give rise to new signatures, which might be testable at the LHC or future linear colliders.

We close with a literal outlook. The upcoming years might see the determination of the remaining unknowns in the neutrino sector—mass scale, hierarchy, nature, and CP violation. Along the way, most of the models presented and discussed in this thesis will be ruled out, while some may survive. Hopefully, the ideas presented here will nonetheless be of use in our common quest for knowledge, if only as a snapshot of these exciting times.

Appendix A

Stückelberg Mechanism

This appendix is devoted to a discussion of the Stückelberg mechanism for abelian gauge boson masses. After a brief technical discussion of the mechanism in Sec. A.1 we will study the implications for the photon, namely a nonzero mass and finite lifetime, in Sec. A.2. The latter is taken almost verbatim from the paper "How stable is the photon?" [9].

A.1 Gauge Boson Mass

A quantum field theory with abelian gauge group $U(1)$ and some charged Dirac fermions Ψ_j is part of most textbooks on relativistic quantum mechanics, as it is not only simple enough for calculations, but works as an amazingly good approximation for electromagnetic interactions under the name of quantum electrodynamics (QED). The gauge boson A_μ associated to the group $U(1)_{\mathrm{EM}}$ is then called the photon, the fermions for example electron or muon. The Lagrangian for this renormalizable theory takes the form

$$\mathcal{L} = -\frac{1}{4} F^{\mu\nu} F_{\mu\nu} + \sum_j \overline{\Psi}_j \left(i\partial\!\!\!/ - g Q_j A\!\!\!/ - m_j \right) \Psi_j \,, \tag{A.1}$$

with the mass m_j and charge Q_j of the fermion Ψ_j, g being the $U(1)$ coupling strength. This Lagrangian is invariant under the local gauge transformation

$$\Psi_j \to \exp\left[-igQ_j\theta(x)\right] \Psi_j \,, \quad A_\mu \to A_\mu - \partial_\mu \theta(x) \,, \tag{A.2}$$

$\theta(x)$ being an arbitrary real scalar function of the position four-vector x_μ.

Adherence to gauge invariance then seems to forbid the inclusion of a mass term $\frac{1}{2} m^2 A_\mu A^\mu$ for the gauge field A_μ; it was however noted long ago that such a gauge boson mass does not, in fact, destroy the renormalizability of the theory but leads to a perfectly valid quantum field theory (a good technical and historical overview can be found in Ref. [210]). The reason for this is the Stückelberg mechanism [211], which reinstates gauge invariance by replacing the seemingly problematic mass term with a coupling to a new field σ

$$\frac{1}{2} m^2 A^\mu A_\mu \quad \to \quad \Delta\mathcal{L} \equiv \frac{1}{2} \left(m A^\mu + \partial^\mu \sigma \right) \left(m A_\mu + \partial_\mu \sigma \right) . \tag{A.3}$$

The so-called Stückelberg field σ is a real scalar field which transforms as

$$\sigma \to \sigma' \equiv \sigma + m\,\theta(x) \tag{A.4}$$

under gauge transformations, rendering $\Delta\mathcal{L}$ gauge invariant. Note that $\Delta\mathcal{L}$ automatically contains the kinetic term for σ, and that no additional couplings, e.g. to the fermions Ψ_j, are allowed due to the affine gauge transformation (A.4).

The full Lagrangian $\mathcal{L}+\Delta\mathcal{L}$ is then again invariant under local gauge transformations, and renormalizability and unitarity follow from standard arguments [210]. Gauge invariance of physical results allows us to perform calculations in a gauge of our choosing, and we can in particular choose $\sigma'(x) = 0$ at every point x_μ, which completely eliminates the Stückelberg scalar from the theory and leaves us with $\mathcal{L} + \frac{1}{2}m^2 A_\mu A^\mu$, i.e. the Proca Lagrangian [212] for a massive abelian vector boson. The Stückelberg mechanism therefore illuminates why we can give a mass to the gauge boson of an abelian symmetry without breaking said symmetry: The mass term should not be viewed as *breaking* gauge invariance, it should be viewed as merely *fixing* a gauge.

We stress that the Stückelberg mechanism does not break the $U(1)$ gauge symmetry in any way, and that the mass m is a free new parameter. A small new scale m is technically natural [65], in that all radiative corrections are again proportional to m. We also point out that the above procedure does not extend to non-abelian symmetries, and is therefore not useful to explain the masses for the Z and $W^\pm$ bosons—the only known way to generate masses for non-abelian gauge bosons is spontaneous symmetry breaking.

Connection to Higgs

It might be worthwhile to provide an interesting view on the Stückelberg mechanism from the more familiar perspective of the Higgs mechanism. The connection presented here is strictly speaking unnecessary for our purposes and hopefully neither distracting nor confusing. We take again our QED-like Lagrangian $\mathcal{L}$ from Eq. (A.1), but also introduce a complex scalar S with $U(1)$ charge q:

$$\mathcal{L}' = \mathcal{L} + |(\partial_\mu - igqA_\mu)S|^2 - \lambda\left(|S|^2 - \frac{v^2}{2}\right)^2 , \tag{A.5}$$

leaving out any Yukawa couplings of S to the fermions of the theory. The scalar potential exhibits a minimum at $\langle S\rangle = v/\sqrt{2}$, allowing us to parametrize the complex scalar S in terms of two real scalar fields h and χ as

$$S(x) = \frac{1}{\sqrt{2}}\left[v + h(x)\right] e^{-i\chi(x)/v} , \tag{A.6}$$

yielding the Lagrangian

$$\begin{aligned}\mathcal{L}' = \mathcal{L} &+ \frac{1}{2}\partial_\mu\chi\partial^\mu\chi + gqvA_\mu\partial^\mu\chi + \frac{1}{2}g^2q^2v^2A_\mu A^\mu \\ &+ \frac{1}{2}\partial_\mu h\partial^\mu h - \lambda v^2h^2 - \lambda vh^3 - \frac{1}{4}\lambda h^4 \\ &+ \left[\partial_\mu\chi\partial^\mu\chi + 2gqvA_\mu\partial^\mu\chi + g^2q^2v^2A_\mu A^\mu\right]\left[\left(\frac{h}{v}\right) + \frac{1}{2}\left(\frac{h}{v}\right)^2\right] .\end{aligned} \tag{A.7}$$

We find the usual: a massless Goldstone boson χ, a massive vector boson A_μ ($m^2 = g^2q^2v^2$), a massive Higgs particle h ($m_h^2 = 2\lambda v^2$), and many interaction terms. Let us now consider

the limits $v \to \infty$ and $q \to 0$, keeping the gauge boson mass $m \propto qv$ and g constant. In this limit, all factors h/v vanish, and the Higgs particle h becomes infinitely heavy and decouples from the theory. Only the first line in Eq. (A.7) survives, which is simply the Stückelberg Lagrangian from before: $\mathcal{L}' \to \mathcal{L} + \Delta\mathcal{L}$. Hence, the gauge boson mass stays finite and χ can be readily identified as the Stückelberg scalar σ from above. Since the symmetry-breaking VEV v is put to infinity, the $U(1)$ is actually *not broken*. The Stückelberg mechanism in this light also nicely illustrates why it only works for *abelian* gauge groups: In order to keep the gauge boson mass $m = |gqv|$ finite in the limit $v \to \infty$, we have to let the scalar charge q go to zero. This is allowed because there are no restrictions on the $U(1)$ charges of particles—anomaly cancellation among chiral fermions aside. In comparison, the charge q of a scalar under a *non-abelian* gauge group is replaced by a set of representation matrices, without any free continuous parameters. The masses of the non-abelian gauge bosons therefore depend only on the free parameters g and v, so a finite mass in the limit $v \to \infty$ would require $g \to 0$ and hence decouple the gauge bosons from all other particles.

A.2 Photon Mass and Lifetime

The previous section can be summarized as follows: Gauge bosons of abelian symmetries are permitted to have mass by means of the Stückelberg mechanism—retaining gauge invariance, unitarity, and renormalizability. In Sec. 2.1 we have already applied this mechanism to $U(1)_{B-L}$, the only subgroup of the SM's symmetry group $\mathcal{G} = U(1)_{B-L} \times U(1)_{L_e-L_\mu} \times U(1)_{L_\mu-L_\tau}$ that is phenomenologically allowed to be unbroken. There is, however, another unbroken abelian symmetry of interest in $G_{\text{SM}} \times \mathcal{G}$: $U(1)_{\text{EM}}$. So, as another application of the Stückelberg mechanism, we can give a mass m to the most famous of abelian gauge bosons: the photon. Following our above discussion, there is no theoretical prejudice against a small m over $m = 0$, so the question of a photon mass in QED is purely experimental, and there already are impressive upper limits of

$$m < 10^{-18}\,\text{eV} \simeq 2 \times 10^{-54}\,\text{kg} \simeq (2 \times 10^{11}\,\text{m})^{-1} \tag{A.8}$$

from astrophysical observations, specifically the magnetic field in the solar wind [16,213]. Even stronger limits exist on galactic-sized fields, but suffer from systematic uncertainties [214].

However, we already know that QED is just the low-energy approximation of the Glashow–Weinberg–Salam model of electroweak interactions, so our above motivation for a nonzero photon mass might be in danger. Fortunately, the electroweak gauge group $SU(2)_L \times U(1)_Y$ still features an abelian factor—the hypercharge $U(1)_Y$—that can be used in a Stückelberg mechanism. The resulting mass for the hypercharge gauge boson eventually generates again a massive photon [215].[1] A detailed discussion of this procedure and its implications can be found in Ref. [210]. Since the Stückelberg mechanism only works for abelian groups, the grand unification of the SM gauge group $SU(3)_C \times SU(2)_L \times U(1)_Y$ into a simple non-abelian group like $SU(5)$, $SO(10)$, or E_6 would necessarily result in a truly massless photon [216].

[1] The same trick works, for example, in simple left–right symmetric models [99–101], where the hypercharge $U(1)_Y$ itself results from the breakdown of $SU(2)_R \times U(1)_{B-L}$: A Stückelberg mass of the $B - L$ boson trickles down and makes the photon massive.

Turning this around, the discovery of a massive photon would exclude a huge number of GUTs—and, obviously, be a spectacular finding in its own right.

Let us now move on to the key point of this section: If one can constrain the *mass* of a photon, one should also be able to constrain its *lifetime*. Massless photons in QED are stable purely due to kinematical reasons, there are no additional quantum numbers that forbid a decay. Recalling the tight upper bound on the photon mass though (A.8), there are not many possible final states—indeed, only one *known* particle could be even lighter than the photon: the lightest neutrino ν_1. This is because current neutrino-oscillation experiments can only fix the two mass-squared differences Δm^2_{31} and Δm^2_{21} of the three neutrinos, leaving the absolute mass scale undetermined (see Sec. 1.1). Kinematically, this opens up the possibility of a decay $\gamma \to \nu_1\nu_1$—should $m_1 < m/2$ hold.[2] We thus find once more a connection between neutrinos and abelian gauge symmetries, making the discussion in this section relevant to the topic of the thesis. The loop-suppressed process $\gamma \to \nu_1\nu_1$ can be calculated in the SM (using e.g. a seesaw mechanism (see Sec. 2.2.1) to make neutrinos massive in a renormalizable way), and is, not surprisingly, ridiculously small [219]—being suppressed by the small photon mass, the heavy particles in the loop and maybe the smallest neutrino mass, depending on the operator that induces this decay. We also note that one of the side effects of a massive hypercharge boson—besides a massive photon—are tiny electric charge shifts of the known (chiral) elementary particles [210, 215]. The neutrino then picks up an electric charge $Q_\nu \propto e\, m^2/M_W^2$, which gives rise to a correspondingly small tree-level decay rate $\gamma \to \nu_1\nu_1$. Still, unmeasurable small SM rates have never stopped anyone from looking for a signal, as it would be a perfect sign for new physics.

Particles beyond the SM could not only increase the rate $\gamma \to \nu_1\nu_1$, but also serve as final states themselves, as some SM extensions feature additional (close to) massless states; examples include sterile neutrinos, hidden photons, Goldstone bosons and axions (cf. Ref. [70]). These weakly interacting sub-eV particles are less constrained than neutrinos, and photon decay might be an indirect effect of these states. Although mainly of academic interest, we also mention that a massive photon provides the *possibility* of faster-than-light particles—and a decaying photon even *predicts* them. The question of photon decay is therefore obviously relevant even if the lightest neutrino turns out to be an inaccessibly heavy final state.

Following the above motivation, we set out to find limits on the photon mass m and lifetime τ_γ as model-independent parameters. Most importantly, we do not care about the daughter particles for now. Because of the small allowed values for m, all measurable photons around us are highly relativistic, making a decay hard to observe due to time dilation. Correspondingly, a good limit on τ_γ requires a large number of low-energy photons from well-known far-away sources. Seeing as we have access to very accurate measurements of the CMB—consisting of the oldest photons in the visible Universe—we will take m and τ_γ as parameters that will modify the black-body radiation law—given by the Planck spectrum—and fit the CMB spectrum to obtain bounds on both parameters. Similar analyses have been performed to obtain a limit on the neutrino lifetime in the channels $\nu_i \to \gamma\, \nu_j$ [220]. In our case, we are

[2] The naive prototype model—augmenting the SM by only two right-handed neutrinos (SM+$2\nu_R$)—is problematic, as the initially massless ν_1 will unavoidably pick up a finite mass at loop level [217], which can be too large for our purposes [218]. Fine-tuned solutions aside, we can obtain a simple valid model by imposing a $B - L$ symmetry on the SM+$2\nu_R$, resulting in two Dirac neutrinos and one exactly massless Weyl neutrino.

not looking for a spectral line on top of the CMB, but rather a diminished overall intensity and change of shape.

Before delving into the details, let us present a back-of-the-envelope estimate: CMB photons with low energies around meV have a lifetime $\tau = \gamma_\mathrm{L}\tau_\gamma$ that is increased by a relativistic Lorentz factor $\gamma_\mathrm{L} = E/m \simeq 1\,\mathrm{meV}/10^{-18}\,\mathrm{eV} = 10^{15}$. This lifetime has to be compared to the age of the Universe $t_0 \simeq 13.8 \times 10^9\,\mathrm{yr}$ (or the corresponding comoving distance). Seeing as an improved accuracy A in the measurements will increase the bound, we can estimate $\tau_\gamma \gtrsim t_0/\gamma_\mathrm{L}A$. We therefore expect a lifetime constraint in the ballpark of years from the very precise CMB measurements ($A \simeq 10^{-4}$), which will be confirmed by the more refined analysis below.

The photon mass m modifies the dispersion relation $p^2 = E^2 - m^2$, which changes the spectral energy density of black-body radiation to

$$\rho(T,E)\,\mathrm{d}E = \frac{1}{\pi^2}\,\frac{E^3\,\mathrm{d}E}{e^{E/T}-1}\,\sqrt{1-\frac{m^2}{E^2}}\,, \tag{A.9}$$

but it is unclear how to include the decay width. The expansion of the Universe also needs to be taken into account, as the black-body spectrum no longer stays in shape for $m \neq 0$. Let us therefore give a brief derivation of the energy spectrum of massive unstable photons during cosmic expansion.

Ignoring the width for a moment, the number density of massive photons right after decoupling (at the time of last scattering $t_L \simeq 400\,000\,\mathrm{years}$) is given by [221]

$$n_0(p,t)\,\mathrm{d}p = \left(\frac{a(t_L)}{a(t)}\right)^3 n_0(p_L,t_L)\,\mathrm{d}p_L = \frac{4\pi g p^2\,\mathrm{d}p/(2\pi)^3}{\exp\left(\sqrt{p^2+m^2\left(\frac{a(t_L)}{a(t)}\right)^2}/T\right)-1}\,, \tag{A.10}$$

where $p = p_L\ a(t_L)/a(t)$ is the redshifted momentum, T the temperature at time t, and g the number of spin states. We take $g = 2$, because only the transverse modes are excited before decoupling—this implicitly constrains m, as discussed below. The chemical potential of *massless* photons is zero, and since we assume that as our initial condition at t_L, we set it to zero in all our calculations.

Including the width, we can write down the differential equation for the time evolution of the number density $n(p,t)$

$$\frac{\mathrm{d}}{\mathrm{d}t}n(p,t) = \frac{\mathrm{d}}{\mathrm{d}t}n_0(p,t) - \Gamma(p)n_0(p,t)\,. \tag{A.11}$$

The first term on the right-hand side describes the number density dilution due to the expansion of the Universe, while the second one is due to photon decay. The width can be obtained from the rest-frame width $\Gamma_0 = 1/\tau_\gamma$ by a Lorentz boost: $\Gamma(p) \simeq \Gamma_0\frac{m}{p}$. We use the boundary condition $n(p,t_L) = n_0(p,t_L)$ and obtain the number density today

$$n(p,t_0) = n_0(p,t_0) - \Gamma_0 \int_{t_L}^{t_0} \frac{m}{p} n_0(p,t)\,\mathrm{d}t\,. \tag{A.12}$$

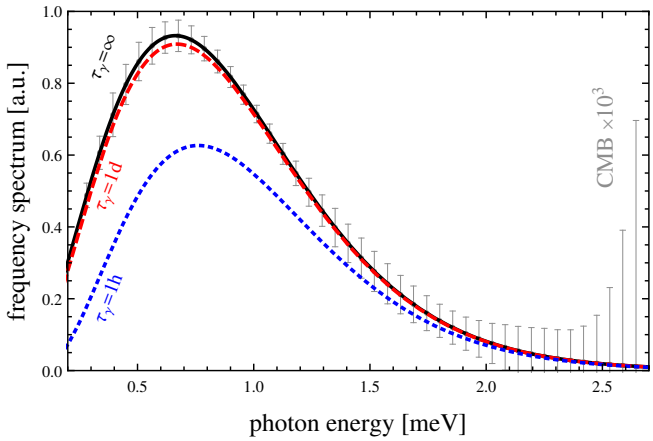

Figure A.1: CMB spectral distribution for $m = 10^{-18}\,\text{eV}$ and $\tau_\gamma = \infty$ (black), $\tau_\gamma = 1\,\text{d}$ (dashed red), and $\tau_\gamma = 1\,\text{h}$ (dotted blue) using Eq. (A.15), as well as the COBE data (error bars multiplied by 10^3 to be visible).

The integral can be evaluated to

$$\int_{t_L}^{t_0} \frac{m}{p} n_0(p,t)\,\mathrm{d}t = \frac{m}{p_L} n_0(p_L,t_L) \int_{t_L}^{t_0} \frac{a(t_L)}{a(t)}\,\mathrm{d}t = \frac{m}{p} n_0(p,t_0)\; d_L\,, \tag{A.13}$$

with the comoving distance of the surface of last scattering $d_L = \int_{t_L}^{t_0} a(t_0)/a(t)\,\mathrm{d}t \simeq 47$ billion lightyears. Overall we have:

$$n(p,t_0) \simeq n_0(p,t_0)\left(1 - \Gamma_0 \frac{m}{p} d_L\right) \simeq n_0(p,t_0) \exp\left(-\Gamma_0 \frac{m}{p} d_L\right). \tag{A.14}$$

The energy density relevant for the CMB spectrum is then obtained by multiplying $n(p,t_0)$ with $E = \sqrt{p^2+m^2}$:

$$\rho(E,T)\,\mathrm{d}E \simeq \frac{1}{\pi^2} \frac{E^3\,\mathrm{d}E}{e^{\sqrt{E^2-m^2}/T} - 1} \sqrt{1 - \frac{m^2}{E^2}}\, \exp\left(-\Gamma_0 \frac{m}{E} d_L\right), \tag{A.15}$$

where we approximated

$$\sqrt{p^2 + m^2 \left(\frac{a(t_L)}{a(t)}\right)^2} \simeq \sqrt{E^2 - m^2} \tag{A.16}$$

because $a(t_L)/a(t_0) \simeq 8 \times 10^{-4}$. Because of this approximation, the limit $\rho(E \to m, T)$ is nonzero, which is, however, of no importance for our CMB analysis.

Equation (A.15) is the key equation of this section and will now be used to set constraints on m and $\Gamma_0 = 1/\tau_\gamma$. For illustrative purposes we show the spectrum for various values in Fig. A.1. As expected from time-dilation arguments, the low-energy part of the spectrum shows the strongest deviations, which fortunately also features the smallest experimental error bars. Using the COBE (COsmic Background Explorer) data set of the CMB [222, 223]

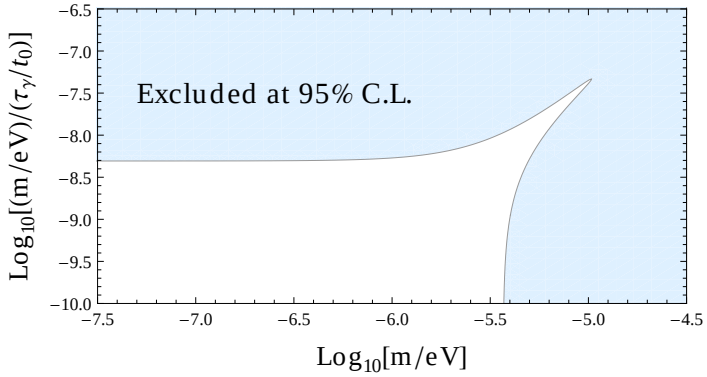

Figure A.2: Constraints on photon mass m and lifetime τ_γ from the CMB spectrum.

we can construct a simple χ^2 function to fit the spectrum from Eq. (A.15).[3] The best fit values are at $m = 0 = \Gamma_0$, so we can only obtain exclusion ranges, shown in Fig. A.2. The limit on the photon mass is not competitive with other experiments—$m < 3 \times 10^{-6}\,\text{eV}$—but for the photon width we find the only existing (and model-independent) bound

$$\tau_\gamma > 3\,\text{yr}\left(\frac{m}{10^{-18}\,\text{eV}}\right) \tag{A.17}$$

at 95% C.L. This would correspond to a photon lifetime of only *three years*, should the photon mass be close to its current bound (A.8). Another useful form of the constraint is given by

$$\left(\frac{m}{10^{-18}\,\text{eV}}\right)\left(\frac{\Gamma_0}{7.5 \times 10^{-24}\,\text{eV}}\right) < 1\,. \tag{A.18}$$

For two-particle fermionic final states X, the decay rate $\gamma \to X\overline{X}$ from (effective) interactions like $g\overline{X}\gamma_\mu X A^\mu$ will be of the form $\Gamma_0 \sim g^2 m/4\pi$ [219]. With Eq. (A.18) we can constrain $g \lesssim 0.03\,e$, which corresponds to a very large effective electric charge and is excluded by other experiments [225].[4] In particular, final state neutrinos are far better constrained by their electric properties to be relevant in photon decay (see for example Ref. [220] for a recent review). Our complementary and model-independent approach should be interesting nonetheless, as it constitutes the only *direct* constraint on the photon lifetime as of yet.

Let us make a couple more comments to illustrate some issues with our above analysis. Our approach basically assumed a vanishing or negligible number density of Stückelberg scalars σ and daughter particles X prior to photon decoupling. To ensure this, m and Γ_0 need to be small: σ has only the interaction $mA^\mu\partial_\mu\sigma$, so for small mass m, it will not be in equilibrium with the rest of the SM. The creation rate of σ via $e\gamma \leftrightarrow e\sigma$ is proportional to $\alpha^2 m^2/T$, which has to be smaller than the expansion rate of the Universe $H(T) \simeq T^2/M_\text{Pl}$—at least before weak decoupling around $T \simeq 1\,\text{MeV}$—in order to not put σ in thermal equilibrium during BBN. For $m < 10^{-3}\,\text{eV}$, only the transverse polarizations of the photon are excited, making it

[3] Ground-based and balloon experiments probe the CMB down to energies $\sim 10^{-6}\,\text{eV}$, which typically have much larger errors. Additionally, there is an excess at low energies that is not understood yet [224], so we do not include those data.

[4] It is of course trivial to reinterpret bounds on millicharged particles [225] in terms of photon decay.

okay to treat the photon as massless before BBN. For the initial condition of our black-body calculation, however, we need to ensure that only the two transverse degrees of freedom of the photon are excited at the surface of last scattering at $T \simeq 0.25\,\mathrm{eV}$. This requires $m < 5 \times 10^{-13}\,\mathrm{eV}$, making our approach a little inconsistent, because at these low masses the primordial plasma—consisting mainly of partly ionized hydrogen and helium—cannot be ignored. We will remark on this below.

On to the daughter particles: The interaction rate of photons with their will-be daughter particles at temperature T will be something like $\Gamma_0 T/m$, as it should be finite in the limit $m \to 0$. This rate has to be smaller than the expansion rate of the Universe at BBN—unless the final daughter particles are neutrinos. This gives the condition $\Gamma_0 \ll 10^{-22} m < 10^{-40}\,\mathrm{eV}$, which is far stronger than the bound we obtained from the CMB analysis above, directly related to the fact that the minicharge of new ultralight particles is tightly constrained [225]. One should be careful with the above constraint though, because additional degrees of freedom at BBN are currently still allowed by cosmological observations [23].

Having discussed the initial conditions of our analysis—which degrees of freedom are present at recombination—it is time to scrutinize our main assumption: that the photons are free streaming. This is usually a very good approximation, as the density of ionized hydrogen is rather small after recombination, but it is still large enough to induce a plasma mass as large as $10^{-9}\,\mathrm{eV}$ to the photon. Further complications arise from the non-ionized hydrogen and helium, as they effectively make the Universe a refractive medium—changing the dispersion relation of on-shell photons even further. This has been emphasized in Ref. [226], where CMB constraints on photon oscillations into hidden photons [227] have been discussed. Their analysis (and phenomenology) is very similar to our discussion of photon decay, but in our case the inclusion of the plasma is more difficult. The photon in a medium requires a careful treatment, as it becomes just one of several quasiparticles that can be excited. (A well-studied example relevant to our discussion is the decay of plasmons—effectively massive photons—into neutrinos as a mechanism to cool stars [220].) This makes it difficult, if not impossible, to constrain the properties of a free photon—namely, m and τ_γ—through a study of these quasiparticles, certainly not in the model-independent way we aspired to. Naively reinterpreting τ_γ as an effective coupling of the daughter particles to the photons—and further ignoring the vacuum mass m in the dense plasma—would lead back to the usual bounds on millicharged particles [225].

In conclusion, a massive photon sounds crazy and exotic, but it really is not. A massless photon is neither a theoretical prediction nor a necessity, but rather a phenomenological curiosity. We should try to understand why this parameter in the Lagrangian (that we can just write down) is so small. This is similar to the strong-CP problem [228], and in both cases experiments so far have only come up with upper bounds for these parameters. Independent of its actual value, a nonzero photon mass immediately opens up the possibility of photon decay—even in the SM—which can, and should, also be constrained. Using the long-lived low-energy photons of the cosmic microwave background, we were able to derive the first direct bound on the photon lifetime in this section. Adopting the largest allowed value for the photon mass from other experiments, $m \simeq 10^{-18}\,\mathrm{eV}$, we find a lower limit of about 3 yr on the photon rest-frame lifetime; for photons in the visible spectrum, this corresponds to a lifetime around 10^{18} yr. A study of the challenging, but important, effects of the primordial plasma on this limit has to be left for future work.

Appendix B

Gauge Boson Mixing

In this appendix we provide a brief discussion of kinetic mixing [73] and, more generally, Z–Z' mixing. This topic is relevant far beyond the topic of this thesis, i.e. the abelian gauge symmetries motivated in Sec. 1.5, as it pertains to all SM extensions by abelian gauge groups, be it motivated by GUTs (for a review and a list of early references see Ref. [72]), flavor symmetries (early treatments of abelian and non-abelian gauged flavor groups include Refs. [229–232]), and DM models [194, 195, 233].

After a brief discussion of the simplest case—kinetic mixing of just two abelian gauge bosons, one of them coupled to hypercharge—we extend the framework to three abelian groups, including also mass mixing. This second part follows closely our paper "Kinetic and mass mixing with three abelian groups" [10] (in collaboration with W. Rodejohann). Note that we will for the most part represent the new gauge boson(s) by X_μ instead of Z'_μ in this appendix, in order to avoid a cluttered notation.

B.1 Kinetic Mixing

Let us first consider the simplest Z–Z' mixing scenario, induced only by a kinetic-mixing term $\sin\chi F_Y^{\mu\nu} F'_{\mu\nu}$. Since the field strength tensors $F_Y^{\mu\nu}$ and $F'_{\mu\nu}$ are gauge invariant under the associated abelian gauge groups $U(1)_Y$ and $U(1)'$, such a cross-coupling term is always allowed in the Lagrangian.[1] Even if the kinetic-mixing angle χ is zero at some scale, it will typically be generated radiatively [73]. In models where scalar fields carry charges under both $U(1)_Y$ *and* $U(1)'$, mass mixing terms like $\delta M^2 Z^\mu X_\mu$ will be generated by their VEVs, further complicating Z–Z' mixing. Since we only considered $U(1)'$ breaking via SM-singlet scalars in this thesis, there is no mass mixing at tree level, allowing us to use the calculations from below. The effect of mass mixing—and more than one $U(1)'$ group—is considered in more generality in Sec. B.2.

The Lagrangian of interest after breaking our extended gauge group $G_{\text{SM}} \times U(1)'$ to $SU(3)_C \times U(1)_{\text{EM}}$ is composed of the parts [234]

$$\begin{aligned}
\mathcal{L}_{\text{SM}} &= -\frac{1}{4}\hat{B}_{\mu\nu}\hat{B}^{\mu\nu} - \frac{1}{4}\hat{W}^a_{\mu\nu}\hat{W}^{a\mu\nu} + \frac{1}{2}\hat{M}_Z^2\hat{Z}_\mu\hat{Z}^\mu - \frac{\hat{e}}{\hat{c}_W}j_Y^\mu\hat{B}_\mu - \frac{\hat{e}}{\hat{s}_W}j_W^{a\mu}\hat{W}^a_\mu\,, \\
\mathcal{L}_X &= -\frac{1}{4}\hat{X}_{\mu\nu}\hat{X}^{\mu\nu} + \frac{1}{2}\hat{M}_X^2\hat{X}_\mu\hat{X}^\mu - \hat{g}j^\mu\hat{X}_\mu\,, \\
\mathcal{L}_{\text{mix}} &= -\frac{\sin\chi}{2}\hat{B}_{\mu\nu}\hat{X}^{\mu\nu}\,,
\end{aligned} \tag{B.1}$$

[1] Since kinetic mixing relies on two abelian factors in the gauge group, the embedding of G_{SM} in a simple non-abelian group like $SO(10)$ in the context of GUTs would render our discussion mute.

with the would-be Weinberg angle $\hat{\theta}_W$ and $\hat{s}_W \equiv \sin\hat{\theta}_W$, $\hat{c}_W \equiv \cos\hat{\theta}_W$. The hypercharge gauge boson and field strength tensor are denoted by $\hat{B}_\mu$ and $\hat{B}_{\mu\nu}$, respectively. The currents are defined as

$$\begin{aligned} j_Y^\mu &= -\frac{1}{2}\sum_{\ell=e,\mu,\tau}\left[\overline{L}_\ell\gamma^\mu L_\ell + 2\,\overline{\ell}_R\gamma^\mu\ell_R\right] + \frac{1}{6}\sum_{\text{quarks}}\left[\overline{Q}_L\gamma^\mu Q_L + 4\,\overline{u}_R\gamma^\mu u_R - 2\,\overline{d}_R\gamma^\mu d_R\right], \\ j_W^{a,\mu} &= \sum_{\ell=e,\mu,\tau}\overline{L}_\ell\gamma^\mu\frac{\sigma^a}{2}L_\ell + \sum_{\text{quarks}}\overline{Q}_L\gamma^\mu\frac{\sigma^a}{2}Q_L\,, \end{aligned} \tag{B.2}$$

with the left-handed $SU(2)_L$ doublets Q_L and L_ℓ and the Pauli matrices σ^a. We also define the electromagnetic current $j_{\text{EM}} \equiv j_W^3 + j_Y$ and the weak neutral current $j_{\text{NC}} \equiv 2j_W^3 - 2\hat{s}_W^2 j_{\text{EM}}$, while the new current j associated to the $U(1)'$ is left unspecified for now. We furthermore introduce the fields $\hat{A} \equiv \hat{c}_W\hat{B} + \hat{s}_W\hat{W}_3$ and $\hat{Z} \equiv \hat{c}_W\hat{W}_3 - \hat{s}_W\hat{B}$, corresponding to the photon and the Z_{SM} boson in the absence of $\mathcal{L}_{\text{mix}}$. Here and in the following we will often omit the Lorentz indices on the currents and gauge fields, expressions such as jA are to be read as $j^\mu A_\mu$.

In our discussion it is actually irrelevant how the $U(1)'$ mass term $\hat{M}_X^2\hat{X}_\mu\hat{X}^\mu$ is generated, be it via spontaneous symmetry breaking or the Stückelberg mechanism (App. A), the latter leaving the group $U(1)'$ unbroken. On to the actual mixing: The Lagrangian $\mathcal{L} = \mathcal{L}_{\text{SM}} + \mathcal{L}_X + \mathcal{L}_{\text{mix}} + \dots$ is written in terms of the *gauge eigenstates* (denoted by hatted fields), but for calculations we need the *mass* eigenstates with definite kinetic terms. To diagonalize the kinetic terms, we define the new fields $X^\mu = \cos\chi\hat{X}^\mu$ and $B^\mu \equiv \hat{B}^\mu + \tan\chi X^\mu$—with corresponding field strength tensors—with standard kinetic terms:

$$-\frac{1}{4}\hat{B}_{\mu\nu}\hat{B}^{\mu\nu} - \frac{1}{4}\hat{X}_{\mu\nu}\hat{X}^{\mu\nu} - \frac{\sin\chi}{2}\hat{B}_{\mu\nu}\hat{X}^{\mu\nu} = -\frac{1}{4}B_{\mu\nu}B^{\mu\nu} - \frac{1}{4}X_{\mu\nu}X^{\mu\nu}\,. \tag{B.3}$$

The neutral vector fields B, X, and $\hat{W}^3 \equiv W^3$ now have properly normalized diagonal kinetic terms, but share a non-diagonal symmetric 3×3 mass matrix, to be read off of Eq. (B.1):

$$\mathcal{M}^2_{B,W^3,X} = \begin{pmatrix} \hat{s}_W^2\hat{M}_Z^2 & -\hat{c}_W\hat{s}_W\hat{M}_Z^2 & -\hat{s}_W^2\tan\chi\hat{M}_Z^2 \\ \cdot & \hat{c}_W^2\hat{M}_Z^2 & \hat{c}_W\hat{s}_W\tan\chi\hat{M}_Z^2 \\ \cdot & \cdot & \hat{M}_X^2/\cos^2\chi + \hat{s}_W^2\tan^2\chi\hat{M}_Z^2 \end{pmatrix}. \tag{B.4}$$

It is easy to check that this matrix has one vanishing eigenvalue, corresponding to a massless leftover photon A_μ. The other two eigenvalues $M_{1,2}^2$ correspond to the masses of the two massive neutral vector bosons $Z_{1,2}$. An *orthogonal* transformation is used to rotate (B, W^3, X) into the mass eigenstates (A, Z_1, Z_2) without re-introducing off-diagonal kinetic terms:

$$\begin{aligned} A_\mu &= \hat{c}_W B_\mu + \hat{s}_W W_\mu^3\,, \\ Z_{1,\mu} &= \cos\xi\left(\hat{c}_W W_\mu^3 - \hat{s}_W B_\mu\right) + \sin\xi X_\mu\,, \\ Z_{2,\mu} &= \cos\xi X_\mu - \sin\xi\left(\hat{c}_W W_\mu^3 - \hat{s}_W B_\mu\right), \end{aligned} \tag{B.5}$$

ξ being a mixing angle that depends on χ and the other parameters in $\mathcal{M}^2_{B,W^3,X}$ [234]. The limit $\xi \to 0$—induced by $\chi \to 0$—obviously brings us back to the SM definition of photon

and Z boson (and the Weinberg angle $\hat{\theta}_W$), the new X boson being decoupled. For $\xi \neq 0$, the coupling strength of the vector boson Z_1 studied at LEP will be reduced by $\cos^2 \xi$ compared to the SM, and the famous relation $\rho \equiv M_W^2/M_Z^2 c_W^2 = 1$ is modified as well, resulting in constraints on ξ; typically, the model-dependent limits are of order $|\xi| \lesssim 10^{-2}$–10^{-3} [72]. Other effects of this Z–Z' mixing can be found in the literature [73, 234–237].

Let us consider the most common limit $\chi \ll 1$ and $\hat{M}_X^2 \gg \hat{M}_Z^2$, leading to a highly suppressed mixing angle $\xi \simeq -\hat{s}_W \chi \hat{M}_Z^2/\hat{M}_X^2$, and the massive vector bosons Z_1 and Z_2 have masses $M_1 \simeq \hat{M}_Z$ and $M_2 \simeq \hat{M}_X$, respectively. We can identify $\hat{e} = e$, and in this limit $\hat{s}_W \simeq s_W$. The dominant effect is then an induced coupling of the new field $Z_2 \simeq X \simeq \hat{X}$ to the hypercharge current:

$$\hat{g} j^\mu \hat{X}_\mu \to \hat{g} j^\mu Z_{2,\mu} - \chi \frac{e}{c_W} j_Y^\mu Z_{2,\mu} \,. \tag{B.6}$$

This is, of course, most exciting for models where j_Y contains particles not found in the $U(1)'$ current j—as is the case for the DM symmetries discussed in Ch. 4—making the Z_2 a mediator between two sectors. For the $B - L$ symmetries discussed in Ch. 2, the above kinetic mixing will induce axial couplings to the otherwise vector-like j_{B-L}.

A quite different limit arises for $\hat{M}_X^2 \ll \hat{M}_Z^2$, i.e. a *light* neutral vector boson. Assuming further that the $U(1)'$ current j_μ contains no SM particles, only the small kinetic-mixing angle $\chi \simeq \xi/s_W \ll 1$ will induce a coupling of $X_\mu \simeq \hat{X}_\mu$ to SM particles. In physical processes with energies far above $\hat{M}_X$, both photons and X bosons can then be emitted, and will actually start to oscillate into each other in complete analogy to neutrino oscillations (Sec. 1.1). Such an oscillation of photons into "hidden photons" can be searched for in various ways, for example by trying to shine light through opaque walls (cf. Ref. [237]).

Let this suffice as an introduction to kinetic mixing; more can be found in Refs. [73, 234, 235], and in the next section.

B.2 Kinetic and Mass Mixing with Three Abelian Groups

The mixing of two abelian groups—one of them being the hypercharge gauge group $U(1)_Y$—is well studied and widely used in model building, but the generalization to more abelian factors is seldom discussed, even though this structure naturally occurs in some string theory and GUT models [238–241], not to mention the symmetry group $\mathcal{G}$ motivated in Sec. 1.5 and studied in this thesis. Renormalizability of the theory requires the gauge group to be free of anomalies, which drastically limits the allowed additional $U(1)'$ groups, unless additional fermions are introduced; the condition of anomaly freedom is, of course, even more constraining in gauge extensions with several new abelian factors. Even without tapping into the various GUT-inspired symmetries, there are several interesting combinations of well-motivated symmetries that lead to valid models, e.g. $U(1)_L \times U(1)_B$ [242–245], $U(1)_B \times U(1)_{\mathrm{DM}}$, or $U(1)_{B-L} \times U(1)_{L_\mu - L_\tau} \subset \mathcal{G}$.

We will present the generalization of the well-studied gauge group $G_{\mathrm{SM}} \times U(1)'$ to $G_{\mathrm{SM}} \times U(1)' \times U(1)''$, which introduces three kinetic-mixing angles and three mass-mixing parameters. To demonstrate possible applications in model building we show that $U(1)_B \times U(1)_{\mathrm{DM}}$ generates isospin-dependent nucleon–DM scattering and that $U(1)_{B-L} \times U(1)_{L_\mu - L_\tau}$ can in principle induce non-standard neutrino interactions.

B.2.1 Kinetic and Mass Mixing

In complete analogy to Sec. B.1, we can parametrize the most general effective Lagrange density after breaking $G_{\text{SM}} \times U(1)_1 \times U(1)_2$ to $SU(3)_C \times U(1)_{\text{EM}}$ as $\mathcal{L} = \mathcal{L}_{\text{SM}} + \mathcal{L}_{X_1} + \mathcal{L}_{X_2} + \mathcal{L}_{\text{mix}}$, with

$$\begin{aligned}
\mathcal{L}_{\text{SM}} &= -\frac{1}{4}\hat{B}_{\mu\nu}\hat{B}^{\mu\nu} - \frac{1}{4}\hat{W}^a_{\mu\nu}\hat{W}^{a\mu\nu} + \frac{1}{2}\hat{M}_Z^2\,\hat{Z}_\mu\hat{Z}^\mu - \frac{\hat{e}}{\hat{c}_W}j_Y^\mu\hat{B}_\mu - \frac{\hat{e}}{\hat{s}_W}j_W^{a\mu}\hat{W}^a_\mu\,, \\
\mathcal{L}_{X_i} &= -\frac{1}{4}\hat{X}_{i\,\mu\nu}\hat{X}_i^{\mu\nu} + \frac{1}{2}\hat{M}_{X_i}^2\hat{X}_{i\,\mu}\hat{X}_i^\mu - \hat{g}_i j_i^\mu\hat{X}_{i\,\mu}\,, \qquad i = 1,2\,, \\
\mathcal{L}_{\text{mix}} &= -\frac{\sin\alpha}{2}\hat{B}_{\mu\nu}\hat{X}_1^{\mu\nu} - \frac{\sin\beta}{2}\hat{B}_{\mu\nu}\hat{X}_2^{\mu\nu} - \frac{\sin\gamma}{2}\hat{X}_{1\,\mu\nu}\hat{X}_2^{\mu\nu} \\
&\quad + m_1^2\,\hat{Z}_\mu\hat{X}_1^\mu + m_2^2\,\hat{Z}_\mu\hat{X}_2^\mu + m_3^2\,\hat{X}_{1\,\mu}\hat{X}_2^\mu\,.
\end{aligned} \tag{B.7}$$

α, β, and γ are kinetic-mixing angles, while m_j^2 are mass-mixing parameters potentially induced by the spontaneous breakdown of $U(1)_Y \times U(1)_1 \times U(1)_2$.

Due to our parametrization of the kinetic-mixing angles, the hypercharge field strength tensor $\hat{B}_{\mu\nu}$ and the field strength tensors $\hat{X}_i^{\mu\nu}$ of $U(1)_1 \times U(1)_2$ share the symmetric mixing matrix

$$\mathcal{L} \supset -\frac{1}{4}\begin{pmatrix}\hat{B}^{\mu\nu}, & \hat{X}_1^{\mu\nu}, & \hat{X}_2^{\mu\nu}\end{pmatrix}\begin{pmatrix}1 & \sin\alpha & \sin\beta \\ \cdot & 1 & \sin\gamma \\ \cdot & \cdot & 1\end{pmatrix}\begin{pmatrix}\hat{B}_{\mu\nu} \\ \hat{X}_{1\,\mu\nu} \\ \hat{X}_{2\,\mu\nu}\end{pmatrix}. \tag{B.8}$$

In complete analogy to Sec. B.1, we can transform the gauge fields $(\hat{B}, \hat{X}_1, \hat{X}_2)$ into a basis (B, X_1, X_2) with canonical (diagonal) kinetic terms by means of a non-unitary transformation

$$\begin{pmatrix}\hat{B} \\ \hat{X}_1 \\ \hat{X}_2\end{pmatrix} = \begin{pmatrix}1 & -t_\alpha & (t_\alpha s_\gamma - s_\beta/c_\alpha)/D \\ 0 & 1/c_\alpha & (t_\alpha s_\beta - s_\gamma/c_\alpha)/D \\ 0 & 0 & c_\alpha/D\end{pmatrix}\begin{pmatrix}B \\ X_1 \\ X_2\end{pmatrix}, \tag{B.9}$$

where $D \equiv \sqrt{1 - s_\alpha^2 - s_\beta^2 - s_\gamma^2 + 2s_\alpha s_\beta s_\gamma}$, $s_x \equiv \sin x$, $c_x \equiv \cos x$, and $t_x \equiv \tan x$. The transformation (B.9) diagonalizes the kinetic terms and yields the massless photon A and the mass matrix for the massive neutral fields in the basis (Z, X_1, X_2)

$$\mathcal{M}^2 = \begin{pmatrix}\hat{M}_Z^2 & m_1^2/c_\alpha + \hat{M}_Z^2\hat{s}_W t_\alpha & M_{13}^2 \\ \cdot & \hat{M}_{X_1}^2/c_\alpha^2 + \hat{s}_W t_\alpha(2m_1^2 + \hat{M}_Z^2\hat{s}_W s_\alpha)/c_\alpha & M_{23}^2 \\ \cdot & \cdot & M_{33}^2\end{pmatrix}, \tag{B.10}$$

with the three extra long expressions

$$\begin{aligned}
M_{13}^2 \cdot c_\alpha D &\equiv (\hat{M}_Z^2\hat{s}_W(s_\beta - s_\alpha s_\gamma) + m_1^2(s_\alpha s_\beta - s_\gamma) + m_2^2 c_\alpha^2)\,, \\
M_{23}^2 \cdot c_\alpha^2 D &\equiv \hat{M}_{X_1}^2(s_\alpha s_\beta - s_\gamma) + \hat{M}_Z^2\hat{s}_W^2 s_\alpha(s_\beta - s_\alpha s_\gamma) + m_1^2\hat{s}_W(s_\beta - 2s_\alpha s_\gamma + s_\beta s_\alpha^2) \\
&\quad + m_2^2\hat{s}_W s_\alpha c_\alpha^2 + m_3^2 c_\alpha^2\,, \\
M_{33}^2 \cdot c_\alpha^2 D^2 &\equiv \hat{M}_{X_2}^2 c_\alpha^4 + \hat{M}_{X_1}^2(s_\gamma - s_\alpha s_\beta)^2 + \hat{M}_Z^2\hat{s}_W^2(s_\beta - s_\alpha s_\gamma)^2 \\
&\quad - 2m_1^2\hat{s}_W(s_\alpha s_\beta - s_\gamma)(s_\alpha s_\gamma - s_\beta) + 2m_2^2 c_\alpha^2\hat{s}_W(s_\beta - s_\alpha s_\gamma) \\
&\quad + 2m_3^2 c_\alpha^2(s_\alpha s_\beta - s_\gamma)\,.
\end{aligned} \tag{B.11}$$

$\mathcal{M}^2$ is a real symmetric matrix and can therefore be diagonalized by an orthogonal matrix U via $U^T\mathcal{M}^2U = \text{diag}(M_1^2, M_2^2, M_3^2)$, M_i being the masses of the physical fields. This diagonalization introduces in general three more mixing angles ξ_i that are connected to the entries in $\mathcal{M}^2$. The gauge eigenstates $\hat{A}$, $\hat{Z}$, $\hat{X}_1$, and $\hat{X}_2$ couple to the currents $\hat{e}j_{\text{EM}}$, $\hat{g}_Z j_{\text{NC}}$,[2] $\hat{g}_1 j_1$, and $\hat{g}_2 j_2$, respectively, and are connected to the physical mass eigenstates A, Z_1, Z_2, and Z_3 via

$$\begin{pmatrix}\hat{A}\\ \hat{Z}\\ \hat{X}_1\\ \hat{X}_2\end{pmatrix} = \begin{pmatrix}1 & 0 & -\hat{c}_W t_\alpha & \hat{c}_W(s_\alpha s_\gamma - s_\beta)/c_\alpha D\\ 0 & 1 & \hat{s}_W t_\alpha & \hat{s}_W(s_\beta - s_\alpha s_\gamma)/c_\alpha D\\ 0 & 0 & 1/c_\alpha & (s_\alpha s_\beta - s_\gamma)/c_\alpha D\\ 0 & 0 & 0 & c_\alpha/D\end{pmatrix} \begin{pmatrix}1 & 0 & 0 & 0\\ 0 & & & \\ 0 & & U & \\ 0 & & & \end{pmatrix} \begin{pmatrix}A\\ Z_1\\ Z_2\\ Z_3\end{pmatrix}, \tag{B.12}$$

or, inverted:

$$\begin{pmatrix}A\\ Z_1\\ Z_2\\ Z_3\end{pmatrix} = \begin{pmatrix}1 & 0 & 0 & 0\\ 0 & & & \\ 0 & & U^T & \\ 0 & & & \end{pmatrix} \begin{pmatrix}1 & 0 & \hat{c}_W s_\alpha & \hat{c}_W s_\beta\\ 0 & 1 & -\hat{s}_W s_\alpha & -\hat{s}_W s_\beta\\ 0 & 0 & c_\alpha & (s_\gamma - s_\alpha s_\beta)/c_\alpha\\ 0 & 0 & 0 & D/c_\alpha\end{pmatrix} \begin{pmatrix}\hat{A}\\ \hat{Z}\\ \hat{X}_1\\ \hat{X}_2\end{pmatrix}. \tag{B.13}$$

Due to our parametrization, we can identify $\hat{e} = e = \sqrt{4\pi\alpha_{\text{EM}}}$ with the usual electric charge. The physical Weinberg angle is defined via

$$s_W^2 c_W^2 = \frac{\pi\alpha_{\text{EM}}(M_1)}{\sqrt{2}G_F M_1^2}, \tag{B.14}$$

which leads to the identity $s_W c_W M_1 = \hat{s}_W \hat{c}_W \hat{M}_Z$ [234].

The general case is complicated to discuss and hardly illuminating, which is why we will work with several approximations from here on out. In the limit $m_i^2 \ll \hat{M}_Z^2, \hat{M}_{X_j}^2$, and $\alpha, \beta, \gamma \ll 1$, the mass matrix (B.10) simplifies to

$$\mathcal{M}^2 \simeq \begin{pmatrix}\hat{M}_Z^2 & \hat{M}_Z^2\hat{s}_W\alpha + m_1^2 & \hat{M}_Z^2\hat{s}_W\beta + m_2^2\\ \cdot & \hat{M}_{X_1}^2 & -\hat{M}_{X_1}^2\gamma + m_3^2\\ \cdot & \cdot & \hat{M}_{X_2}^2\end{pmatrix}. \tag{B.15}$$

Diagonalization leads to the resulting connection between gauge and mass eigenstates

$$\begin{pmatrix}\hat{A}\\ \hat{Z}\\ \hat{X}_1\\ \hat{X}_2\end{pmatrix} \simeq \begin{pmatrix}1 & 0 & -\hat{c}_W\alpha & -\hat{c}_W\beta\\ 0 & 1 & \frac{\hat{s}_W\alpha\hat{M}_{X_1}^2 + m_1^2}{\hat{M}_{X_1}^2 - \hat{M}_Z^2} & \frac{\hat{s}_W\beta\hat{M}_{X_2}^2 + m_2^2}{\hat{M}_{X_2}^2 - \hat{M}_Z^2}\\ 0 & -\frac{\hat{s}_W\alpha\hat{M}_Z^2 + m_1^2}{\hat{M}_{X_1}^2 - \hat{M}_Z^2} & 1 & -\frac{\gamma\hat{M}_{X_2}^2 - m_3^2}{\hat{M}_{X_2}^2 - \hat{M}_{X_1}^2}\\ 0 & -\frac{\hat{s}_W\beta\hat{M}_Z^2 + m_2^2}{\hat{M}_{X_2}^2 - \hat{M}_Z^2} & \frac{\gamma\hat{M}_{X_1}^2 - m_3^2}{\hat{M}_{X_2}^2 - \hat{M}_{X_1}^2} & 1\end{pmatrix} \begin{pmatrix}A\\ Z_1\\ Z_2\\ Z_3\end{pmatrix}, \tag{B.16}$$

and one can calculate the mass shift of the Z boson

$$M_1^2/\hat{M}_Z^2 \simeq 1 + \frac{\left(\hat{s}_W\alpha + m_1^2/\hat{M}_Z^2\right)^2}{1 - \hat{M}_{X_1}^2/\hat{M}_Z^2} + \frac{\left(\hat{s}_W\beta + m_2^2/\hat{M}_Z^2\right)^2}{1 - M_{X_2}^2/\hat{M}_Z^2}. \tag{B.17}$$

[2] Here we defined the coupling strength of the $\hat{Z}$ boson $\hat{g}_Z \equiv \hat{e}/2\hat{c}_W\hat{s}_W$.

With this formula we can express $\hat{M}_Z^2$ in terms of measurable masses:

$$\frac{\hat{M}_Z^2}{M_1^2} = \frac{s_W^2 c_W^2}{\hat{s}_W^2 \hat{c}_W^2} \simeq 1 - \frac{\left(s_W \alpha + m_1^2/M_1^2\right)^2}{1 - M_2^2/M_1^2} - \frac{\left(s_W \beta + m_2^2/M_1^2\right)^2}{1 - M_3^2/M_1^2} \,. \tag{B.18}$$

The direction of the shift depends on the hierarchy of $\hat{M}_Z^2$ and $\hat{M}_{X_i}^2$; a cancellation is possible for $\hat{M}_{X_1}^2 < \hat{M}_Z^2 < \hat{M}_{X_2}^2$, which would reduce stringent constraints from the ρ parameter (hiding one Z' with another). A different way of relaxing the limits on a Z' model by adding additional heavy bosons with specific charges was discussed in Ref. [246]. For completeness we show the effects of heavy Z' bosons in terms of the oblique parameters S and T, which can be read off the modified Z_1 couplings to j_W^3 and j_{EM} in the limit $\hat{g}_{1,2} \equiv 0$ [234]:

$$\begin{aligned} \alpha_{\text{EM}} T &\simeq \frac{s_W^2 \alpha^2 - m_1^4/M_1^4}{1 - M_2^2/M_1^2} + \frac{s_W^2 \beta^2 - m_2^4/M_1^4}{1 - M_3^2/M_1^2} \,, \\ \alpha_{\text{EM}} S &\simeq 4 s_W c_W^2 \alpha \, \frac{s_W \alpha + m_1^2/M_1^2}{1 - M_2^2/M_1^2} + 4 s_W c_W^2 \beta \, \frac{s_W \beta + m_2^2/M_1^2}{1 - M_3^2/M_1^2} \,. \end{aligned} \tag{B.19}$$

B.2.2 Applications

We will now show some applications of the framework laid out above. It is not our intention to examine the models in complete detail, but only to consider a few interesting effects. In most cases it suffices to work with the approximation in Eq. (B.16), which is used to read off the couplings of the mass eigenstates to the different currents/particles. Once a proper model is defined by additional scalars and fermions, one can perform more sophisticated analyses which make use of numerical diagonalization of the neutral boson mass matrix in Eq. (B.10). In particular, loop-induced kinetic mixing angles can be calculated in specific models.

Crossing the Streams

Model building with mixing between $U(1)_1$ and $U(1)_2$ often makes use of the induced coupling of currents, i.e. $\mathcal{L}_{\text{mix}} \sim \varepsilon \, j_1 j_2$, which connects the two gauge sectors even if no particle is charged under both groups. We will now derive a necessary condition for such a non-diagonal term at tree level. Taking all of the mixing parameters in Eq. (B.7) to be zero except for m_3 and γ, we obtain the coupling of the mass eigenstates Z_2 and Z_3 to the currents

$$\mathcal{L} \supset -\begin{pmatrix} \hat{g}_1 j_1 \,, & \hat{g}_2 j_2 \end{pmatrix} \begin{pmatrix} 1 & -t_\gamma \\ 0 & 1/c_\gamma \end{pmatrix} \begin{pmatrix} c_\xi & -s_\xi \\ s_\xi & c_\xi \end{pmatrix} \begin{pmatrix} Z_2 \\ Z_3 \end{pmatrix} \equiv -\begin{pmatrix} \hat{g}_1 j_1 \,, & \hat{g}_2 j_2 \end{pmatrix} V_\gamma U_\xi \begin{pmatrix} Z_2 \\ Z_3 \end{pmatrix} , \tag{B.20}$$

where U_ξ diagonalizes the mass matrix. Integrating out the heavy mass eigenstates yields an effective four-fermion interaction of the form

$$\begin{aligned} \mathcal{L}_{\text{eff}} &= -\frac{1}{2} \begin{pmatrix} \hat{g}_1 j_1 \,, & \hat{g}_2 j_2 \end{pmatrix} V_\gamma U_\xi \begin{pmatrix} 1/M_2^2 & 0 \\ 0 & 1/M_3^2 \end{pmatrix} U_\xi^T V_\gamma^T \begin{pmatrix} \hat{g}_1 j_1 \\ \hat{g}_2 j_2 \end{pmatrix} \\ &= -\frac{1}{2} \begin{pmatrix} \hat{g}_1 j_1 \,, & \hat{g}_2 j_2 \end{pmatrix} \begin{pmatrix} \hat{M}_{X_1}^2 & m_3^2 \\ m_3^2 & \hat{M}_{X_2}^2 \end{pmatrix}^{-1} \begin{pmatrix} \hat{g}_1 j_1 \\ \hat{g}_2 j_2 \end{pmatrix} . \end{aligned} \tag{B.21}$$

It is obvious that the coupling matrix is diagonal if $m_3 = 0$, independent of γ. An analogous calculation can be performed for the coupling of j_i to j_{NC} via m_i and α, β, respectively, although it is a bit more tedious because of the additional Weinberg rotation. Nevertheless, the result is the same: An off-diagonal effective coupling $j_i\, j_{\text{NC}}$ only arises for $m_i \neq 0$, i.e. $\mathcal{L}_{\text{eff}} \propto m_{1,2}^2\, j_{1,2}\, j_{\text{NC}}$. Since the Weinberg rotation induces a coupling of j_i to the electromagnetic current (first row in Eq. (B.16)), interesting couplings can arise even for $m_{1,2} = 0$.

Up until now we discussed only one nonzero m_i and kinetic mixing angle at a time, corresponding to the well-known case of Z–Z' mixing. A more general analysis including all our mixing parameters from Eq. (B.7) yields the effective four-fermion interactions

$$\mathcal{L}_{\text{eff}} = -\frac{1}{2} \begin{pmatrix} \hat{g}_Z j_{\text{NC}} \\ \hat{g}_1 j_1 - e\hat{c}_W s_\alpha j_{\text{EM}} \\ \hat{g}_2 j_2 - e\hat{c}_W s_\beta j_{\text{EM}} \end{pmatrix}^T \begin{pmatrix} \hat{M}_Z^2 & m_1^2 & m_2^2 \\ \cdot & \hat{M}_{X_1}^2 & m_3^2 \\ \cdot & \cdot & \hat{M}_{X_2}^2 \end{pmatrix}^{-1} \begin{pmatrix} \hat{g}_Z j_{\text{NC}} \\ \hat{g}_1 j_1 - e\hat{c}_W s_\alpha j_{\text{EM}} \\ \hat{g}_2 j_2 - e\hat{c}_W s_\beta j_{\text{EM}} \end{pmatrix}. \tag{B.22}$$

Because the 3×3 coupling matrix takes the explicit form

$$\begin{pmatrix} \hat{M}_Z^2 & m_1^2 & m_2^2 \\ \cdot & \hat{M}_{X_1}^2 & m_3^2 \\ \cdot & \cdot & \hat{M}_{X_2}^2 \end{pmatrix}^{-1} = \frac{1}{\Delta^6} \begin{pmatrix} \hat{M}_{X_1}^2 \hat{M}_{X_2}^2 - m_3^4 & m_2^2 m_3^2 - m_1^2 \hat{M}_{X_2}^2 & m_1^2 m_3^2 - \hat{M}_{X_1}^2 m_2^2 \\ \cdot & \hat{M}_Z^2 \hat{M}_{X_2}^2 - m_2^4 & m_1^2 m_2^2 - \hat{M}_Z^2 m_3^2 \\ \cdot & \cdot & \hat{M}_Z^2 \hat{M}_{X_1}^2 - m_1^4 \end{pmatrix}, \tag{B.23}$$

with $\Delta^6 \equiv \hat{M}_Z^2 \hat{M}_{X_1}^2 \hat{M}_{X_2}^2 - \hat{M}_Z^2 m_3^4 - \hat{M}_{X_2}^2 m_2^4 - \hat{M}_{X_2}^2 m_1^4 + 2 m_1^2 m_2^2 m_3^2$, we end up with new off-diagonal couplings like $m_2^2 m_3^2\, j_1\, j_{\text{NC}}$, even if there is no *direct coupling* $m_1^2\, j_1\, j_{\text{NC}}$.

Isospin-Violating Dark Matter

In our introduction to dark matter in Sec. 1.3 we have claimed that direct-detection experiments provide strong *limits* on DM–nucleon cross sections, without mentioning the existing *hints* for actual DM observation by DAMA [247] (sodium and iodine target), CoGeNT [248] (germanium), CRESST [249] (calcium tungstate), and CDMS [250] (germanium and silicon). Even though the positive signals at these experiments all point to a similar region in parameter space—dark matter mass $\mathcal{O}(10)\,\text{GeV}$, spin-independent DM–proton cross section 10^{-42}–$10^{-40}\,\text{cm}^2$—they are overall incompatible with each other. Furthermore, such large spin-independent DM–nucleon cross sections are naively excluded by xenon-based DM experiments like XENON100 [43] and, most recently, LUX [251]. There are obviously some problems with *at least* one of the mentioned experiments, and it is not our intention to select the most reputable of the bunch or discuss experimental issues. Taking seriously any one of the hints for DM, we are faced with the stringent exclusion limits from the xenon-based experiments. This tension can, however, be alleviated if DM were xenophobic, i.e. would couple weaker to xenon than to other elements. A ridiculous idea at first, but due to the different proton-to-neutrino ratio in the relevant elements, it actually goes a long way to consider *isospin-violating* DM [252], which is not *as* far fetched. The destructive interference of the DM scattering off protons and neutrons can then be used to reduce the effective DM coupling to xenon, with less pronounced reduction in light elements like germanium. Due to the variety of xenon isotopes employed by the experiments, it is impossible to obtain truly

xenophobic DM in this way, but taking a DM coupling to neutrons and protons in the ratio $f_n/f_p \simeq -0.7$ [252–254] at least weakens the xenon constraints by some orders of magnitude. It is not our intention to review the current state of this approach (see e.g. Ref. [255] for that), let us rather demonstrate our Z–Z'–Z'' mixing ansatz at the slightly outdated example of DAMA/CoGeNT and XENON100.

Many models have been brought forward to alleviate the tension between the potential DM signals in DAMA/CoGeNT and the null results in XENON100 using isospin-dependent couplings of nucleons to dark matter [252–254, 256–261]. One of the models used in Ref. [262] to explain this coupling is based on gauged baryon number $U(1)_1 \equiv U(1)_B$.[3] With dark matter charged under this gauge group, the resulting cross section turns out to be too small to explain the observed events, unless the coupling of Z' to dark matter is significantly stronger than to quarks (i.e. DM carries a large baryon number). However, in a model with another gauge group $U(1)_2 \equiv U(1)_{\text{DM}}$—acting only on the DM sector—the dark matter coupling constant g_{DM} can be naturally large compared to g_B, which allows for a sizable cross section as long as the mass mixing between the groups is not too small.[4] We therefore consider vector boson mixing with the gauge group $U(1)_Y \times U(1)_B \times U(1)_{\text{DM}}$; we only introduce one DM Dirac fermion χ, so the $U(1)_2$ current takes the simple form $j_2^\mu = j_{\text{DM}}^\mu = \overline{\chi}\gamma^\mu\chi$. For clarity we take all mixing parameters in Eq. (B.7) to be zero—except for m_3 and β—and assume $Z_{2,3}$ to be light ($M_{2,3}^2 \ll M_1^2$) to generate a large cross section. Eq. (B.16) then gives the approximate couplings

$$\begin{aligned}\mathcal{L} \supset & -\left(\frac{e}{2c_W s_W} j_{\text{NC}} + \beta s_W g_{\text{DM}} j_{\text{DM}}\right) Z_1 - \left(g_B j_B - g_{\text{DM}} \frac{m_3^2}{M_3^2 - M_2^2} j_{\text{DM}}\right) Z_2 \\ & - \left(g_{\text{DM}} j_{\text{DM}} - \beta c_W e j_{\text{EM}} + g_B \frac{m_3^2}{M_3^2 - M_2^2} j_B\right) Z_3 \,.\end{aligned} \tag{B.24}$$

These terms couple dark matter to nucleons via m_3, and because of β, proton and neutron couple differently, i.e. the interaction is isospin dependent. Integrating out all the gauge bosons gives the effective vector–vector interactions in the usual parametrization

$$\mathcal{L}_{\text{eff}} \supset f_p\, \overline{\chi}\gamma_\mu\chi\, \overline{p}\gamma^\mu p + f_n\, \overline{\chi}\gamma_\mu\chi\, \overline{n}\gamma^\mu n \,, \tag{B.25}$$

with the ratio of the neutron and proton couplings

$$f_n/f_p = \frac{1}{1+r} \,, \qquad \text{with} \qquad r \simeq e c_W \frac{\beta}{g_B} \frac{M_2^2}{m_3^2} \,. \tag{B.26}$$

We can easily find parameters to generate $f_n/f_p \simeq -0.7$, corresponding to $r \simeq -2.4$. The overall DM–neutron cross section can be calculated to be [267]

$$\sigma_n = \frac{1}{64\pi}\left(\frac{m_\chi m_n}{m_\chi + m_n}\right)^2 f_n^2 \simeq \frac{m_n^2}{64\pi}\left(g_B g_{\text{DM}} \frac{m_3^2}{M_2^2 M_3^2}\right)^2 \simeq 2\,\alpha_{\text{DM}}\beta^2 \left(\frac{1\,\text{GeV}}{M_3}\right)^4 10^{-31}\,\text{cm}^2 \,, \tag{B.27}$$

[3] It was pointed out in Ref. [263–265] that a gauge boson coupled to the baryon number B can be light. The drawback of such a symmetry is the unavoidable introduction of new chiral fermions to cancel occurring triangle anomalies. An anomaly-free symmetry (SM + right-handed neutrinos) with similarly weak constraints is $U(1)_{B-3L_\tau}$ [110–112, 115], a subgroup of $\mathcal{G}$ from Eq. (1.52).

[4] A similar model was proposed in the same context in Ref. [266].

where we defined $\alpha_{\rm DM} \equiv g_{\rm DM}^2/4\pi$ and assumed $m_\chi \gg m_n$. To obtain the last equation we replaced $g_B\, m_3^2$ with the demanded value for r from Eq. (B.26). For $\beta \sim 10^{-3}$ it is possible to generate the required DAMA/CoGeNT cross section $\sigma_n \sim 10^{-38}$–$10^{-37}\,\mathrm{cm}^2$ [252, 252–254, 257–261] without being in conflict with other constraints [69, 263–265, 268]. We note that the dark matter fine-structure constant $\alpha_{\rm DM}$ is not restricted to be small.

Due to the required nonzero m_3^2 we will have a non-trivial scalar sector that also serves as a mediator between the SM and the dark sector. We assume these scalars to be heavy enough not to alter our foregoing discussion.

Aside from the group $U(1)_B \times U(1)_{\rm DM}$ discussed above, further interesting models using this framework in the dark matter sector could be build using leptophilic groups like $U(1)_{L_\mu - L_\tau} \times U(1)_{\rm DM}$, with the possibility to resolve the PAMELA positron excess via the small leptophilic admixture [269].

Non-Standard Neutrino Interactions

We have shown in Sec. 1.5 that the group $G_{\rm SM} \times U(1)_{B-L} \times U(1)_{L_e - L_\mu} \times U(1)_{L_\mu - L_\tau}$ is free of anomalies after introducing three right-handed neutrinos ν_R. Having focused on $U(1)'$ subgroups of $U(1)_{B-L} \times U(1)_{L_e-L_\mu} \times U(1)_{L_\mu - L_\tau}$ in the main part of this thesis, let us take a look at the effect of a $U(1)_1 \times U(1)_2$ subgroup. This group is necessarily flavored, because there is only one unflavored $U(1)$ subgroup ($B - L$, as discussed in Ch. 2). We choose $U(1)_1 \equiv U(1)_{B-L}$ and $U(1)_2 \equiv U(1)_{L_\mu - L_\tau}$ for the flavored part, $L_\mu - L_\tau$ being favored over any other $U(1)' \subset U(1)_{L_e-L_\mu} \times U(1)_{L_\mu - L_\tau}$ because of a more reasonable structure of the neutrino mass matrix (see Sec. 3.3). The gauge boson $Z_2 = Z_{B-L}$ is highly constrained by collider experiments ($M_{B-L}/g_{B-L} \gtrsim 7\,\mathrm{TeV}$ from Sec. 2.1.1),[5] but $Z_3 = Z_{L_\mu - L_\tau}$ can have a mass around the electroweak scale and there is actually a preferred region around $M_{L_\mu - L_\tau}/g_{L_\mu - L_\tau} \simeq 200\,\mathrm{GeV}$ that ameliorates the tension between the theoretical and experimental values for the muon's magnetic moment (see Sec. 3.3.2).

In $U(1)_{B-L} \times U(1)_{L_\mu - L_\tau}$ models with non-vanishing mass mixing the parameter m_3 induces an effective coupling of the currents $j_{L_\mu - L_\tau}$ and j_{B-L} (see Sec. B.2.2), which leads for example to non-standard neutrino interactions, usually parametrized by the non-renormalizable effective Lagrangian [270]

$$\mathcal{L}_{\rm eff}^{\rm NSI} = -2\sqrt{2} G_F \varepsilon_{\alpha\beta}^{fP} \left[\bar{f}\gamma^\mu P f\right] \left[\bar{\nu}_\alpha \gamma_\mu P_L \nu_\beta\right]. \tag{B.28}$$

The model at hand induces $\varepsilon_{\mu\mu}^{fP} = -\varepsilon_{\tau\tau}^{fP}$, easily read off from Eq. (B.21):

$$\begin{aligned} \varepsilon_{\mu\mu}^{eV} &\simeq -\frac{1}{2\sqrt{2}G_F} g_1 g_2 \frac{m_3^2}{M_2^2 M_3^2} \\ &\simeq -10^{-6}\, \frac{1}{g_1 g_2} \left(\frac{m_3}{10\,\mathrm{GeV}}\right)^2 \left(\frac{7\,\mathrm{TeV}}{M_2/g_1}\right)^2 \left(\frac{200\,\mathrm{GeV}}{M_3/g_2}\right)^2, \\ \varepsilon_{\mu\mu}^{uV} &= \varepsilon_{\mu\mu}^{dV} = -\varepsilon_{\mu\mu}^{eV}/3\,, \end{aligned} \tag{B.29}$$

which are in general too small to be observable in current experiments [270]. Larger NSIs can be generated at the price of introducing mass mixing of $Z_{L_\mu - L_\tau}$ with $Z_{\rm SM}$ via m_2 (using the

[5] The limits from LEP-2 and Tevatron have strictly speaking been derived under the assumption of just *one* additional gauge boson, but still hold approximately when additional bosons are included [246].

more general Eq. (B.22)). Even though this kind of mixing is highly constrained by collider experiments, the arising NSIs are testable in future facilities for $M_2 < M_1$ [4]. Substituting $U(1)_{B-L}$ in Eq. (B.29) with less constrained symmetries like $U(1)_{B-3L_\tau}$ or $U(1)_B$ (including fermions to cancel arising anomalies) allows for lighter gauge bosons and therefore also larger NSIs; a recent discussion of additional constraints on Z' bosons with non-universal couplings to charged leptons can be found in Ref. [271]. This framework comes down to Z'–Z'' mixing; it does not involve mixing with the SM gauge bosons—at least at tree level—so the bounds on the mixing parameters are less stringent.

B.2.3 Conclusion

The extension of the Standard Model by an additional abelian factor $U(1)'$ is a well motivated and frequently discussed area in model building. It is not far fetched to extend this even further to $G_{\mathrm{SM}} \times [U(1)']^n$—especially following our motivation in Sec. 1.5—provided the full gauge group stays free of anomalies. We discussed the most general low-energy Lagrangian for the case $n = 2$, including kinetic mixing among the abelian groups, $n > 2$ being hardly more difficult. We showed how the mixing among several gauge groups—such as $U(1)_{B-L}$, $U(1)_{L_\mu - L_\tau}$, and $U(1)_{\mathrm{DM}}$—can lead to interesting effects like non-standard neutrino interactions and isospin-dependent dark matter scattering, opening up new and exciting possibilities in model building.

List of Abbreviations and Acronyms

$0\nu2\beta$ ..... Neutrinoless Double Beta Decay

$0\nu4\beta$ ..... Neutrinoless Quadruple Beta Decay

$\mathcal{G}$ ..... $U(1)_{B-L} \times U(1)_{L_e-L_\mu} \times U(1)_{L_\mu-L_\tau}$

$\overline{L}$ ..... $L_e - L_\mu - L_\tau$

B ..... Baryon Number

G_{SM} ..... Standard Model Gauge Group $SU(3)_C \times SU(2)_L \times U(1)_Y$

L ..... Lepton Number

M_{Pl} ..... Planck Mass, approx. 1.22×10^{19} GeV

BAU ..... Baryon Asymmetry of the Universe

BBN ..... Big Bang Nucleosynthesis

C.L. ..... Confidence Level

CDMS ..... Cryogenic Dark Matter Search

CKM ..... Cabibbo–Kobayashi–Maskawa

CMB ..... Cosmic Microwave Background

COBE ..... COsmic Background Explorer

CoGeNT ..... Coherent Germanium Neutrino Technology

CP ..... Charge Parity

CRESST ..... Cryogenic Rare Event Search with Superconducting Thermometers

DAMA ..... DArk MAtter Collaboration

DM ..... Dark Matter

EC ..... Electron Capture

EM ..... ElectroMagnetism

EWPT ..... ElectroWeak Phase Transition

EWSB ..... ElectroWeak Symmetry Breaking

EXO ..... Enriched Xenon Observatory

GAPP ..... Global Analysis of Particle Properties

GERDA ..... GERmanium Detector Array

GUT ..... Grand Unified Theory

IH ..... Inverted Hierarchy

KATRIN ..... KArlsruhe TRItium Neutrino Experiment

LEP ..... Large Electron–Positron Collider

LHC ..... Large Hadron Collider

LNV ..... Lepton Number Violation

LSND ..... Liquid Scintillator Neutrino Detector

LUX ..... Large Underground Xenon experiment

MES ..... Minimal Extended Seesaw

MiniBooNE ..... Mini Booster Neutrino Experiment

NA ..... Natural Abundance

NEMO ..... Neutrino Ettore Majorana Observatory

NH ..... Normal Hierarchy

NSI ..... Non-Standard Neutrino Interaction

PAMELA ..... Payload for Antimatter–Matter Exploration and Light-nuclei Astrophysics

PMNS ..... Pontecorvo–Maki–Nakagawa–Sakata

QCD ..... Quantum ChromoDynamics

QD ..... Quasi-Degenerate Spectrum

QED ..... Quantum ElectroDynamics

RHN ..... Right-Handed Neutrino

SM ..... Standard Model

VEV ..... Vacuum Expectation Value

WIMP ..... Weakly Interacting Massive Particle

WMAP ..... Wilkinson Microwave Anisotropy Probe

Bibliography

[1] J. Heeck and W. Rodejohann, "*Neutrinoless quadruple beta decay*," Europhys. Lett. **103** (2013) 32001, arXiv:1306.0580.

[2] J. Heeck, "*Leptogenesis with lepton-number-violating Dirac neutrinos*," Phys. Rev. D **88** (2013) 076004, arXiv:1307.2241.

[3] J. Heeck and W. Rodejohann, "*Neutrino hierarchies from a gauge symmetry*," Phys. Rev. D **85** (2012) 113017, arXiv:1203.3117.

[4] J. Heeck and W. Rodejohann, "*Gauged $L_\mu - L_\tau$ symmetry at the electroweak scale*," Phys. Rev. D **84** (2011) 075007, arXiv:1107.5238.

[5] T. Araki, J. Heeck, and J. Kubo, "*Vanishing minors in the neutrino mass matrix from abelian gauge symmetries*," JHEP **1207** (2012) 083, arXiv:1203.4951.

[6] I. de Medeiros Varzielas, C. Hambrock, G. Hiller, M. Jung, *et al.*, "*Proceedings of the 2nd workshop on flavor symmetries and consequences in accelerators and cosmology (FLASY12)*," arXiv:1210.6239.

[7] J. Heeck, "*Gauged flavor symmetries*," Nucl. Phys. Proc. Suppl. **237–238** (2013) 336–338.

[8] J. Heeck and H. Zhang, "*Exotic charges, multicomponent dark matter and light sterile neutrinos*," JHEP **1305** (2013) 164, arXiv:1211.0538.

[9] J. Heeck, "*How stable is the photon?*," Phys. Rev. Lett. **111** (2013) 021801, arXiv:1304.2821.

[10] J. Heeck and W. Rodejohann, "*Kinetic and mass mixing with three abelian groups*," Phys. Lett. B **705** (2011) 369–374, arXiv:1109.1508.

[11] J. Heeck and W. Rodejohann, "*'Hidden' $O(2)$ and $SO(2)$ symmetry in lepton mixing*," JHEP **1202** (2012) 094, arXiv:1112.3628.

[12] J. Heeck, "*Seesaw parametrization for n right-handed neutrinos*," Phys. Rev. D **86** (2012) 093023, arXiv:1207.5521.

[13] J. Heeck and W. Rodejohann, "*Sterile neutrino anarchy*," Phys. Rev. D **87** (2013) 037301, arXiv:1211.5295.

[14] **ATLAS Collaboration**, G. Aad *et al.*, "*Observation of a new particle in the search for the Standard Model Higgs boson with the ATLAS detector at the LHC*," Phys. Lett. B **716** (2012) 1–29, arXiv:1207.7214.

[15] **CMS Collaboration**, S. Chatrchyan *et al.*, "*Observation of a new boson at a mass of 125 GeV with the CMS experiment at the LHC*," Phys. Lett. B **716** (2012) 30–61, arXiv:1207.7235.

[16] **Particle Data Group**, J. Beringer *et al.*, "*Review of particle physics*," Phys. Rev. D **86** (2012) 010001. See http://pdg.lbl.gov for the 2013 partial update.

[17] D. Dinh, S. Petcov, N. Sasao, M. Tanaka, and M. Yoshimura, "*Observables in Neutrino Mass Spectroscopy Using Atoms*," Phys. Lett. B **719** (2013) 154–163, arXiv:1209.4808.

[18] E. K. Akhmedov and J. Kopp, "*Neutrino oscillations: Quantum mechanics vs. quantum field theory*," JHEP **1004** (2010) 008, arXiv:1001.4815.

[19] M. Gonzalez-Garcia, M. Maltoni, J. Salvado, and T. Schwetz, "*Global fit to three neutrino mixing: critical look at present precision*," JHEP **1212** (2012) 123, arXiv:1209.3023. Updated version 1.2 from http://www.nu-fit.org.

[20] S. F. King and C. Luhn, "*Neutrino Mass and Mixing with Discrete Symmetry*," Rept. Prog. Phys. **76** (2013) 056201, arXiv:1301.1340.

[21] K. Abazajian *et al.*, "*Light sterile neutrinos: a white paper*," arXiv:1204.5379.

[22] A. D. Dolgov, "*Neutrinos in cosmology*," Phys. Rept. **370** (2002) 333–535, arXiv:hep-ph/0202122.

[23] **Planck Collaboration**, P. Ade *et al.*, "*Planck 2013 results. XVI. Cosmological parameters*," arXiv:1303.5076.

[24] C. Kraus, B. Bornschein, L. Bornschein, J. Bonn, B. Flatt, *et al.*, "*Final results from phase II of the Mainz neutrino mass search in tritium beta decay*," Eur. Phys. J. C **40** (2005) 447–468, arXiv:hep-ex/0412056.

[25] **KATRIN Collaboration**, A. Osipowicz *et al.*, "*KATRIN: A Next generation tritium beta decay experiment with sub-eV sensitivity for the electron neutrino mass. Letter of intent*," arXiv:hep-ex/0109033.

[26] R. Foot, H. Lew, X. He, and G. C. Joshi, "*Seesaw neutrino masses induced by a triplet of leptons*," Z. Phys. C **44** (1989) 441.

[27] S. Weinberg, "*Baryon and lepton nonconserving processes*," Phys. Rev. Lett. **43** (1979) 1566–1570.

[28] B. Grzadkowski, M. Iskrzynski, M. Misiak, and J. Rosiek, "*Dimension-Six Terms in the Standard Model Lagrangian*," JHEP **1010** (2010) 085, arXiv:1008.4884.

[29] J. Schechter and J. Valle, "*Neutrinoless double-beta decay in $SU(2) \times U(1)$ theories*," Phys. Rev. D **25** (1982) 2951.

[30] **GERDA Collaboration**, M. Agostini *et al.*, "*Results on neutrinoless double-β decay of ^{76}Ge from GERDA Phase I*," Phys. Rev. Lett. **111** (2013) 122503, arXiv:1307.4720.

[31] W. Rodejohann, "*Neutrino-less double beta decay and particle physics*," Int. J. Mod. Phys. E **20** (2011) 1833–1930, arXiv:1106.1334.

[32] S. Luo and Z.-Z. Xing, "*Theoretical overview on the flavor issues of massive neutrinos*," Int. J. Mod. Phys. A **27** (2012) 1230031, arXiv:1211.4331.

[33] L. Canetti, M. Drewes, and M. Shaposhnikov, "*Matter and Antimatter in the Universe*," New J. Phys. **14** (2012) 095012, arXiv:1204.4186.

[34] C. Caprini, S. Biller, and P. Ferreira, "*Constraints on the electrical charge asymmetry of the universe*," JCAP **0502** (2005) 006, arXiv:hep-ph/0310066.

[35] G. Steigman, "*Primordial nucleosynthesis: the predicted and observed abundances and their consequences*," PoS NIC **XI** (2010) 001, arXiv:1008.4765.

[36] **WMAP Collaboration**, G. Hinshaw *et al.*, "*Nine-Year Wilkinson Microwave Anisotropy Probe (WMAP) Observations: Cosmological Parameter Results*," Astrophys. J. Suppl. **208** (2013) 19, arXiv:1212.5226.

[37] A. D. Linde, "*Inflationary Cosmology*," Lect. Notes Phys. **738** (2008) 1–54, arXiv:0705.0164.

[38] A. Ijjas, P. Steinhardt, and A. Loeb, "*Inflationary paradigm in trouble after Planck2013*," Phys. Lett. B **723** (2013) 261–266, arXiv:1304.2785.

[39] A. D. Dolgov, "*NonGUT baryogenesis*," Phys. Rept. **222** (1992) 309–386.

[40] A. Sakharov, "*Violation of CP Invariance, C Asymmetry, and Baryon Asymmetry of the Universe*," Pisma Zh. Eksp. Teor. Fiz. **5** (1967) 32–35.

[41] J. L. Feng, "*Dark Matter Candidates from Particle Physics and Methods of Detection*," Ann. Rev. Astron. Astrophys. **48** (2010) 495–545, arXiv:1003.0904.

[42] E. W. Kolb and M. S. Turner, *The Early Universe*. Addison-Wesley, 1990.

[43] **XENON100 Collaboration**, E. Aprile *et al.*, "*Dark Matter Results from 225 Live Days of XENON100 Data*," Phys. Rev. Lett. **109** (2012) 181301, arXiv:1207.5988.

[44] S. L. Adler, "*Axial vector vertex in spinor electrodynamics*," Phys. Rev. **177** (1969) 2426–2438.

[45] J. Bell and R. Jackiw, "*A PCAC puzzle:* $\pi^0 \to \gamma\gamma$ *in the* σ*-model*," Nuovo Cim. A **60** (1969) 47–61.

[46] G. 't Hooft, "*Symmetry breaking through Bell–Jackiw anomalies*," Phys. Rev. Lett. **37** (1976) 8–11.

[47] S. Davidson, E. Nardi, and Y. Nir, "*Leptogenesis*," Phys. Rept. **466** (2008) 105–177, arXiv:0802.2962.

[48] W. Buchmüller, "*Baryogenesis, dark matter and the maximal temperature of the early universe*," Acta Phys. Polon. B **43** (2012) 2153, arXiv:1212.3554.

[49] M. B. Green and J. H. Schwarz, "*Anomaly cancellation in supersymmetric* $D = 10$ *gauge theory and superstring theory*," Phys. Lett. B **149** (1984) 117–122.

[50] L. Alvarez-Gaumé and E. Witten, "*Gravitational anomalies*," Nucl. Phys. B **234** (1984) 269.

[51] C. Geng and R. Marshak, "*Uniqueness of quark and lepton representations in the Standard Model from the anomalies viewpoint*," Phys. Rev. D **39** (1989) 693.

[52] R. Foot, "*New physics from electric charge quantization?*," Mod. Phys. Lett. A **6** (1991) 527–530.

[53] X.-G. He, G. C. Joshi, H. Lew, and R. Volkas, "*Simplest* Z' *model*," Phys. Rev. D **44** (1991) 2118–2132.

[54] R. Foot, X.-G. He, H. Lew, and R. Volkas, "*Model for a light* Z' *boson*," Phys. Rev. D **50** (1994) 4571–4580, arXiv:hep-ph/9401250.

[55] D. Feldman, P. Fileviez Perez, and P. Nath, "*R-parity Conservation via the Stueckelberg Mechanism: LHC and Dark Matter Signals*," JHEP **1201** (2012) 038, arXiv:1109.2901.

[56] H. Murayama and A. Pierce, "*Realistic Dirac leptogenesis*," Phys. Rev. Lett. **89** (2002) 271601, arXiv:hep-ph/0206177.

[57] M. Roncadelli and D. Wyler, "*Naturally light Dirac neutrinos in gauge theories*," Phys. Lett. B **133** (1983) 325.

[58] P. Roy and O. U. Shanker, "*Observable neutrino Dirac mass and supergrand unification*," Phys. Rev. Lett. **52** (1984) 713–716.

[59] F. Wang, W. Wang, and J. M. Yang, "*Split two-Higgs-doublet model and neutrino condensation*," Europhys. Lett. **76** (2006) 388–394, arXiv:hep-ph/0601018.

[60] S. Gabriel and S. Nandi, "*A new two Higgs doublet model*," Phys. Lett. B **655** (2007) 141–147, arXiv:hep-ph/0610253.

[61] S. M. Davidson and H. E. Logan, "*Dirac neutrinos from a second Higgs doublet*," Phys. Rev. D **80** (2009) 095008, arXiv:0906.3335.

[62] T. Wagner, S. Schlamminger, J. Gundlach, and E. Adelberger, "*Torsion-balance tests of the weak equivalence principle*," Class. Quant. Grav. **29** (2012) 184002, arXiv:1207.2442.

[63] T. Lee and C.-N. Yang, "*Conservation of heavy particles and generalized gauge transformations*," Phys. Rev. **98** (1955) 1501.

[64] L. Okun, "*On muonic charge and muonic photons*," Yad. Fiz. **10** (1969) 358–362.

[65] G. 't Hooft, "*Naturalness, chiral symmetry, and spontaneous chiral symmetry breaking*," NATO Adv. Study Inst. Ser. B Phys. **59** (1980) 135.

[66] **LEP Collaboration, ALEPH Collaboration, DELPHI Collaboration, L3 Collaboration, OPAL Collaboration, LEP Electroweak Working Group, SLD Electroweak Group, SLD Heavy Flavor Group**, D. Abbaneo *et al.*, "*A Combination of preliminary electroweak measurements and constraints on the standard model*," arXiv:hep-ex/0312023.

[67] M. S. Carena, A. Daleo, B. A. Dobrescu, and T. M. Tait, "*Z' gauge bosons at the Tevatron*," Phys. Rev. D **70** (2004) 093009, arXiv:hep-ph/0408098.

[68] G. Cacciapaglia, C. Csáki, G. Marandella, and A. Strumia, "*The minimal set of electroweak precision parameters*," Phys. Rev. D **74** (2006) 033011, arXiv:hep-ph/0604111.

[69] M. Williams, C. Burgess, A. Maharana, and F. Quevedo, "*New constraints (and motivations) for abelian gauge bosons in the MeV–TeV mass range*," JHEP **1108** (2011) 106, arXiv:1103.4556.

[70] R. Essig, J. A. Jaros, W. Wester, P. H. Adrian, S. Andreas, *et al.*, "*Dark Sectors and New, Light, Weakly-Coupled Particles*," arXiv:1311.0029.

[71] L. Basso, A. Belyaev, S. Moretti, and C. H. Shepherd-Themistocleous, "*Phenomenology of the minimal $B-L$ extension of the Standard model: Z' and neutrinos*," Phys. Rev. D **80** (2009) 055030, arXiv:0812.4313.

[72] P. Langacker, "*The physics of heavy Z' gauge bosons*," Rev. Mod. Phys. **81** (2009) 1199–1228, arXiv:0801.1345.

[73] B. Holdom, "*Two $U(1)$'s and Epsilon Charge Shifts*," Phys. Lett. B **166** (1986) 196.

[74] K. Dick, M. Lindner, M. Ratz, and D. Wright, "*Leptogenesis with Dirac neutrinos*," Phys. Rev. Lett. **84** (2000) 4039–4042, arXiv:hep-ph/9907562.

[75] V. Kuzmin, V. Rubakov, and M. Shaposhnikov, "*On the anomalous electroweak baryon number nonconservation in the early universe*," Phys. Lett. B **155** (1985) 36.

[76] R. Marshak and R. N. Mohapatra, "*Quark–Lepton Symmetry and $B-L$ as the $U(1)$ Generator of the Electroweak Symmetry Group*," Phys. Lett. B **91** (1980) 222–224.

[77] R. N. Mohapatra and R. Marshak, "*Local $B-L$ Symmetry of Electroweak Interactions, Majorana Neutrinos and Neutron Oscillations*," Phys. Rev. Lett. **44** (1980) 1316–1319.

[78] P. Minkowski, "$\mu \to e\gamma$ *at a rate of one out of 1-billion muon decays?*," Phys. Lett. B **67** (1977) 421.

[79] T. Yanagida, "*Horizontal gauge symmetry and masses of neutrinos*," in *Proc. Workshop on the Baryon Number of the Universe and Unified Theories*, O. Sawada and A. Sugamoto, eds., pp. 95–99. 1979.

[80] R. N. Mohapatra and G. Senjanović, "*Neutrino mass and spontaneous parity violation*," Phys. Rev. Lett. **44** (1980) 912.

[81] M. Gell-Mann, P. Ramond, and R. Slansky, "*Complex spinors and unified theories*," in *Supergravity*, P. van Nieuwenhuizen and D. Z. Freedman, eds., pp. 315–321. 1979. arXiv:1306.4669.

[82] S. Antusch, C. Biggio, E. Fernandez-Martinez, M. Gavela, and J. Lopez-Pavon, "*Unitarity of the leptonic mixing matrix*," JHEP **0610** (2006) 084, arXiv:hep-ph/0607020.

[83] A. Atre, T. Han, S. Pascoli, and B. Zhang, "*The search for heavy Majorana neutrinos*," JHEP **0905** (2009) 030, arXiv:0901.3589.

[84] C. S. Fong, E. Nardi, and A. Riotto, "*Leptogenesis in the Universe*," Adv. High Energy Phys. **2012** (2012) 158303, arXiv:1301.3062.

[85] M. Fukugita and T. Yanagida, "*Baryogenesis without grand unification*," Phys. Lett. B **174** (1986) 45.

[86] J. A. Harvey and M. S. Turner, "*Cosmological baryon and lepton number in the presence of electroweak fermion number violation*," Phys. Rev. D **42** (1990) 3344–3349.

[87] L. Basso, S. Moretti, and G. M. Pruna, "*Phenomenology of the minimal $B - L$ extension of the Standard Model: the Higgs sector*," Phys. Rev. D **83** (2011) 055014, arXiv:1011.2612.

[88] J. M. No and M. Ramsey-Musolf, "*Probing the Higgs Portal at the LHC Through Resonant di-Higgs Production*," arXiv:1310.6035.

[89] S. Blanchet, Z. Chacko, S. S. Granor, and R. N. Mohapatra, "*Probing Resonant Leptogenesis at the LHC*," Phys. Rev. D **82** (2010) 076008, arXiv:0904.2174.

[90] A. de Gouvêa and J. Jenkins, "*A Survey of Lepton Number Violation Via Effective Operators*," Phys. Rev. D **77** (2008) 013008, arXiv:0708.1344.

[91] **KamLAND Collaboration**, T. Araki *et al.*, "*Search for the invisible decay of neutrons with KamLAND*," Phys. Rev. Lett. **96** (2006) 101802, arXiv:hep-ex/0512059.

[92] E. Witten, "*Lepton number and neutrino masses*," Nucl. Phys. Proc. Suppl. **91** (2001) 3–8, arXiv:hep-ph/0006332.

[93] National Nuclear Data Center. Information extracted from the chart of nuclides database, online under http://www.nndc.bnl.gov/chart. See also the Wikipedia pages http://en.wikipedia.org/wiki/Beta-decay_stable_isobars and http://en.wikipedia.org/wiki/Table_of_nuclides_(complete) for useful overviews (accessed on 19.4.2013).

[94] **EXO-200 Collaboration**, N. Ackerman *et al.*, "*Observation of two-neutrino double-beta decay in ^{136}Xe with EXO-200*," Phys. Rev. Lett. **107** (2011) 212501, arXiv:1108.4193.

[95] **NEMO-3 Collaboration**, J. Argyriades *et al.*, "*Measurement of the two neutrino double beta decay half-life of Zr-96 with the NEMO-3 detector*," Nucl. Phys. A **847** (2010) 168–179, arXiv:0906.2694.

[96] **NEMO Collaboration**, J. Argyriades *et al.*, "*Measurement of the double beta decay half-life of Nd-150 and search for neutrinoless decay modes with the NEMO-3 detector*," Phys. Rev. C **80** (2009) 032501, arXiv:0810.0248.

[97] S. Eliseev, Y. Novikov, and K. Blaum, "*Search for resonant enhancement of neutrinoless double-electron capture by high-precision Penning-trap mass spectrometry*," J. Phys. G **39** (2012) 124003.

[98] J. Suhonen and O. Civitarese, "*Weak-interaction and nuclear-structure aspects of nuclear double beta decay*," Phys. Rept. **300** (1998) 123–214.

[99] J. C. Pati and A. Salam, "*Lepton number as the fourth color*," Phys. Rev. D **10** (1974) 275–289.

[100] R. Mohapatra and J. C. Pati, "*A natural left-right symmetry*," Phys. Rev. D **11** (1975) 2558.

[101] G. Senjanović and R. N. Mohapatra, "*Exact left-right symmetry and spontaneous violation of parity*," Phys. Rev. D **12** (1975) 1502.

[102] M. S. Bilenky and A. Santamaria, "*'Secret' neutrino interactions*," arXiv:hep-ph/9908272.

[103] P. Benes, A. Faessler, F. Simkovic, and S. Kovalenko, "*Sterile neutrinos in neutrinoless double beta decay*," Phys. Rev. D **71** (2005) 077901, arXiv:hep-ph/0501295.

[104] M. Mitra, G. Senjanović, and F. Vissani, "*Neutrinoless double beta decay and heavy sterile neutrinos*," Nucl. Phys. B **856** (2012) 26–73, arXiv:1108.0004.

[105] E. Ma, "*Naturally small seesaw neutrino mass with no new physics beyond the TeV scale*," Phys. Rev. Lett. **86** (2001) 2502–2504, arXiv:hep-ph/0011121.

[106] S. M. Davidson and H. E. Logan, "*LHC phenomenology of a two-Higgs-doublet neutrino mass model*," Phys. Rev. D **82** (2010) 115031, arXiv:1009.4413.

[107] M.-C. Chen, M. Ratz, C. Staudt, and P. K. Vaudrevange, "*The mu term and neutrino masses*," Nucl. Phys. B **866** (2013) 157–176, arXiv:1206.5375.

[108] A. Kartavtsev, "*Baryon and lepton numbers in two scenarios of leptogenesis*," Phys. Rev. D **73** (2006) 023514, arXiv:hep-ph/0511059.

[109] L. A. Anchordoqui, H. Goldberg, and G. Steigman, "*Right-handed neutrinos as the dark radiation: status and forecasts for the LHC*," Phys. Lett. B **718** (2013) 1162–1165, arXiv:1211.0186.

[110] E. Ma, "*Gauged $B - 3L_\tau$ and radiative neutrino masses*," Phys. Lett. B **433** (1998) 74–81, arXiv:hep-ph/9709474.

[111] E. Ma and D. Roy, "*Phenomenology of the $B - 3L_\tau$ gauge boson*," Phys. Rev. D **58** (1998) 095005, arXiv:hep-ph/9806210.

[112] E. Ma and U. Sarkar, "*Gauged $B - 3L_\tau$ and baryogenesis*," Phys. Lett. B **439** (1998) 95–102, arXiv:hep-ph/9807307.

[113] E. Ma, D. Roy, and U. Sarkar, "*A Seesaw model for atmospheric and solar neutrino oscillations*," Phys. Lett. B **444** (1998) 391–396, arXiv:hep-ph/9810309.

[114] E. Ma and D. Roy, "*Minimal seesaw model for atmospheric and solar neutrino oscillations*," Phys. Rev. D **59** (1999) 097702, arXiv:hep-ph/9811266.

[115] L. N. Chang, O. Lebedev, W. Loinaz, and T. Takeuchi, "*Constraints on gauged $B - 3L_\tau$ and related theories*," Phys. Rev. D **63** (2001) 074013, arXiv:hep-ph/0010118.

[116] E. Salvioni, A. Strumia, G. Villadoro, and F. Zwirner, "*Non-universal minimal Z' models: present bounds and early LHC reach*," JHEP **1003** (2010) 010, arXiv:0911.1450.

[117] H.-S. Lee and E. Ma, "*Gauged $B - x_i L$ origin of R parity and its implications*," Phys. Lett. B **688** (2010) 319–322, arXiv:1001.0768.

[118] H. Davoudiasl, H.-S. Lee, and W. J. Marciano, "*Long-range lepton flavor interactions and neutrino oscillations*," Phys. Rev. D **84** (2011) 013009, arXiv:1102.5352.

[119] S. Choubey and W. Rodejohann, "*A Flavor symmetry for quasi-degenerate neutrinos: $L_\mu - L_\tau$*," Eur. Phys. J. C **40** (2005) 259–268, arXiv:hep-ph/0411190.

[120] G. Branco, W. Grimus, and L. Lavoura, "*The seesaw mechanism in the presence of a conserved lepton number*," Nucl. Phys. B **312** (1989) 492.

[121] S. Petcov, "*On pseudodirac neutrinos, neutrino oscillations and neutrinoless double beta decay*," Phys. Lett. B **110** (1982) 245–249.

[122] C. N. Leung and S. Petcov, "*A comment on the coexistence of Dirac and Majorana massive neutrinos*," Phys. Lett. B **125** (1983) 461.

[123] R. Barbieri, L. Hall, D. Tucker-Smith, A. Strumia, and N. Weiner, "*Oscillations of solar and atmospheric neutrinos*," JHEP **9812** (1998) 017, arXiv:hep-ph/9807235.

[124] A. S. Joshipura and S. D. Rindani, "*Vacuum solutions of neutrino anomalies through a softly broken U(1) symmetry*," Eur. Phys. J. C **14** (2000) 85–89, arXiv:hep-ph/9811252.

[125] R. Mohapatra, A. Pérez-Lorenzana, and C. A. de Sousa Pires, "*Type II seesaw and a gauge model for the bimaximal mixing explanation of neutrino puzzles*," Phys. Lett. B **474** (2000) 355–360, arXiv:hep-ph/9911395.

[126] Y. Nir, "*Pseudo-Dirac solar neutrinos*," JHEP **0006** (2000) 039, arXiv:hep-ph/0002168.

[127] L. Lavoura, "*New model for the neutrino mass matrix*," Phys. Rev. D **62** (2000) 093011, arXiv:hep-ph/0005321.

[128] L. Lavoura and W. Grimus, "*Seesaw model with softly broken $L_e - L_\mu - L_\tau$*," JHEP **0009** (2000) 007, arXiv:hep-ph/0008020.

[129] W. Grimus and L. Lavoura, "*Softly broken lepton numbers and maximal neutrino mixing*," JHEP **0107** (2001) 045, arXiv:hep-ph/0105212.

[130] Q. Shafi and Z. Tavartkiladze, "*Anomalous flavor $U(1)$: Predictive texture for bimaximal neutrino mixing*," Phys. Lett. B **482** (2000) 145–149, arXiv:hep-ph/0002150.

[131] G. Fogli, E. Lisi, A. Marrone, A. Palazzo, and A. Rotunno, "*Evidence of $\theta_{13} > 0$ from global neutrino data analysis*," Phys. Rev. D **84** (2011) 053007, arXiv:1106.6028.

[132] S. Khalil and A. Masiero, "*Radiative $B - L$ symmetry breaking in supersymmetric models*," Phys. Lett. B **665** (2008) 374–377, arXiv:0710.3525.

[133] P. Fileviez Perez and S. Spinner, "*The fate of R-parity*," Phys. Rev. D **83** (2011) 035004, arXiv:1005.4930.

[134] B. O'Leary, W. Porod, and F. Staub, "*Mass spectrum of the minimal SUSY $B - L$ model*," JHEP **1205** (2012) 042, arXiv:1112.4600.

[135] J. Erler and P. Langacker, "*Constraints on extended neutral gauge structures*," Phys. Lett. B **456** (1999) 68–76, arXiv:hep-ph/9903476.

[136] J. Erler, "*Global fits to electroweak data using GAPP*," arXiv:hep-ph/0005084.

[137] J. Schechter and J. Valle, "*Neutrino masses in $SU(2) \times U(1)$ theories*," Phys. Rev. D **22** (1980) 2227.

[138] W. Grimus and L. Lavoura, "*Softly broken lepton number $L_e - L_\mu - L_\tau$ with non-maximal solar neutrino mixing*," J. Phys. G **31** (2005) 683–692, arXiv:hep-ph/0410279.

[139] R. Mohapatra and W. Rodejohann, "*Scaling in the neutrino mass matrix*," Phys. Lett. B **644** (2007) 59–66, arXiv:hep-ph/0608111.

[140] A. Blum, R. Mohapatra, and W. Rodejohann, "*Inverted mass hierarchy from scaling in the neutrino mass matrix: Low and high energy phenomenology*," Phys. Rev. D **76** (2007) 053003, arXiv:0706.3801.

[141] S. Ray, W. Rodejohann, and M. A. Schmidt, "*Lower bounds on the smallest lepton mixing angle*," Phys. Rev. D **83** (2011) 033002, arXiv:1010.1206.

[142] N. Okada and O. Seto, "*Higgs portal dark matter in the minimal gauged $U(1)_{B-L}$ model*," Phys. Rev. D **82** (2010) 023507, arXiv:1002.2525.

[143] S. Kanemura, O. Seto, and T. Shimomura, "*Masses of dark matter and neutrino from TeV scale spontaneous $U(1)_{B-L}$ breaking*," Phys. Rev. D **84** (2011) 016004, arXiv:1101.5713.

[144] G. Belanger, F. Boudjema, A. Pukhov, and A. Semenov, "*micrOMEGAs 2.0: A Program to calculate the relic density of dark matter in a generic model*," Comput. Phys. Commun. **176** (2007) 367–382, arXiv:hep-ph/0607059.

[145] G. Belanger, F. Boudjema, A. Pukhov, and A. Semenov, "*Dark matter direct detection rate in a generic model with micrOMEGAs 2.2*," Comput. Phys. Commun. **180** (2009) 747–767, arXiv:0803.2360.

[146] G. Belanger, F. Boudjema, A. Pukhov, and A. Semenov, "*micrOMEGAs: A Tool for dark matter studies*," Nuovo Cim. C **33** (2010) no. 2, 111–116, arXiv:1005.4133.

[147] S. Kanemura, T. Nabeshima, and H. Sugiyama, "*TeV-scale seesaw with loop-induced Dirac mass term and dark matter from $U(1)_{B-L}$ gauge symmetry breaking*," Phys. Rev. D **85** (2012) 033004, arXiv:1111.0599.

[148] N. Okada and Y. Orikasa, "*Dark matter in the classically conformal $B - L$ model*," Phys. Rev. D **85** (2012) 115006, arXiv:1202.1405.

[149] Z. M. Burell and N. Okada, "*Supersymmetric minimal $B - L$ model at the TeV scale with right-handed Majorana neutrino dark matter*," Phys. Rev. D **85** (2012) 055011, arXiv:1111.1789.

[150] M. Freytsis and Z. Ligeti, "*On dark matter models with uniquely spin-dependent detection possibilities*," Phys. Rev. D **83** (2011) 115009, arXiv:1012.5317.

[151] **XENON100 Collaboration**, E. Aprile *et al.*, "*Dark matter results from 100 live days of XENON100 data*," Phys. Rev. Lett. **107** (2011) 131302, arXiv:1104.2549.

[152] J. Heeck, "*Phenomenology of a gauged $L_\mu - L_\tau$ symmetry*," Diploma Thesis, University of Heidelberg, 2011.

[153] J. Heeck and W. Rodejohann, "*Gauged $L_\mu - L_\tau$ and different muon neutrino and anti-neutrino oscillations: MINOS and beyond*," J. Phys. G **38** (2011) 085005, arXiv:1007.2655.

[154] J. P. Leveille, "*The second order weak correction to $g - 2$ of the muon in arbitrary gauge models*," Nucl. Phys. B **137** (1978) 63.

[155] E. Ma, D. Roy, and S. Roy, "*Gauged $L_\mu - L_\tau$ with large muon anomalous magnetic moment and the bimaximal mixing of neutrinos*," Phys. Lett. B **525** (2002) 101–106, arXiv:hep-ph/0110146.

[156] S. Baek, N. Deshpande, X. He, and P. Ko, "*Muon anomalous $g-2$ and gauged $L_\mu - L_\tau$ models*," Phys. Rev. D **64** (2001) 055006, arXiv:hep-ph/0104141.

[157] E. Ma and D. P. Roy, "*Anomalous neutrino interaction, muon $g-2$, and atomic parity nonconservation*," Phys. Rev. D **65** (2002) 075021.

[158] K. Harigaya, T. Igari, M. M. Nojiri, M. Takeuchi, and K. Tobe, "*Muon $g-2$ and LHC phenomenology in the $L_\mu - L_\tau$ gauge symmetric model*," JHEP **1403** (2014) 105, arXiv:1311.0870.

[159] H. Fritzsch, Z.-Z. Xing, and S. Zhou, "*Two-zero textures of the Majorana neutrino mass matrix and current experimental tests*," JHEP **1109** (2011) 083, arXiv:1108.4534.

[160] M. Berger and K. Siyeon, "*Discrete flavor symmetries and mass matrix textures*," Phys. Rev. D **64** (2001) 053006, arXiv:hep-ph/0005249.

[161] P. H. Frampton, S. L. Glashow, and D. Marfatia, "*Zeroes of the neutrino mass matrix*," Phys. Lett. B **536** (2002) 79–82, arXiv:hep-ph/0201008.

[162] P. H. Frampton, M. C. Oh, and T. Yoshikawa, "*Majorana mass zeroes from triplet VEV without majoron problem*," Phys. Rev. D **66** (2002) 033007, arXiv:hep-ph/0204273.

[163] A. Kageyama, S. Kaneko, N. Shimoyama, and M. Tanimoto, "*Seesaw realization of the texture zeros in the neutrino mass matrix*," Phys. Lett. B **538** (2002) 96–106, arXiv:hep-ph/0204291.

[164] L. Lavoura, "*Zeros of the inverted neutrino mass matrix*," Phys. Lett. B **609** (2005) 317–322, arXiv:hep-ph/0411232.

[165] E. Lashin and N. Chamoun, "*Zero minors of the neutrino mass matrix*," Phys. Rev. D **78** (2008) 073002, arXiv:0708.2423.

[166] W. Grimus, A. S. Joshipura, L. Lavoura, and M. Tanimoto, "*Symmetry realization of texture zeros*," Eur. Phys. J. C **36** (2004) 227–232, arXiv:hep-ph/0405016.

[167] T. Banks and N. Seiberg, "*Symmetries and Strings in Field Theory and Gravity*," Phys. Rev. D **83** (2011) 084019, arXiv:1011.5120.

[168] E. Lashin and N. Chamoun, "*One-zero textures of Majorana neutrino mass matrix and current experimental tests*," Phys. Rev. D **85** (2012) 113011, arXiv:1108.4010.

[169] E. Lashin and N. Chamoun, "*One vanishing minor in the neutrino mass matrix*," Phys. Rev. D **80** (2009) 093004, arXiv:0909.2669.

[170] D. Meloni, A. Meroni, and E. Peinado, "*Two-zero Majorana textures in the light of the Planck results*," Phys. Rev. D **89** (2014) 053009, arXiv:1401.3207.

[171] D. Meloni and G. Blankenburg, "*Fine-tuning and naturalness issues in the two-zero neutrino mass textures*," Nucl. Phys. B **867** (2013) 749–762, arXiv:1204.2706.

[172] C. Froggatt and H. B. Nielsen, "*Hierarchy of quark masses, Cabibbo angles and CP violation*," Nucl. Phys. B **147** (1979) 277.

[173] L. M. Krauss and F. Wilczek, "*Discrete gauge symmetry in continuum theories*," Phys. Rev. Lett. **62** (1989) 1221.

[174] C. Giunti and M. Laveder, "*3+1 and 3+2 sterile neutrino fits*," Phys. Rev. D **84** (2011) 073008, arXiv:1107.1452.

[175] J. Kopp, M. Maltoni, and T. Schwetz, "*Are there sterile neutrinos at the eV scale?*," Phys. Rev. Lett. **107** (2011) 091801, arXiv:1103.4570.

[176] **LSND Collaboration**, A. Aguilar-Arevalo *et al.*, "*Evidence for neutrino oscillations from the observation of anti-neutrino(electron) appearance in a anti-neutrino(muon) beam*," Phys. Rev. D **64** (2001) 112007, arXiv:hep-ex/0104049.

[177] **MiniBooNE Collaboration**, A. Aguilar-Arevalo *et al.*, "*Event excess in the MiniBooNE search for $\bar{\nu}_\mu \to \bar{\nu}_e$ oscillations*," Phys. Rev. Lett. **105** (2010) 181801, arXiv:1007.1150.

[178] **MiniBooNE Collaboration**, A. Aguilar-Arevalo *et al.*, "*Improved search for $\bar{\nu}_\mu \to \bar{\nu}_e$ oscillations in the MiniBooNE experiment*," Phys. Rev. Lett. **110** (2013) 161801, arXiv:1207.4809.

[179] C. Giunti, M. Laveder, Y. Li, and H. Long, "*Pragmatic View of Short-Baseline Neutrino Oscillations*," Phys. Rev. D **88** (2013) 073008, arXiv:1308.5288.

[180] J. Hamann, S. Hannestad, G. G. Raffelt, I. Tamborra, and Y. Y. Wong, "*Cosmology seeking friendship with sterile neutrinos*," Phys. Rev. Lett. **105** (2010) 181301, arXiv:1006.5276.

[181] J. Hamann, S. Hannestad, G. G. Raffelt, and Y. Y. Wong, "*Sterile neutrinos with eV masses in cosmology: How disfavoured exactly?*," JCAP **1109** (2011) 034, arXiv:1108.4136.

[182] S. Joudaki, K. N. Abazajian, and M. Kaplinghat, "*Are light sterile neutrinos preferred or disfavored by cosmology?*," Phys. Rev. D **87** (2013) 065003, arXiv:1208.4354.

[183] H. Motohashi, A. A. Starobinsky, and J. Yokoyama, "*Cosmology based on $f(R)$ gravity admits 1 eV sterile neutrinos*," Phys. Rev. Lett. **110** (2013) 121302, arXiv:1203.6828.

[184] A. de Gouvêa, "*See-saw energy scale and the LSND anomaly*," Phys. Rev. D **72** (2005) 033005, arXiv:hep-ph/0501039.

[185] J. Barry, W. Rodejohann, and H. Zhang, "*Light sterile neutrinos: models and phenomenology*," JHEP **1107** (2011) 091, arXiv:1105.3911.

[186] H. Zhang, "*Light sterile neutrino in the minimal extended seesaw*," Phys. Lett. B **714** (2012) 262–266, arXiv:1110.6838.

[187] E. Ma and P. Roy, "*Model of four light neutrinos prompted by all desiderata*," Phys. Rev. D **52** (1995) 4780–4783, arXiv:hep-ph/9504342.

[188] E. Chun, A. S. Joshipura, and A. Y. Smirnov, "*Models of light singlet fermion and neutrino phenomenology*," Phys. Lett. B **357** (1995) 608–615, arXiv:hep-ph/9505275.

[189] K. Babu and G. Seidl, "*Simple model for (3+2) neutrino oscillations*," Phys. Lett. B **591** (2004) 127–136, arXiv:hep-ph/0312285.

[190] K. Babu and G. Seidl, "*Chiral gauge models for light sterile neutrinos*," Phys. Rev. D **70** (2004) 113014, arXiv:hep-ph/0405197.

[191] J. Sayre, S. Wiesenfeldt, and S. Willenbrock, "*Sterile neutrinos and global symmetries*," Phys. Rev. D **72** (2005) 015001, arXiv:hep-ph/0504198.

[192] P. Batra, B. A. Dobrescu, and D. Spivak, "*Anomaly-free sets of fermions*," J. Math. Phys. **47** (2006) 082301, arXiv:hep-ph/0510181.

[193] B. Patt and F. Wilczek, "*Higgs-field portal into hidden sectors*," arXiv:hep-ph/0605188.

[194] G. Belanger, A. Pukhov, and G. Servant, "*Dirac neutrino dark matter*," JCAP **0801** (2008) 009, arXiv:0706.0526.

[195] Y. Mambrini, "*The Z–Z' kinetic mixing in the light of the recent direct and indirect dark matter searches*," JCAP **1107** (2011) 009, arXiv:1104.4799.

[196] X. Chu, T. Hambye, and M. H. Tytgat, "*The four basic ways of creating dark matter through a portal*," JCAP **1205** (2012) 034, arXiv:1112.0493.

[197] A. Falkowski, J. Juknevich, and J. Shelton, "*Dark matter through the neutrino portal*," arXiv:0908.1790.

[198] M. Lindner, A. Merle, and V. Niro, "*Enhancing dark matter annihilation into neutrinos*," Phys. Rev. D **82** (2010) 123529, arXiv:1005.3116.

[199] Y. Farzan, "*Flavoring monochromatic neutrino flux from dark matter annihilation*," JHEP **1202** (2012) 091, arXiv:1111.1063.

[200] C. Boehm, P. Fayet, and J. Silk, "*Light and heavy dark matter particles*," Phys. Rev. D **69** (2004) 101302, arXiv:hep-ph/0311143.

[201] E. Ma, "*Supersymmetric model of radiative seesaw Majorana neutrino masses*," Annales Fond. Broglie **31** (2006) 285, arXiv:hep-ph/0607142.

[202] L. Lopez-Honorez, T. Schwetz, and J. Zupan, "*Higgs portal, fermionic dark matter, and a Standard Model like Higgs at 125 GeV*," Phys. Lett. B **716** (2012) 179–185, arXiv:1203.2064.

[203] S. Hannestad, I. Tamborra, and T. Tram, "*Thermalisation of light sterile neutrinos in the early universe*," JCAP **1207** (2012) 025, arXiv:1204.5861.

[204] **IceCube Collaboration**, R. Abbasi *et al.*, "*Search for neutrinos from annihilating dark matter in the direction of the galactic center with the 40-string IceCube neutrino observatory*," arXiv:1210.3557.

[205] G. Karagiorgi, A. Aguilar-Arevalo, J. Conrad, M. Shaevitz, K. Whisnant, *et al.*, "*Leptonic CP violation studies at MiniBooNE in the (3+2) sterile neutrino oscillation hypothesis*," Phys. Rev. D **75** (2007) 013011, arXiv:hep-ph/0609177.

[206] A. Donini, P. Hernandez, J. Lopez-Pavon, M. Maltoni, and T. Schwetz, "*The minimal $3+2$ neutrino model versus oscillation anomalies*," JHEP **1207** (2012) 161, arXiv:1205.5230.

[207] J. Conrad, C. Ignarra, G. Karagiorgi, M. Shaevitz, and J. Spitz, "*Sterile neutrino fits to short baseline neutrino oscillation measurements*," Adv. High Energy Phys. **2013** (2013) 163897, arXiv:1207.4765.

[208] M. Pospelov, "*Neutrino physics with dark matter experiments and the signature of new baryonic neutral currents*," Phys. Rev. D **84** (2011) 085008, arXiv:1103.3261.

[209] M. Pospelov and J. Pradler, "*Elastic scattering signals of solar neutrinos with enhanced baryonic currents*," Phys. Rev. D **85** (2012) 113016, arXiv:1203.0545.

[210] H. Ruegg and M. Ruiz-Altaba, "*The Stueckelberg field*," Int. J. Mod. Phys. A **19** (2004) 3265–3348, arXiv:hep-th/0304245.

[211] E. Stückelberg, "*Interaction energy in electrodynamics and in the field theory of nuclear forces*," Helv. Phys. Acta **11** (1938) 225–244.

[212] A. Proca, "*Sur la theorie ondulatoire des electrons positifs et negatifs*," J. Phys. Radium **7** (1936) 347–353.

[213] D. Ryutov, "*Using Plasma Physics to Weigh the Photon*," Plasma Phys. Control. Fusion **49** (2007) B429.

[214] A. S. Goldhaber and M. M. Nieto, "*Photon and graviton mass limits*," Rev. Mod. Phys. **82** (2010) 939–979, arXiv:0809.1003.

[215] S. Kuzmin and D. McKeon, "*Stueckelberg mass in the Glashow–Weinberg–Salam model*," Mod. Phys. Lett. A **16** (2001) 747–753.

[216] D. McKeon and T. Marshall, "*Radiative properties of the Stueckelberg mechanism*," Int. J. Mod. Phys. A **23** (2008) 741–748, arXiv:hep-th/0610034.

[217] S. Petcov and S. Toshev, "*Conservation of lepton charges, massive Majorana and massless neutrinos*," Phys. Lett. B **143** (1984) 175.

[218] S. Davidson, G. Isidori, and A. Strumia, "*The smallest neutrino mass*," Phys. Lett. B **646** (2007) 100–104, arXiv:hep-ph/0611389.

[219] M. Hare, "*Photon stability*," Lett. Nuovo Cim. **4** (1972) 693–694.

[220] C. Broggini, C. Giunti, and A. Studenikin, "*Electromagnetic properties of neutrinos*," Adv. High Energy Phys. **2012** (2012) 459526, arXiv:1207.3980.

[221] H.-B. Zhang, "*Note on the thermal history of decoupled massive particles*," Class. Quant. Grav. **25** (2008) 208001, arXiv:0808.1552.

[222] J. C. Mather, E. Cheng, D. Cottingham, R. Eplee, D. Fixsen, *et al.*, "*Measurement of the Cosmic Microwave Background spectrum by the COBE FIRAS instrument*," Astrophys. J. **420** (1994) 439–444.

[223] D. Fixsen, E. Cheng, J. Gales, J. C. Mather, R. Shafer, *et al.*, "*The Cosmic Microwave Background spectrum from the full COBE FIRAS data set*," Astrophys. J. **473** (1996) 576, arXiv:astro-ph/9605054.

[224] D. Fixsen, A. Kogut, S. Levin, M. Limon, P. Lubin, *et al.*, "*ARCADE 2 measurement of the extra-galactic sky temperature at 3-90 GHz*," arXiv:0901.0555.

[225] S. Davidson, S. Hannestad, and G. Raffelt, "*Updated bounds on millicharged particles*," JHEP **0005** (2000) 003, arXiv:hep-ph/0001179.

[226] A. Mirizzi, J. Redondo, and G. Sigl, "*Microwave background constraints on mixing of photons with hidden photons*," JCAP **0903** (2009) 026, arXiv:0901.0014.

[227] H. Georgi, P. H. Ginsparg, and S. Glashow, "*Photon oscillations and the cosmic background radiation*," Nature **306** (1983) 765–766.

[228] J. E. Kim and G. Carosi, "*Axions and the strong CP problem*," Rev. Mod. Phys. **82** (2010) 557–602, arXiv:0807.3125.

[229] R. N. Mohapatra, "*Gauge model for chiral symmetry breaking and muon electron mass ratio*," Phys. Rev. D **9** (1974) 3461.

[230] S. M. Barr and A. Zee, "*Calculating the electron mass in terms of measured quantities*," Phys. Rev. D **17** (1978) 1854.

[231] C. Ong, "*Adding a horizontal gauge symmetry to the Weinberg–Salam model: an eight quark model*," Phys. Rev. D **19** (1979) 2738.

[232] F. Wilczek and A. Zee, "*Horizontal interaction and weak mixing angles*," Phys. Rev. Lett. **42** (1979) 421.

[233] B. de Carlos and J. Espinosa, "*Cold dark matter candidate in a class of supersymmetric models with an extra $U(1)$*," Phys. Lett. B **407** (1997) 12–21, arXiv:hep-ph/9705315.

[234] K. Babu, C. F. Kolda, and J. March-Russell, "*Implications of generalized Z–Z' mixing*," Phys. Rev. D **57** (1998) 6788–6792, arXiv:hep-ph/9710441.

[235] B. Holdom, "*Oblique electroweak corrections and an extra gauge boson*," Phys. Lett. B **259** (1991) 329–334.

[236] F. del Aguila, M. Masip, and M. Perez-Victoria, "*Physical parameters and renormalization of $U(1)_a \times U(1)_b$ models*," Nucl. Phys. B **456** (1995) 531–549, arXiv:hep-ph/9507455.

[237] J. Jaeckel and A. Ringwald, "*The low-energy frontier of particle physics*," Ann. Rev. Nucl. Part. Sci. **60** (2010) 405–437, arXiv:1002.0329.

[238] F. del Aguila, G. Coughlan, and M. Quiros, "*Gauge coupling renormalization with several $U(1)$ factors*," Nucl. Phys. B **307** (1988) 633.

[239] M.-X. Luo and Y. Xiao, "*Renormalization group equations in gauge theories with multiple $U(1)$ groups*," Phys. Lett. B **555** (2003) 279–286, arXiv:hep-ph/0212152.

[240] S. Abel, M. Goodsell, J. Jaeckel, V. Khoze, and A. Ringwald, "*Kinetic mixing of the photon with hidden $U(1)$s in string phenomenology*," JHEP **0807** (2008) 124, arXiv:0803.1449.

[241] M. Goodsell, J. Jaeckel, J. Redondo, and A. Ringwald, "*Naturally light hidden photons in LARGE volume string compactifications*," JHEP **0911** (2009) 027, arXiv:0909.0515.

[242] P. Fileviez Perez and M. B. Wise, "*Baryon and lepton number as local gauge symmetries*," Phys. Rev. D **82** (2010) 011901, arXiv:1002.1754.

[243] T. R. Dulaney, P. Fileviez Perez, and M. B. Wise, "*Dark matter, baryon asymmetry, and spontaneous B and L breaking*," Phys. Rev. D **83** (2011) 023520, arXiv:1005.0617.

[244] P. Fileviez Perez and M. B. Wise, "*Low energy supersymmetry with baryon and lepton number gauged*," Phys. Rev. D **84** (2011) 055015, arXiv:1105.3190.

[245] P. Fileviez Perez and M. B. Wise, "*Breaking local baryon and lepton number at the TeV scale*," JHEP **1108** (2011) 068, arXiv:1106.0343.

[246] F. del Aguila, J. de Blas, P. Langacker, and M. Perez-Victoria, "*Impact of extra particles on indirect Z' limits*," Phys. Rev. D **84** (2011) 015015, arXiv:1104.5512.

[247] **DAMA Collaboration, LIBRA Collaboration**, R. Bernabei *et al.*, "*New results from DAMA/LIBRA*," Eur. Phys. J. C **67** (2010) 39–49, arXiv:1002.1028.

[248] **CoGeNT Collaboration**, C. Aalseth *et al.*, "*Results from a Search for Light-Mass Dark Matter with a P-type Point Contact Germanium Detector*," Phys. Rev. Lett. **106** (2011) 131301, arXiv:1002.4703.

[249] G. Angloher, M. Bauer, I. Bavykina, A. Bento, C. Bucci, *et al.*, "*Results from 730 kg days of the CRESST-II Dark Matter Search*," Eur. Phys. J. C **72** (2012) 1971, arXiv:1109.0702.

[250] **CDMS Collaboration**, R. Agnese *et al.*, "*Silicon Detector Dark Matter Results from the Final Exposure of CDMS II*," Phys. Rev. Lett. **111** (2013) 251301, arXiv:1304.4279.

[251] **LUX Collaboration**, D. Akerib *et al.*, "*First results from the LUX dark matter experiment at the Sanford Underground Research Facility*," Phys. Rev. Lett. **112** (2014) 091303, arXiv:1310.8214.

[252] A. Kurylov and M. Kamionkowski, "*Generalized analysis of weakly interacting massive particle searches*," Phys. Rev. D **69** (2004) 063503, arXiv:hep-ph/0307185.

[253] S. Chang, J. Liu, A. Pierce, N. Weiner, and I. Yavin, "*CoGeNT interpretations*," JCAP **1008** (2010) 018, arXiv:1004.0697.

[254] J. L. Feng, J. Kumar, D. Marfatia, and D. Sanford, "*Isospin-violating dark matter*," Phys. Lett. B **703** (2011) 124–127, arXiv:1102.4331.

[255] E. Del Nobile, G. B. Gelmini, P. Gondolo, and J.-H. Huh, "*Update on Light WIMP Limits: LUX, lite and Light*," JCAP **1403** (2014) 014, arXiv:1311.4247.

[256] F. Giuliani, "*Are direct search experiments sensitive to all spin-independent WIMP candidates?*," Phys. Rev. Lett. **95** (2005) 101301, arXiv:hep-ph/0504157.

[257] M. T. Frandsen, F. Kahlhoefer, J. March-Russell, C. McCabe, M. McCullough, *et al.*, "*On the DAMA and CoGeNT modulations*," Phys. Rev. D **84** (2011) 041301, arXiv:1105.3734.

[258] E. Del Nobile, C. Kouvaris, and F. Sannino, "*Interfering composite asymmetric dark matter for DAMA and CoGeNT*," Phys. Rev. D **84** (2011) 027301, arXiv:1105.5431.

[259] T. Schwetz and J. Zupan, "*Dark matter attempts for CoGeNT and DAMA*," JCAP **1108** (2011) 008, arXiv:1106.6241.

[260] M. Farina, D. Pappadopulo, A. Strumia, and T. Volansky, "*Can CoGeNT and DAMA modulations be due to dark matter?*," JCAP **1111** (2011) 010, arXiv:1107.0715.

[261] X. Gao, Z. Kang, and T. Li, "*Origins of the isospin violation of dark matter interactions*," JCAP **1301** (2013) 021, arXiv:1107.3529.

[262] M. T. Frandsen, F. Kahlhoefer, S. Sarkar, and K. Schmidt-Hoberg, "*Direct detection of dark matter in models with a light Z'*," JHEP **1109** (2011) 128, arXiv:1107.2118.

[263] C. D. Carone and H. Murayama, "*Possible light $U(1)$ gauge boson coupled to baryon number*," Phys. Rev. Lett. **74** (1995) 3122–3125, arXiv:hep-ph/9411256.

[264] C. D. Carone and H. Murayama, "*Realistic models with a light $U(1)$ gauge boson coupled to baryon number*," Phys. Rev. D **52** (1995) 484–493, arXiv:hep-ph/9501220.

[265] A. Aranda and C. D. Carone, "*Limits on a light leptophobic gauge boson*," Phys. Lett. B **443** (1998) 352–358, arXiv:hep-ph/9809522.

[266] J. M. Cline and A. R. Frey, "*Minimal hidden sector models for CoGeNT/DAMA events*," Phys. Rev. D **84** (2011) 075003, arXiv:1108.1391.

[267] G. Jungman, M. Kamionkowski, and K. Griest, "*Supersymmetric dark matter*," Phys. Rept. **267** (1996) 195–373, arXiv:hep-ph/9506380.

[268] A. Hook, E. Izaguirre, and J. G. Wacker, "*Model independent bounds on kinetic mixing*," Adv. High Energy Phys. **2011** (2011) 859762, arXiv:1006.0973.

[269] S. Baek and P. Ko, "*Phenomenology of $U(1)(L_\mu - L_\tau)$ charged dark matter at PAMELA and colliders*," JCAP **0910** (2009) 011, arXiv:0811.1646.

[270] C. Biggio, M. Blennow, and E. Fernandez-Martinez, "*General bounds on non-standard neutrino interactions*," JHEP **0908** (2009) 090, arXiv:0907.0097.

[271] C.-W. Chiang, Y.-F. Lin, and J. Tandean, "*Probing leptonic interactions of a family-nonuniversal Z' boson*," JHEP **1111** (2011) 083, arXiv:1108.3969.